Niche Contributions to Bone Marrow (Re)generation

Keane Jared Guillaume Kenswil

Erasmus MC
University Medical Center Rotterdam

ISBN: 978-94-6361-426-9
Layout: E.C.M.M. Simons
Cover: L. Rebollar, N. Orteu, E.C.M.M. Simons, K.J.G. Kenswil
Printing: Optima Grafische Communicatie (www.ogc.nl)

The work described in this dissertation was performed at the Department of Hematology of the Erasmus Medical Center, Rotterdam, the Netherlands. Printing of this dissertation was financially supported by Erasmus University Rotterdam and the Erasmus MC Vriendenfonds.

Niche Contributions to Bone Marrow (Re)generation

De rol van de niche in beenmerg vorming en herstel

Doctoral dissertation

to obtain the degree of Doctor from the
Erasmus University Rotterdam
by command of the
rector magnificus

Prof.dr. R.C.M.E. Engels

and in accordance with the decision of the Doctorate Board.

The public defence shall be held on

Tuesday, 19 May 2020 at 15:30 hrs

by

Keane Jared Guillaume Kenswil

born in Paramaribo, Suriname

Erasmus University Rotterdam

DOCTORAL COMMITTEE

Promotors: Prof.dr. H.G.P. Raaijmakers
Prof.dr. I.P. Touw

Other members: Prof.dr. P. ten Dijke
Prof.dr. W. E. Fibbe
Dr. E. Farrell

CONTENTS

1

INTRODUCTION

INTRODUCTION

Blood cells have a limited life-span and must be continuously replenished throughout mammalian life, in a process termed hematopoiesis. Hematopoiesis is maintained by the proliferation and differentiation of a very small population of pluripotent hematopoietic stem cells (HSCs) and their progeny that reside in bone marrow (BM) (Figure 1). Together they provide a steady-supply of red blood cells (that enable O_2/CO_2 exchange), thrombocytes (needed for blood clot formation), and leukocytes (essential for the protection against pathogens).

Chemo- and radiotherapy (chemo/radiotherapy) are among the most commonly used treatments for patients with cancer. Both inhibit cell division by differing modes of action, and once combined, can synergistically arrest growth and induce death of rapidly dividing malignant (cancerous) cells. However, this means that "healthy" non-malignant cells undergoing DNA replication are also affected, which may result in unwanted deleterious effects, such as BM suppression.

BM suppression, also known as myelosuppression, generally refers to the depletion of hematopoietic cells: red blood cells (anemia), thrombocytes (thrombocytopenia), and leukocytes (leukopenia). Anemia is associated with fatigue, dizziness, and heart palpitations, while thrombocytopenia is commonly accompanied by increased risks of bruises and bleedings. Leukopenia in particular is concerning since it leaves patients susceptible to opportunistic infections (including viral infections and fungal infections and fever/febrile episodes. The time needed for patients to achieve full hematopoietic recovery can be considerable and is a significant cause of morbidity, especially for patients with a delayed hematopoietic recovery.

In response to chemo/radiotherapy-induced damage, HSCs become activated to generate progenitors and mature blood cells to replenish those lost during injury. However, how and what drives this activation of HSCs remains incompletely understood. Over the past two decades we have come to realize that HSC function can be greatly influenced by its surrounding microenvironment in the BM. The BM microenvironment for HSCs, often referred to as the HSC niche, can be considered an ancillary meshwork of heterogeneous cells that may facilitate HSC fate by various mechanisms, such as paracrine signaling mediated by secretion of growth factors (cytokines).

Given the key role of niche cells in HSC maintenance and proliferation, it is reasonable to think that a better understanding of the HSC niche, specifically upon regeneration (after chemotherapeutic injury), may lead to the identification of niche cells and niche-derived factors that promote hematopoietic recovery. This may enable us to develop novel treatments that reduce the time needed for patients to recover from chemotherapy-induced myelosuppression.

1.1 BM regeneration

1.1.1 Homeostatic hematopoiesis

Under homeostatic conditions, the hematopoietic system depends on a small pool of pluripotent HSCs. In general, HSCs rarely divide and can generate virtually identical HSCs (a hallmark ability termed self-renewal) or progeny that are more highly proliferative but also more lineage-committed. These progenitors in turn mature into terminally differentiated cells that constitute the entire blood system. A simplified view of hematopoiesis (Figure 1) is to consider the hematopoietic system as a hierarchy of different blood cells that either fall under the myeloid or lymphoid branch with HSCs at the apex.

HSCs are heterogeneous and can be subdivided into long-term and short-term HSCs (LT-HSCs and ST-HSCs) based on their self-renewal capacity and degree of quiescence, with the more dormant LT-HSCs giving rise to multipotent progenitors (MPPs) via the more proliferative ST-HTCs (Passegue et al., 2003). MPPs lack self-renewal ability but retain full-lineage differentiation potential. MPPs in turn differentiate into oligo-potent progenitors, namely the common lymphoid progenitor (CLP) and the common myeloid progenitor (CMP). Further downstream, the CLP develops into cells of the lymphoid lineage, such as the natural killer (NK) cells, B and T lymphocytes. The CMP gives rise to the granulocytic/macrophage progenitor (GMP) and the megakaryocytic/erythroid progenitor (MEP) that together will generate granulocytes (neutrophils, eosinophils, and basophils), mononuclear cells (monocytes, macrophages), megakaryocytes, and erythrocytes.

Erythrocytes, also known as red blood cells (RBCs), provide O_2/CO_2 exchange and are the most abundant cell-type in peripheral blood (PB). Granulocytes and mononuclear cells are the first line of defense against pathogens and foreign material (innate immunity), and are involved in the removal of damaged cells. Megakaryocytes associate with BM sinusoidal vessels and release thrombocytes (platelets) in the peripheral circulation, which are essential for clot formation in case of damage to blood vessels. The lymphoid cells provide long-term memory for protection against recurring pathogens (adaptive immunity).

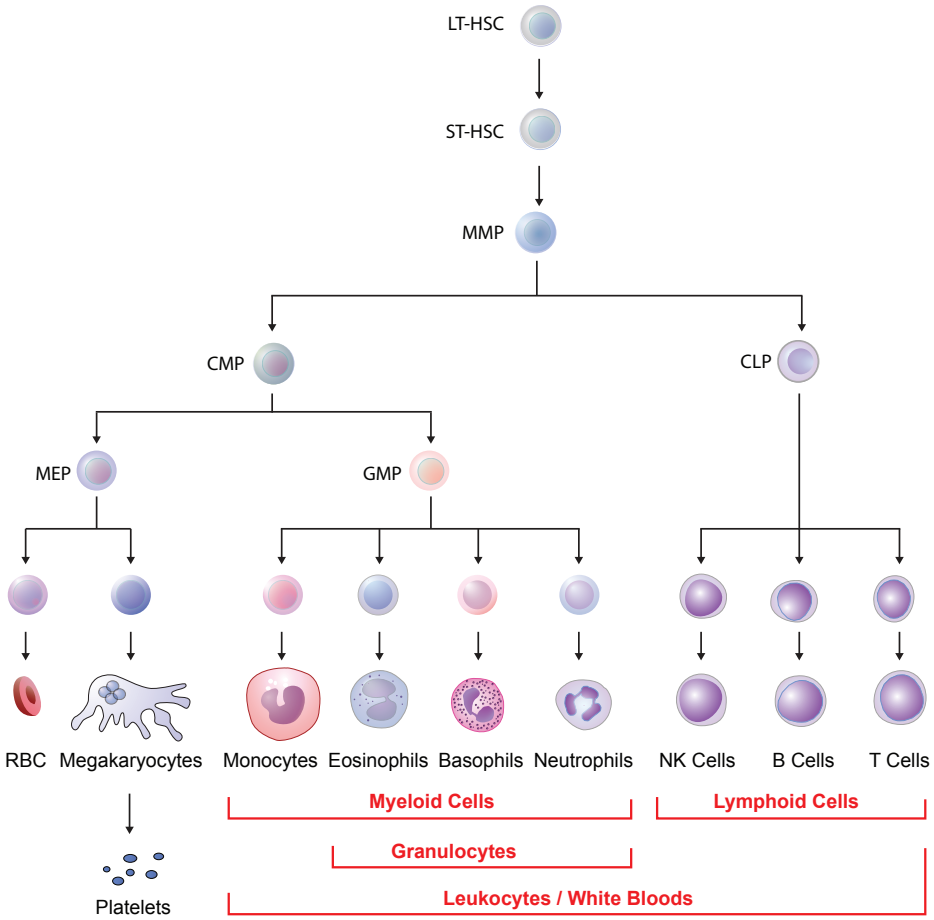

Figure 1. Simplified overview of hematopoiesis. Continuous production of mature blood cells and components depends on the self-renewal and differentiation of HSCs. HSCs give rise to MPPs that develop into more committed progenitors. CMPs give rise to erythrocytes, platelets, and myeloid cells, whereas CLPs differentiate into lymphoid cells. The myeloid cells consist of monocytes/macrophages, and granulocytes, the latter consisting of eosinophils, basophils and neutrophils. The lymphoid cells include the NK cells, and the B and T lymphocytes. Collectively, the granulocytes and lymphoid cells are referred to as leukocytes/white blood cells.

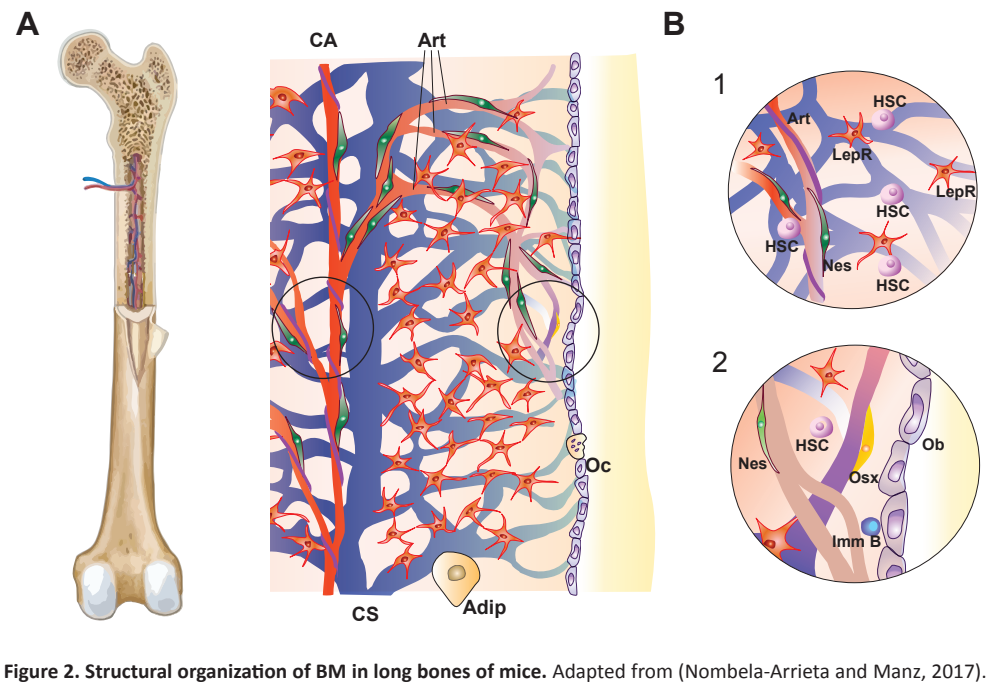

Figure 2. Structural organization of BM in long bones of mice. Adapted from (Nombela-Arrieta and Manz, 2017).
a. Simplified overview of the BM microarchitecture in the mouse femur. The central artery (CA) divides into arterioles (Art) that extend to the endosteal surface which develop into smaller endosteal capillaries (purple) that connect to the complex sinusoidal network (blue) which merges into the central sinus (CS) in the middle of the BM cavity. The distinct blood vessels are aligned by various stromal cells. Bone-degrading cells, called osteoclasts (Oc), line the endosteal surface. Adipocytes (Adip) also reside in the marrow and progressively increase upon aging.
b. 1. While most hematopoietic stem cells (HSCs) are adjacent to the sinusoids (blue), some HSCs preferentially localize to arteries (red). Arteries are enwrapped by sympathetic nervous system (SNS) fibers (purple) and Nestin-GFP^{bright}NG2^{+} cells (green), whereas sinusoids are associated with LEPR^{+}Nestin-GFP^{dim} cells. 2. Endosteal capillaries (purple) are associated with Osterix^{+} cells (Osx, orange). Bone-lining osteoprogenitors/osteoblasts (Ob) regulate lymphoid progenitor (Imm B) number.

1.1.2 HSC niches

Architecture of the BM microenvironment

Whether hematopoietic stem and progenitor cells (HSPCs) become activated (to differentiate and proliferate) or remain in a dormant state is partially determined by extracellular cues derived from their BM microenvironment. These extrinsic cues include secretion of regulatory factors, cell-cell interactions, interaction with the extracellular matrix, and regulation of reactive species oxygen (ROS) levels. In long bones, the architecture of BM is characterized by a complex and dynamic arrangement of hematopoietic niches with distinct compositions (Figure 2A).

BM is a very cell-dense and highly vascularized tissue (Draenert and Draenert, 1980; Nombela-Arrieta and Manz, 2017; Ramasamy, 2017). Blood is supplied to BM by multiple

arteries which divide into smaller arterioles that move towards the endosteal region (the inner-surface of bone), where they further divide into small-diameter endosteal arterioles/ capillaries. These endosteal capillaries transit into downstream sinusoidal vessels, which form a complex network that extends inwards to the medullary cavity, and merge with the central sinus/vein. Despite high vascular density, BM is relatively hypoxic (<32 mmHg), with the lowest oxygen tensions found near sinusoids in the central cavity, due to high oxygen demand associated with its high cellular density (Spencer et al., 2014). Many niche cells are adjacent to these diverse BM blood vessels (Crane et al., 2017), which, besides oxygen, also provide access to nutrients and other metabolites derived from circulating blood, and regulate cellular trafficking. Of note, both bone and BM are extensively innervated by the sympathetic nervous system (SNS). Furthermore, while human BM hardly contains any fat at birth, adipocytes (fat-producing cells) gradually increase with age, leading to a shift from red (hematopoietic-rich) marrow to yellow (fatty) marrow.

The discovery of surface markers for HSCs and BM microenvironmental cells, as well as, advances in imaging techniques and transgenic mouse models, have enabled studies to better define the cellular components and function of the HSC niche. Studies in mice suggest that within adult BM numerous cell-types constitute the HSC niche, with the majority being non-hematopoietic (stromal) cells and an increasingly recognized minor subset consisting of (mature) hematopoietic cells, as will be discussed in more detail in the following section. In particular, BM blood vessels seem to take on a critical role, which will be highlighted in their own separate section following the introduction of the HSC niche.

HSC-regulatory factors derived from niche cells essential for HSC maintenance

One of the ways to define niche cells is by their ability to synthesize factors that sustain HSC survival. Stem cell factor (SCF) and C-X-C motif chemokine ligand 12 (CXCL12) are the quintessential example of such HSC-regulatory factors and are probably among the best characterized niche-derived cytokines.

SCF is an agonist for the c-KIT receptor (Williams et al., 1990), which is expressed by HSCs (Kiel et al., 2005). Membrane-bound and soluble forms of SCF exist, and *in vivo* studies revealed that transgenic mice only expressing the soluble form of SCF have decreased HSC number (Barker, 1994, 1997), indicating that the membrane-bound form is critical for HSC maintenance. This finding also implies that SCF-expressing niche cells are in direct cell-cell contact with HSCs.

CXCL12, in addition to regulating HSC number, is also required for HSC retention in BM (Ara et al., 2003; Sugiyama et al., 2006; Tzeng et al., 2011). Mutant mice lacking CXCL12 fail to initiate hematopoiesis in fetal BM due to impaired colonialization by LT-HSCs (Ara et al., 2003). Additional genetic studies showed that abrogating expression of CXCL12 or its receptor CXCR4 in adulthood lead to depletion of BM HSCs (Sugiyama et al., 2006; Tzeng et al., 2011).

Advances in mouse genetics have enabled conditional and inducible abrogation of *CXCL12*, *SCF*, and other genes encoding for HSC regulatory factors in restricted cell populations by means of various Cre recombinases expressed under the control of (in theory) cell type-specific promoters. This has become an essential tool to test if and when expression of a single factor by a candidate cell type is required for HSC regulation.

HSC maintenance during steady-state: Osteoblasts

Osteoblasts reside at the endosteal surface of BM and are indispensable for *de novo* bone formation, secreting numerous extracellular proteins, such as type 1 collagen, osteocalcin (Ocn), and alkaline phosphatase (Figure 2B). Initially, *in vivo* studies using genetically engineered mice suggested that osteoblasts were important for regulating HSC number (Calvi et al., 2003; Zhang et al., 2003). Mice deficient for bone morphogenetic protein receptor type IA (BMPR1A) have an increased number of spindle-shaped N-cadherin-expressing osteoblastic cells which was associated with increased HSC number. Using 5-bromodeoxyuridine (BrdU)-labelling, researchers found that BrdU-retaining (a surrogate marker for LT-HSCs) cells were adjacent to these osteoblasts (Zhang et al., 2003). In line with these findings was the observation that expansion of osteoblasts, mediated by constitutively active PTH/ PTHrP receptor (PPR) signaling that was restricted to maturing osteoblastic cells, also lead to more HSCs (Calvi et al., 2003).

However, follow-up studies using other transgenic mouse lines and more specific markers for HSCs have since disputed a direct role for osteoblasts in regulating HSC number under homeostatic conditions. While conditional ablation of maturing osteoblasts in transgenic mice (that express herpesvirus thymidine kinase under control of a rat type 1 collagen promotor (*Col 2.3*)) upon ganciclovir injection eventually resulted in loss of BM HSCs (Visnjic et al., 2004); subsequent analyses showed that the decrease in HSC number (28 days post-injection) is preceded by early loss of B-lymphoid progenitors (8 days post-injection), suggesting that osteoblasts play a more direct role in B lymphopoiesis rather than in HSC regulation (Zhu et al., 2007).

This view was later supported by two companion papers from the laboratories of Drs. Daniel Link (using *Ocn*-Cre transgenic mice) and Sean Morrison (using *Col2.3*-Cre transgenic mice) both demonstrating that conditional deletion of *CXCL12* in osteoblasts did not deplete HSC number (Ding et al., 2012; Greenbaum et al., 2013). Furthermore, it had been shown that BM osteoblasts lack SCF expression and conditional deletion of *SCF* in mature osteoblasts had no effect on HSCs (Ding et al., 2012). Lastly, the group lead by Sean Morrison also demonstrated that c-kit^{+}Sca-1^{+}Lin^{-} BM cells with distinct expression of signaling lymphocyte activation molecules (SLAM) – CD150^{+}, CD48^{-}, and CD41^{-} – enriched for functional HSCs and the majority of these cells localized close to sinusoidal blood vessels, rather than the endosteum (Kiel et al., 2005) (Figure 2B).

Taken together, these studies still support a regulatory function of osteoblasts in unperturbed hematopoiesis, albeit at more committed stages of hematopoietic differentiation and perhaps not directly at HSC level. Hence, focus had shifted to other cellular components in the BM to uncover which niches directly control the HSC population.

HSCs niches under steady-state conditions: Perivascular stromal cells

Multipotency is not limited to HSCs in the BM. BM also contains stromal cells that form fibroblast colonies in culture (colony-forming unit-fibroblasts (CFU-Fs)) that exhibit multi-lineage differentiation capacity; fibroblasts expand extensively and can differentiate into cells of different mesenchymal fates, including osteoblasts, adipocytes, and chondrocytes (*ex vivo*). These multipotent bone marrow stromal cells (BMSCs) are very heterogeneous *in situ* (ability to give rise to different mesenchymal lineages, ancestry, and marker expression) and can be found on the abluminal surface of BM blood vessels (Crisan et al., 2008; Sacchetti et al., 2007). Intriguingly, *ex vivo* expanded BMSCs have previously been shown to form ectopic BM upon transplantation, forming donor-derived bone housing recipient-derived hematopoietic cells, making them attractive HSC niche candidates (Friedenstein et al., 1974). Considering that the majority of immunophenotypic HSCs were found to be associated with sinusoidal blood vessels (Kiel et al., 2005), and also with CXCL12-abundant reticular (CAR) cells – the main source of BM CXCL12 – which themselves often surrounded sinusoids (Sugiyama et al., 2006), studies started dissecting (1) the precise role of perivascular stromal cells in HSC maintenance and (2) their relation to BMSCs due to similar perivascular localization and reticular morphology.

In 2010, two independent studies by Mendez-Ferrer *et al* and Omatsu *et al* were among the first to demonstrate that perivascular stromal cells in postnatal marrow of mice are essential for regulating BM HSCs number and that some physiologically resembled BMSCs (Méndez-Ferrer et al., 2010; Omatsu et al., 2010). Using *Nes*-GFP transgenic mice, in which GFP expression is driven by the second intronic enhancer of *nestin*, the group of Paul Frenette demonstrated that *Nes*-GFP+ cells marked perivascular stromal cells that expressed *CXCL12* and *SCF*, and ablation of Nestin-expressing cells lead to reduced BM HSC number and HSC mobilization to the spleen. Provocatively, *Nes*-GFP+ cells (1%) were enriched for CFU-Fs and were able to differentiate into osteoblasts and chondrocytes *in vivo*, and proved to be serially transplantable: demonstrating their self-renewal capacity (Méndez-Ferrer et al., 2010). Congruent with these findings were the observations that (1) CAR cells depletion in postnatal marrow lead to a decreased HSC number and (2) CAR cells were able to differentiate into adipocytes and osteogenic cells *in vivo* (Omatsu et al., 2010). These landmark studies were the first to provide proof of principle that HSC and BMSC biology may be coupled under physiological conditions.

Subsequent work demonstrated that the *Nes*-GFP+ population could be subdivided in two populations based on GFP expression and their specific perivascular localization (Kunisaki et al., 2013). *Nes*-GFP^{bright} cells marked rare peri-arteriolar cells and were labelled by the pericyte marker NG2, while *Nes*-GFP^{dim} cells were much more abundant reticular stromal cells that largely associated with sinusoidal vessels (peri-sinusoidal). Though the authors also confirmed that the majority of the HSCs were closest to sinusoids, a subset of quiescent HSCs localized closer than expected to *Nes*-GFP^{bright}-enwrapped arterioles assuming a random distribution pattern (Figure 2B). Of note, most of the CFU-F content was confined to *Nes*-GFP^{dim} cells, despite exhibiting lower CFU-F frequency (1% vs 4%), due to their higher total cell count (3,500 vs 300 cells per femur).

Meanwhile the studies from the laboratories of Drs. Daniel Link and Sean Morrison, in which researchers systematically abolished CXCL12 and SCF expression in candidate niche cells, demonstrated that *Prx1*-Cre and *LepR*-Cre activity also marked perivascular stromal cells that expressed both CXCL12 and SCF in postnatal marrow (Ding and Morrison, 2013; Ding et al., 2012; Greenbaum et al., 2013). It was initially suggested that *LepR*-Cre cells partially overlapped with *Nes*-GFP+ cells (Ding et al., 2012). In fact, it was later demonstrated that *LepR*-Cre cells highly overlapped (98%) with Nes-GFP+ cells (Zhou et al., 2014) and that 80-90% Nes-GFP^{dim} cells coincided with *LepR*-Cre cells (Kunisaki et al., 2013; Zhou et al., 2014). Nes-GFP^{bright} cells did not strongly overlap with *LepR*-Cre (Kunisaki et al., 2013), only 9% of Nes-GFP^{bright} cells coincided with LepR-Cre (Zhou et al., 2014). In addition, Zhou *et al* showed that nearly all Leptin receptor (LepR)-expressing cells in postnatal BM were positive for *Prx1*-Cre and vice versa.

Conditional deletion of *CXCL12* and *SCF* revealed distinct contributions of perivascular stromal cells to HSC maintenance; abrogation of CXCL12 expression in *Prx1*-Cre and *LepR*-Cre transgenic mice induced HSC mobilization in both cases, but only HSC depletion in *Prx1*-Cre mice (Ding and Morrison, 2013; Greenbaum et al., 2013), whereas abrogation of SCF expression in *LepR*-Cre did deplete HSC number (Ding and Morrison, 2013). This was later confirmed in follow-up work by the group of Dr. Paul Fernette, in which they reproduced the effects of *LepR*-Cre mediated *SCF* and *CXCL12* deletion on HSC maintenance. They also showed that inducible targeted deletion of *CXCL12* induced in 2 week-old *NG2*-CreER mice (supposedly targeting peri-arteriolar *Nes*-GFP^{bright} stromal cells), resulted in HSC number depletion, while observing no effect of *SCF* deletion on HSC number.

Although it was also demonstrated that the majority of LepR-expressing perivascular cells enwrapped sinusoids, a minority was also found around some arterioles. Intriguingly, 10% of the BM cells marked by *LepR*-Cre gave rise to CFU-Fs that were able to differentiate into osteoblasts, adipocytes and chondrocytes *ex vivo* (Zhou et al., 2014). Lineage-tracing studies revealed that *LepR*-Cre cells arose postnatally and were a major source of bone and fat in postnatal BM.

Collectively, these studies further redefined the role of perivascular stromal cells as key components of the HSC niche and their associated BMSC activity, and indicated that perivascular stromal cells are diverse and consist of distinct subsets that exhibit specific spatial characteristics in the BM, and differentially contribute to the HSC niche (Figure 2B).

HSCs niches under steady-state conditions: Other cells

Hematopoietic cells derived from HSCs can convey signals to HSCs and thereby create a feedback loop. Three-dimensional whole-mount imaging demonstrated that a subset of HSCs associate with megakaryocytes (Bruns et al., 2014). Depletion of megakaryocytes leads to HSC proliferation and expansion, and megakaryocytes-derived chemokine C-X-C motif ligand 4 (CXCL4) (Bruns et al., 2014) and TGFβ-1 (Zhao et al., 2014) have been suggested to contribute to the maintenance of HSC quiescence (Figure 2B).

Recent work by Hur *et al* also proposed that HSC quiescence is controlled by niche-mediated activation of TGFβ signaling in HSCs. These researchers suggested that activation of TGFβ–SMAD3 signaling was dependent on stabilization of CD82 (expressed on dormant HSCs) by engaging with its binding partner DARC/CD234, which is expressed by a subset of macrophages (Hur et al., 2016). Previously, macrophages were thought to have more indirect contributions on HSCs by acting via niche cells. In mice, HSC lodgment in the BM was severely disrupted upon targeted depletion of CD169+ macrophages and this coincided with a substantial loss of CXCL12, indicating that macrophages may act via niche cells by regulating their expression of HSC-retention factors (such as CXCL12 by Nestin-GFP+ cells) (Chow et al., 2011). CXCL12 expression can also be regulated by the removal of aged neutrophils from the circulation and their subsequent engulfment by macrophages (Casanova-Acebes et al., 2013), suggesting that interactions between mature hematopoietic cells (macrophages and neutrophils) can affect the HSC niche. A more direct role for (mature) myeloid cells was suggested by a recent study that demonstrated that myeloid cells form a spatial cluster around a subset of HSCs and conferred their quiescence by histamine secretion (Chen et al., 2017).

Differentiated lymphoid cells have also been implicated to play a role in hematopoiesis. IFNγ produced by cytotoxic CD8+ T cells was shown to induce IL-6 production by BMSCs, and thereby enhanced proliferation and myeloid differentiation of early hematopoietic progenitor cells during acute viral infection (Schürch et al., 2014). More recently, a subset of FoxP3+ regulatory T cells marked by CD150 expression was shown to closely associate with HSCs and maintained HSC quiescence by protecting HSCs from oxidative stress under homeostatic conditions (Hirata et al., 2018).

The SNS also seems to play an important role in HSC regulation. Adrenergic nerves from the SNS have been shown to control HSC egress into the circulation by regulating cyclical expression of niche-derived CXCL12 (in a circadian manner) (Méndez-Ferrer et al., 2008) and it was later revealed that these sympathetic nerves innervated Nes-GFP+ stromal cells (Méndez-Ferrer et al., 2010). Furthermore, it has been reported that sympathetic nerve-associated nonmyelinating Schwann cells can promote HSC maintenance by regulating proteolytic activation of latent TGFβ in the BM (Yamazaki et al., 2011).

Lastly, adipocytes have been suggested to play a negative role in the HSC niche; adipocyte-rich BM (such as the vertebrae of the mouse tails) was shown to contain fewer HSPCs compared to adipocyte-free BM (vertebrae of the thorax) (Naveiras et al., 2009), but direct evidence, particularly during homeostasis, is lacking (Figure 2).

HSC niches in humans

Knowledge on the specific cellular components of the human HSC niche (in adult BM) has until recently been limited compared to that generated by studies performed on mice. Much attention has been placed on identifying human BMSCs considering data from murine models strongly argue that mesenchymal progenitor cells fulfill a crucial role in regulating HSC function.

Ironically, one of the first studies that managed to prospectively isolate human BMSCs with bona-fide self-renewal capacity and the ability to create a hematopoietic-supporting microenvironment, preceded the transgenic mice studies that initially identified BMSCs as important HSC niche components (Méndez-Ferrer et al., 2010; Zhou et al., 2014). By using a single positive marker, CD146, the group of Paolo Bianco demonstrated that CD146 labelled adventitial (abluminal surface of blood vessels) reticular cells in adult BM that were enriched for CFU-Fs and upon xenogenic transplantation in mice, formed heterotopic ossicles harboring (1) murine-derived hematopoietic tissue and (2) phenotypically identical CD146+ BMSCs (Sacchetti et al., 2007). Later it was revealed that CD146 marked a perivascular subset of the CD271-expressing BMSCs, while the CD271+ subset lacking CD146 expression exhibited an endosteal localization, and together contained virtually all the CFU-Fs in adult BM (Tormin et al., 2011). Both CD271+ subsets co-localized with CD34+ HSPCs *in situ* and were equally capable of forming ectopic bone and BM upon transplantation (Tormin et al., 2011). Of note, work of the group of Dr. Simón Méndez-Ferrer suggested that a combination of the cell surface markers CD105 and CD146 could be used to prospectively isolate the human equivalent of Nestin-GFP+ cells. CD105+CD146+ cells obtained from adult BM were able to generate mesenchymal spheres *in vitro* that were able to support the expansion of HPCs capable of engrafting immunocompromised mice (Isern et al., 2014).

Despite the considerable effort spent on identifying human BMSCs, evidence for their hematopoietic-supporting capacity and potential underlying mechanisms is still relatively lacking compared to that generated by studies using genetically engineered mice. It remains to be seen to what extent findings in mice are relevant for human biology.

1.1.3 HSCs and their niche during regeneration

Impact of chemo/radiotherapeutic stress on the hematopoietic system

In the treatment of various malignancies, chemotherapy and radiotherapy are often used to eradicate malignant cells, but can also have unwanted harmful effects on hematopoiesis. In general, chemo/radiotherapy works by causing DNA damage and consequently inducing senescence or death of cells. The severity of the damage to the hematopoietic system depends on the treatment regimen.

Ionizing radiation (IR) can induce DNA damage in cells by the formation of reactive oxygen species (ROS). Cells harbor antioxidant systems to scavenge excess ROS, but can become overwhelmed if ROS reach high enough levels. This overabundance of ROS can damage macromolecules within cells (such as lipids, proteins, and DNA) and if not timely repaired, may lead to cell death (Azzam et al., 2012). In severe cases, this oxidative stress persists because pro-inflammatory cytokines are often up-regulated by ROS, and these re-inforce the production of ROS (cytokine storm) (Kim et al., 2014). IR can also directly damage cells by inducing double-stranded breaks in DNA.

Chemotherapy makes use of cytotoxic drugs that inhibit cell division. Chemotherapeutic agents are diverse, and include alkylating agents, antimetabolites, and anthracyclines (Cheung-Ong et al., 2013). Alkylating agents, such as cyclophosphamide act by forming cross-links in DNA double-helix strands, while antimetabolites, like cytarabine, compete with nucleosides for incorporation into DNA. Anthracyclines can interact with DNA in different ways, including intercalation (insertion between the base pairs) and poisoning of topoisomerase II.

In general, cycling cells are in particular sensitive to the effects of chemo/radiotherapy, which means that committed myeloid progenitors giving rise to mature blood cells are more affected compared to the more dormant/quiescent HSCs (Lerner and Harrison, 1990; Mohrin et al., 2010). Consequently, peripheral blood cell counts often decrease after chemotherapy, and exhibit a progressive decline based on the intrinsic lifespan of the cell, with granulocytes declining prior to platelets followed by erythrocytes (Mauch et al., 1995). This sequence and rate of decline of peripheral blood cells is similar for radiotherapy. The resulting granulocytopenia and thrombocytopenia leave patients especially at risk for opportunistic infections and bleedings, and are major cause of morbidity in the treatment of cancer.

Upon stress conditions dormant HSCs become activated to replenish lost cells (Wilson et al., 2008), but how the niche might mediate dormant HSC activation has remained obscure until recently. Spurred on by the increased knowledge on which BM microenvironmental cells constitute the HSC niche and with advances in the tools to identify specific subsets of HSPC populations, studies have started focusing on dissecting the role of the niche cells in BM regeneration in response to chemoradiotherapeutic stress.

Impact of chemoradiotherapeutic stress on the HSC niche and consequences

Cytotoxic damage resulting from chemo/radiotherapy is not limited to the hematopoietic system, micro-environmental cells in the BM can also suffer damage depending on the treatment regimen.

Cao *et al* reported that femur irradiation at a dose of 20 Gray can robustly alter the BM architecture of mice and saw that BM exhibited increased adipogenesis, reduced CFU-F efficiency, and a disrupted vasculature network (Cao et al., 2011). Similarly, chemotherapeutic agents, such as cyclophosphamide and methotrexate (an antimetabolite), have also been associated with increased marrow adipocyte content, bone loss, and regression of BM blood vessels in murines (Georgiou et al., 2012; Shirota and Tavassoli, 1991).

Osteolineage cells

Although recent work has toned down the importance of osteoblasts in regulating HSC number during homeostasis, numerous studies have suggested that bone-lineage cells play a prominent role after BM injury. For instance, studies have demonstrated that transplanted HSPCs localize near the endosteal surface and osteolineage cells of irradiated mice (Lo Celso et al., 2009; Dominici et al., 2009; Jiang et al., 2009). Irradiation was associated with a reversible expansion of N-cadherin+ osteoblasts and concomitant CXCL12 expression (Dominici et al., 2009). These findings were in line with previous work that demonstrated that CXCL12 levels were increased after conditioning with DNA-damage agents (ionizing irradiation, cyclophosphamide, and 5-fluorouracil) (Ponomaryov et al., 2000). This is especially clinically relevant in the context of HSPC recovery after BM transplantation, which is preceded by conditioning regimens consisting of chemo/radiotherapy.

Recent work has suggested that the subset of osteoblasts expressing N-cadherin can normally maintain HSC quiescence via non-canonical WNT signaling and after 5-FU challenge this signaling becomes attenuated and HSCs subsequently enter cell cycle (Sugimura et al., 2012). Furthermore, single-cell analysis of osteoblasts from irradiated mice in direct contact with transplanted HSCs lead to the discovery of 3 novel HSPC regulatory factors: Embigin, IL-18 and angiogenin (Silberstein et al., 2016). Remarkably, angiogenin was found to regulate hematopoietic recovery after myeoablation by specifically promoting proliferation of committed progenitors, while inducing quiescence in HSCs (Goncalves et al., 2016). More recently, it was reported that dickkopf-1 (DKK1) released by osteoprogenitors could promote HSC reconstitution following irradiation by suppressing mitochondrial ROS levels and senescence (Himburg et al., 2017).

Together these studies indicate that bone-lining/osteoprogenitor cells take on a prominent role in hematopoietic recovery after chemoradiotherapeutic insult.

Perivascular stromal cells

The group of Dr. Paul Frenette was one of the first to describe the role of BMSCs upon regeneration by challenging *Nes*-GFP mice with 5-FU (Kunisaki et al., 2013). Kunisaki et al observed that the *Nes*-GFP^{bright} cells were relatively quiescent compared to sinusoid-associated *Nes*-GFP^{dim} cells, and were subsequently also more chemoresistant upon 5-FU challenge. Intriguingly, the proportion of HSCs near *Nes*-GFP^{bright} cells was initially increased after 5-FU treatment, and as regeneration progressed this proportion steadily decreased. The authors proposed that *Nes*-GFP^{bright} cells might somehow shield HSCs from genotoxic insult by mediating HSC quiescence in a protective milieu, but the direct role of *Nes*-GFP^{bright} cells or protective signals involved remains unclear.

The role of LepR-expressing BMSCs is more clear and has been recently described by multiple groups (Himburg et al., 2018; Zhou et al., 2017). The Morrison laboratory reported that SCF derived from cells marked by *LepR*-cre mediated hematopoietic regeneration after HSC transplantation in irradiated mice, as well as, in mice treated with 5-FU (Zhou et al., 2017). Notably, Zhou et al observed that LepR+ cells actually declined after chemo/radiotherapy and that SCF derived from adipocytes, presumably descendants of LepR+ cells (95% of the BM adipocytes were previously shown to be marked Lepr-Cre after irradiation), promoted hematopoietic regeneration. In addition, pleiotrophin (PTN), a novel HSPC regulatory factor, was identified in BM cells marked by *LepR*-cre and was suggested to mediate acute hematologic recovery and survival following irradiation (Himburg et al., 2018).

Collectively these studies suggest that BMSC niche cells respond differently to cytotoxic challenge. While Nestin-GFP^{bright} cells may be relatively chemoresistant and are associated with a subset of quiescent HSCs, their exact role in BM regeneration is not well described. LepR+ cells on the other hand seem to be more sensitive to chemoradiotherpeutic stress, but together with their descendants mediate hematopoietic recovery by secreting SCF and PTN.

Nerve cells

Impaired adrenergic signaling in 5-FU treated mice resulted in reduced number of Nestin-GFP+, as well as, endothelial cells and delayed hematopoietic recovery (Lucas et al., 2013). These findings imply that the SNS indirectly plays a role in BM regeneration by ensuring survival of other HSC niche components after chemotherapy. Interestingly, while the number of sympathetic fibers was unaltered after IR or 5FU treatment, peripheral nerve damage did occur in mice that received cisplatin, indicating that the response of HSC niche cells depends on the type of cytotoxic stressor.

Megakaryocytes

In response to chemotherapeutic stress megakaryocytes were shown to up-regulate fibroblast growth factor (FGF1) to promote HSC expansion (Zhao et al., 2014). Furthermore, megakaryocytes accumulate in the BM after cytotoxic stress (Hérault et al., 2017; Kopp et al., 2005) and megakaryocyte-derived cytokines were previously implicated as a possible mediator of the transient osteoblast expansion after irradiation (Dominici et al., 2009).

Conclusion

Taken together, emerging evidence from mice studies indicate that the HSC niche is not limited to a single cell type or anatomical location in BM. It has been proposed that there are multiple HSC niches situated in BM, perhaps reflecting (or contributing to?) the heterogeneity within the HSC pool (Haas et al., 2018). Individual niche components may have a specific contribution to HSC regulation, but most likely there is a complex interdependency and crosstalk between the different niches that enable fine-tuned regulation of the HSC pool under specific circumstances. In the following section, the specialized role of BM blood vessels will be discussed.

1.2 The role of endothelial cells in BM regeneration

1.2.1 General

Endothelial cells (ECs), collectively termed endothelium, form a monolayer of cells that constitute the inner-lining of blood vessels and are most commonly known for facilitating blood flow and enabling exchange of nutrients and waste products. ECs are also widely recognized for their role in regulating vascular tone, blood clotting, and migration of hematopoietic cells. However, these cells perform other critical physiological tasks as well – signals from ECs guide the development, maintenance, and regeneration of their surrounding tissue. This has been shown to be especially true for BM physiology, and by extension, BM hematopoiesis.

ECs have been shown to play a critical role during endochondral ossification, which is required for the formation of long bones and subsequent BM (Chan et al., 2009). Invading blood vessels are attracted to the cartilage template of bone by VEGF from hypertrophic chondrocytes (Gerber et al., 1999), and together with the latter, as well as, with osteoblasts and osteoclasts, will coordinate the development of bone. It is thought that during this process ECs express factors (angiocrine factors) that support osteogenesis. The expression of EC-derived osteogenic factors has been reported for specific endosteal blood vessels recently characterized in (postnatal) mice (Kusumbe et al., 2014).

1.2.2 Endothelial cells

The importance of BM ECs for hematopoiesis first emerged in studies that focused on hematopoietic recovery following chemo/radiotherapy. The group of Dr. Shahin Rafii revealed that chemo/radiotherapy can severely disrupt the sinusoidal network, with the extent of damage depending on the type and magnitude of the cytotoxic agent used (Hooper et al., 2009; Kopp et al., 2005). Importantly, blocking regeneration of sinusoidal vessels after

irradiation by inhibiting VEGFR2 signaling impaired engraftment and reconstitution of HSPCs. In line with these findings was the observation that targeted deletion of pro-apoptotic genes *Bak* and *Bax* in endothelium (using either *Tie2*-Cre or *VEcadherin*-Cre mice) preserved the integrity of BM vasculature following lethal irradiation, which was associated with improved survival of mice (Doan et al., 2013a). These studies indicate that BM ECs might mediate HSPC reconstitution after myelosuppresive injury, but the precise mechanisms involved were unclear.

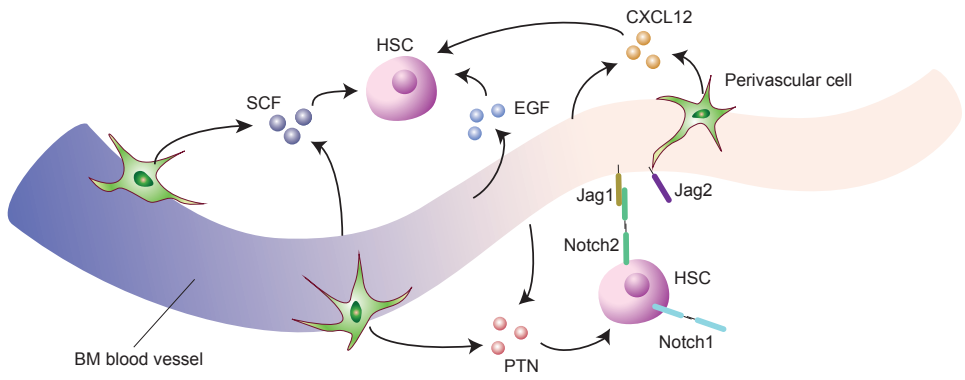

Figure 3. Regeneration-associated paracrine factors in the bone marrow (BM) vascular niche. Adapted from (Sasine et al., 2017). A schematic diagram of a BM blood vessel aligned with perivascular stromal cells in longitudinal view and representation of several paracrine factors that are secreted by BM endothelial cells and perivascular cells. Abbreviations: CXCL12, C-X-C chemokine ligand 12; CXCR4, C-X-C chemokine receptor type 4; EGF, epidermal growth factor; EGFR, epidermal growth factor receptor; HSC, hematopoietic stem cell; Jag1, Jagged-1; Jag2, Jagged-2; PTN, pleiotrophin; PTP-z, protein receptor tyrosine phosphatase-z; SCF, stem cell factor.

1.2.3 Endothelial cell-derived instructive (angiocrine) factors

Follow-up work revealed that BM ECs can mediate hematopoietic recovery following injury in a perfusion-independent manner (Figure 3). Butler *et al* demonstrated that inhibition of VEGFR2 signaling diminished endothelial expression of Notch ligands, Jagged1 and Jagged2, indicating that BM ECs may mediate the reconstitution of hematopoiesis by expressing HSPC-instructive factors (Butler et al., 2010). Indeed, it was later suggested by specifically disrupting Jagged1 and Jagged2 expression in ECs (using *VEcadherin*-Cre mice) that both Notch ligands can contribute to hematopoietic recovery after myelosuppressive injury (Guo et al., 2017; Poulos et al., 2013). Subsequently, other studies have identified additional angiocrine factors that may regulate HSPC recovery by mediating cell-to-cell or cell-extracellular matrix interactions, such as sinusoidal E-selectin (Winkler et al., 2012) and extracellular matrix protein developmental endothelial locus (Del)-1 (Mitroulis et al., 2017). The team of Dr. John Chute reported that paracrine factors released by BM ECs can also mediate HSPC regeneration following myelosuppression. These include epidermal growth factor (EGF) (Doan et al., 2013b) and PTN (Himburg et al., 2010, 2018), with EGF preventing

radiation-induced apoptosis of HSCs, while PTN was associated with HSC expansion via activation of the RAS pathway (Himburg et al., 2014). Of note, it has been demonstrated that during steady-state conditions BM ECs also release CXCL12 and SCF, and abrogating CXCL12 or SCF expression in BM ECs lead to decreased HSC number (Ding and Morrison, 2013; Ding et al., 2012; Greenbaum et al., 2013). The effects on HSPC regeneration following injury were not explored, but a previous report did describe that 5FU treated mice had a dramatic increase in SCF expression by sinusoidal ECs (Kimura et al., 2011). These studies indicate that ECs express instructive factors that may be involved in both HSC maintenance and regeneration.

1.2.4 Crosstalk with other niche cells

Other niche cells can indirectly regulate hematopoietic recovery via BM ECs. DKK1 released by osteoprogenitors induced upregulation of EGF expression by BM ECs, which contributed to hematopoietic recovery following irradiation (Himburg et al., 2017). In addition, BM granulocytes were recently reported to promote EC survival and vessel growth following irradiation by delivering tumor necrosis factor-alpha (TNFα) to regenerative vasculature, which resulted in improved hematopoietic engraftment (Bowers et al., 2018). Also, as previously mentioned, the SNS has been suggested to mediate EC survival following chemotherapy.

1.2.5 Specialized endothelium

It has recently become clear that BM blood vessels are very heterogeneous. Besides structure and morphology, ECs of BM blood vessels differ in respect to their sensitivity to cytotoxic stress, expression of angiocrine factors, and their associated function.

For example, the endosteal capillaries that connect arterioles with sinusoids have been attributed with a number of specific characteristics (Kusumbe et al., 2014; Ramasamy et al., 2014) (Figure 2B). Endosteal capillaries, also termed Type H capillaries due to their high expression of CD31 and endomucin, were reported to be relatively radioresistant compared to sinusoidal ECs, and intriguingly, were suggested to couple BM angiogenesis and osteogenesis in a Notch-dependent manner by angiocrine release of Noggin. These endosteal capillaries were also tightly associated with perivascular osteoprogenitors marked by Osterix expression. Remarkably, activated Notch signaling in BM ECs also lead to HSC expansion (Kusumbe et al., 2016).

Another study demonstrated that some non-sinusoidal BM ECs expressed thrombomodulin and maintained the retention of a small subset of LT-HSCs (marked by EPCR expression) in the BM by inhibiting NO production (Gur-Cohen et al., 2015). Subsequent work by the same lab indicated that due to leaky nature of sinusoidal ECs, HSCs exposed to plasma components exhibit increased ROS and are more active, while less permeable arterial ECs maintain lower levels of ROS and thereby confer quiescence to HSCs (Itkin et al., 2016).

Further supporting the notion that sinusoidal and arterial ECs exhibit specific roles was a very recent report that indicated that arterial ECs are the main source of endothelial SCF, which regulated HSC number under steady-state conditions, as well as, HSPC reconstitution after 5-FU challenge (Xu et al., 2018).

Taken together these studies indicate that ECs are important and versatile. In addition to their conventional function, ECs are needed for HSC maintenance and regeneration, and can mediate these functions in a perfusion-independent manner by expressing angiocrine factors. Not only do they affect HSPCs, but they can also couple angiogenesis and osteogenesis by secreting osteogenic factors.

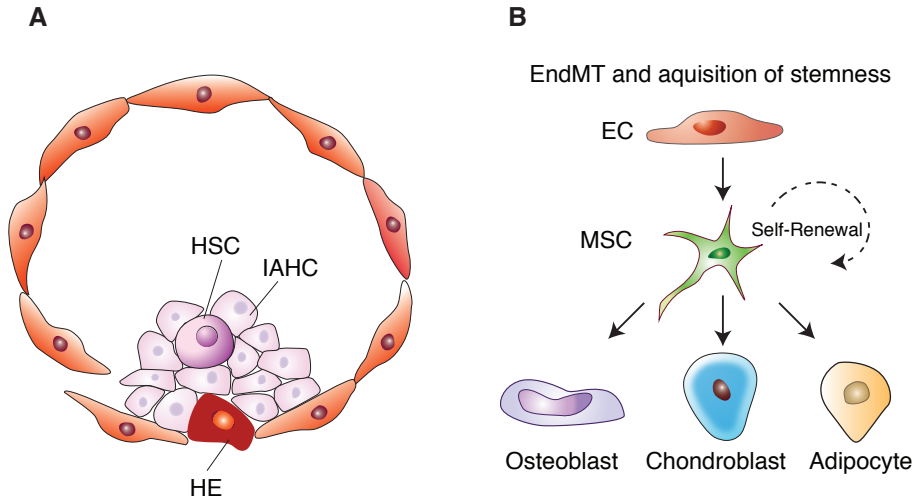

Figure 4. Plasticity of endothelium.
a. Adapted from (Kauts et al., 2016). Hemogenic endothelium gives rise to intra-aortic hematopoietic clusters that contain hematopoietic stem cells (HSCs) at embryonic day 10.5 (E10.5).
b. Hypothetical model of endothelium giving rise to mesenchymal multipotent stromal cells (MSCs) capable of self-renewal and differentiating into multiple skeletal lineages.

1.3 Plasticity of endothelial cells

1.3.1 Endothelial-to-Hematopoietic transition and Endothelial-to-Mesenchymal transition

The intimate relationship between ECs and HSCs is not surprising considering that definitive HSCs arise from ECs during embryogenesis. In mice at embryonic day (E) 10.5, specialized ECs in the aorta-gonad-mesonephros (AGM) region, called hemogenic endothelium, start giving rise to hematopoietic clusters by undergoing endothelial to hematopoietic transition (EHT) (Figure 4A). These hematopoietic clusters contain the HSCs that will give a life-long supply of blood cells and components (de Bruijn et al., 2002). Of note, the actual number of HSCs in these clusters is very low (2/700) (Yokomizo and Dzierzak, 2010), indicating that

in addition to EHT, HSC-precursors need to undergo a molecular program that specifies HSC fate. The AGM itself is thought to originate from embryonic mesoderm, specifically the splanchnopleural mesoderm (Rosselló Castillo et al., 2013). Ultimately, the generated HSCs migrate to fetal liver where they will undergo massive expansion prior to colonizing the BM of fetal long bones.

In addition to giving rise to HSPCs at the AGM, ECs of other tissues can directly contribute to organogenesis by transforming into other cell types. For example, ECs of the embryonic heart (endothelial endocardial cells) can give rise to mesenchymal cells necessary for proper heart development by undergoing endothelial to mesenchymal transition (EndMT). EndMT is required for the generation of the atrioventricular valves, as well as, the formation of endocardial cushion (Liebner et al., 2004) and a substantial portion of the cardiac pericytes and vascular smooth muscle cells (Chen et al., 2016). Intriguingly, endothelial endocardium-derived cells have been reported to give rise to osteogenic and adipogenic cells (Pu et al., 2016; Wylie-Sears et al., 2011). This remarkable plasticity of endothelium was also observed in ECs of human skeletal muscle that were reported to be able to differentiate into myogenic, osteogenic and chondrogenic cells in culture (Zheng et al., 2007) (Figure 4B).

1.4 Scope and outline of this thesis

Recent studies in mice have led to the recognition of BM ECs as critical HSC niche components that can mediate hematologic recovery after injury. Furthermore, these studies also identified specialized subsets of endothelium that not only regulate the hematopoietic system, but also couple osteogenesis and angiogenesis. Importantly, insights into the molecular programs underlying the specialized function of these endothelial subsets have enabled targeted interventions in mice, such as pharmacologic manipulation that enhanced bone formation or administration of recombinant proteins that promoted hematologic recovery after injury. However, the relevance of these findings for human biology remains relatively unknown. In particular, studies in humans that have attempted to unravel the specific contributions of BM ECs to hematologic recovery are scarce. To identify potential targets for therapeutic modulation to accelerate hematologic recovery in humans, a better understanding of the relevant cellular constituents and molecular pathways underlying hematologic recovery is needed.

In this thesis, we aimed to better define cellular and molecular events that occur in the human bone marrow during (re)generation, in order to identify novel cellular programs and mechanisms that might be exploitable for therapeutic modulation.

To this end, we defined two distinct (patho)physiologic conditions associated with BM (re)generation, requiring coordinated activation of osteogenesis, angiogenesis, and hematopoiesis, namely (1) regeneration after chemotherapeutically-induced injury and (2) bone marrow generation in human fetal development upon migration from hematopoiesis from the fetal liver to the bone at week 15–20 post gestation.

In **chapter 2**, we characterized human BM ECs associated with BM (re)generation in these conditions by flow-cytometry. Massive parallel sequencing was employed in EC subsets to identify candidate angiocrine factors that might drive hematologic recovery. This led to the identification of IL-33 which was subsequently functionally interrogated for its regenerative potential in bone and marrow. In **chapter 3**, we build upon the observation in chapter 2 that BM ECs exist that co-express mesenchymal markers, suggesting the possibility that specific BM ECs might contribute to BM regeneration by giving rise to mesenchymal progenitors (via EndMT). This notion is tested by extensive experimentation in both human cells and mice, leading to the postulation of EndMT as novel concept in bone marrow (re)generation and the *de novo* generation of MSCs in the mammalian BM. IL-33 is subsequently identified as a driver of this process.

As immune cells have also been implicated to regulate HSPC behavior, we dissected the BM lymphoid composition of the AML patients recovering (from remission induction chemotherapy) to determine whether specific immune subsets are associated with hematologic recovery in **chapter 4**. Finally, in **chapter 5** the findings in this thesis are summarized and their relevance for the field of BM regeneration, including future perspectives, are discussed.

REFERENCE LIST

Ara, T., Tokoyoda, K., Sugiyama, T., Egawa, T., Kawabata, K., and Nagasawa, T. (2003). Long-term hematopoietic stem cells require stromal cell-derived factor-1 for colonizing bone marrow during ontogeny. Immunity *19*, 257–267.

Azzam, E.I., Jay-Gerin, J.-P., and Pain, D. (2012). Ionizing radiation-induced metabolic oxidative stress and prolonged cell injury. Cancer Lett. *327*, 48–60.

Barker, J.E. (1994). Sl/Sld hematopoietic progenitors are deficient in situ. Exp. Hematol. *22*, 174–177.

Barker, J.E. (1997). Early transplantation to a normal microenvironment prevents the development of Steel hematopoietic stem cell defects. Exp. Hematol. *25*, 542–547.

Bianco, P., Cao, X., Frenette, P.S., Mao, J.J., Robey, P.G., Simmons, P.J., and Wang, C.Y. (2013). The meaning, the sense and the significance: Translating the science of mesenchymal stem cells into medicine. Nat. Med. *19*, 35–42.

Bowers, E., Slaughter, A., Frenette, P.S., Kuick, R., Pello, O.M., and Lucas, D. (2018). Granulocyte-derived TNFα promotes vascular and hematopoietic regeneration in the bone marrow. Nat. Med. *24*, 95–102.

de Bruijn, M.F.T.., Ma, X., Robin, C., Ottersbach, K., Sanchez, M., and Dzierzak, E. (2002). Hematopoietic Stem Cells Localize to the Endothelial Cell Layer in the Midgestation Mouse Aorta. Immunity *16*, 673–683.

Bruns, I., Lucas, D., Pinho, S., Ahmed, J., Lambert, M.P., Kunisaki, Y., Scheiermann, C., Schiff, L., Poncz, M., Bergman, A., et al. (2014). Megakaryocytes regulate hematopoietic stem cell quiescence through CXCL4 secretion. Nat. Med. *20*, 1315–1320.

Butler, J.M., Nolan, D.J., Vertes, E.L., Varnum-Finney, B., Kobayashi, H., Hooper, A.T., Seandel, M., Shido, K., White, I.A., Kobayashi, M., et al. (2010). Endothelial Cells Are Essential for the Self-Renewal and Repopulation of Notch-Dependent Hematopoietic Stem Cells. Cell Stem Cell *6*, 251–264.

Calvi, L.M., Adams, G.B., Weibrecht, K.W., Weber, J.M., Olson, D.P., Knight, M.C., Martin, R.P., Schipani, E., Divieti, P., Bringhurst, F.R., et al. (2003). Osteoblastic cells regulate the haematopoietic stem cell niche. Nature *425*, 841–846.

Cao, X., Wu, X., Frassica, D., Yu, B., Pang, L., Xian, L., Wan, M., Lei, W., Armour, M., Tryggestad, E., et al. (2011). Irradiation induces bone injury by damaging bone marrow microenvironment for stem cells. Proc. Natl. Acad. Sci. U. S. A. *108*, 1609–1614.

Casanova-Acebes, M., Pitaval, C., Weiss, L.A., Nombela-Arrieta, C., Chèvre, R., A-González, N., Kunisaki, Y., Zhang, D., van Rooijen, N., Silberstein, L.E., et al. (2013). Rhythmic modulation of the hematopoietic niche through neutrophil clearance. Cell *153*, 1025–1035.

Lo Celso, C., Fleming, H.E., Wu, J.W., Zhao, C.X., Miake-Lye, S., Fujisaki, J., Côté, D., Rowe, D.W., Lin, C.P., and Scadden, D.T. (2009). Live-animal tracking of individual haematopoietic stem/progenitor cells in their niche. Nature *457*, 92–96.

Chan, C.K.F., Chen, C.-C., Luppen, C.A., Kim, J.-B., DeBoer, A.T., Wei, K., Helms, J.A., Kuo, C.J., Kraft, D.L., and Weissman, I.L. (2009). Endochondral ossification is required for haematopoietic stem-cell niche formation. Nature *457*, 490–494.

Chen, Q., Zhang, H., Liu, Y., Adams, S., Eilken, H., Stehling, M., Corada, M., Dejana, E., Zhou, B., and Adams, R.H. (2016). Endothelial cells are progenitors of cardiac pericytes and vascular smooth muscle cells. Nat. Commun. *7*, 12422.

Chen, X., Deng, H., Churchill, M.J., Luchsinger, L.L., Du, X., Chu, T.H., Friedman, R.A., Middelhoff, M., Ding, H., Tailor, Y.H., et al. (2017). Bone Marrow Myeloid Cells Regulate Myeloid-Biased Hematopoietic Stem Cells via a Histamine-Dependent Feedback Loop. Cell Stem Cell *21*, 747–760.e7.

Cheung-Ong, K., Giaever, G., and Nislow, C. (2013). DNA-damaging agents in cancer chemotherapy: Serendipity and chemical biology. Chem. Biol. *20*, 648–659.

Chow, A., Lucas, D., Hidalgo, A., Méndez-Ferrer, S., Hashimoto, D., Scheiermann, C., Battista, M., Leboeuf, M., Prophete, C., van Rooijen, N., et al. (2011). Bone marrow CD169 + macrophages promote the retention of hematopoietic stem and progenitor cells in the mesenchymal stem cell niche. J. Exp. Med. *208*, 261–271.

Crane, G.M., Jeffery, E., and Morrison, S.J. (2017). Adult haematopoietic stem cell niches. Nat. Rev. Immunol. *17*, 573–590.

Crisan, M., Yap, S., Casteilla, L., Chen, C.W., Corselli, M., Park, T.S., Andriolo, G., Sun, B., Zheng, B., Zhang, L., et al. (2008). A Perivascular Origin for Mesenchymal Stem Cells in Multiple Human Organs. Cell Stem Cell *3*, 301–313.

Ding, L., and Morrison, S.J. (2013). Haematopoietic stem cells and early lymphoid progenitors occupy distinct bone marrow niches. Nature *495*, 231–235.

Ding, L., Saunders, T.L., Enikolopov, G., and Morrison, S.J. (2012). Endothelial and perivascular cells maintain haematopoietic stem cells. Nature *481*, 457–462.

Doan, P.L., Russell, J.L., Himburg, H.A., Helms, K., Harris, J.R., Lucas, J., Holshausen, K.C., Meadows, S.K., Daher, P., Jeffords, L.B., et al. (2013a). Tie2 + Bone Marrow Endothelial Cells Regulate Hematopoietic Stem Cell Regeneration Following Radiation Injury. Stem Cells *31*, 327–337.

Doan, P.L., Himburg, H.A., Helms, K., Russell, J.L., Fixsen, E., Quarmyne, M., Harris, J.R., Deoliviera, D., Sullivan, J.M., Chao, N.J., et al. (2013b). Epidermal growth factor regulates hematopoietic regeneration after radiation injury. Nat. Med. *19*, 295–304.

Dominici, M., Le Blanc, K., Mueller, I., Slaper-Cortenbach, I., Marini, F.C., Krause, D.S., Deans, R.J., Keating, A., Prockop, D.J., and Horwitz, E.M. (2006). Minimal criteria for defining multipotent mesenchymal stromal cells. The International Society for Cellular Therapy position statement. Cytotherapy *8*, 315–317.

Dominici, M., Rasini, V., Bussolari, R., Chen, X., Hofmann, T.J., Spano, C., Bernabei, D., Veronesi, E., Bertoni, F., Paolucci, P., et al. (2009). Restoration and reversible expansion of the osteoblastic hematopoietic stem cell niche after marrow radioablation. Blood *114*, 2333–2343.

Draenert, K., and Draenert, Y. (1980). The vascular system of bone marrow. Scan. Electron Microsc. 113–122.

Friedenstein, A.J., Chailakhyan, R.K., Latsinik, N. V, Panasyuk, A.F., and Keiliss-Borok, I. V (1974). Stromal cells responsible for transferring the microenvironment of the hemopoietic tissues. Cloning in vitro and retransplantation in vivo. Transplantation *17*, 331–340.

Georgiou, K.R., Scherer, M.A., Fan, C.-M., Cool, J.C., King, T.J., Foster, B.K., and Xian, C.J. (2012). Methotrexate chemotherapy reduces osteogenesis but increases adipogenic potential in the bone marrow. J. Cell. Physiol. *227*, 909–918.

Gerber, H.P., Vu, T.H., Ryan, A.M., Kowalski, J., Werb, Z., and Ferrara, N. (1999). VEGF couples hypertrophic cartilage remodeling, ossification and angiogenesis during endochondral bone formation. Nat. Med. *5*, 623–628.

Goncalves, K.A., Silberstein, L., Li, S., Severe, N., Hu, M.G., Yang, H., Scadden, D.T., and Hu, G. fu (2016). Angiogenin Promotes Hematopoietic Regeneration by Dichotomously Regulating Quiescence of Stem and Progenitor Cells. Cell *166*, 894–906.

Greenbaum, A., Hsu, Y.M.S., Day, R.B., Schuettpelz, L.G., Christopher, M.J., Borgerding, J.N., Nagasawa, T., and Link, D.C. (2013). CXCL12 in early mesenchymal progenitors is required for haematopoietic stem-cell maintenance. Nature *495*, 227–230.

Guo, P., Poulos, M.G., Palikuqi, B., Badwe, C.R., Lis, R., Kunar, B., Ding, B.-S., Rabbany, S.Y., Shido, K., Butler, J.M., et al. (2017). Endothelial jagged-2 sustains hematopoietic stem and progenitor reconstitution after myelosuppression. J. Clin. Invest. *127*, 4242–4256.

Gur-Cohen, S., Itkin, T., Chakrabarty, S., Graf, C., Kollet, O., Ludin, A., Golan, K., Kalinkovich, A., Ledergor, G., Wong, E., et al. (2015). PAR1 signaling regulates the retention and recruitment of EPCR-expressing bone marrow hematopoietic stem cells. Nat. Med. *21*, 1307–1317.

Haas, S., Trumpp, A., and Milsom, M.D. (2018). Causes and Consequences of Hematopoietic Stem Cell Heterogeneity. Cell Stem Cell *22*, 627–638.

Hérault, A., Binnewies, M., Leong, S., Calero-Nieto, F.J., Zhang, S.Y., Kang, Y.-A., Wang, X., Pietras, E.M., Chu, S.H., Barry-Holson, K., et al. (2017). Myeloid progenitor cluster formation drives emergency and leukaemic myelopoiesis. Nature *544*, 53–58.

Himburg, H.A., Muramoto, G.G., Daher, P., Meadows, S.K., Russell, J.L., Doan, P., Chi, J.T., Salter, A.B., Lento, W.E., Reya, T., et al. (2010). Pleiotrophin regulates the expansion and regeneration of hematopoietic stem cells. Nat. Med. *16*, 475–482.

Himburg, H.A., Yan, X., Doan, P.L., Quarmyne, M., Micewicz, E., McBride, W., Chao, N.J., Slamon, D.J., and Chute, J.P. (2014). Pleiotrophin mediates hematopoietic regeneration via activation of RAS. J. Clin. Invest. *124*, 4753–4758.

Himburg, H.A., Doan, P.L., Quarmyne, M., Yan, X., Sasine, J., Zhao, L., Hancock, G. V., Kan, J., Pohl, K.A., Tran, E., et al. (2017). Dickkopf-1 promotes hematopoietic regeneration via direct and niche-mediated mechanisms. Nat. Med. *23*, 91–99.

Himburg, H.A., Termini, C.M., Schlussel, L., Kan, J., Li, M., Zhao, L., Fang, T., Sasine, J.P., Chang, V.Y., and Chute, J.P. (2018). Distinct Bone Marrow Sources of Pleiotrophin Control Hematopoietic Stem Cell Maintenance and Regeneration. Cell Stem Cell *23*, 370–381.e5.

Hirata, Y., Furuhashi, K., Ishii, H., Li, H.W., Pinho, S., Ding, L., Robson, S.C., Frenette, P.S., and Fujisaki, J. (2018). CD150highBone Marrow Tregs Maintain Hematopoietic Stem Cell Quiescence and Immune Privilege via Adenosine. Cell Stem Cell *22*, 445–453.e5.

Hooper, A.T., Butler, J.M., Nolan, D.J., Kranz, A., Iida, K., Kobayashi, M., Kopp, H.-G., Shido, K., Petit, I., Yanger, K., et al. (2009). Engraftment and Reconstitution of Hematopoiesis Is Dependent on VEGFR2-Mediated Regeneration of Sinusoidal Endothelial Cells. Cell Stem Cell *4*, 263–274.

Hur, J., Choi, J. Il, Lee, H., Nham, P., Kim, T.W., Chae, C.W., Yun, J.Y., Kang, J.A., Kang, J., Lee, S.E., et al. (2016). CD82/KAI1 Maintains the Dormancy of Long-Term Hematopoietic Stem Cells through Interaction with DARC-Expressing Macrophages. Cell Stem Cell *18*, 508–521.

Isern, J., García-García, A., Martín, A.M., Arranz, L., Martín-Pérez, D., Torroja, C., Sánchez-Cabo, F., and Méndez-Ferrer, S. (2014). The neural crest is a source of mesenchymal stem cells with specialized hematopoietic stem cell niche function. Elife *3*, 1–28.

Itkin, T., Gur-Cohen, S., Spencer, J.A., Schajnovitz, A., Ramasamy, S.K., Kusumbe, A.P., Ledergor, G., Jung, Y., Milo, I., Poulos, M.G., et al. (2016). Distinct bone marrow blood vessels differentially regulate haematopoiesis. Nature *532*, 323–328.

Jiang, Y., Bonig, H., Ulyanova, T., Chang, K., and Papayannopoulou, T. (2009). On the adaptation of endosteal stem cell niche function in response to stress. Blood *114*, 3773–3782.

Kauts, M.L., Vink, C.S., and Dzierzak, E. (2016). Hematopoietic (stem) cell development — how divergent are the roads taken? FEBS Lett. *590*, 3975–3986.

Kiel, M.J., Yilmaz, Ö.H., Iwashita, T., Yilmaz, O.H., Terhorst, C., and Morrison, S.J. (2005). SLAM family receptors distinguish hematopoietic stem and progenitor cells and reveal endothelial niches for stem cells. Cell *121*, 1109–1121.

Kim, J., Kim, W., Le, H.T., Moon, U.J., Tran, V.G., Kim, H.J., Jung, S., Nguyen, Q.-T., Kim, B.-S., Jun, J.-B., et al. (2014). IL-33–Induced Hematopoietic Stem and Progenitor Cell Mobilization Depends upon CCR2. J. Immunol. *193*, 3792–3802.

Kimura, Y., Ding, B., Imai, N., Nolan, D.J., Butler, J.M., and Rafii, S. (2011). c-Kit-Mediated Functional Positioning of Stem Cells to Their Niches Is Essential for Maintenance and Regeneration of Adult Hematopoiesis. PLoS One *6*, e26918.

Komada, Y., Yamane, T., Kadota, D., Isono, K., Takakura, N., Hayashi, S.-I., and Yamazaki, H. (2012). Origins and Properties of Dental, Thymic, and Bone Marrow Mesenchymal Cells and Their Stem Cells. PLoS One *7*, e46436.

Kopp, H.G., Avecilla, S.T., Hooper, A.T., Shmelkov, S. V., Ramos, C.A., Zhang, F., and Rafii, S. (2005). Tie2 activation contributes to hemangiogenic regeneration after myelosuppression. Blood *106*, 505–513.

Kunisaki, Y., Bruns, I., Scheiermann, C., Ahmed, J., Pinho, S., Zhang, D., Mizoguchi, T., Wei, Q., Lucas, D., Ito, K., et al. (2013). Arteriolar niches maintain haematopoietic stem cell quiescence. Nature *502*, 637–643.

Kusumbe, A.P., Ramasamy, S.K., and Adams, R.H. (2014). Coupling of angiogenesis and osteogenesis by a specific vessel subtype in bone. Nature *507*, 323–328.

Kusumbe, A.P., Ramasamy, S.K., Itkin, T., Mäe, M.A., Langen, U.H., Betsholtz, C., Lapidot, T., and Adams, R.H. (2016). Age-dependent modulation of vascular niches for haematopoietic stem cells. Nature *532*, 380–384.

Lerner, C., and Harrison, D.E. (1990). 5-Fluorouracil spares hemopoietic stem cells responsible for long-term repopulation. Exp. Hematol. *18*, 114–118.

Liebner, S., Cattelino, A., Gallini, R., Rudini, N., Iurlaro, M., Piccolo, S., and Dejana, E. (2004). B-Catenin Is Required for Endothelial-Mesenchymal Transformation During Heart Cushion Development in the Mouse. J. Cell Biol. *166*, 359–367.

Lucas, D., Scheiermann, C., Chow, A., Kunisaki, Y., Bruns, I., Barrick, C., Tessarollo, L., and Frenette, P.S. (2013). Chemotherapy-induced bone marrow nerve injury impairs hematopoietic regeneration. Nat. Med. *19*, 695–703.

Mauch, P., Constine, L., Greenberger, J., Knospe, W., Sullivan, J., Liesveld, J.L., and Deeg, H.J. (1995). Hematopoietic stem cell compartment: Acute and late effects of radiation therapy and chemotherapy. Int. J. Radiat. Oncol. *31*, 1319–1339.

Méndez-Ferrer, S., Lucas, D., Battista, M., and Frenette, P.S. (2008). Haematopoietic stem cell release is regulated by circadian oscillations. Nature *452*, 442–447.

Méndez-Ferrer, S., Michurina, T. V, Ferraro, F., Mazloom, A.R., MacArthur, B.D., Lira, S. a, Scadden, D.T., Ma□ayan, A., Enikolopov, G.N., and Frenette, P.S. (2010). Mesenchymal and haematopoietic stem cells form a unique bone marrow niche. Nature *466*, 829–834.

Mitroulis, I., Chen, L.-S., Singh, R.P., Kourtzelis, I., Economopoulou, M., Kajikawa, T., Troullinaki, M., Ziogas, A., Ruppova, K., Hosur, K., et al. (2017). Secreted protein Del-1 regulates myelopoiesis in the hematopoietic stem cell niche. J. Clin. Invest. *127*, 3624–3639.

Mizuhashi, K., Ono, W., Matsushita, Y., Sakagami, N., Takahashi, A., Saunders, T.L., Nagasawa, T., Kronenberg, H.M., and Ono, N. (2018). Resting zone of the growth plate houses a unique class of skeletal stem cells. Nature *563*, 254–258.

Mohrin, M., Bourke, E., Alexander, D., Warr, M.R., Barry-Holson, K., Le Beau, M.M., Morrison, C.G., and Passegué, E. (2010). Hematopoietic stem cell quiescence promotes error-prone DNA repair and mutagenesis. Cell Stem Cell *7*, 174–185.

Morikawa, S., Mabuchi, Y., Niibe, K., Suzuki, S., Nagoshi, N., Sunabori, T., Shimmura, S., Nagai, Y., Nakagawa, T., Okano, H., et al. (2009). Development of mesenchymal stem cells partially originate from the neural crest. Biochem. Biophys. Res. Commun. *379*, 1114–1119.

Naveiras, O., Nardi, V., Wenzel, P.L., Hauschka, P. V., Fahey, F., and Daley, G.Q. (2009). Bone-marrow adipocytes as negative regulators of the haematopoietic microenvironment. Nature *460*, 259–263.

Niibe, K., Morikawa, S., Mabuchi, Y., Araki, D., Nakagawa, T., Okano, H., and Matsuzaki, Y. (2011). Mesp1+ early paraxial mesodermal cells supply initial bone marrow mesenchymal stem cells capable of differentiating into neural crest lineage cells. Inflamm. Regen. *31*, 116–124.

Nombela-Arrieta, C., and Manz, M.G. (2017). Quantification and three-dimensional microanatomical organization of the bone marrow. Blood Adv. *1*, 407–416.

Omatsu, Y., Sugiyama, T., Kohara, H., Kondoh, G., Fujii, N., Kohno, K., and Nagasawa, T. (2010). The Essential Functions of Adipo-osteogenic Progenitors as the Hematopoietic Stem and Progenitor Cell Niche. Immunity *33*, 387–399.

Ono, N., Ono, W., Mizoguchi, T., Nagasawa, T., Frenette, P.S., and Kronenberg, H.M. (2014a). Vasculature-associated cells expressing nestin in developing bones encompass early cells in the osteoblast and endothelial lineage. Dev. Cell *29*, 330–339.

Ono, N., Ono, W., Nagasawa, T., and Kronenberg, H.M. (2014b). A subset of chondrogenic cells provides early mesenchymal progenitors in growing bones. Nat. Cell Biol. *16*, 1157–1167.

Passegue, E., Jamieson, C.H.M., Ailles, L.E., and Weissman, I.L. (2003). Normal and leukemic hematopoiesis: Are leukemias a stem cell disorder or a reacquisition of stem cell characteristics? Proc. Natl. Acad. Sci. *100*, 11842–11849.

Ponomaryov, T., Peled, A., Petit, I., Taichman, R.S., Habler, L., Sandbank, J., Arenzana-Seisdedos, F., Magerus, A., Caruz, A., Fujii, N., et al. (2000). Induction of the chemokine stromal-derived factor-1 following DNA damage improves human stem cell function. J. Clin. Invest. *106*, 1331–1339.

Poulos, M.G., Guo, P., Kofler, N.M., Pinho, S., Gutkin, M.C., Tikhonova, A., Aifantis, I., Frenette, P.S., Kitajewski, J., Rafii, S., et al. (2013). Endothelial Jagged-1 Is Necessary for Homeostatic and Regenerative Hematopoiesis. Cell Rep. *4*, 1022–1034.

Pu, W., Hu, S., He, L., Zhang, L., Zhang, H., Liu, Q., Huang, X., Zhou, B., Lui, K.O., Nie, Y., et al. (2016). Endocardium Contributes to Cardiac Fat. Circ. Res. *118*, 254–265.

Ramasamy, S.K. (2017). Structure and Functions of Blood Vessels and Vascular Niches in Bone. Stem Cells Int. *2017*.

Ramasamy, S.K., Kusumbe, A.P., Wang, L., and Adams, R.H. (2014). Endothelial Notch activity promotes angiogenesis and osteogenesis in bone. Nature *507*, 376–380.

Robey, P.G. (2018). Skeletal Stem Cells/Bone Marrow Stromal Cells. In Genetics of Bone Biology and Skeletal Disease, (Elsevier), pp. 241–260.

Rosselló Castillo, C., Lempereur, A., Souyri, M., Speck, N.A., Jaffredo, T., Piwarzyk, E., Bollérot, K., Canto, P.-Y., Drevon, C., Richard, C., et al. (2013). Endothelio-Mesenchymal Interaction Controls runx1 Expression and Modulates the notch Pathway to Initiate Aortic Hematopoiesis. Dev. Cell *24*, 600–611.

Sacchetti, B., Funari, A., Michienzi, S., Di Cesare, S., Piersanti, S., Saggio, I., Tagliafico, E., Ferrari, S., Robey, P.G., Riminucci, M., et al. (2007). Self-renewing osteoprogenitors in bone marrow sinusoids can organize a hematopoietic microenvironment. Cell *131*, 324–336.

Sasine, J.P., Yeo, K.T., and Chute, J.P. (2017). Concise Review: Paracrine Functions of Vascular Niche Cells in Regulating Hematopoietic Stem Cell Fate. Stem Cells Transl. Med. *6*, 482–489.

Schürch, C.M., Riether, C., and Ochsenbein, A.F. (2014). Cytotoxic CD8+ T cells stimulate hematopoietic progenitors by promoting cytokine release from bone marrow mesenchymal stromal cells. Cell Stem Cell *14*, 460–472.

Shirota, T., and Tavassoli, M. (1991). Cyclophosphamide-induced alterations of bone marrow endothelium: implications in homing of marrow cells after transplantation. Exp. Hematol. *19*, 369–373.

Silberstein, L., Goncalves, K.A., Kharchenko, P. V., Turcotte, R., Kfoury, Y., Mercier, F., Baryawno, N., Severe, N., Bachand, J., Spencer, J.A., et al. (2016). Proximity-Based Differential Single-Cell Analysis of the Niche to Identify Stem/Progenitor Cell Regulators. Cell Stem Cell *19*, 530–543.

Spencer, J.A., Ferraro, F., Roussakis, E., Klein, A., Wu, J., Runnels, J.M., Zaher, W., Mortensen, L.J., Alt, C., Turcotte, R., et al. (2014). Direct measurement of local oxygen concentration in the bone marrow of live animals. Nature *508*, 269–273.

Sugimura, R., He, X.C., Venkatraman, A., Arai, F., Box, A., Semerad, C., Haug, J.S., Peng, L., Zhong, X.-B., Suda, T., et al. (2012). Noncanonical Wnt signaling maintains hematopoietic stem cells in the niche. Cell *150*, 351–365.

Sugiyama, T., Kohara, H., Noda, M., and Nagasawa, T. (2006). Maintenance of the Hematopoietic Stem Cell Pool by CXCL12-CXCR4 Chemokine Signaling in Bone Marrow Stromal Cell Niches. Immunity *25*, 977–988.

Takashima, Y., Era, T., Nakao, K., Kondo, S., Kasuga, M., Smith, A.G., and Nishikawa, S.I. (2007). Neuroepithelial Cells Supply an Initial Transient Wave of MSC Differentiation. Cell *129*, 1377–1388.

Tormin, A., Li, O., Brune, J.C., Walsh, S., Schutz, B., Ehinger, M., Ditzel, N., Kassem, M., and Scheding, S. (2011). CD146 expression on primary nonhematopoietic bone marrow stem cells is correlated with in situ localization. Blood *117*, 5067–5077.

Tzeng, Y.-S., Li, H., Kang, Y.-L., Chen, W.-C., Cheng, W.-C., and Lai, D.-M. (2011). Loss of Cxcl12/Sdf-1 in adult mice decreases the quiescent state of hematopoietic stem/progenitor cells and alters the pattern of hematopoietic regeneration after myelosuppression. Blood *117*, 429–439.

Visnjic, D., Kalajzic, Z., Rowe, D.W., Katavic, V., Lorenzo, J., and Aguila, H.L. (2004). Hematopoiesis is severely altered in mice with an induced osteoblast deficiency. Blood *103*, 3258–3264.

Williams, D.E., Eisenman, J., Baird, A., Rauch, C., Van Ness, K., March, C.J., Park, L.S., Martin, U., Mochizukl, D.Y., Boswell, H.S., et al. (1990). Identification of a ligand for the c-kit proto-oncogene. Cell *63*, 167–174.

Wilson, A., Laurenti, E., Oser, G., van der Wath, R.C., Blanco-Bose, W., Jaworski, M., Offner, S., Dunant, C.F., Eshkind, L., Bockamp, E., et al. (2008). Hematopoietic Stem Cells Reversibly Switch from Dormancy to Self-Renewal during Homeostasis and Repair. Cell *135*, 1118–1129.

Winkler, I.G., Barbier, V., Nowlan, B., Jacobsen, R.N., Forristal, C.E., Patton, J.T., Magnani, J.L., and Lévesque, J.-P. (2012). Vascular niche E-selectin regulates hematopoietic stem cell dormancy, self renewal and chemoresistance. Nat. Med. *18*, 1651–1657.

Worthley, D.L., Churchill, M., Compton, J.T., Tailor, Y., Rao, M., Si, Y., Levin, D., Schwartz, M.G., Uygur, A., Hayakawa, Y., et al. (2015). Gremlin 1 identifies a skeletal stem cell with bone, cartilage, and reticular stromal potential. Cell *160*, 269–284.

Wylie-Sears, J., Aikawa, E., Levine, R.A., Yang, J.H., and Bischoff, J. (2011). Mitral valve endothelial cells with osteogenic differentiation potential. Arterioscler. Thromb. Vasc. Biol. *31*, 598–607.

Xu, C., Gao, X., Wei, Q., Nakahara, F., Zimmerman, S.E., Mar, J., and Frenette, P.S. (2018). Stem cell factor is selectively secreted by arterial endothelial cells in bone marrow. Nat. Commun. *9*, 1–13.

Yamazaki, S., Ema, H., Karlsson, G., Yamaguchi, T., Miyoshi, H., Shioda, S., Taketo, M.M., Karlsson, S., Iwama, A., and Nakauchi, H. (2011). Nonmyelinating Schwann cells maintain hematopoietic stem cell hibernation in the bone marrow niche. Cell *147*, 1146–1158.

Yokomizo, T., and Dzierzak, E. (2010). Three-dimensional cartography of hematopoietic clusters in the vasculature of whole mouse embryos. Development *137*, 3651–3661.

Zhang, J., Niu, C., Ye, L., Huang, H., He, X., Tong, W.-G., Ross, J., Haug, J., Johnson, T., Feng, J.Q., et al. (2003). Identification of the haematopoietic stem cell niche and control of the niche size. Nature *425*, 836–841.

Zhao, M., Perry, J.M., Marshall, H., Venkatraman, A., Qian, P., He, X.C., Ahamed, J., and Li, L. (2014). Megakaryocytes maintain homeostatic quiescence and promote post-injury regeneration of hematopoietic stem cells. Nat. Med. *20*, 1321–1326.

Zheng, B., Cao, B., Crisan, M., Sun, B., Li, G., Logar, A., Yap, S., Pollett, J.B., Drowley, L., Cassino, T., et al. (2007). Prospective identification of myogenic endothelial cells in human skeletal muscle. Nat. Biotechnol. *25*, 1025–1034.

Zhou, B.O., Yue, R., Murphy, M.M., Peyer, J.G., and Morrison, S.J. (2014). Leptin-receptor-expressing mesenchymal stromal cells represent the main source of bone formed by adult bone marrow. Cell Stem Cell *15*, 154–168.

Zhou, B.O., Yu, H., Yue, R., Zhao, Z., Rios, J.J., Naveiras, O., and Morrison, S.J. (2017). Bone marrow adipocytes promote the regeneration of stem cells and haematopoiesis by secreting SCF. Nat. Cell Biol. *19*, 891–903.

Zhu, J., Garrett, R., Jung, Y., Zhang, Y., Kim, N., Wang, J., Joe, G.J., Hexner, E., Choi, Y., Taichman, R.S., et al. (2007). Osteoblasts support B-lymphocyte commitment and differentiation from hematopoietic stem cells. Blood *109*, 3706–3712.

2

CHARACTERIZATION OF ENDOTHELIAL CELLS ASSOCIATED WITH HEMATOPOIETIC NICHE FORMATION IN HUMANS IDENTIFIES IL-33 AS AN ANABOLIC FACTOR

Keane Jared Guillaume Kenswil[1], Adrian Jaramillo Mantilla[1], Zhen Ping[1], Si Chen[1], Remco Michiel Hoogenboezem[1], Maria Athina Mylona[1], Maria Niken Adisty[1], Eric Moniqué Johannes Bindels[1], Pieter Koen Bos[2], Hans Stoop[3], King Hong Lam[3], Bram van der Eerden[4], Tom Cupedo[1], Marc Hermanus Gerardus Petrus Raaijmakers[1,5,*]

[1]Department of Hematology, Erasmus MC Cancer Institute, Rotterdam 3015CN, The Netherlands
[2]Department of Orthopaedics, Erasmus MC, Rotterdam 3015CN, The Netherlands
[3]Department of Pathology, Erasmus MC, Rotterdam 3015CN, The Netherlands
[4]Department of Internal Medicine, Laboratory for Calcium and Bone Metabolism, Rotterdam, The Netherlands.
[5]Lead Contact: m.h.g.raaijmakers@erasmusmc.nl
*Correspondence: m.h.g.raaijmakers@erasmusmc.nl

Cell Reports 2018

SUMMARY

Bone marrow formation requires an orchestrated interplay between osteogenesis, angiogenesis and hematopoiesis that is thought to be mediated by endothelial cells. The nature of the endothelial cells and the molecular mechanisms underlying these events remain unclear in humans. Here, we identify a subset of endoglin-expressing, endothelial cells enriched in human bone marrow during fetal ontogeny and upon regeneration after chemotherapeutic injury. Comprehensive transcriptional characterization by massive parallel RNA sequencing of these cells reveals a phenotypic and molecular similarity to murine H endothelium, and activation of angiocrine factors implicated in hematopoiesis, osteogenesis and angiogenesis. IL-33 was significantly overexpressed in these endothelial cells and promoted the expansion of distinct subsets of hematopoietic precursor cells, endothelial cells, as well as osteogenic differentiation. The identification and molecular characterization of these human regeneration-associated endothelial cells is thus anticipated to instruct the discovery of angiocrine factors driving bone marrow formation and recovery after injury.

KEYWORDS

Endothelial, bone marrow, niche, regeneration, development, hematopoietic stem/progenitor cell, bone formation, interleukin-33

INTRODUCTION

Endothelial cells (ECs) govern tissue development and regeneration by signaling molecules on their cell surface and the release of factors such as cytokines and extracellular matrix proteins. This angiocrine function of the endothelium drives tissue development and regeneration in multiple organs.

In the hematopoietic system, studies in mice have revealed pivotal contributions of ECs to the formation and regeneration of bone and bone marrow (BM) (Hooper et al., 2009; Ramasamy et al., 2016). Coordinated activation of osteogenesis, angiogenesis and hematopoiesis is required for BM regeneration after tissue injury (Rafii et al., 2016; Ramasamy et al., 2015) induced by irradiation or chemotherapy. ECs support the proper regeneration of the hematopoietic system following myeloablation (Butler et al., 2010; Hooper et al., 2009; Kobayashi et al., 2010). Engraftment and repopulation of hematopoietic stem and progenitor cells (HSPCs) in mice is dependent on regeneration of sinusoid ECs which are vulnerable to toxic injury (Hooper et al., 2009). Sinusoid regeneration is mediated through vascular endothelial growth factor receptor 2 (VEGFR2) signaling, blockage of which resulted in delayed reconstitution of peripheral blood values in irradiated mice (Hooper et al., 2009).

ECs do not seem to be created equally in their ability to drive or contribute to bone and hematopoietic development and regeneration. Recent studies in mice have identified a specialized endothelial subset that controls HSPC number in addition to coupling angiogenesis and osteogenesis (Kusumbe et al., 2016, 2014; Ramasamy et al., 2014). This endothelial subtype, dubbed type H endothelium for its high expression of endomucin and CD31, is enriched in the bone metaphysis at the endosteal surface where it is adjacent to osteoprogenitor cells and gives rise to sinusoidal endothelial vessels. Importantly, insight into the molecular programs underlying the capacity of this endothelial subtype to drive angiogenesis and osteogenesis enabled its pharmacologic manipulation in mice resulting in increased bone formation (Kusumbe et al., 2014; Ramasamy et al., 2015).

Taken together, various studies indicate that specified EC-derived signals can orchestrate complex multicellular network interactions in the mammalian marrow driving bone formation and regeneration under stress conditions. These findings in murine models open the perspective of EC-instructed strategies to regenerate bone and marrow in humans, both in degenerative conditions as well as after injury such as chemotherapy and irradiation. Translation of these important findings to human regenerative medicine, however, will be critically dependent on our ability to identify and interrogate molecularly equivalent human ECs driving ontogeny and regeneration.

Here, we describe the identification of a human EC subtype that is strongly associated with human fetal BM development and regeneration after chemotherapeutic injury. This EC displays striking immunophenotypic and molecular commonalities with type H endothelium

in mice, including transcriptional activation of programs and angiocrine factors previously related to BM recovery in mice. Interleukin 33 (IL-33 is) identified as a putative regenerative factor facilitating hematopoietic expansion and bone mineralization *ex vivo*, thus supporting the notion that the transcriptome of this human EC may serve as an important resource instructing discovery as well as validating the relevance of findings in murine models to human regenerative medicine.

RESULTS

Identification of endoglin (CD105)-expressing ECs associated with bone marrow regeneration after chemotherapeutic injury

To identify niche cells potentially implicated in regeneration of the hematopoietic system in humans, we interrogated the composition of the hematopoietic niche upon recovery after chemotherapeutic injury. Chemotherapeutic exposure causes damage to endothelial, hematopoietic and osteolineage cells within the BM (Hooper et al., 2009; Kopp et al., 2009; Lerner and Harrison, 1990; Xian et al., 2006) resulting in a prolonged neutropenia associated with considerable morbidity and mortality in humans. Flow-cytometric assessment of the niche ($7AAD^-CD45^-CD235a^-$, Figure 1A) composition in the regenerating BM of acute myeloid leukemia (AML) patients (see 'experimental procedures') revealed an unaltered frequency of ECs ($CD31^+CD9^+$) (Barreiro et al., 2005) in comparison to marrow under homeostatic conditions (healthy donors) (22.1% ± 2.24 vs 31.57% ± 9.66; p=0.15 by unpaired student t-test) (Figure 1A, B). To identify putative immuno-markers of EC subtypes emerging during regeneration, we performed massive parallel sequencing (RNAseq) of the fluorescence-activated cell sorting (FACS)-purified endothelial compartment ($CD31^+CD9^+$) (Figure 1A). 903 transcripts were found to be significantly differentially expressed in ECs in the regenerative marrow in comparison to ECs from normal, steady-state, marrow (GLM LRT Edge R; FDR <0.05). The top 200 overexpressed transcripts contained 16 genes encoding for cluster of differentiation (CD) molecules, among which CD105 (*endoglin*) (Table S1), a co-receptor for transforming growth factor β (TGFβ) promoting angiogenesis (Cheifetz et al., 1992; Duff et al., 2003) (Miller et al., 1999) and previously associated with tissue injury (Wang et al., 1995). CD105 protein levels, assessed by FACS analysis (Figure 1C), identified a distinct subset of CD105-expressing ECs, strongly enriched in the regenerative marrow compared to normal BM (10.81% ± 2.14 vs 0.48% ± 0.24 of $CD31^+CD9^+$; p=0.043) (Figure 1D). The presence of this endoglin-expressing subset was temporally restricted, as it was (virtually) absent in AML patients at diagnosis (0% ± 0 of $CD31^+CD9^+$) or after full recovery of peripheral blood values (in complete remission) (1.27% ± 0.66 of $CD31^+CD9^+$) (Figure 1E).

Endoglin-expressing ECs are enriched in the mouse bone marrow after chemotherapeutic myeloablation

To confirm our observation that the CD105 expressing subset of endothelial cells is enriched during bone marrow regeneration and establish a broader relevance for mammalian biology, we next translated our observations to an experimental setting in which we exposed C57BL/6 wild-type mice to a myeloablative dose of the chemotherapeutic agent 5-fluorouracil (5FU) or PBS (vehicle control). The endoglin-expressing subset constituted a rare subpopulation of endothelial ($CD31^+CD9^+$) cells in the steady-state adult BM niche (0.05% ± 0.02 of $CD45^-Ter119^-$ cells) and in the collagenased bone niche (0.42% ± 0.12 of $CD45^-Ter119^-$ cells) (Figure

2A, B and S1A, B). This fraction increased significantly after administration of 5FU in the BM (0.65% ± 0.15 of CD45$^-$Ter119$^-$ cells, fold-change (FC) increase of 13.6 ± 3.2, p=0.026) and collagenased bone (8.18% ± 1.43 of CD45$^-$Ter119$^-$ cells, FC increase of 19.6 ± 3.4, p=0.007) (Figure 2A, B and S1A, B), confirming a relative increase of this specific subset in the regenerative phase after myeloablation. Of note, the absolute number of CD31$^+$CD105$^+$ ECs in the bone marrow did not increase after exposure to 5FU (Figure 2C), suggesting that selection of these cells under chemotherapeutic pressure (rather than absolute expansion) may be implicated.

Endoglin-expressing ECs are enriched in the human bone marrow during fetal development

The temporally restricted enrichment of CD105-expressing ECs during recovery after chemotherapeutic injury suggests that this cell type could potentially be implicated in regeneration and hematopoietic niche formation. To corroborate this notion, we sought to define other conditions in human biology where angiogenesis, osteogenesis and hematopoiesis are synergistically activated. In human fetal bone development, hematopoiesis shifts from the fetal liver to the bones starting from week 10 after gestation. During this process angiogenesis, osteogenesis and hematopoiesis are tightly coupled to allow coordinated bone and hematopoietic development (Coşkun et al., 2014; Jagannathan-Bogdan and Zon, 2013; Medvinsky et al., 2011). Invasion of blood vessels into the mesenchymal condensate is crucial for the coordinated activity of chondrocytes, osteoblasts and each of these cell types stands in spatial and molecular interaction with ECs (Maes, 2013; Salazar et al., 2016).

Flow cytometric dissection of the endothelial composition of fetal bone marrow at gestational week 15-20 revealed a striking predominance of CD105-expressing cells within the endothelial compartment (62.8% ± 5.9 of CD31$^+$CD9$^+$) (Figure 3A, B). Massive parallel sequencing of these cells confirmed overexpression of genes encoding CD markers identified in the endothelial cells in regenerating bone marrow (Figure S2A), supporting the notion that the enrichment of these transcripts in ECs in the regenerative marrow is caused by overexpression in the subset of CD105$^+$ ECs.

The frequency of CD105-expressing ECs within the endothelial compartment was even higher when examining collagenased fetal bone fractions (average 82.65% ± 2.5 of CD31$^+$CD9$^+$) (Figure 3A, B), suggesting that this endothelial subpopulation might preferentially localize to the endosteal surface of fetal long bones. In line with this, CD105-expressing ECs were identified, albeit at considerably lower frequency, in collagenased bone fractions of human adult postnatal bone (average 25.9% ± 5.0 of CD31$^+$CD9$^+$) (Figure 3A,B).

To provide anatomical context for this CD31$^+$CD105$^+$ EC subset, we performed *in situ* immunohistochemistry and immunofluorescence on fetal femurs and core hip bone biopsies obtained from adults. CD31$^+$CD105$^+$ EC were observed in the trabecular bone area of the metaphysis of fetal femurs (Figure 3C and S3A, B) at a significant higher frequency than in the trabecular bone of adult bone marrow. The majority of vascular structures in both fetal and adult human bone were lined with CD31$^-$CD105$^+$ endothelial cells, previously shown to be sinusoid endothelial cells. CD31$^+$CD105$^-$ cells were present sporadically in adult bone.

Collectively, these findings identify a human endothelial subtype that is enriched in collagenased bone fractions, prevalent during human fetal bone development, declines in frequency upon aging and emerges, in a temporally restricted fashion, in the BM during regeneration after chemotherapeutic injury. Henceforward, we will refer to this EC type as 'human regeneration-associated EC' or hREC.

hRECs share immunophenotypic and molecular similarities with murine type H endothelium and express key regulators of angiogenesis and osteogenesis

Interestingly, similarities exist between hRECs and the recently described specialized endothelium coordinating osteo- and angiogenesis in mice, termed type H endothelium (Kusumbe et al., 2016, 2014; Ramasamy et al., 2014). These include the enrichment at the bone surface, reduced frequencies upon aging and an increase in frequency upon genotoxic stress, suggesting that hRECs may reflect human equivalents of mouse 'type H endothelium'. To further investigate this, differentially expressed transcripts in CD31$^+$CD9$^+$CD105$^+$ hRECs isolated from human fetal bone (in comparison to steady-state postnatal CD31$^+$CD9$^+$CD105$^-$ cells) were related to genes reported to be overexpressed in H-endothelium. This confirmed elevated expression of many transcripts previously reported to be enriched in type H endothelium, including genes encoding the signature markers CD31 (*PECAM1*) and mucin-like sialoglycoprotein endomucin (*EMCN*) (Figure 4A) and vessel guidance molecules (Ramasamy et al., 2014) (Figure 4B). Most of these genes were similarly enriched in the CD31$^+$CD9$^+$ fraction of regenerative BM (Figure 4A, B) (the limited number of CD105$^+$ precluded RNA-sequencing of this specific subset). In total, 3718 genes were differentially expressed (GLM LRT Edge R; FDR < 0.05) in fetal bone hRECs in comparison to steady-state postnatal BM ECs. Among the overexpressed genes were HSPC niche factors (Figure 4C) and known angiocrine anabolic regulators of osteogenesis and angiogenesis (Figure 4D), further suggesting that hREC might be involved in hematopoietic niche formation.

Next, transcriptional programs and signatures were interrogated in hRECs using gene set enrichment analysis (GSEA) (Subramanian et al., 2005). Activated Notch signaling and stabilization of HIF1a have been identified in H endothelium as key promotors of the formation of type H capillaries and release of osteogenic factors that enhance osteogenesis (Kusumbe et al., 2014; Ramasamy et al., 2014). In line with this, key NOTCH regulators such as Jagged-1, DLL4, NOTCH 1 and NOTCH4 (receptors of DLL4) were upregulated in fetal hRECs (Figure 4E), reflected in activation of downstream transcriptional NOTCH signaling, as demonstrated by GSEA (Figure 4F). Similarly, gene sets related to the HIF1a pathway were enriched in fetal hREC according to GSEA (Figure S2B). Other relevant molecular

signatures that were identified to be significantly enriched in hRECs include 'angiogenesis'- and 'stemness'- signatures, among which VEGF and WNT-signaling (Figure S2C). Together, the data indicate that hRECs share immunophenotypic and molecular commonalities with murine type H ECs and have a transcriptional wiring that may be congruent with the view that these cells are implicated in the coupling of hematopoiesis, osteogenesis and angiogenesis in regeneration.

Interleukin-33 is expressed by hRECs and promotes angiogenesis, osteogenesis and the expansion of hematopoietic precursor cells

We thus hypothesized that elucidation of the transcriptome of ECs related to hematopoietic niche formation might instruct the discovery of pathways or proteins facilitating niche formation. In particular, angiocrine factors may be identified that facilitate angiogenesis, osteogenesis and hematopoiesis. To provide proof of principle for this assumption, we focused our attention on genes encoding secreted factors that were both significantly enriched in fetal hRECs and regenerative BM ECs. In total 237 genes were significantly enriched, of which 34 are genes encoding known secreted factors with a strong correlation in levels of expression (Figure 5A). Of interest, the canonical receptors of many of these secreted proteins were overexpressed in fetal hRECs, (MMRN2-CLEC14A, BMP4-BMPR2, EFNA1-EPHA2/EPHA4/EPHA7, EDN1-EDNRB, SEMA3A-NRP1/NRP2/PLXNA2, ADM-RAMP2/CALCRL) (Figure S2D), suggesting the possibility of autocrine signaling.

In addition to secreted factors with a known role in regulating HSPC behavior, such as plasminogen activator (*PLAT*) (Ibrahim et al., 2014) and tissue factor pathway inhibitor (*TFPI*) (Khurana et al., 2013), we found significant overexpression of interleukin-33 (*IL33*) in hRECs (Figure 5A).

IL-33 is a pro-inflammatory cytokine and a chromatin-associated nuclear factor (Carriere et al., 2007). IL-33 protein expression in fetal hREC was confirmed using fluorescence microscopy (Figure 5B) and IL-33 was differentially overexpressed in murine $CD31^+CD105^+$ endothelial cells in comparison to their $CD105^-$ counterparts during regeneration (Figure 2D, E). The inability to propagate sorted hRECs *ex vivo* (data not shown), precluded the possibility to perform co-culture blocking experiments to assess the contribution of hREC-derived IL-33 to angiogenesis, hematopoiesis and osteogenesis. As an alternative strategy, we exposed relevant cell types to recombinant human IL-33 (rhIL-33).

Hematopoiesis

To test if IL-33 facilitates human hematopoiesis *in vitro*, we exposed cord blood (CB) $CD34^+$ HSPCs to rhIL-33 or vehicle control for a week in serum-free medium containing SCF. rhIL-33 expanded the total number of hematopoietic cells (total MNCs) (3.4-fold increase ± 0.29; $p<0.01$) with a concomitant expansion of hematopoietic progenitors cells (HPCs), specifically immunophenotypic multipotent progenitors (MPPs) (2.5-fold increase ± 0.43; $p<0.05$) and multilymphoid progenitors (MLPs) (2.7-fold increase ± 0.15; $p<0.01$) (Figure 5C, S4). Immunophenotypic HSC numbers were not affected by exposure to IL-33. Expansion of myeloid progenitor cells was confirmed in colony-forming assays (CFU-C) demonstrating an increase in CFU-GMs (2.27-fold increase ± 0.21; $p<0.05$) (Figure 5D).

Osteogenesis

Next, we interrogated a potential role of IL-33 in bone formation. In human fetal bone development (endochondral ossification), vascular invasion of chondrocytes coincides with expansion of osteoblasts and mineralization of the matrix (Charbord et al., 1996; Ramasamy et al., 2016). To test the role of IL-33 in this process, the effect of rhIL-33 on the osteogenic differentiation of human BM-derived stromal cells (BMDSCs) was assessed. Addition of rhIL-33 to osteogenic induction medium accelerated terminal differentiation of BMDSCs towards matrix-depositing osteoblasts as suggested by Alizarin red-staining (Figure 6A), indicating increased calcific matrix deposition. To confirm this finding, we performed colorimetric assessment of calcium deposition, demonstrating a striking 3.61-fold ± 0.63 ($p<0.02$) increase in calcium deposition of IL-33-exposed BMDSCs in comparison to BMDSCs cultured in osteogenic induction medium alone (Figure 6B). The proliferation of BMDSCs was not affected by rhIL-33 (Figure S5A, B), suggesting that IL-33 exerted its osteogenic effect by promoting osteoblastic differentiation or the secretion of matrix proteins by osteoblasts, rather than expanding primitive mesenchymal cells.

Angiogenesis

In line with earlier reports (Choi et al., 2009), we confirmed that IL-33 is an angiogenic factor. shRNA mediated-knockdown of IL-33 (Figure S5D, E) from HUVECs dramatically impaired their expansion in culture (Figure 6C), indicating that IL-33 promotes angiogenesis in an autocrine fashion.

IL-33 promotes expansion of hematopoietic precursor cells and alters the architecture of the bone marrow niche in mice

We next studied the *in vivo* relevance of these effects of IL-33 on distinct cellular components of the human bone marrow. Administration of recombinant murine IL-33 (rmIL-33) compared to PBS control resulted in expansion of immature (Lin^-) (Figure S6A) and primitive progenitor (LKS) hematopoietic cells, in particular the HPC-1 population (Figure 7A, B), earlier shown to contain restricted hematopoietic precursor cells with myeloid and lymphoid lineage potential (Oguro et al., 2013). Expansion of a myeloid progenitor population was confirmed with CFU-C assays (Figure S6B). Total BM cellularity, and $Lin^-Kit^+Sca1^-$ cell counts remained unchanged (Figure S6C). In addition, the number of granulocyte-macrophage progenitors (GMPs) and myeloid cells increased after IL-33 administration (Figure 7A, B, and Figure S6D, E), recapitulating the expansion of human hematopoietic, myeloid, precursors *in vitro*. Congruent with our findings in human hematopoietic cells, immunophenotypic HSCs were not numerically affected by IL-33 (Figure 7A, B). Interestingly, IL-33 also expanded significantly the population of $Lin^-Kit^-Sca1^+$ bone marrow cells, previously shown to contain

early lymphoid-committed precursors with T cell, B-cell and NK cell potential (Kumar et al., 2008) and innate lymphoid cells (Brickshawana et al., 2011). Hematopoietic changes were accompanied by a relative increase in $CD31^{+}CD105^{+}$ ECs as well as $Lin^{-}Ter119^{-}CD51^{+}Sca^{-}$ cells (earlier shown to contain lineage committed/osteoblastic cells) (Schepers et al., 2012), albeit not reaching statistical significance, within the niche compartment (Figure S7A, B).

Collectively, the *in vitro* and *in vivo* data indicate that IL-33 modulates distinct cellular components of the hematopoietic tissue and has the potential to facilitate angiogenesis, hematopoiesis and osteogenesis, supporting the view that elucidation of the transcriptome of hRECs may instruct the identification of modulators of these processes.

DISCUSSION

Injury to the hematopoietic system, caused by chemotherapy or irradiation, is a significant cause of morbidity and mortality in the treatment of malignant hematopoietic disease. Studies in mice have demonstrated a pivotal role of specific BM niche cells and secreted molecules in hematopoietic recovery. Translation of these findings to the clinic, however, is hampered, principally by insufficient understanding of the niche cells and molecular programs governing niche formation and hematopoietic recovery in humans. Here, by cellular dissection of the BM niche in humans during fetal development and regeneration after chemotherapeutic injury we reveal the existence of a specific EC type (hREC) associated with these conditions. hRECs share phenotypic and molecular similarities with specialized EC driving hematopoietic niche formation in mice, expressing critical regulators of hematopoiesis, osteogenesis and angiogenesis. The data comprises, to our knowledge, the first comprehensive molecular characterization of human ECs upon tissue regeneration after injury.

We identified the TGF-β1 receptor endoglin (CD105) as a marker of endothelium associated with BM (re)generation in fetal development and after chemotherapeutic injury. Endoglin-expressing ECs have earlier been associated with angiogenesis in tumors and inflammation (Kumar et al., 1996) and loss of endoglin results in defective angiogenesis in mice (Li et al., 1999), supporting the view that it mediates signals governing blood vessel formation. The data indicate that endoglin with concomitant CD31 expression marks a specific subset of angiogenic endothelial cells which is further supported by observations that endoglin expression is strongly elevated in ECs of small capillary-like vessels at tumor edges (Miller et al., 1999; Yoshitomi et al., 2008). Endoglin thus likely identifies a subset of endothelium during ontogeny and regeneration that marks an angiogenic subset, in line with observations in different settings.

This subset revealed remarkable molecular congruence with EC subsets identified in murine studies driving bone and BM regeneration after injury. ECs in mice support the regeneration of the hematopoietic system following injury such as myeloablation (Butler et al., 2010; Hooper et al., 2009; Kobayashi et al., 2010) and in recent years several markers of specified endothelial subsets exerting this function as well as the underlying mechanisms have been revealed. Interestingly, hREC share many characteristics with the ECs described in these studies, including expression of the cell surface proteins Tie2/TEK (Figure S2E) (Doan et al., 2013; Kopp et al., 2005), EMCN (Kusumbe et al., 2014; Ramasamy et al., 2014), Jagged1 and activation of specific signaling pathways, including NOTCH (Butler et al., 2010; Poulos et al., 2013). Also, hRECs express many molecules previously shown to regulate HSPC behaviour in mice such as *PLAT* (Ibrahim et al., 2014), *TFPI* (Khurana et al., 2013), E-selectin *(ESELE)* (Figure S2E) (Winkler et al., 2012), thrombomodulin *(TMBD)* (Figure S2E) (Gur-Cohen et al., 2015), tenascin C (*TNC)* (Figure S2E) (Nakamura-Ishizu et al., 2012).

In particular, hRECs displayed striking commonalities with H endothelium, a murine EC subtype that has recently been functionally implicated in EC-driven formation of the niche through activation of NOTCH and HIF1 signaling (Kusumbe et al., 2014; Ramasamy et al., 2014). Commonalities with the now identified hRECs include enrichment at the bone surface, reduction in frequency upon ageing, resistance to stress conditions, expression of markers typical for both arterial (Ephn2b, Nestin, Nrp1, Sox17, VEGFR2), and sinusoidal vessels (VEGFR3, EMCN) and activation of the NOTCH and HIF1 pathways driving regeneration.

Expression of CD105 was not addressed in the studies on H endothelium but our data in mice show that a rare population of endoglin expressing endothelial cells increases in frequency in the regenerative phase after chemotherapy, likely reflecting increased resistance to myeloablative stress. It is noteworthy that $CD105^+$ ECs associated with elevated HIF-1a expression have been described in the BM of mice upon regeneration following 5-FU treatment (Nombela-Arrieta et al., 2013) making it tempting to hypothesize that these represent similar or overlapping cell types.

Taken together, these immunophenotypic and molecular similarities between hRECs and murine endothelial subtypes implicated in hematopoietic niche formation point towards evolutionary conservation of these cells between mammalian species. They thus provide human relevance to findings in murine studies, supporting the notion that ECs are implicated in niche regeneration in humans.

Providing experimental support for this view is challenging by limitations inherent to the study of human cells as well as the inability to propagate highly purified hRECs *ex vivo*, precluding co-culture studies. As an alternative approach, we exploited elucidation of their transcriptome to identify candidate factors driving EC-driven formation of the hematopoietic niche and regeneration of HSPCs. We identified IL-33, a cytokine typically associated with innate immunity and inflammation (Cayrol and Girard, 2014) as a candidate factor. IL33 was overexpressed in human hRECs and expression was increased in murine $CD31^+CD105^+$ ECs upon exposure to 5FU. Hematopoietic niche regenerating properties of IL33 was demonstrated by its *ex vivo* capacity to facilitate hematopoiesis (increased numbers of HPCs), osteogenesis (accelerating terminal differentiation of BMDSCs towards matrix-depositing osteoblasts), and angiogenesis (expansion of HUVECs). The data follow recent reports demonstrating IL-33 to predominantly act as an “alarmin”, released by cells undergoing necrosis after tissue damage or active secretion (Kakkar et al., 2012; Lee et al., 2015) and playing anabolic roles in angiogenesis (Choi et al., 2009; Shan et al., 2016) and osteogenesis (Saleh et al., 2011). Our finding that human recombinant IL-33 increased the numbers of HPCs *ex vivo* seems congruent with recent observations in mice where administration of IL-33 promoted myelopoiesis (Kim et al., 2014). Of considerable interest, rhIL-33 in our experiments expanded both immunophenotypic MLPs and MPPs, in line with observations in experiments in mice where expansion of splenic lymphoid progenitors after IL-33 administration resulted in enhanced defense against opportunistic infection (Kim et al., 2014). Formal demonstration that secretion by a defined subset of ECs is required for the regenerative actions of IL-33 will have to await *in vivo* targeted deletion experiments, as it is currently challenging to maintain this particular subset of ECs *ex vivo* to enable co-culture experiments. The profound effect of IL33 knockdown on HUVEC proliferation and maintenance precluded use of this *ex vivo* system to address this question.

The combined findings point to a unique role of IL-33 in mammalian species facilitating the reconstitution of both hematopoietic lineages, which may be of considerable importance to prepare the hematopoietic system for extra-uterine environment in ontogeny but also for immune reconstitution after injury, e.g. hematopoietic stem cell transplantation characterized by long-term lymphocyte depletion and ensuing opportunistic infections.

The exact molecular mechanisms by which IL-33 exerts these effects (either direct or indirect) remain to be fully elucidated. IL-33 expression in HUVECs has been associated with a quiescent cellular state (Küchler et al., 2008) and, although we did not examine the cell cycle status of $CD31^+CD105^+$, IL-33 ^{high} hRECs, this might help explain the notion that they may be relatively resistant to chemotherapeutic myeloablation. We can speculate that quiescent $CD31^+CD105^+$, IL-33 ^{high} hRECs survive chemotherapy and are ‘activated’ to release IL-33 as an anabolic hematopoietic factor. In this context it is noteworthy that hRECs display transcriptional activation of DLL4 and the Notch pathway, earlier shown to be an important driver of IL-33 expression (Sundlisæter et al., 2012).

Regardless the underlying molecular mechanisms of IL-33 expression, the data support the notion that elucidation of the transcriptome of hRECs may instruct the identification of proteins and pathways driving niche formation after injury. It is conceivable that receptor-ligand interactions allows targeting of these cells to drive regeneration (as previously shown by pharmacologic modulation of NOTCH signaling in mice (Ramasamy et al., 2014). In this context, it is noteworthy that transcriptional profiling of fetal hRECs revealed overexpression of genes encoding secreted factors as well as their receptors suggesting potential relevance of autocrine signaling in the biology of hRECs. Alternatively, it will be worthwhile testing the ability of identified secreted factors to expand human HSPC *ex vivo*, either direct or in co-culture settings with mesenchymal elements.

Collectively, the identification of human ECs associated with hematopoietic niche formation and elucidation of their transcriptome is anticipated to provide a valuable resource for the regenerative community to relate findings in animal models to human biology and to instruct *in vivo* and *ex vivo* approaches to foster EC-driven regeneration of the hematopoietic system after injury.

Figure 1

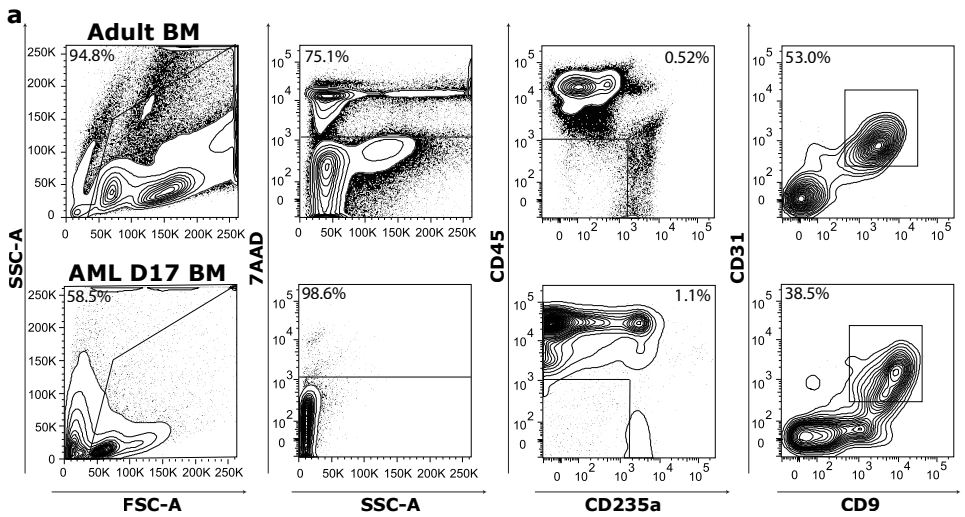

Figure 1. Identification of CD105 (endoglin)-expressing endothelial cells associated with bone marrow regeneration after chemotherapeutic injury

Bone marrow (BM) obtained by aspirates upon recovery after chemotherapeutic injury (AML D17) was compared to normal adult BM.

a. Gating strategy for identification and isolation of endothelial cells (ECs). After doublet exclusion, 7AAD$^-$ mononuclear cells (MNCs) were gated based on low/negative CD45 and CD235a expression to identify niche cells. ECs were identified as CD31$^+$CD9$^+$ cells within the niche.

b. Frequency of ECs within the niche in adult steady-state (n=9) and regenerative (n=48) BM.

c. Representative FACS plots revealing the existence of a CD105-expressing endothelial subset in regeneration.

d. The frequency of CD105$^+$ cells in the endothelial niche in normal BM (n=9) and during regeneration after chemotherapy (n=48).

e. The frequency of CD105$^+$ cells in the endothelial niche in BM aspirates of AML patients at diagnosis (n=4), and after recovery in complete remission (n=3).

Data represent mean ± s.e.m. *p <0.05, two-tailed unpaired t-test. AML=Acute Myeloid Leukemia. BM=Bone marrow. D17=Day 17. CR=Complete Remission.

Figure 2

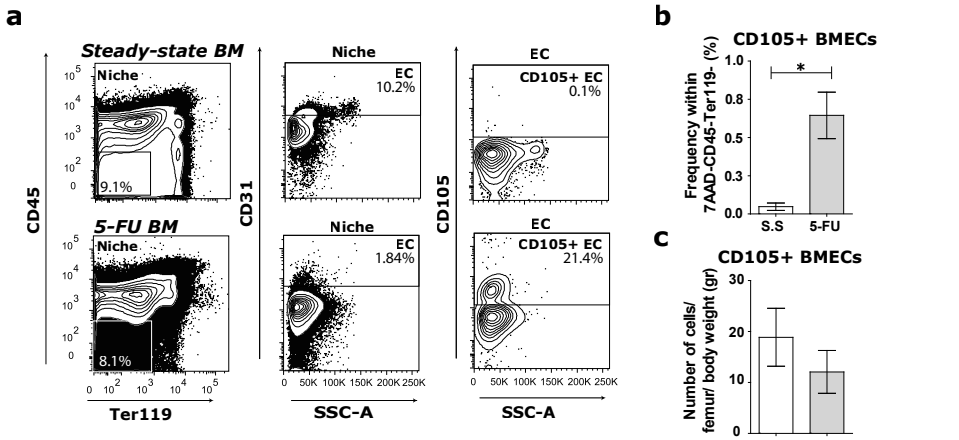

Figure 2. CD105-expressing endothelial cells are enriched in mice during regeneration after chemotherapeutic injury

a. Representative FACS plots for identification of murine BM ECs. After doublet exclusion, 7AAD$^-$ mononuclear cells (MNCs) were gated based on low/negative CD45/ Ter119 expression to select for BM niche cells. BM ECs were identified by CD31 and CD105 expression.

b. Frequency of CD105$^+$ ECs within the murine BM niche during S.S (n=3 mice) and upon recovery after 5-FU (n=5 mice).

c. Numbers of CD105$^+$ BM ECs during S.S (n=3) and after 5-FU treatment (n=5).

d,e. CD105$^+$ BM ECs differentially express IL-33 upon injury. (d) Representative FACS plots. (e) IL-33 expression in CD105$^+$ BM ECs and CD105$^-$ BM ECs in S.S (n=3) and after 5-FU treatment (n=5).

Data represent mean ± s.e.m. *p <0.05, two-tailed unpaired t-test. S.S=Steady-state. 5-FU=5-fluorouracil.

Figure 3

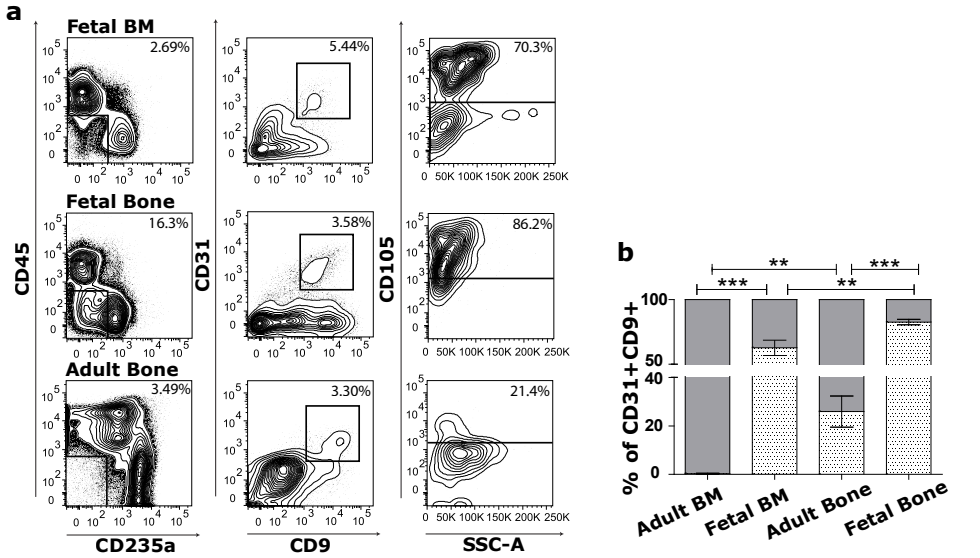

Figure 3. CD105-expressing endothelial cells are enriched in fetal development and collagenized bone fractions

a. Representative FACS plots identifying CD105-expressing ECs in fetal BM, fetal bone and adult bone.

b. Frequency of CD105$^+$ cells in the endothelial compartment in healthy adult BM aspirates (n=9), fetal BM (n=15), fetal bone (n=21), and adult bone (n=9). Data represent mean ± s.e.m. **p <0.01, ***p <0.001, one-way ANOVA (p< 0.0001) followed by Bonferroni's Multiple Comparison Test. BM= Bone marrow.

c. *In situ* immunofluorescence demonstrating the existence of capillary structures in the trabecular area of fetal long bone comprised of CD31$^+$CD105$^+$ endothelial cells (arrowheads). Sinusoid structures are CD31^{lo}CD105$^+$. In human adult BM, the majority of CD31$^+$ endothelial cells lacks CD105 expression (asterisks). Area within the dotted line in the adult BM represent bone tissue. 20x magnification. White scale bar represents 100 µm.

Figure 4

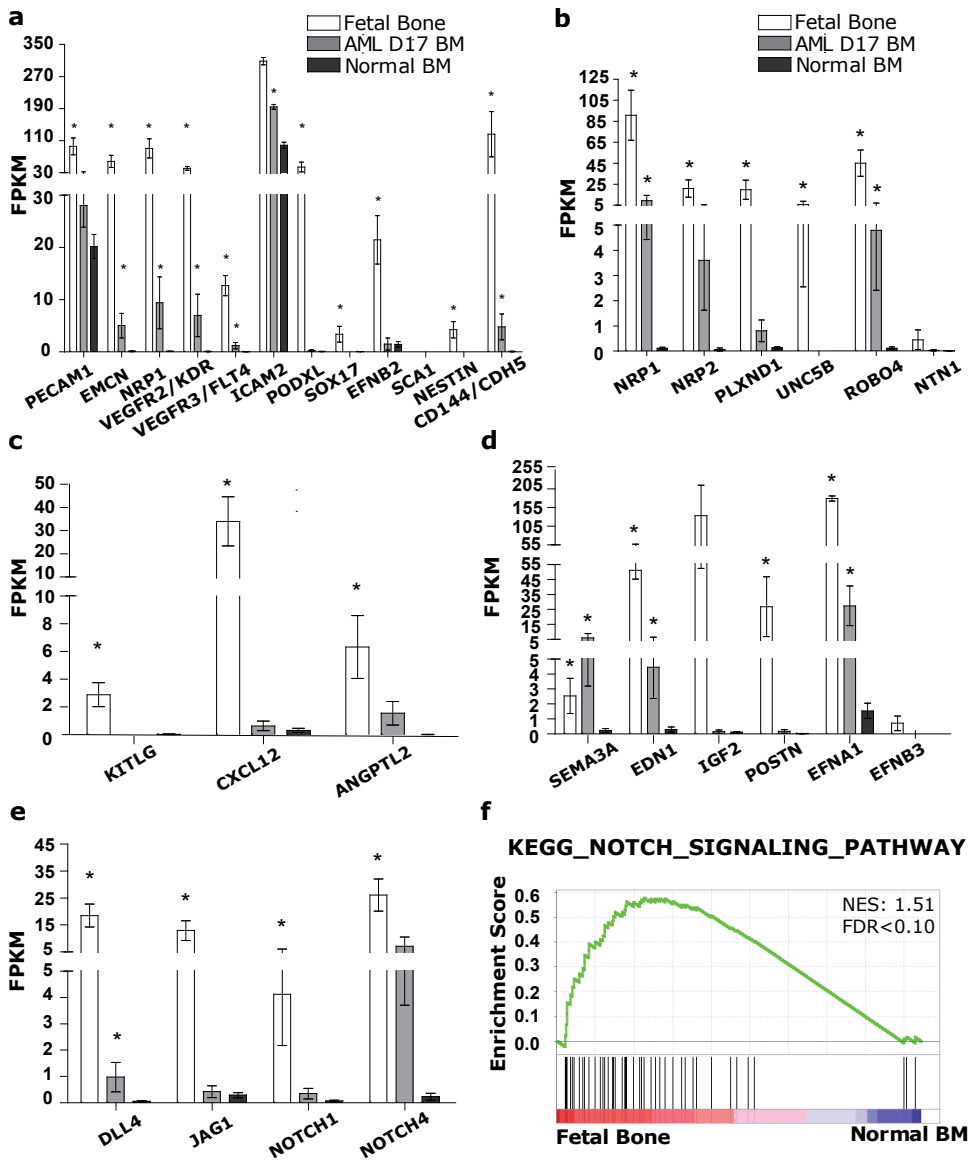

Figure 4. hRECs express transcriptional programs defining niche-forming endothelial cells in mice

Transcriptomes of hRECS isolated from human fetal bone ($CD45^-CD235^-CD31^+CD9^+CD105^+$)(n=3) and regenerative bone marrow ($CD45^-CD235^-CD31^+CD9^+$)(n=3) were compared to postnatal steady-state BM ECs ($CD45^-CD235^-CD31^+CD9^+$)(n=7).

a,b. Expression of genes previously reported to be overexpressed in murine type H endothelial cells (Itkin et al., 2016; Kusumbe et al., 2016, 2014; Ramasamy et al., 2014). Note, Sca-1 has no known human homolog (Holmes and Stanford, 2007).

c. Expression of established hematopoiesis-supporting cytokines (Broudy, 1997; Sugiyama et al., 2006; Zhang et al., 2006).

d. Expression of genes encoding anabolic regulators of angiogenesis and osteogenesis (Blumenfeld et al., 2002; Clines et al., 2007; Edwards and Mundy, 2008; Oshima et al., 2002; Salani et al., 2000; Salvucci and Tosato, 2012; Serini et al., 2003; Shao et al., 2004; Shigematsu et al., 1999; Tamagnone and Giordano, 2006).

e,f. Expression of genes encoding critical NOTCH pathway components (e) and activation of Notch- signaling (f) as demonstrated gene sets enrichment analysis (GSEA).

FPKM: fragments per kilobase of exon per million fragments mapped. NES: normalized enrichment score. FDR: false discovery rate. *FDR<0.05.

Figure 5

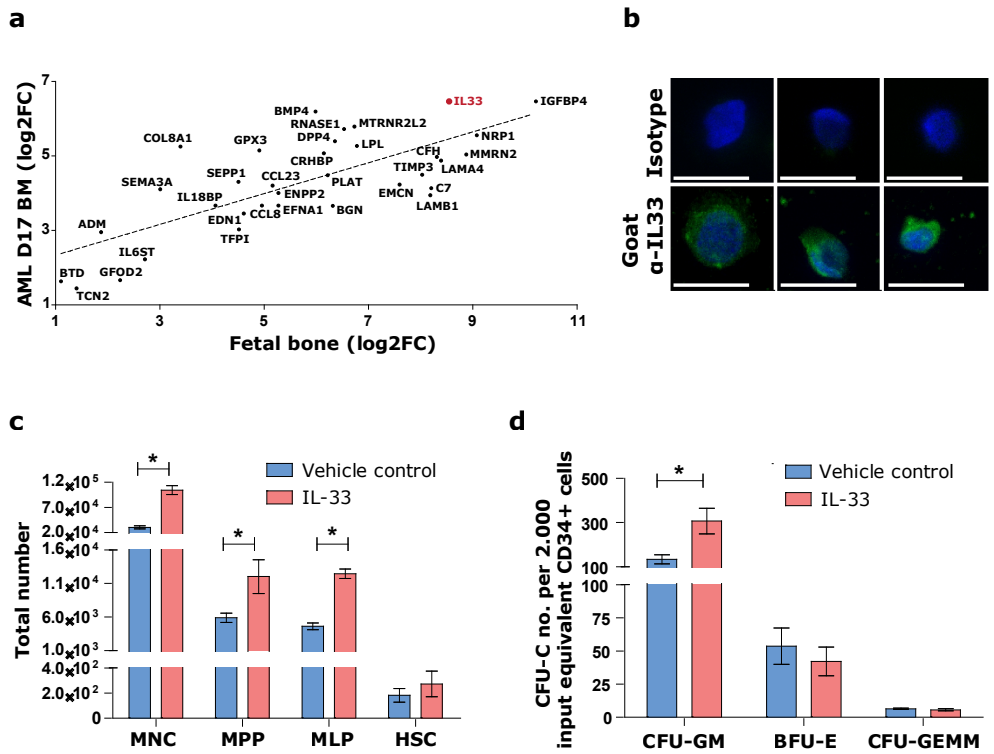

Figure 5. Identification of IL-33 as a hematopoietic niche factor

a. Transcript expression of 34 genes encoding secreted factors significantly enriched (FDR<0.05) in fetal bone and regenerating BM ECs (Log2 fold change in comparison to steady-state bone marrow). FDR: false discovery rate. FC: Fold Change.

b. 3x magnification cropped pictures of immunostained fetal hRECs demonstrating protein expression of IL-33. White scale bar represents 20 μm.

c,d. IL-33 mediated expansion of cord blood derived myeloid and lymphoid progenitor cells as demonstrated by flow-cytometric cell counting (c) (MPP, multipotent progenitor, $CD90^{-}CD45RA^{-}$; MLP, multilymphoid progenitor, $CD90^{-}CD45RA^{+}$; HSC, hematopoietic stem cell, $CD90^{+}CD45RA^{-}$) (n= 4 independent experiments) and colony-forming assays (CFU-C) (d) confirming an increase in CFU-GMs (n= 3 independent experiments).

Data represent mean ± s.e.m. *p<0.05, two-tailed unpaired t-test.

Figure 6

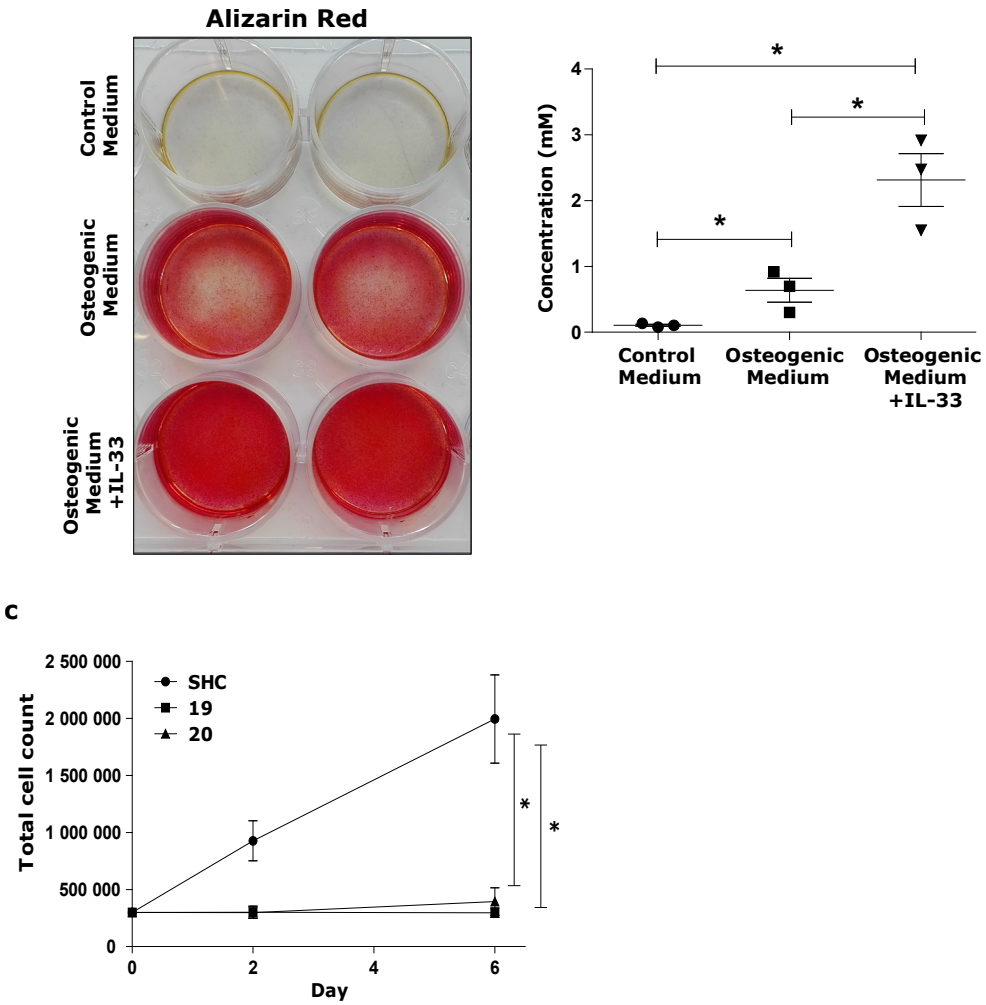

Figure 6. IL-33 promotes osteogenesis and angiogenesis *in vitro*

a,b. IL-33 accelerates terminal differentiation of mesenchymal cells towards matrix-depositing osteoblasts as demonstrated by Alizarin red-staining (a) and colorimetric assessment of calcium deposition (b) (n= 3 independent experiments).

c. Knockdown of IL-33 inhibits expansion of HUVECs. Quantification of the total number of HUVECs over time (combined data of n= 3 independent experiments).

Data represent mean ± s.e.m. *p <0.05, two-tailed unpaired t-test.

Figure 7

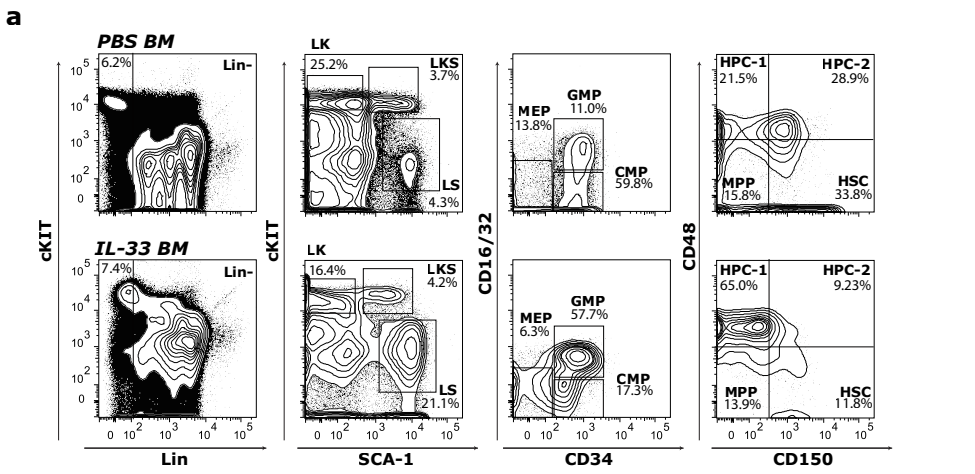

Figure 7. Recombinant IL-33 expands hematopoietic progenitors *in vivo*

a. Representative FACS plots of PBS vs IL-33 treated mice depicting the distribution of hematopoietic (progenitor) populations. **Lin-**: Lineage-negative cells. **LK**: Lin$^-$, c-KIT$^+$, Sca-1$^-$ cells. **LKS**: Lin$^-$, c-KIT$^+$, Sca-1$^+$ cells. **LS**: Lin$^-$, c-KIT$^-$, Sca-1$^+$ cells. **MEP**: LK, CD16/32$^-$, CD34$^-$ cells, megakaryocyte-erythroid progenitor. **GMP**: LK, CD16/32$^+$, CD34$^+$ cells, granulocyte-macrophage progenitor. **CMP**: LK, CD16/32$^-$, CD34$^+$ cells, common myeloid progenitor. **HPC-1**: LKS, CD48$^+$, CD150$^-$ cells, hematopoietic progenitor -1. **HPC-2**: LKS, CD48$^+$,CD150$^+$ cells, hematopoietic progenitor-2. **MPP**: LKS, CD48$^-$CD150$^-$ cells, multipotent progenitor. **HSC**: LKS, CD48$^-$CD150$^+$ cells, hematopoietic stem cell.

b. Total BM counts of GMP, LKS, HPC-1, HSC and LS populations in PBS (n=10) and IL-33 (n=5) treated mice.

Data represent mean ± s.e.m. *p<0.05, **p<0.01, two-tailed unpaired t-test.

EXPERIMENTAL PROCEDURES

Human bone marrow samples

Bone marrow (BM) aspirates of AML patients were collected at diagnosis, 17 days after start chemotherapy (3+7 schedule anthracycline and cytarabin) and upon achievement of complete remission (median age: 65 years, range 28-76). The time point of 17 days after start of chemotherapy represents the neutropenic phase, 10 days after administration of chemotherapy and on average 4 days before recovery of neutropenia. Control marrow was obtained by aspiration from donors for allogeneic transplantation (median age: 40 years, range 39-48) after written informed consent. In addition, trabecular hip bone was collected from patients undergoing hip replacement surgery (median age: 55 years, range 22-71). Human fetal long bones (median age: 18 gestational weeks, range 15-20) were obtained from elective abortions. Gestational age was confirmed by ultrasonic measurement by measurement of skull diameter and femoral length. The use of human samples was approved by the Institutional Review Board of the Erasmus Medical Center, the Netherlands, in accordance with the declaration of Helsinki with informed consent.

RNA Sequencing and GSEA analysis

RNA of sorted cells was extracted according to the manufacturer's instructions for RNA isolation with GenElute LPA (Sigma). cDNA was prepared using the SMARTer procedure (SMARTer Ultra Low RNA Kit (Clonetech). Library preparation and RNA-sequencing was performed as previously described and validated for low-input (Chen et al., 2016). Finally gene set enrichment analysis (GSEA) was performed on the FPKM values using the curated C2 collection of gene sets within MSigDB (Subramanian et al., 2005).

Mice and *in vivo* procedures

C57BL/6JOlaHsd wild-type mice were purchased from Envigo. Animals were maintained in specific pathogen free conditions in the Experimental Animal Center of Erasmus MC (EDC). To study the murine niche in regenerative conditions, adult mice (7-12 weeks old) were intraperitoneally administered with 250 mg/kg 5-fluorouracil (5-FU) and then sacrificed 7 days after 5-FU treatment. To study the effect of rmIL-33 on steady-state hematopoiesis and the BM niche, adult mice (7-14 weeks old) were intraperitoneally injected with 2 µg of recombinant IL-33 (580504, Biolegend) or PBS vehicle control daily for 6 consecutive days and then sacrificed.

All mice were sacrificed by cervical dislocation. Mouse bone marrow (BM) and bone fraction cells were isolated as previously described (Zambetti et al., 2016). Peripheral blood was collected from the submandibular vein in K2EDTA-coated microtainers (BD) and analyzed using a Vet ABC counter (Scil Animal Care). Animal studies were approved by the Animal Welfare/Ethics Committee of the EDC in accordance with legislation in the Netherlands (approval No. EMC 4015).

Liquid culture of CD34$^+$ cord blood cells

20,000 CD34$^+$ cord blood (CB) cells in 200 µl per well were cultured in StemSpan™ SFEM (Stem cell technologies, cat. 9600) with Stem Cell Factor (SCF) (50 ng/ml, Cellgenix, Freiburg, Germany), in a flat-bottom 96-well plate, at 37ºC and 5% CO2. 2 µl mQ solution containing only recombinant human IL-33 protein (ProSpec, cat. CYT-425) or just mQ (vehicle control) was added to the medium for a final concentration of 25 ng/ml IL-33 or 1% mQ, respectively. The medium was refreshed every 3 or 4 days and cells collected at day 7 for FACs analysis or for hematopoietic colony forming-unit assay.

Culture of human BM-derived mesenchymal stromal cells

Human BM-derived mesenchymal stromal cells (BMDSCs) (PT-2501, Lonza) were cultured as described previously (Brum et al., 2015). For osteogenic differentiation, BMDSCs were cultured in osteogenic induction medium (αMEM medium containing 10% heat-inactivated FCS supplemented with 100 nM dexamethasone, 10 mM β-glycerophosphate) with recombinant human IL-33 (250 ng/ml) or mQ vehicle control for 3 weeks. Medium was refreshed every 3-4 days.

Culture of and shRNA-mediated knockdown of IL-33 in HUVECs

Human umbilical vein endothelial cells (HUVECs) were expanded in EGM-2 Bulletkit medium (CC-3156 & CC-4176, Lonza). RNA interference was achieved by lentiviral transduction. Briefly, short hairpin RNAs against *IL-33* (sh19:TRCN0000135845 and sh20: TRCN0000135846) and a non-target control (shControl: SHC002 [SHC]) cloned in the pLKO.1 backbones were obtained from the Mission TRC shRNA library (Sigma-Aldrich). Lentiviral shRNAs were produced in HEK293T cells after cotransfection of shControl, sh19, or sh20 together with the packaging plasmids pSPAX2 and pMDG.2. HUVECs were infected with lentivirus for 24 hours and selected for 5 days with 2µg/mL of puromycin.

Statistics

Statistical analyses were performed using Prism 5 (GraphPad Software). Unless otherwise specified, unpaired, 2-tailed Student's t test (single test for comparison of two means) or 1-way analysis of variance followed by Bonferroni correction for multiple comparisons were used to evaluate statistical significance, defined as $P<0.05$. All results in bar graphs are mean value ± standard error of the mean.

AUTHOR CONTRIBUTIONS

K.K. designed and performed experiments, analyzed data, made figures, and wrote the manuscript. A.J.M designed and performed experiments and analyzed data. Z.P., S.C., E.B, and H.S. provided input on and performed experiments. R.H performed bioinformatics analysis for RNA-seq data. M.M, and M.A FACS-sorted and performed RNA-Seq. K.L provided core hip bone biopsies. P.B. provided human hip bone samples. B.E provided BMDSCs and necessary reagents. T.C. provided human fetal samples and input on experiments. M.R. designed experiments, analyzed data, wrote the manuscript, supervised the study, and acquired funding.

ACCESSION NUMBERS

The accession number for the RNA-seq data, submitted to the European Genome-phenome Archive, derived from human healthy adults, AML day 17 patients, and fetal bone specimens is EGAS00001002736.

ACKNOWLEDGEMENTS

We would like to thank Dr. Eric Braakman, Lucia Duinhouwer, and Mariëtte ter Borg for providing CD34$^+$ cells; Nathalie Papazian for helping to process fetal tissue. Kirsten van Lom for coordinating human sampling. Marijke Koedam for preparing and culture of BMDSCs. Dr. Moniek de Maat for providing HUVECs. Dr. Elwin Rombouts, Peter van Geel, Paulette van Strien and Michael Vermeulen for operating the BD FACSARIA III; Noemi Zambetti, Onno Roovers, Jyotirmaya Behera, Lucia Duinhouwer, Marijke Koedam, Inge Snoeren, Almira Henić, Dr. Rebekka Schneider and Gert-Jan Kremers for providing technical assistance; members of the Erasmus MC Department of Hematology for providing scientific discussion.

DECLARATION OF INTERESTS

The authors declare no competing interests.

REFERENCES

Barreiro, O., Yáñez-Mó, M., Sala-Valdés, M., Gutiérrez-López, M.D., Ovalle, S., Higginbottom, A., Monk, P.N., Cabañas, C., Sánchez-Madrid, F., 2005. Endothelial tetraspanin microdomains regulate leukocyte firm adhesion during extravasation. Blood 105, 2852–2861. https://doi.org/10.1182/blood-2004-09-3606

Blumenfeld, I., Srouji, S., Lanir, Y., Laufer, D., Livne, E., 2002. Enhancement of bone defect healing in old rats by TGF-β and IGF-1. Exp. Gerontol. 37, 553–565. https://doi.org/10.1016/S0531-5565(01)00215-7

Brickshawana, A., Shapiro, V.S., Kita, H., Pease, L.R., 2011. Lineage(-)Sca1+c-Kit(-)CD25+ cells are IL-33-responsive type 2 innate cells in the mouse bone marrow. J. Immunol. 187, 5795–804. https://doi.org/10.4049/jimmunol.1102242

Broudy, V.C., 1997. Stem cell factor and hematopoiesis. Blood 90, 1345–64.

Brum, A.M., van de Peppel, J., van der Leije, C.S., Schreuders-Koedam, M., Eijken, M., van der Eerden, B.C.J., van Leeuwen, J.P.T.M., 2015. Connectivity Map-based discovery of parbendazole reveals targetable human osteogenic pathway. Proc. Natl. Acad. Sci. 112, 12711–12716. https://doi.org/10.1073/pnas.1501597112

Butler, J.M., Nolan, D.J., Vertes, E.L., Varnum-Finney, B., Kobayashi, H., Hooper, A.T., Seandel, M., Shido, K., White, I.A., Kobayashi, M., Witte, L., May, C., Shawber, C., Kimura, Y., Kitajewski, J., Rosenwaks, Z., Bernstein, I.D., Rafii, S., 2010. Endothelial Cells Are Essential for the Self-Renewal and Repopulation of Notch-Dependent Hematopoietic Stem Cells. Cell Stem Cell 6, 251–264. https://doi.org/10.1016/j.stem.2010.02.001

Carriere, V., Roussel, L., Ortega, N., Lacorre, D.-A., Americh, L., Aguilar, L., Bouche, G., Girard, J.-P., 2007. IL-33, the IL-1-like cytokine ligand for ST2 receptor, is a chromatin-associated nuclear factor in vivo. Proc. Natl. Acad. Sci. 104, 282–287. https://doi.org/10.1073/pnas.0606854104

Cayrol, C., Girard, J.P., 2014. IL-33: An alarmin cytokine with crucial roles in innate immunity, inflammation and allergy. Curr. Opin. Immunol. 31, 31–37. https://doi.org/10.1016/j.coi.2014.09.004

Charbord, P., Tavian, M., Humeau, L., Peault, B., 1996. Early ontogeny of the human marrow from long bones: an immunohistochemical study of hematopoiesis and its microenvironment. Blood 87, 4109–4119. https://doi.org/10.1182/blood.V87.10.4109.bloodjournal87104109

Cheifetz, S., Bellón, T., Calés, C., Vera, S., Bernabeu, C., Massagué, J., Letarte, M., 1992. Endoglin is a component of the transforming growth factor-beta receptor system in human endothelial cells. J. Biol. Chem. 267, 19027–30.

Chen, S., Zambetti, N.A., Bindels, E.M.J., Kenswill, K., Mylona, A.M., Adisty, N.M., Hoogenboezem, R.M., Sanders, M.A., Cremers, E.M.P., Westers, T.M., Jansen, J.H., van de Loosdrecht, A.A., Raaijmakers, M.H.G.P., 2016. Massive parallel RNA sequencing of highly purified mesenchymal elements in low-risk MDS reveals tissue-context-dependent activation of inflammatory programs. Leukemia 30, 1938–42. https://doi.org/10.1038/leu.2016.91

Choi, Y., Choi, H., Min, J., Pyun, B., Maeng, Y., Park, H., Kim, J., Kim, Y., Kwon, Y., 2009. ST2 / TRAF6-mediated endothelial nitric oxide production Interleukin-33 induces angiogenesis and vascular permeability through ST2 / TRAF6-mediated endothelial nitric oxide production. Blood 114, 3117–3126. https://doi.org/10.1182/blood-2009-02-203372.The

Clines, G. a, Mohammad, K.S., Bao, Y., Stephens, O.W., Suva, L.J., Shaughnessy, J.D., Fox, J.W., Chirgwin, J.M., Guise, T. a, 2007. Dickkopf Homolog 1 Mediates Endothelin-1-Stimulated New Bone Formation. Mol. Endocrinol. 21, 486–498. https://doi.org/10.1210/me.2006-0346

Coşkun, S., Chao, H., Vasavada, H., Heydari, K., Gonzales, N., Zhou, X., de Crombrugghe, B., Hirschi, K.K., 2014. Development of the fetal bone marrow niche and regulation of HSC quiescence and homing ability by emerging osteolineage cells. Cell Rep. 9, 581–90. https://doi.org/10.1016/j.celrep.2014.09.013

Doan, P.L., Russell, J.L., Himburg, H.A., Helms, K., Harris, J.R., Lucas, J., Holshausen, K.C., Meadows, S.K., Daher, P., Jeffords, L.B., Chao, N.J., Kirsch, D.G., Chute, J.P., 2013. Tie2 + Bone Marrow Endothelial Cells Regulate Hematopoietic Stem Cell Regeneration Following Radiation Injury. Stem Cells 31, 327–337. https://doi.org/10.1002/stem.1275

Duff, S.E., Li, C., Garland, J.M., Kumar, S., 2003. CD105 is important for angiogenesis: evidence and potential applications. FASEB J. 17, 984–992. https://doi.org/10.1096/fj.02-0634rev

Edwards, C.M., Mundy, G.R., 2008. Eph receptors and ephrin signaling pathways: A role in bone homeostasis. Int. J. Med. Sci. 5, 263–272. https://doi.org/10.7150/ijms.5.263

Gur-Cohen, S., Itkin, T., Chakrabarty, S., Graf, C., Kollet, O., Ludin, A., Golan, K., Kalinkovich, A., Ledergor, G., Wong, E., Niemeyer, E., Porat, Z., Erez, A., Sagi, I., Esmon, C.T., Ruf, W., Lapidot, T., 2015. PAR1 signaling regulates the retention and recruitment of EPCR-expressing bone marrow hematopoietic stem cells. Nat. Med. 21, 1307–17. https://doi.org/10.1038/nm.3960

Holmes, C., Stanford, W.L., 2007. Concise Review: Stem Cell Antigen-1: Expression, Function, and Enigma. Stem Cells 25, 1339–1347. https://doi.org/10.1634/stemcells.2006-0644

Hooper, A.T., Butler, J.M., Nolan, D.J., Kranz, A., Iida, K., Kobayashi, M., Kopp, H.-G., Shido, K., Petit, I., Yanger, K., James, D., Witte, L., Zhu, Z., Wu, Y., Pytowski, B., Rosenwaks, Z., Mittal, V., Sato, T.N., Rafii, S., 2009. Engraftment and Reconstitution of Hematopoiesis Is Dependent on VEGFR2-Mediated Regeneration of Sinusoidal Endothelial Cells. Cell Stem Cell 4, 263–274. https://doi.org/10.1016/j.stem.2009.01.006

Ibrahim, A.A., Yahata, T., Onizuka, M., Dan, T., Van Ypersele De Strihou, C., Miyata, T., Ando, K., 2014. Inhibition of plasminogen activator inhibitor type-1 activity enhances rapid and sustainable hematopoietic regeneration. Stem Cells 32, 946–958. https://doi.org/10.1002/stem.1577

Itkin, T., Gur-Cohen, S., Spencer, J.A., Schajnovitz, A., Ramasamy, S.K., Kusumbe, A.P., Ledergor, G., Jung, Y., Milo, I., Poulos, M.G., Kalinkovich, A., Ludin, A., Kollet, O., Shakhar, G., Butler, J.M., Rafii, S., Adams, R.H., Scadden, D.T., Lin, C.P., Lapidot, T., 2016. Distinct bone marrow blood vessels differentially regulate haematopoiesis. Nature 532, 323–328. https://doi.org/10.1038/nature17624

Jagannathan-Bogdan, M., Zon, L.I., 2013. Hematopoiesis. Development 140, 2463–7. https://doi.org/10.1242/dev.083147

Kakkar, R., Hei, H., Dobner, S., Lee, R.T., 2012. Interleukin 33 as a mechanically responsive cytokine secreted by living cells. J. Biol. Chem. 287, 6941–6948. https://doi.org/10.1074/jbc.M111.298703

Khurana, S., Margamuljana, L., Joseph, C., Schouteden, S., Buckley, S.M., Verfaillie, C.M., 2013. Glypican-3-mediated inhibition of CD26 by TFPI: a novel mechanism in hematopoietic stem cell homing and maintenance. Blood 121, 2587–2595. https://doi.org/10.1182/blood-2012-09-456715

Kim, J., Kim, W., Le, H.T., Moon, U.J., Tran, V.G., Kim, H.J., Jung, S., Nguyen, Q.-T., Kim, B.-S., Jun, J.-B., Cho, H.R., Kwon, B., 2014. IL-33–Induced Hematopoietic Stem and Progenitor Cell Mobilization Depends upon CCR2. J. Immunol. 193, 3792–3802. https://doi.org/10.4049/jimmunol.1400176

Kobayashi, H., Butler, J.M., O'Donnell, R., Kobayashi, M., Ding, B.-S., Bonner, B., Chiu, V.K., Nolan, D.J., Shido, K., Benjamin, L., Rafii, S., 2010. Angiocrine factors from Akt-activated endothelial cells balance self-renewal and differentiation of haematopoietic stem cells. Nat. Cell Biol. 12, 1046–1056. https://doi.org/10.1038/ncb2108

Kopp, H.G., Avecilla, S.T., Hooper, A.T., Shmelkov, S. V., Ramos, C.A., Zhang, F., Rafii, S., 2005. Tie2 activation contributes to hemangiogenic regeneration after myelosuppression. Blood 106, 505–513. https://doi.org/10.1182/blood-2004-11-4269

Kopp, H.G., Hooper, A.T., Avecilla, S.T., Rafii, S., 2009. Functional heterogeneity of the bone marrow vascular niche. Ann. N. Y. Acad. Sci. 1176, 47–54. https://doi.org/10.1111/j.1749-6632.2009.04964.x

Küchler, A.M., Pollheimer, J., Balogh, J., Sponheim, J., Manley, L., Sorensen, D.R., De Angelis, P.M., Scott, H., Haraldsen, G., 2008. Nuclear Interleukin-33 Is Generally Expressed in Resting Endothelium but Rapidly Lost upon Angiogenic or Proinflammatory Activation. Am. J. Pathol. 173, 1229–1242. https://doi.org/10.2353/ajpath.2008.080014

Kumar, P., Wang, J.M., Bernabeu, C., 1996. CD 105 and angiogenesis. J. Pathol. 178, 363–6. https://doi.org/10.1002/(SICI)1096-9896(199604)178:4<363::AID-PATH491>3.0.CO;2-8

Kumar, R., Fossati, V., Israel, M., Snoeck, H.-W., 2008. Lin-Sca1+Kit- Bone Marrow Cells Contain Early Lymphoid-Committed Precursors That Are Distinct from Common Lymphoid Progenitors. J. Immunol. 181, 7507–7513. https://doi.org/10.4049/jimmunol.181.11.7507

Kusumbe, A.P., Ramasamy, S.K., Adams, R.H., 2014. Coupling of angiogenesis and osteogenesis by a specific vessel subtype in bone. Nature 507, 323–328. https://doi.org/10.1038/nature13145

Kusumbe, A.P., Ramasamy, S.K., Itkin, T., Mäe, M.A., Langen, U.H., Betsholtz, C., Lapidot, T., Adams, R.H., 2016. Age-dependent modulation of vascular niches for haematopoietic stem cells. Nature 532, 380–384. https://doi.org/10.1038/nature17638

Lee, E.-J., Kim, J.W., Yoo, H., Kwak, W., Choi, W.H., Cho, S., Choi, Y.J., Lee, Y.-J., Cho, J., 2015. Single high-dose irradiation aggravates eosinophil-mediated fibrosis through IL-33 secreted from impaired vessels in the skin compared to fractionated irradiation. Biochem. Biophys. Res. Commun. 464, 20–26. https://doi.org/10.1016/j.bbrc.2015.05.081

Lerner, C., Harrison, D.E., 1990. 5-Fluorouracil spares hemopoietic stem cells responsible for long-term repopulation. Exp. Hematol. 18, 114–8.

Li, D.Y., Sorensen, L.K., Brooke, B.S., Urness, L.D., Davis, E.C., Taylor, D.G., Boak, B.B., Wendel, D.P., 1999. Defective angiogenesis in mice lacking endoglin. Science. 284, 1534–7. https://doi.org/10.1126/science.284.5419.1534

Maes, C., 2013. Role and regulation of vascularization processes in endochondral bones. Calcif. Tissue Int. 92, 307–323. https://doi.org/10.1007/s00223-012-9689-z

Medvinsky, A., Rybtsov, S., Taoudi, S., 2011. Embryonic origin of the adult hematopoietic system: advances and questions. Development 138, 1017–31. https://doi.org/10.1242/dev.040998

Miller, D.W., Graulich, W., Karges, B., Stahl, S., Ernst, M., Ramaswamy, A., Sedlacek, H.H., Müller, R., Adamkiewicz, J., 1999. Elevated expression of endoglin, a component of the TGF-beta-receptor complex, correlates with proliferation of tumor endothelial cells. Int. J. cancer 81, 568–72.

Nakamura-Ishizu, A., Okuno, Y., Omatsu, Y., Okabe, K., Morimoto, J., Uede, T., Nagasawa, T., Suda, T., Kubota, Y., 2012. Extracellular matrix protein tenascin-C is required in the bone marrow microenvironment primed for hematopoietic regeneration. Blood 119, 5429–5437. https://doi.org/10.1182/blood-2011-11-393645

Nombela-Arrieta, C., Pivarnik, G., Winkel, B., Canty, K.J., Harley, B., Mahoney, J.E., Park, S.-Y., Lu, J., Protopopov, A., Silberstein, L.E., 2013. Quantitative imaging of haematopoietic stem and progenitor cell localization and hypoxic status in the bone marrow microenvironment. Nat. Cell Biol. 15, 533–543. https://doi.org/10.1038/ncb2730

Oguro, H., Ding, L., Morrison, S.J., 2013. SLAM family markers resolve functionally distinct subpopulations of hematopoietic stem cells and multipotent progenitors. Cell Stem Cell 13, 102–16. https://doi.org/10.1016/j.stem.2013.05.014

Oshima, A., Tanabe, H., Yan, T., Lowe, G.N., Glackin, C.A., Kudo, A., 2002. A novel mechanism for the regulation of osteoblast differentiation: Transcription of periostin, a member of the fasciclin I family, is regulated by the bHLH transcription factor, Twist. J. Cell. Biochem. 86, 792–804. https://doi.org/10.1002/jcb.10272

Poulos, M.G., Guo, P., Kofler, N.M., Pinho, S., Gutkin, M.C., Tikhonova, A., Aifantis, I., Frenette, P.S., Kitajewski, J., Rafii, S., Butler, J.M., 2013. Endothelial Jagged-1 Is Necessary for Homeostatic and Regenerative Hematopoiesis. Cell Rep. 4, 1022–1034. https://doi.org/10.1016/j.celrep.2013.07.048

Rafii, S., Butler, J.M., Ding, B.-S., 2016. Angiocrine functions of organ-specific endothelial cells. Nature 529, 316–325. https://doi.org/10.1038/nature17040

Ramasamy, S.K., Kusumbe, A.P., Adams, R.H., 2015. Regulation of tissue morphogenesis by endothelial cell-derived signals. Trends Cell Biol. 25, 148–157. https://doi.org/10.1016/j.tcb.2014.11.007

Ramasamy, S.K., Kusumbe, A.P., Itkin, T., Gur-Cohen, S., Lapidot, T., Adams, R.H., 2016. Regulation of Hematopoiesis and Osteogenesis by Blood Vessel–Derived Signals. Annu. Rev. Cell Dev. Biol. 32, 649–675. https://doi.org/10.1146/annurev-cellbio-111315-124936

Ramasamy, S.K., Kusumbe, A.P., Wang, L., Adams, R.H., 2014. Endothelial Notch activity promotes angiogenesis and osteogenesis in bone. Nature 507, 376–380. https://doi.org/10.1038/nature13146

Salani, D., Taraboletti, G., Rosanò, L., Di Castro, V., Borsotti, P., Giavazzi, R., Bagnato, A., 2000. Endothelin-1 Induces an Angiogenic Phenotype in Cultured Endothelial Cells and Stimulates Neovascularization In Vivo. Am. J. Pathol. 157, 1703–1711. https://doi.org/10.1016/S0002-9440(10)64807-9

Salazar, V.S., Gamer, L.W., Rosen, V., 2016. BMP signalling in skeletal development, disease and repair. Nat. Rev. Endocrinol. 12, 203–221. https://doi.org/10.1038/nrendo.2016.12

Saleh, H., Eeles, D., Hodge, J.M., Nicholson, G.C., Gu, R., Pompolo, S., Gillespie, M.T., Quinn, J.M.W., 2011. Interleukin-33, a target of parathyroid hormone and oncostatin m, increases osteoblastic matrix mineral deposition and inhibits osteoclast formation in vitro. Endocrinology 152, 1911–1922. https://doi.org/10.1210/en.2010-1268

Salvucci, O., Tosato, G., 2012. Essential Roles of EphB Receptors and EphrinB Ligands in Endothelial Cell Function and Angiogenesis, in: Advances in Cancer Research. pp. 21–57. https://doi.org/10.1016/B978-0-12-386503-8.00002-8

Schepers, K., Hsiao, E.C., Garg, T., Scott, M.J., Passegue, E., 2012. Activated Gs signaling in osteoblastic cells alters the hematopoietic stem cell niche in mice. Blood 120, 3425–3435. https://doi.org/10.1182/blood-2011-11-395418

Serini, G., Valdembri, D., Zanivan, S., Morterra, G., Burkhardt, C., Caccavari, F., Zammataro, L., Primo, L., Tamagnone, L., Logan, M., Tessier-Lavigne, M., Taniguchi, M., Puschel, A.W., Bussolino, F., 2003. Class 3 semaphorins control vascular morphogenesis by inhibiting integrin function. Nature 424, 391–397. https://doi.org/10.1038/nature01784\rnature01784 [pii]

Shan, S., Li, Y., Wang, J., Lv, Z., Yi, D., Huang, Q., Corrigan, C.J., Wang, W., Quangeng, Z., Ying, S., 2016. Nasal administration of interleukin-33 induces airways angiogenesis and expression of multiple angiogenic factors in a murine asthma surrogate. Immunology 148, 83–91. https://doi.org/10.1111/imm.12589

Shao, R., Bao, S., Bai, X., Blanchette, C., Anderson, R.M., Dang, T., Gishizky, M.L., Marks, J.R., Wang, X., 2004. Acquired expression of periostin by human breast cancers promotes tumor angiogenesis through up-regulation of vascular endothelial growth factor receptor 2 expression. Mol. Cell. Biol. 24, 3992–4003. https://doi.org/10.1128/MCB.24.9.3992

Shigematsu, S., Yamauchi, K., Nakajima, K., Iijima, S., Aizawa, T., Hashizume, K., 1999. IGF-1 regulates migration and angiogenesis of human endothelial cells. Endocr. J. 46 Suppl, S59–S62. https://doi.org/10.1507/endocrj.46.Suppl_S59

Subramanian, A., Tamayo, P., Mootha, V.K., Mukherjee, S., Ebert, B.L., Gillette, M. a, Paulovich, A., Pomeroy, S.L., Golub, T.R., Lander, E.S., Mesirov, J.P., 2005. Gene set enrichment analysis: A knowledge-based approach for interpreting genome-wide expression profiles. Proc. Natl. Acad. Sci. 102, 15545–15550. https://doi.org/10.1073/pnas.0506580102

Sugiyama, T., Kohara, H., Noda, M., Nagasawa, T., 2006. Maintenance of the Hematopoietic Stem Cell Pool by CXCL12-CXCR4 Chemokine Signaling in Bone Marrow Stromal Cell Niches. Immunity 25, 977–988. https://doi.org/10.1016/j.immuni.2006.10.016

Sundlisæter, E., Edelmann, R.J., Hol, J., Sponheim, J., Kchler, A.M., Weiss, M., Udalova, I.A., Midwood, K.S., Kasprzycka, M., Haraldsen, G., 2012. The alarmin IL-33 is a notch target in quiescent endothelial cells. Am. J. Pathol. 181, 1099–1111. https://doi.org/10.1016/j.ajpath.2012.06.003

Tamagnone, L., Giordano, S., 2006. Semaphorin pathways orchestrate osteogenesis. Nat. Cell Biol. 8, 545–547. https://doi.org/10.1038/ncb0606-545

Wang, J.M., Kumar, S., Van Agthoven, A., Kumar, P., Pye, D., Hunter, R.D., 1995. Irradiation induces up-regulation of E9 protein (CD105) in human vascular endothelial cells. Int. J. Cancer 62, 791–796. https://doi.org/10.1002/ijc.2910620624

Winkler, I.G., Barbier, V., Nowlan, B., Jacobsen, R.N., Forristal, C.E., Patton, J.T., Magnani, J.L., Lévesque, J.-P., 2012. Vascular niche E-selectin regulates hematopoietic stem cell dormancy, self renewal and chemoresistance. Nat. Med. 18, 1651–1657. https://doi.org/10.1038/nm.2969

Xian, C.J., Cool, J.C., Pyragius, T., Foster, B.K., 2006. Damage and recovery of the bone growth mechanism in young rats following 5-fluorouracil acute chemotherapy. J. Cell. Biochem. 99, 1688–1704. https://doi.org/10.1002/jcb.20889

Yoshitomi, H., Kobayashi, S., Ohtsuka, M., Kimura, F., Shimizu, H., Yoshidome, H., Miyazaki, M., 2008. Specific expression of endoglin (CD105) in endothelial cells of intratumoral blood and lymphatic vessels in pancreatic cancer. Pancreas 37, 275–281. https://doi.org/10.1097/mpa.0b013e3181690b97

Zambetti, N.A., Ping, Z., Chen, S., Kenswil, K.J.G., Mylona, M.A., Sanders, M.A., Hoogenboezem, R.M., Bindels, E.M.J., Adisty, M.N., Van Strien, P.M.H., van der Leije, C.S., Westers, T.M., Cremers, E.M.P., Milanese, C., Mastroberardino, P.G., van Leeuwen, J.P.T.M., van der Eerden, B.C.J., Touw, I.P., Kuijpers, T.W., Kanaar, R., van de Loosdrecht, A.A., Vogl, T., Raaijmakers, M.H.G.P., 2016. Mesenchymal Inflammation Drives Genotoxic Stress in Hematopoietic Stem Cells and Predicts Disease Evolution in Human Pre-leukemia. Cell Stem Cell 19, 613–627. https://doi.org/10.1016/j.stem.2016.08.021

Zhang, C.C., Kaba, M., Ge, G., Xie, K., Tong, W., Hug, C., Lodish, H.F., 2006. Angiopoietin-like proteins stimulate ex vivo expansion of hematopoietic stem cells. Nat. Med. 12, 240–245. https://doi.org/10.1038/nm1342

SUPPLEMENTAL INFORMATION

Table S1

Gene Name	Cluster of differentation	FDR	FC	Avg FPKM AML D17	Avg FPKM Healthy CTRL
DPP4	CD26	4.30E-06	42.06162224	1.447326333	0.018322079
ENG	CD105	1.61E-03	8.55449896	15.62384567	1.547395714
VCAM1	CD106	3.81E-06	50.16296233	88.93116733	0.804735029
LIFR	CD118	2.08E-02	10.1185124	0.1064362	0.016143224
IL1R1	CD121a	1.54E-03	22.29341884	1.835577597	0.040494024
CDH5	CD144	4.26E-03	22.72755944	4.79532	0.072456899
CXCR3	CD183	1.04E-02	6.439581287	4.524633333	1.938153714
CCR2	CD192	1.09E-03	5.554609242	17.7306	4.429592857
PROCR	CD201	1.03E-03	19.40383328	7.131228667	0.224176357
TSPAN7	CD231	2.61E-05	24.32565573	54.17457	1.558463086
TNFSF10	CD253	1.16E-02	5.826945634	10.84400633	1.776891571
CD300LG	CD300g	1.90E-04	38.86795899	14.576502	0.166514471
NRP1	CD304	3.82E-06	47.01754435	9.396109867	0.113237357
KDR	CD309	1.69E-02	18.71674562	6.977216	0.077225637
FZD4	CD344	1.50E-06	45.00592407	2.850081333	0.043208416
S1PR1	CD363	1.33E-03	13.72492829	11.43101533	0.575994457

Supplemental Table 1. Related to Figure 1. Differential expression of candidate membrane markers of endothelial cells associated with regeneration after chemotherapy

Genes encoding cluster of differentiation antigens overexpressed in endothelial cells ($CD45^-CD235^-CD31^+CD9^+$) in aspirates obtained from regenerative marrow (n= 3) compared to postnatal steady-state BM (n= 7). FC: Fold change. FPKM: fragments per kilobase of exon per million fragments mapped. BM: bone marrow. FDR: false discovery rate.

SUPPLEMENTAL FIGURES

Figure S1

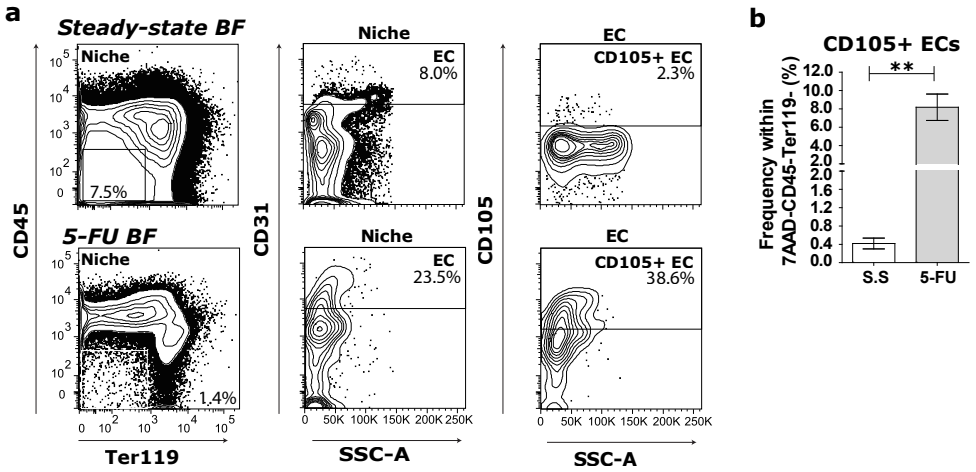

Supplementary Figure 1. Related to Figure 2. CD105-expressing endothelial cells are enriched in collagenased bone of mice after chemotherapeutic injury

a. Representative FACS plots revealing the enrichment of a CD105-expressing endothelial cells (ECs) in collagenased bone after administration of 5-fluoroucil. Gating strategy for identification of murine ECs is also depicted (see also figure 2). BF=Bone fraction.

b. Frequency of CD105⁺ ECs within collagenased bone of mice in steady-state (n=3) and after administration of 5-fluoroucil (n=5). Data represent mean ± s.e.m. **p <0.01, two-tailed unpaired t-test. S.S=Steady-state. 5-FU=5-fluorouracil.

Figure S2

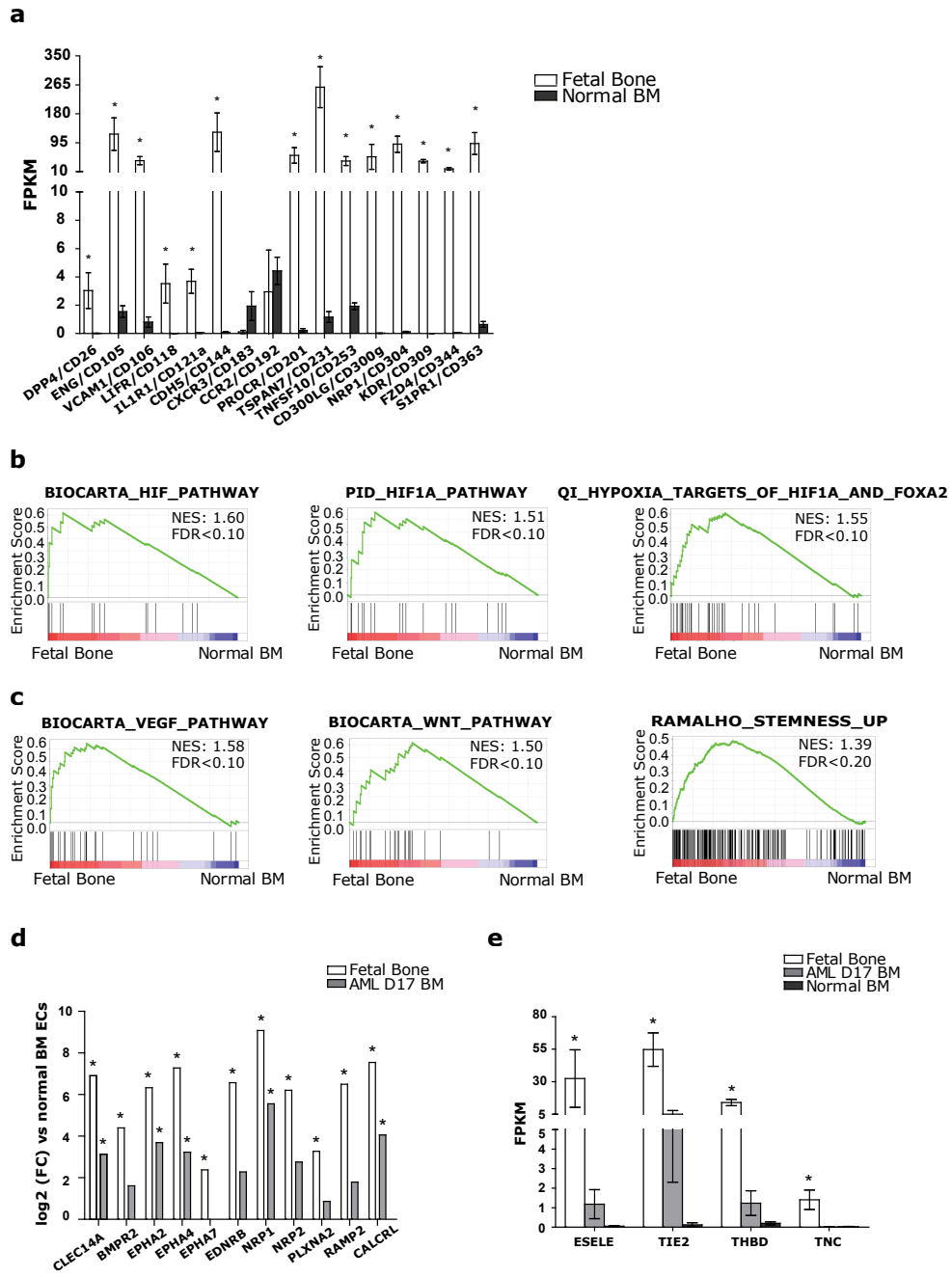

Supplementary Figure 2. Related to Supplemental Table 1, Figure 4 and 5. Transcriptional signatures of fetal CD105+ ECs

a. Transcript expression of membrane proteins (CD markers) in fetal bone $CD31^+CD105^+$ ECs compared to steady-state BM ECs. The overlap with transcripts identified in ECs isolated from D17 BM (Table S1) supports the notion that the enrichment of these transcripts in ECs in the regenerative marrow is caused by overexpression in the subset of $CD105^+$ ECs.

b,c. GSEA plots demonstrating activation of HIF1a signaling (b) and gene sets associated with VEGF, WNT and stem cells (c) in fetal hRECs compared to steady-state BM. GSEA: gene sets enrichment analysis.

d. Transcript expression (Log 2 fold change) of cognate receptors of candidate secreted proteins (Figure 5A) in fetal hRECs and ECs of regenerative marrow compared to steady-state bone marrow.

e. Transcript abundance of molecules associated with regeneration previously described in murine studies (Doan et al., 2013; Gur-Cohen et al., 2015; Kopp et al., 2005; Nakamura-Ishizu et al., 2012; Winkler et al., 2012).

*<FDR 0.05. FDR: false discovery rate. FPKM: fragments per kilobase of exon per million fragments mapped. BM: bone marrow. NES: normalized enrichment score. FC: Fold Change.

Figure S3

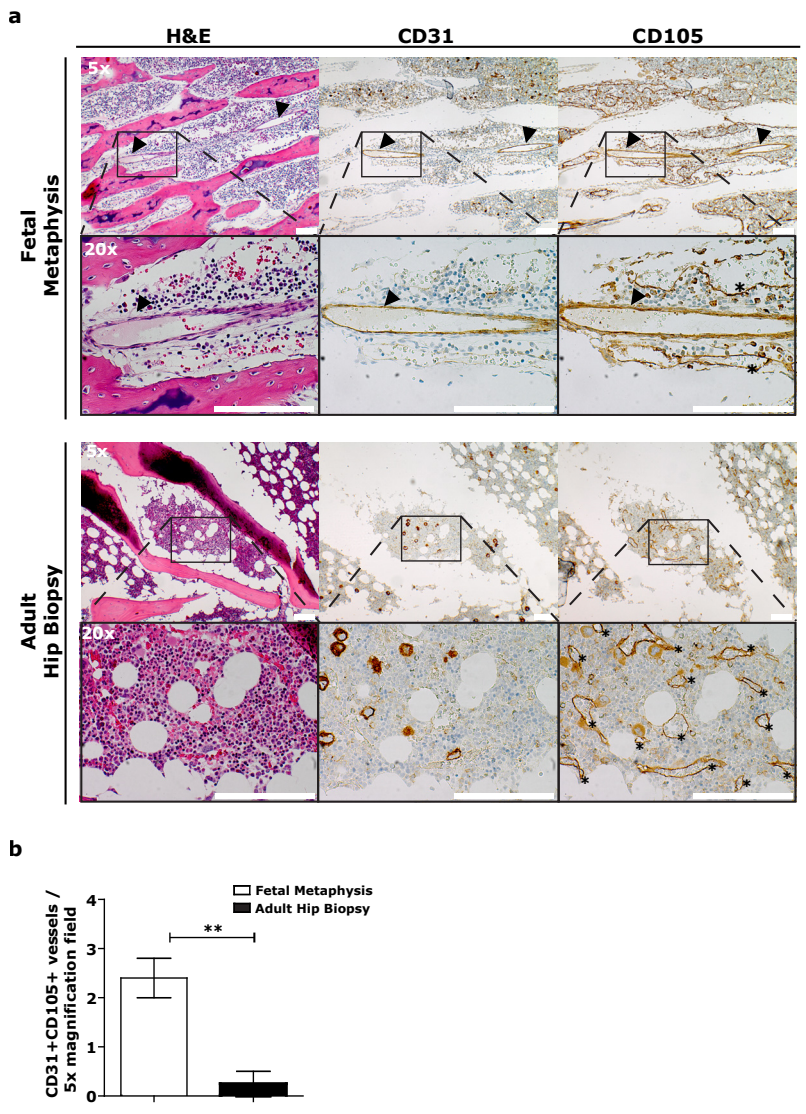

Supplementary Figure 3. Related to Figure 3. *In situ* immunohistochemistry of $CD31^+CD105^+$ endothelial cells in human fetal and postnatal bone marrow

a. Hematoxylin and eosin, CD31, and CD105 staining in consecutive serial sections of fetal and adult trabecular bone. $CD31^+CD105^+$ vessels (indicated by black arrowheads) were readily detected in the fetal bone, but at much lower frequency in postnatal trabecular bone. Asterisks highlight sinusoidal endothelium, marked by CD105 expression and concomitant low or lack of CD31 expression. Note: hematopoietic elements with high CD31 expression (indicated by black arrows) represent megakaryocytes. Representative 5x and 20x magnified images. Scale bars represent 100 µm.

b. Quantified total number of $CD31^+CD105^+$ vessels per 5x magnification field in trabecular areas of human fetal (n=5) and postnatal trabecular bone (n=4). Data represent mean ± s.e.m. **p <0.01, two-tailed unpaired t-test.

Figure S4

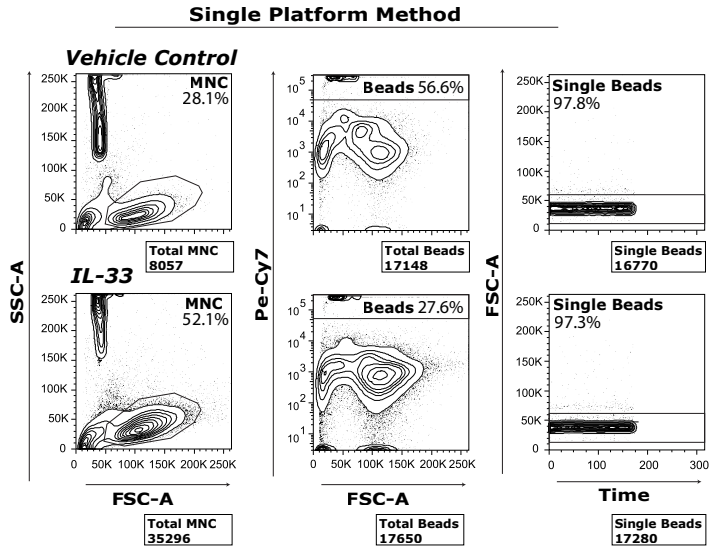

Supplementary Figure 4. Related to Figure 5. Representative FACS plots of cord blood stem/progenitor cells exposed to recombinant IL-33 for one week

Top, representative example of the single platform flow cytometric assay to quantify total cell number. Total number of mononuclear cells were calculated using the total number of MNC and beads events recorded using the quantification formula described in Experimental Procedures. Note that the MNC/Beads ratio in the vehicle control (VC) sample approximates 0.5, whereas the IL-33 treated sample is 2.0, indicating an a 4-fold increase of MNC in comparison with VC.

Bottom, characterization of the MNCs based on CD marker expression. $CD34^{+}CD38^{lo}$ MNCs were identified as hematopoietic stem and progenitor cells (HSPCs). HSPCs were further subdivided based on CD90 and CD45RA expression. $CD90^{+}CD45RA^{-}$ cells were defined as hematopoietic stem cells (HSCs), CD90-$CD45RA^{-}$ cells classified as multipotent progenitor cells (MPP), and $CD90^{-}CD45RA^{+}$ cells as multilymphoid progenitors (MLP).

Figure S5

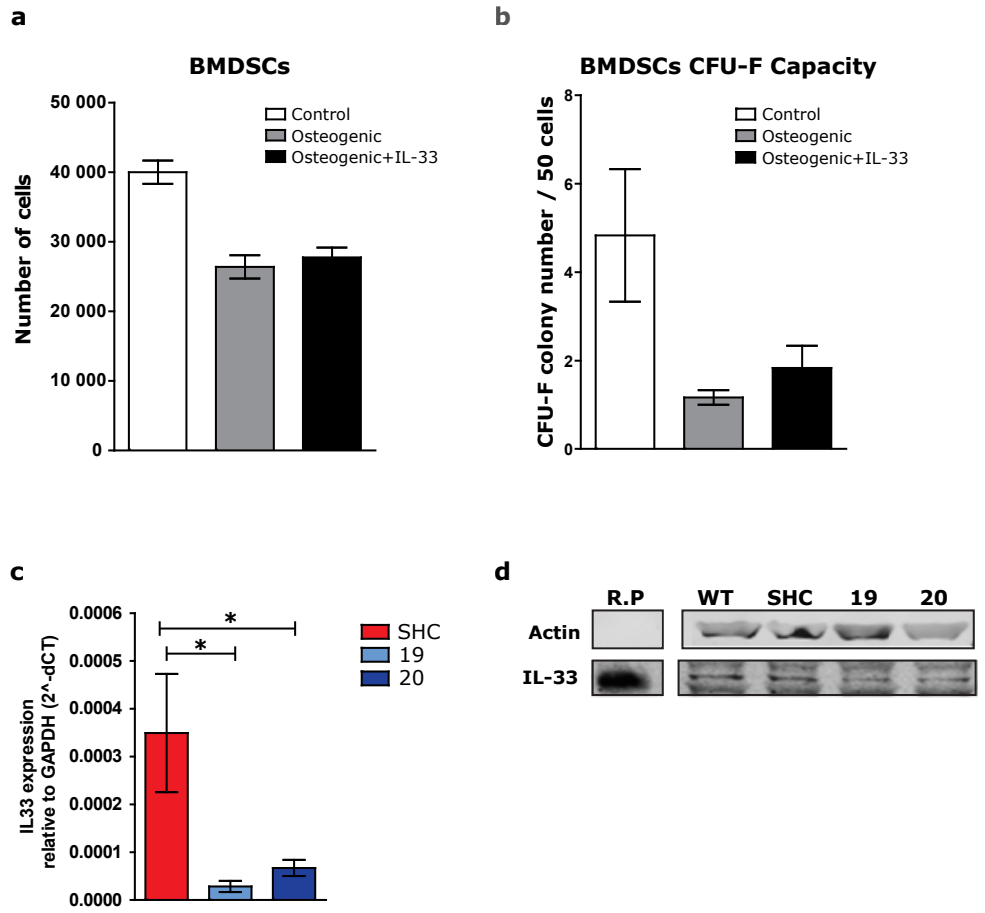

Supplementary Figure 5. Related to Figure 6. Effect of recombinant IL-33 on bone marrow-derived stromal cells and validation of shRNA-mediated IL-33 knockdown in HUVECs

a,b. The total number of bone marrow-derived mesenchymal cells (BMDSCs) and their CFU-F capacity is not affected after treatment with recombinant IL-33 in osteogenic conditions. (a) Quantification of the total number of BMDSCs kept in regular culture medium (n=2), osteogenic induction medium (n=2) and osteogenic induction medium containing recombinant IL-33 (n=2). (b) Quantification of the colony-forming unit-fibroblast (CFU-F) capacity of BMDSCs kept in regular culture medium (n=2), osteogenic induction medium (n=2) and osteogenic induction medium containing recombinant IL-33 (n=2).

c,d. Validation of shRNA-mediated IL-33 knockdown in HUVECs. (c) Transcript analysis of IL-33 by quantitative polymerase chain reaction (qPCR) demonstrates efficient knockdown of IL-33 in HUVECs transduced with two independent shRNA (sh19 and sh20) compared to a scramble hairpin control (SHC). (n= 4 independent experiments). (d) Representative Western Blot analysis confirming knockdown of IL33 at the protein level. R.P=recombinant protein IL-33. Protein ladder has been cropped out from both gel figures.

Data represent mean ± s.e.m. *p <0.05, two-tailed unpaired t-test.

Figure S6

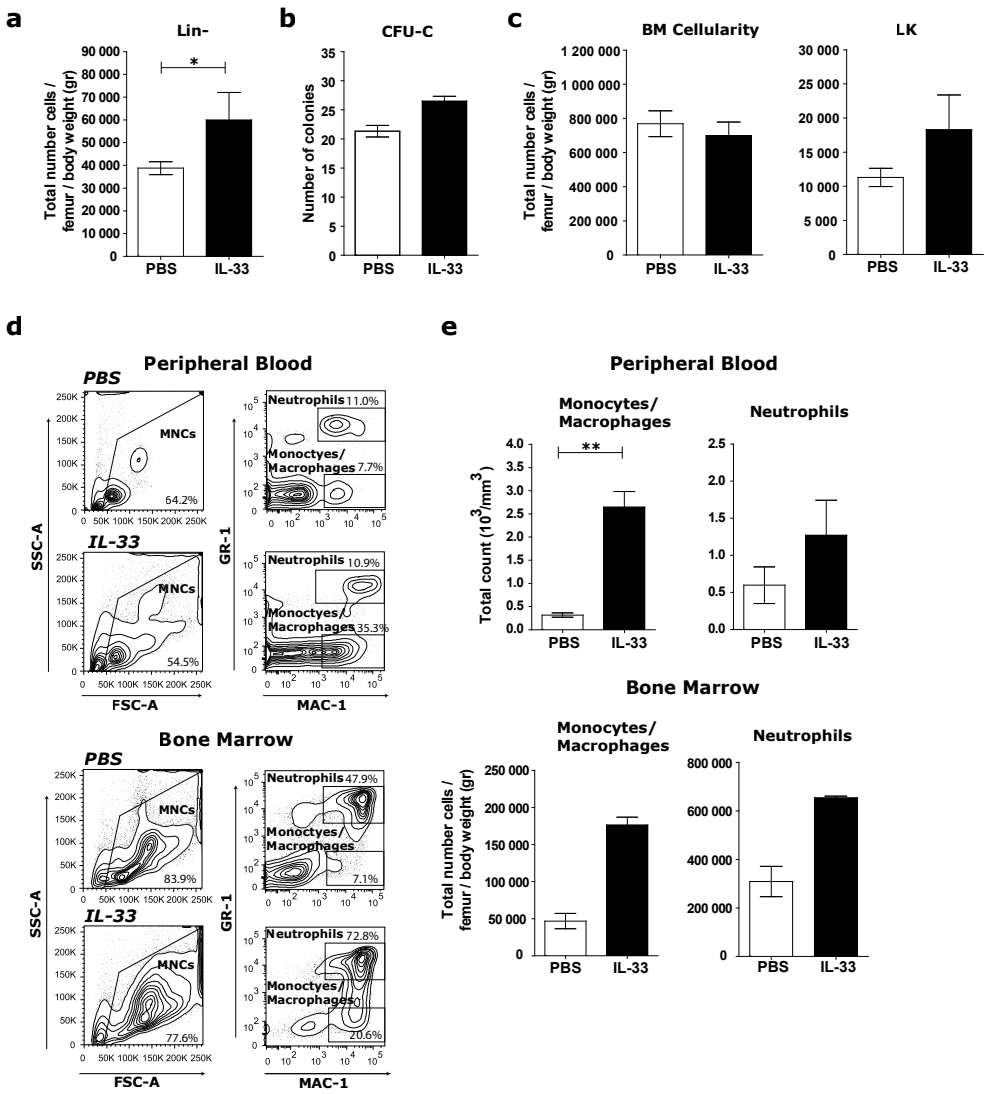

Supplementary Figure 6. Related to Figure 7. IL-33 promotes expansion of myeloid cells

a. Total lineage-negative cell counts in PBS (n=10) and IL-33 treated (n=5) mice. Data represent mean ± s.e.m. *p<0.05, unpaired t-test.

b. Colony-forming assay (CFU-C) on total BM of PBS (n=2) and IL-33 (n=2) treated mice. Data represent mean ± s.e.m. Experiments were performed in triplicate.

c. Total bone marrow cellularity and Lin-, c-KIT+, Sca-1- cell counts in PBS (n=10) and IL-33 treated (n=5) mice. Data represent mean ± s.e.m.

d. Representative FACS plots demonstrating an increased frequency of monocytes/macrophages in the peripheral blood (PB) and bone marrow (BM) of IL-33 treated mice.

e. Total PB and BM counts of monocytes/macrophages and neutrophils in PBS-treated (n=3 for PB and n=2 for BM) and IL-33 treated (n=3 for PB and n=2 for BM) mice.

Data represent mean ± s.e.m. **p<0.01, two-tailed unpaired t-test.

Figure S7

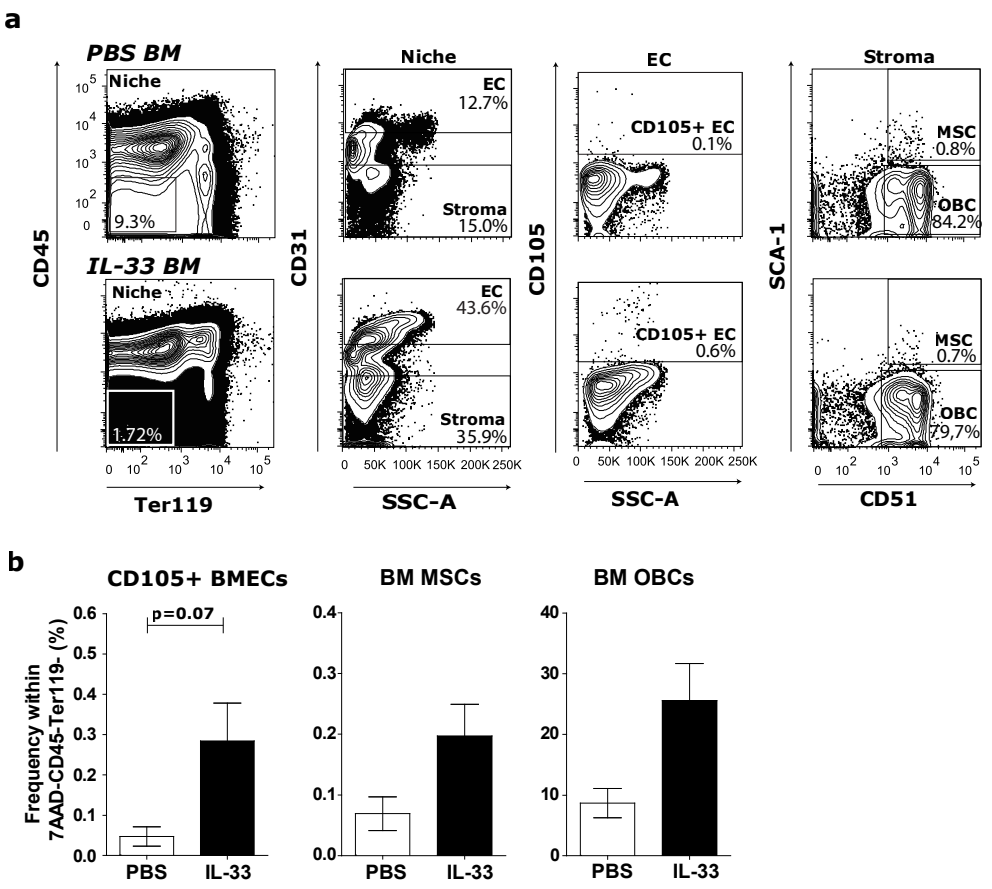

Supplementary Figure 7. Related to Figure 7. Recombinant IL-33 alters the architecture of the BM niche

a,b. Representative FACS plots of PBS (n=3) vs IL-33 treated (n=3) mice depicting the distribution of niche ($CD45^-Ter119^-$) cells within the BM. ECs were identified by CD31. Stromal ($CD31^-$) cells were further defined as SCA-1+CD51+ cells (MSCs) or SCA-1-CD51+ cells (OBCs). IL33 administration resulted in a relative increase of $CD31^+CD105^+$, MSC and OBC populations within the niche.

Data represent mean ± s.e.m. *p<0.05, two-tailed unpaired t-test.

SUPPLEMENTAL EXPERIMENTAL PROCEDURES

Cell isolation from human bone (marrow)

Freshly obtained BM aspirates of AML Day 17 patients were diluted 1:25 with red blood cell lysis solution (NH4Cl 0.155 M, KHCO3 0.01 M, EDTA-Na2.2H2O 0.1 M, pH 7.4) and incubated for 10 min at room temperature. Mononuclear cells (MNCs) were collected by centrifugation and washed once with PBS+0.5%FCS.

Fetal BM MNCs were isolated by gently crushing fetal long bones (femora, tibiae, fibulae, humeri, radii and ulna) in PBS+0.5%FCS using a mortar and pestle and passing subsequent cell suspension through a 40-µm filter in a 50 ml collection tube. Simultaneously, bone fragments were digested with 0.25% collagenase type I (Stem Cell. Cat#07902) for 45 minutes at 37°C, vortexing every 15 minutes. Excess PBS was added to the solution and filtered through a 40-µm filter in a collection tube. Next, both BM and bone fragment cell suspensions were washed once with PBS+0.5%FCS and were subsequently cleared from erythrocytes with IOtest3 lysing solution (Beckman Coulter. Cat#A07799), according to manufacturer's instructions.

For adult hip bone cells, trabecular bone was gently crushed using a mortar and pestle and resulting bone fragments were processed as described for fetal bone cells.

Fluorescence active cells-sorting (FACS) of human BM niche cells

Prior to cell sorting, FACS antibody incubations were performed in PBS+0.5%FCS for 20 minutes on ice in the dark with the following antibodies using optimized dilutions: CD45 (clone HI30, 1:100), CD271 (clone ME20.4, 1:100), CD235a (clone HI264, 1:100), CD31 (clone WM59, 1:100), CD9 (clone HI9a, 1:100) from Biolegend, and CD105 (clone SN6, 1:50) from eBioscience. The indicated populations of interest were sorted using a FACS ARIAIII Cell Sorter (BD Biosciences). Dead cells were gated out using 7AAD (Stem-Kit Reagents) after MNC selection and doublets exclusion. For RNASeq, cells were directly sorted in 800µl Trizol (Ambion) for RNA isolation. RNAse free non-stick micro-tubes (Ambion) were used to prevent pre-digestion of RNA.

Flow cytometry on murine peripheral blood and bone (marrow) cells

To identify murine hematopoietic stem and progenitor cells (HSPCs), BM cells were first co-stained with a cocktail of biotin-labelled antibodies against the following lineage (Lin) markers: Gr1 (RB6-8C5), Mac1 (M1/70), Ter119 (TER-119), CD3e (145-2C11), CD4 (GK1.5), CD8 (53-6.7) and B220 (RA3-6B2) (all from BD Biosciences). After washing, cells were incubated with Pacific Orange-conjugated streptavidin (Life Technologies) and the following antibodies: APC anti-c-Kit (2B8), PE anti-CD34 (HM34), Pacific Blue anti-Sca1 (D7), Alexa Fluor 700 anti-CD48 (HM48-1), PE-Cy7 anti-CD150 (TC15-12F12.2) (all from Biolegend), and APC/Cy7 anti-CD16/32 (56054, from BD Biosciences). To analyze murine differentiated cells, we used APC anti-Gr1 (RB6-8C5), PE-Cy7 anti-Mac1 (M1/70), Pacific Blue anti-B220 (RA3-6B2) antibodies (all from Biolegend). To define murine niche cells, BM and bone fraction cell suspensions were stained with the following antibodies: APC-Cy7 anti-CD45.2 (104), BV510 anti-Ter119 (TER-119), PE-Cy7 anti-CD105 (MJ7/18), PE anti-CD51 (RMV-7), Pacific Blue anti-Sca1 (D7) (all from Biolegend), and PE-CF594 anti-CD31 (MEC 13.3, BD Biosciences). IL-33 expression was assessed in BM cells fixed and permeabilized with Cytofix/Cytoperm Fixation/Permeabilization Solution Kit (BD Biosciences) by incubating cells with PE anti-IL33 (IC3626P, R&D Systems) diluted in 1X Perm/Wash buffer (BD Biosciences).

CD31 and CD105 in situ immunofluorescence and immunohistochemistry

4 µm thick sections of paraffin-embedded BM biopsies were obtained from benign lymphoma patients without evidence of intramedullary localization. Fetal femurs were fixed in 4% formaldehyde for 24 hours and decalcified in 12.5% EDTA overnight. Fetal femurs were subsequently embedded in paraffin and sliced with a Micron HM355Smicrotome (Thermo Scientific) to create 4 µm thick sections.

For in situ immunofluorescence, deparaffinizing and antigen retrieval of the sections were performed with CC1 (Ventana 900-124) at 97oC for 64 minutes in a Ventana BenchMark ULTRA automatic staining system (Ventana Medical Systems, Tuscon, AZ). Next, murine anti-human CD31 (Cell Marque 760-4378) and rabbit anti-human CD105 (Genetex GTX100508_25ul,1:100) primary antibodies were manually added to the sections and incubated in the Ventana BenchMark ULTRA automatic staining system for 60 minutes at 36oC. After thorough washing with PBS/Tween 0.1%, sections were incubated for 30 minutes with a biotinylated rabbit anti-mouse secondary antibody lacking the FC fragment (DAKO E413), followed by washing in PBS/Tween20 0.1% and a 30 minute incubation with Cy™3-streptavidin (Jackson ImmunoResearch 016-0160-084). Next, avidin/biotin blocking was performed (Vector Laboratories P-2001). After thorough washing with PBS/Tween 0.1%, sections were incubated for 30 minutes with a biotinylated swine anti-rabbit secondary antibody (DAKO E431), followed by washing in PBS/Tween20 0.1% and a 30 minute incubation with FITC- streptavidin (Jackson ImmunoResearch 016-010-084). Finally, sections were mounted with DAPI-containing (1:2.000) vectashield (Vector Laboratories H-1000). 20x magnified Z-series images were acquired with a Leica TCS SP5 confocal microscope using the LAS software (Leica Microsystems). Briefly, after deparaffinization sectioned specimens were processed for 64-minute antigen retrieval with CC1. After 20-minute incubation at 36°C with either previously described primary antibodies for CD31 and CD105 (1:500), detection was performed using UltraView DAB IHC Detection Kit (760-500, Ventana). The sections stained with CD31 and CD105 were counterstained with hematoxylin II (Ventana Ref.: 790-2208). Images were acquired with a ZEISS AxioPhot microscope using cellSens Entry 1.9 software (Olympus Corporation).

IL-33 immunofluorescence

FACS-isolated hRECs, obtained from fetal bones and BM, were collected in PBS, cytospun on a glass slide for 3 minutes at 500 rpm using a Cytospin 4 centrifuge (Thermo Scientific), and fixed in 3% PFA/PBS for 15 minutes on ice. After washing with PBS 3 times, cells were permeabilized for 2 minutes in 0.15% Triton-X100/PBS and then incubated in 1%BSA/PBS for 1 hour at room temperature to block aspecific binding sites. Cells were next stained overnight at 4°C with polyclonal goat anti-human IL-33 antibody (AF3625, R&D, 20 µg/ml in 1%BSA/PBS) or goat IgG isotype control antibody(Catalog # AB-108-C). Slides were washed twice with PBS for 5 minutes and incubated for 1 hour at 37°C with Alexa Fluor 488-conjugated donkey anti-goat antibody (A-11055, Invitrogen, 1:200, in 1%BSA/PBS). After 2 washes in PBS, slides were mounted in VECTASHIELD Mounting Medium with DAPI (Vector Laboratories). 63x magnified Z-series images were acquired with a Leica TCS SP5 confocal microscope using the LAS software (Leica Microsystems). For *in situ* immunohistochemistry consecutive serial sections of the benign lymphoma patients and fetal femur biopsies were stained for hematoxylin and eosin, CD31 and CD105 separately with the Ventana Benchmark Ultra automated staining system.

Hematopoietic stem progenitor cell isolation from umbilical cord blood

Umbilical cord blood (CB) was collected in a 300 ml bag filled with 20ml of the anticoagulant citrate phosphate dextrose (T2950, Fresenius Kabi), after receiving informed consent from the mother, and retrieved within 24 hours after collection. MNCs were obtained by using a standard Ficoll gradient protocol (1114547, Axis-Shield). CD34+ CB HSPCs were further isolated by magnetic-activated cell sorting (MACS). Briefly, MNCs were incubated with a magnetically coated anti-CD34 antibody (120-000-268, Miltenyi Biotec) and FcR blocking reagent (120-000-265, Miltenyi Biotec) in MACS buffer at 4°C for 30 minutes. After washing, CD34+ CB HSPCs were isolated using a LS column (130-042-401, Miltenyi Biotec) and purity was further enriched by performing an additional MACS selection using two MS columns (130-042-201, Miltenyi Biotec). Purity of the isolated cell population was confirmed with fluorescence-activated cell sorting (FACS).

Quantification and multiparametric immunophenotyping of cultured CB CD34+ cells

Cultured CB cells were thoroughly resuspended and collected for the single platform flowcytometric assay (to determine absolute cell counts) and for immunophenotyping (to specify HSPC subpopulations), respectively. For the single platform flowcytometric assay, cultured cells were incubated with CD34-PE-Cy7 (348811, BD Biosciences, 1:50) and CD45-PE-Cy5 (557075, BD Biosciences, 1:50) antibodies, and a calibrated number of flow-count fluorosphere beads (7547053, Beckman Coulter). In addition, 4',6-diamidino-2-phenylindole (DAPI) (1:5.000) was used to distinguish between living and dead cells. The total number of living MNC per µl in (n) a well was calculated using the following formula: n= ((number of MNC events recorded * bead concentration)/number of recorded single beads)/ (volume cells/ volume beads). For immunophenotyping, cultured cells were incubated with Lin-FITC (22-7778-72, eBiosciences, 1:25), CD34-PE-Cy7 (348811, BD Biosciences, 1:50), CD38-PerCP-Cy5.5 (561106, BD Pharmingen, 1:60), CD90-PE (12-0909-42, eBiosciences, 1:30), CD45RA-APC-H7 (560674, BD Pharmingen, 1:30) and DAPI. Antibody incubation for FACs took place as previously described. The total number of a specific subpopulations was determined by multiplying the absolute number of living MNCs with the frequencies of the populations, determined with immunophenotyping, of interest. Flowcytometric analysis was performed using a BD LSRII (BD Biosciences, San Jose, CA, USA) and data was analyzed using FlowJo software (Tree Star Inc, Ashland, OR, USA).

Human hematopoietic colony forming-unit assay

To further assess the effect of recombinant human IL-33 on the hematopoietic potential of cultured CB cells, we performed a colony-forming unit assay (CFU). Input equivalent of 2000 7-days cultured CD34+ cells of each condition (rhIL-33 vs vehicle control) was resuspended in 400 µl Iscove's Modified Dulbecco's Medium (IMDM) and transferred to 3.6 ml of methylcellulose (MethoCult H84434, StemCell Technologies). Cells were then plated in triplicate in 1 cm^2 petri-dishes(1 ml/dish) and were kept at 37ºC and 5% CO2. Colonies were counted after 12-14 days.

Osteogenic differentiation and mineralization assays

BMDSC extracts were harvested at the end of culture by scraping the cells in PBS/triton 1% and storing them at −80 °C for biochemical analyses (Bruedigam et al., 2011). After scraping, PBS/triton 1%/0.24 M HCL was added to the wells and kept overnight at 4 °C to release calcium ions from the matrix deposition. Cell extracts were briefly sonicated (Soniprep 150, Sanyo) to produce cell lysates and incubated overnight with 6 M HCL. In short, calcium content was determined colorimetrically by adding o-cresolphthalein complexone to the well contents and cell lysates and measuring the absorbance of the resulting chromophore-complex at 595 nm.

Alternatively, cells were fixed in 70% ethanol (vol/vol) on ice for an hour and after washing with PBS, stained for 10–20 min with alizarin Red S solution (saturated Alizarin Red S (Sigma) in demineralized water adjusted to pH 4.2 using 0.5% ammonium hydroxide).

Human bone marrow fibroblast colony-forming unit assay

BMDSCs were first either cultured in αMEM medium containing 10% heat-inactivated FCS, or osteogenic induction medium containing recombinant human IL-33 (250 ng/ml) or mQ vehicle control for 1 week. After culture, total number of cells per condition were quantified with a Bürker counting chamber. Next, 50 cells per 0.32 cm2 (1 well of a 96-well plate) were seeded in αMEM supplemented with 20% fetal bovine serum and 1% penicillin/

streptomycin. On day 14, dishes were fixed with 70% ethanol (vol/vol) and stained with Giemsa. CFU-F colonies were counted as previously described (Chen et al., 2016).

Validation of IL-33 knockdown in HUVECs

For transcriptional analyses, HUVECs were harvested and collected after puromycin selection in TRIzol Reagent (Life Technologies). RNA isolation, conversion to cDNA and qPCR were performed accordingly to previously described methods (Zambetti et al., 2015) using the SuperScript II Reverse Transcriptase (Thermo Fisher Scientific). For qPCR, expression levels were obtained using the ddCt method using GAPDH as an internal control. The following primers were used: GAPDH-Fw: GTCGGAGTCAACGGATT; GAPDH-Rv: AAGCTTCCCGTTCTCAG; IL-33-Fw: GGAAGAACACAGCAAGCAAAGCCT; IL-33-Rv: TAAGGCCAGAGCGGAGCTTCATAA.

For protein analyses, cells were lysed in Carin lysis buffer (20 mM Tris-HCl pH 8.0, 138 mM NaCl, 10mM EDTA, 100 mM NaF, 1% Nonidet P-40, 10% glycerol, 2mM NA-vanadate) supplemented with 0.5 mM DTT and the protease inhibitor SigmaFast (Sigma Aldrich). Equal amounts of proteins were denatured and separated on a Novex NuPage 4-12% Bis-Tris Gradient gel (Life Technologies) and transferred to Protran BA83 blotting paper (GE Healthcare Sciences). After blocking with 5% BSA, membranes were incubated overnight at 4°C with a polyclonal goat anti-IL-33 primary antibody (AF3625, R&D systems). Actin was used as a loading control and detected with a mouse anti-actin antibody (A5441 Sigma Aldrich). Western blots were scanned and processed using an Odyssey Infrared Imager (Li-COR Biosciences).

To monitor the expansion of HUVECs after shRNA mediated knockdown of IL-33 after puromycin selection, HUVECs were re-plated and seeded at 300.000 cells in a T-25 flask and grown in EGM-2 medium containing 2µg/ml of puromycin. HUVECs were passaged every 2 to 4 days and total number of cells were quantified using a Casy counter (Roche Innovatis).

Murine hematopoietic colony forming-unit assay

To assess the myeloid progenitor capacity of whole BM from mice treated with PBS or IL-33, BM cells were cultured in methylcellulose containing murine SCF (10 ng/ml), IL-3 (100 ng/ml, purified from supernatant of CHO cells), IL-6 (10 ng/ml) and GM-CSF (10 ng/ml). Cytokines were purchased from PeproTech, if not otherwise mentioned. Specifically, 20000 BM cells per condition were resuspended in 400 µl IMDM and transferred to 3.6 ml of Methocult 3231 (StemCell Technologies). Cells were then plated in triplicate in 1 cm^2 petri-dishes(1 ml/dish) and were kept at 37ºC and 5% CO2. Colonies were counted after 5-7 days.

SUPPLEMENTAL REFERENCES

Bruedigam, C., van Driel, M., Koedam, M., van de Peppel, J., van der Eerden, B.C.J., Eijken, M., van Leeuwen, J.P.T.M., 2011. Basic techniques in human mesenchymal stem cell cultures: Differentiation into osteogenic and adipogenic lineages, genetic perturbations, and phenotypic analyses. Curr. Protoc. Stem Cell Biol. 1–20. doi:10.1002/9780470151808.sc01h03s17

Doan, P.L., Russell, J.L., Himburg, H.A., Helms, K., Harris, J.R., Lucas, J., Holshausen, K.C., Meadows, S.K., Daher, P., Jeffords, L.B., Chao, N.J., Kirsch, D.G., Chute, J.P., 2013. Tie2(+) bone marrow endothelial cells regulate hematopoietic stem cell regeneration following radiation injury. Stem Cells 31, 327–37. doi:10.1002/stem.1275

Gur-Cohen, S., Itkin, T., Chakrabarty, S., Graf, C., Kollet, O., Ludin, A., Golan, K., Kalinkovich, A., Ledergor, G., Wong, E., Niemeyer, E., Porat, Z., Erez, A., Sagi, I., Esmon, C.T., Ruf, W., Lapidot, T., 2015. PAR1 signaling regulates the retention and recruitment of EPCR-expressing bone marrow hematopoietic stem cells. Nat. Med. 21, 1307–17. doi:10.1038/nm.3960

Kopp, H.G., Avecilla, S.T., Hooper, A.T., Shmelkov, S. V., Ramos, C.A., Zhang, F., Rafii, S., 2005. Tie2 activation contributes to hemangiogenic regeneration after myelosuppression. Blood 106, 505–513. doi:10.1182/blood-2004-11-4269

Nakamura-Ishizu, A., Okuno, Y., Omatsu, Y., Okabe, K., Morimoto, J., Uede, T., Nagasawa, T., Suda, T., Kubota, Y., 2012. Extracellular matrix protein tenascin-C is required in the bone marrow microenvironment primed for hematopoietic regeneration. Blood 119, 5429–5437. doi:10.1182/blood-2011-11-393645

Winkler, I.G., Barbier, V., Nowlan, B., Jacobsen, R.N., Forristal, C.E., Patton, J.T., Magnani, J.L., Lévesque, J.-P., 2012. Vascular niche E-selectin regulates hematopoietic stem cell dormancy, self renewal and chemoresistance. Nat. Med. 18, 1651–7. doi:10.1038/nm.2969

Zambetti, N.A., Bindels, E.M.J., Van Strien, P.M.H., Valkhof, M.G., Adisty, M.N., Hoogenboezem, R.M., Sanders, M.A., Rommens, J.M., Touw, I.P., Raaijmakers, M.H.G.P., 2015. Deficiency of the ribosome biogenesis gene Sbds in hematopoietic stem and progenitor cells causes neutropenia in mice by attenuating lineage progression in myelocytes. Haematologica 100, 1285–1293. doi:10.3324/haematol.2015.131573

3

ENDOTHELIAL-DERIVED MESENCHYMAL CELLS CONTRIBUTE TO HEMATOPOIETIC NICHE FORMATION IN HUMANS

RUNNING TITLE: A HUMAN BONE MARROW ENDOTHELIAL PRECURSOR FOR MULTIPOTENT STROMAL CELLS

Keane Jared Guillaume Kenswil[1], Gonzalo Sánchez-Duffhues[2], Andrea Lolli[3], Claire van Dijk[1], Callie Knuth[3], Byambasuren Vanchin[4], Adrian Christopher Jaramillo[1], Remco Michiel Hoogenboezem[1], Tom Cupedo[1], Eric Moniqué Johannes Bindels[1], Bianca Blom[5], Pieter Koen Bos[6], Marie-Jose Goumans[2], Peter ten Dijke[2,7], Eric Farrell[3], Guido Krenning[4], Marc Hermanus Gerardus Petrus Raaijmakers[1,8,*]

[1]Department of Hematology, Erasmus MC Cancer Institute, Rotterdam 3015CN, The Netherlands.
[2]Department of Cell and Chemical Biology, Leiden University Medical Centre, Leiden 2300 RC, The Netherlands.
[3]Department of Oral and Maxillofacial Surgery, Erasmus MC, University Medical Center Rotterdam, Rotterdam 3000 DR, The Netherlands.
[4]Cardiovascular Regenerative Medicine Research Group, Department of Pathology and Medical Biology, University Medical Center Groningen, University of Groningen, Groningen 9713 GZ, The Netherlands.
[5]Department of Cell Biology & Histology, Center for Immunology of Amsterdam, Academic Medical Center, University of Amsterdam, Amsterdam 1105 AZ, The Netherlands.
[6]Department of Orthopaedics, Erasmus MC, Rotterdam 3015CE, The Netherlands.
[7]Oncode Institute, Leiden University Medical Centre, Leiden 2300 RC, The Netherlands.
[8]Lead Contact: m.h.g.raaijmakers@erasmusmc.nl
*Correspondence: m.h.g.raaijmakers@erasmusmc.nl, tel: +31107043756

Manuscript in submission

Graphical Abstract

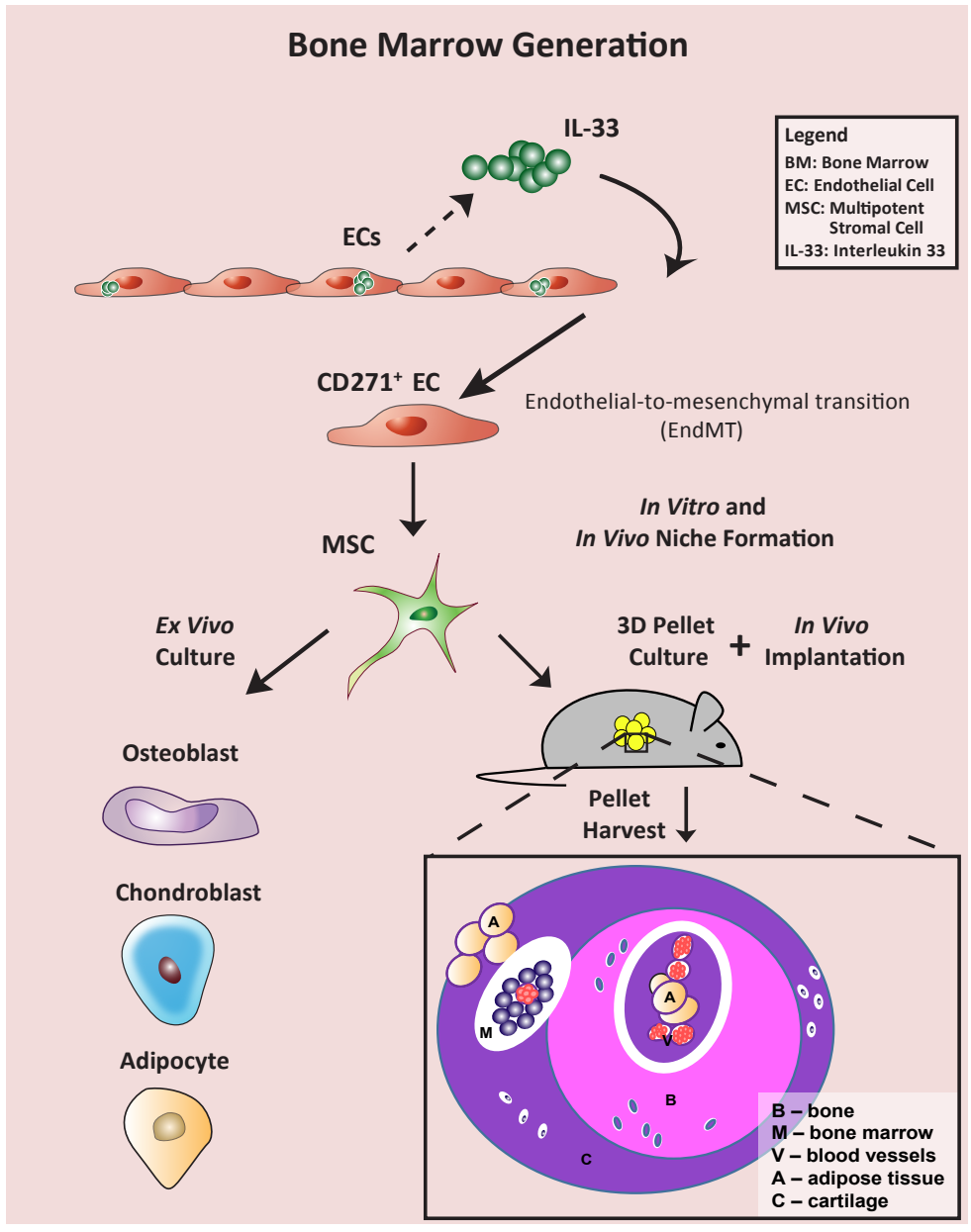

Highlights

1. LNGFR$^+$ ECs emerge in the human bone marrow during development and regeneration
2. LNGFR$^+$ ECs are the result of EndMT and capable of hematopoietic niche formation
3. Endothelial-derived BM mesenchymal cells constitute a distinct niche subset in mice
4. IL-33 drives the conversion of human ECs to MSCs

eTOC Blurb

Endothelial cells (ECs) may contribute to tissue development and regeneration. Here, Kenswil et al. identify specialized ECs in the human bone marrow with the potential to generate the hematopoietic niche by IL-33 driven acquisition of mesenchymal stemness and multilineage differentiation capacity. This finding is anticipated to instruct novel insights into bone marrow disease and herald novel directions for bone and marrow regeneration.

ABSTRACT

Mesenchymal multipotent stromal cells (MSCs) in the bone marrow (BM) play pivotal roles in tissue maintenance and regeneration. Their origins, however, remain incompletely understood. Here, we identify a rare subset of endothelial cells (ECs) in the human BM that expresses mesenchymal markers, including low-affinity nerve growth factor receptor (LNGFR/CD271). LNGFR$^+$ ECs are prevalent during fetal development and re-emerge during regeneration after injury. They display transcriptional reprogramming consistent with endothelial-to-mesenchymal transition (EndMT), reflected in their potential to generate colony-forming unit fibroblasts (CFU-Fs) with multilineage skeletogenic differentiation and *in vivo* BM niche-forming capacity. Lineage tracing in mice confirmed the endothelial origin of distinct mesenchymal cells expressing hematopoietic niche factors. Mechanistically, IL-33, overexpressed in EC subsets, is identified as a driver of EndMT via ST2-receptor signaling. The data reveal *de novo* generation of MSCs from ECs in BM formation. Elucidation of its molecular programs may instruct novel directions for human tissue regeneration.

Keywords

Niche; development; regeneration; endothelial; mesenchymal; transdifferentiation; endothelial-mesenchymal transition (EndMT); hematopoietic stem cell

INTRODUCTION

Mesenchymal multipotent stromal cells (MSCs) contain adult putative stem cells that emerge during development and have a, tissue-restricted, multilineage differentiation capacity (Bianco et al., 2008; Dominici et al., 2006). In the bone marrow (BM), mesenchymal MSCs are a heterogeneous population with putative roles in maintaining tissue homeostasis and driving regeneration of the tissue after injury (Kfoury and Scadden, 2015). Mesenchymal cells in the BM play critical roles in skeletogenesis (Chan et al., 2015; Worthley et al., 2015) and they are components of the hematopoietic stem cell niche (Greenbaum et al., 2013; Méndez-Ferrer et al., 2010). The ability to expand these cells *ex vivo* and differentiate them into different mesenchymal lineages has made them attractive candidates to explore a potential role in regenerative medicine and tissue engineering (Galipeau and Sensébé, 2018).

The origin of BM MSCs remains incompletely understood. The prevailing notion is that a reservoir of tissue-specific MSCs is generated during development. These pools of 'primordial' MSCs may be derived from different germ layers, i.e. the paraxial or lateral plate mesoderm (Olsen et al., 2000) and the neural crest (Isern et al., 2014; Morikawa et al., 2009a; Takashima et al., 2007), and serve as ontogenically distinct ancestors of stromal cells with heterogeneous function in the postnatal marrow (Kfoury and Scadden, 2015).

A key open question remains whether the BM tissue pool size of MSCs is developmentally restricted or that it can be modulated by *de novo* generation of MSCs in conditions of tissue demand, such as injury. Endothelial cells (ECs) are among the first cells to reemerge in the BM after injury (Rafii et al., 2016) and orchestrate tissue development, maintenance, and regeneration by providing instructive angiocrine signals (Ramasamy et al., 2015). Specific subsets of ECs that drive regeneration of the bone and BM have recently been identified in mice (Kusumbe et al., 2014, 2016; Ramasamy et al., 2016) and their human counterparts are beginning to be identified (Kenswil et al., 2018).

ECs can be coerced *ex vivo* towards mesenchymal cells through a process of transdifferentiation called endothelial-to-mesenchymal transition (EndMT) (Dejana et al., 2017; Sanchez-Duffhues et al., 2016). Human umbilical vein ECs (HUVECs) have been reported to transition into mesenchymal cells with multipotent stem-like properties under defined experimental conditions *ex vivo* (Medici et al., 2010), but the relevance of this finding to human bone physiology has remained controversial.

Here, we identify an EC type in the human BM that appears under conditions requiring tissue formation with the capacity to generate mesenchymal multipotent stem cell-like cells able to reconstitute the entire hematopoietic niche *in vivo*. Lineage tracing experiments in mice confirm a robust contribution of specialized, endothelial-derived, mesenchymal cells to the hematopoietic BM niche. Interleukin (IL)-33 is identified as a novel factor driving the conversion of human ECs to such 'mesenchyme-primed' ECs.

RESULTS

Identification of a rare LNGFR-expressing human EC enriched in regenerative and fetal bone marrow

Recently, we identified human ECs associated with BM regeneration and development (Kenswil et al., 2018). These Endoglin (CD105) expressing ECs, dubbed $CD31^+CD9^+CD105^+$ human Regeneration-associated ECs (or hRECs), constituted a fraction of ECs, emerging during fetal development and regeneration after chemotherapy (conditions in which angiogenesis, hematopoiesis and osteogenesis are tightly coupled) with a distinct transcriptional landscape (Kenswil et al., 2018). Interestingly, when examining the transcriptome of hRECs we observed expression of transcripts typically associated with mesenchymal cell fates, including *MCAM* (CD146), *THY1* (CD90), and *NGFR* (CD271) (Table S1), suggesting the possibility that a subset of hRECs with mesenchymal properties might exist during human fetal development.

Protein expression of LNGFR (CD271), a well-established marker of primary human BM mesenchymal cells (Jones et al., 2010; Quirici et al., 2002; Tormin et al., 2011), encoded by the *NGFR* gene, was confirmed in a subset of fetal hRECs by flow-cytometry (Figure 1A, B). This subset of LNGFR-expressing hRECs was virtually absent in human adult BM under steady state (isolated from healthy BM donors) (0.27% ± 0.1 of $CD31^+CD9^+$ ECs), but highly enriched in human fetal BM (gestational weeks 15-20) (6.47% ± 1.5 of $CD31^+CD9^+$ ECs; one-way ANOVA [$p< 0.0001$], followed by Bonferroni's Multiple Comparison Test [$p=0.001$]), and human BM upon recovery following chemotherapeutic injury (17 days after start of chemotherapy for acute myeloid leukemia [AML]) (Kenswil et al., 2018) (1.15% ± 0.3 of the $CD31^+CD9^+$ EC population, Bonferroni's Multiple Comparison Test [$p=0.14$]). In addition, $LNGFR^+$ hRECs expressed other *bona fide* markers of endothelium such as CD34 and CD144 (VE-Cadherin) (Figure 1C, D), stressing their endothelial identity.

Previously, we showed that hRECs are enriched in collagenase treated human bone fractions (Kenswil et al., 2018). $LNGFR^+$ cells were identified within this hREC fraction both in collagenased adult bone (obtained from patients undergoing hip replacement surgery) (2.7% ± 0.7 of $CD31^+CD9^+$ ECs) (Figure S1A, S1B) and fetal bone fractions (4.1% ± 1.0 of $CD31^+CD9^+$ ECs) (Figure S1A, S1B).

Finally, to exclude the possibility that co-expression of both endothelial and mesenchymal markers reflects close proximity of two cells (identified as a single event in flow cytometry despite 'doublet' exclusion), $LNGFR^+$ hRECs were sorted by fluorescence-activated cell sorting (FACS) and co-expression of CD31, CD105, and LNGFR was confirmed at the single cell level by immunocytochemistry (Figure 1E, Figure S1C-E).

Taken together, the data demonstrates that a rare subtype of $LNGFR^+$ hREC exists in the human bone and marrow that is highly enriched in frequency during development and regeneration.

LNGFR-expressing ECs display a molecular signature of cells undergoing endothelial-to-mesenchymal transition

We next hypothesized that this rare EC subtype might reflect specialized endothelium with the capacity to convert to a mesenchymal cell fate. ECs undergoing EndMT have previously been characterized by down-regulation of endothelial makers and increased expression of mesenchymal markers (Dejana et al., 2017; Souilhol et al., 2018).

To begin addressing in more detail whether $LNGFR^+$ hRECs ($CD31^+CD9^+CD105^+$ cells) fulfill this criterium, we interrogated by massive parallel RNA sequencing the transcriptome of highly FACS-purified $LNGFR^+$ hRECs, in comparison to other endothelial ($LNGFR^-$ hRECs) and mesenchymal ($CD31^-LNGFR^+$ mesenchymal cells) subsets sorted from the same BM samples. Hierarchical clustering by principal component analysis of transcriptomes revealed a strikingly separate clustering for the sorted endothelial and mesenchymal populations (Figure 2A). Remarkably, the transcriptome of $LNGFR^+$ hRECs clustered in-between those of $LNGFR^-$ hRECs and $CD31^-LNGFR^+$ mesenchymal cells, suggesting that $LNGFR^+$ hRECs have a transcriptional signature with similarities to both endothelial and mesenchymal cells.

Transcript analysis confirmed the robust expression of multiple *bona fide* markers of ECs in $LNGFR^+$ hRECs, including *PECAM1*, *CDH5* (encoding CD144/VE-Cadherin), and others (Figure 2B). Expression of *PECAM1* (CD31) and other endothelial markers was consistently lower in $LNGFR^+$ hRECs in comparison to $LNGFR^-$ hRECs, in line with the finding of reduced CD31 protein expression by immunocytochemistry (Figure 1E and S1C).

In addition to reduced expression of endothelial markers, $LNGFR^+$ hRECs displayed increased expression of multiple markers typically associated with primitive mesenchymal cells such as *MCAM* (CD146), *LEPR* and *PDGFRA* (CD140a) (Figure 2C) at levels comparable to those of mesenchymal BM cells. Genes encoding markers of bone progenitor cells were highly or uniquely overexpressed in $LNGFR^+$ hRECs in comparison to $LNGFR^-$ hRECs (Figure 2D).

Importantly, the distinct expression of endothelial markers confirms their endothelial nature and clearly separates these cells from perivascular stromal cells/pericytes, which lack expression of these endothelial markers (Crisan et al., 2008).

Collectively, the unique transcriptional feature of reduced expression of endothelial markers concomitant with the activation of mesenchymal programs suggests that $LNGFR^+$ hRECs may refer to ECs undergoing EndMT.

Further supporting this notion, analysis of transcriptional programs by gene set enrichment analysis (GSEA) revealed remarkable enrichment of transcriptional signatures associated with transition to mesenchymal cell fates in $LNGFR^+$ hRECs in comparison to $LNGFR^-$ hRECs (Figure 2E and S2A). Similarly, gene ontologies (GO) term analysis revealed biologic programs related to mesenchymal cells in $LNGFR^+$ hRECs, including extracellular matrix production and ossification (Table S2).

Gene sets associated with signaling pathways previously shown to regulate epithelial-mesenchymal transition (EMT) as well as EndMT, including the transforming growth factor-β (TGF-β) (Azhar et al., 2009), fibroblast growth factor (FGF) (Lee et al., 2004), Hedgehog (Syn et al., 2009), and WNT (Hurlstone et al., 2003) signaling pathways, were significantly enriched in LNGFR$^+$ hRECs (Figure S2B-E). These signaling pathways have been shown to activate the transcription factors driving EndMT (Pardali et al., 2017), including members of the Snail (Kokudo et al., 2008; Mahmoud et al., 2017), Twist (Ansieau et al., 2008; Chakraborty et al., 2010), and ZEB (Bracken et al., 2008) transcription factor families. Strikingly, many of these key transcription factors driving EndMT (*SNAI2* [Slug], *TWIST1*, *TWIST2*, *YAP1*, *ZEB2)* were overexpressed in LNGFR$^+$ hRECs compared to LNGFR$^-$ hRECs (Figure 2F). This simultaneous overexpression of transcriptional mediators has been previously described as an important feature of ECs undergoing EndMT (Wesseling et al., 2018).

Collectively, the data indicate that LNGFR$^+$ hRECs exhibit molecular characteristics congruent with ECs undergoing mesenchymal transition and might be potentially capable of giving rise to primitive mesenchymal cells and downstream differentiated progeny cell types.

LNGFR$^+$ ECs display transcriptional features of stemness and give rise to stem cell-like mesenchymal progenitors with multilineage differentiation capacity

The conversion of vascular ECs into mesenchymal stem-like cells has previously been postulated and is experimentally supported by *ex vivo* observations in HUVECs (Medici et al., 2010), but whether a primary EC with this capacity exists in the human BM, and contributes to human physiology has remained elusive. Acquisition of stem-cell defining transcriptional programs in LNGFR$^+$ hRECs was suggested by both GSEA and GO analyses (Figure 3A and Table S2). GO-term analysis further revealed enrichment of gene sets associated with skeletal and neuronal development (Table S2), suggesting that LNGFR$^+$ hRECs might have the potential to contribute to skeletogenesis.

LNGFR$^+$ hRECs, when cultured in endothelium supporting medium (EGM-2), formed a stromal layer of cells morphologically resembling fibroblasts after 6-7 days of culture (Figure 3B). Flow cytometric analyses of these stromal cells revealed robust expression of typical markers used to define MSCs (Dominici et al., 2006), including CD105, CD73, CD90, CD51, CD146 (Figure 3C) with loss of endothelial markers (CD34 and CD31) (Figure 3D).

The ability to form stromal colonies (CFU-F capacity) was restricted to LNGFR$^+$ hRECs and not found in other endothelial subsets (Table S3). Single cell sorting revealed the frequency of cells with CFU-F forming capacity within the LNGFR$^+$ hRECs to be 1 in 10 ± 0.1, in comparison to 1 in 6 ± 1.5 of CD31$^-$ LNGFR$^+$ mesenchymal cells (Figure 3E).

LNGFR$^+$ hREC-derived mesenchymal cells were able to expand extensively and demonstrated extensive serial replating capacity (performed until 15 passages without signs of exhaustion) (data not shown), indicative of the acquisition of self-renewal capacity. Multilineage differentiation capacity of mesenchymal cells derived from LNGFR$^+$ hRECs

was also demonstrated by their ability to differentiate into osteoblastic, chondrogenic and adipocytic cells under defined culture conditions (Figure 3F), thus fulfilling the criteria of the International Society for Cellular Therapy (ISCT) for mesenchymal MSCs (Dominici et al., 2006).

The vast majority of LNGFR$^+$ hRECs (> 80%) expresses CD144 (*CDH5*), as a *bona fide* and specific marker of ECs (Figure 1C and S3). To further confirm that this subset of ECs can give rise to mesenchymal progenitor cells, sorting and *ex vivo* culture of the LNGFR$^+$CD144$^+$ hREC population was performed (Figure S3A), which demonstrated that this particular endothelial subset harbors cells with the ability to form CFU-Fs with serial replating (Figure S3B) and multilineage differentiation capacity (Figure S3C-D). These *ex vivo* mesenchymal progenitors lacked protein expression of markers typical for hematopoietic and ECs (CD45, CD34, CD31, CD144) (Figure S3E), and expressed markers associated with MSCs (CD105, CD73, CD90, and CD146) (Figure S3F).

Finally, the primitive mesenchymal cells derived from LNGFR$^+$ hREC were able to support hematopoietic stem/progenitor cells (HSPCs) (Figure S4A and S4B). Co-culture of umbilical cord blood (UCB) derived CD34$^+$ HSPCs resulted in expansion of these cells to the level of CD31$^-$ LNGFR$^+$ mesenchymal cells, that have previously been shown to support expansion of HSPCs (Li et al., 2014). Hematopoietic-supporting capacity coincided with high expression of HSC regulating genes such as *VCAM1*, *SELE* and *CXCL12,* and *ANGPT1* (Figure S4C).

Taken together, the data demonstrate that LNGFR$^+$ hREC have the capacity to convert to a mesenchymal stem cell-like cell with expression of stem cell transcriptional signatures, the ability to form CFU-F with serial replating ability and multilineage differentiation capacity. These cells have the potential of contributing to BM development by transdifferentiation into bone lineages and by providing support to the nascent hematopoiesis.

LNGFR$^+$ EC-derived mesenchymal progenitors form an *in vivo* bone marrow niche

The ability of LNGR$^+$ ECs for multilineage skeletal differentiation and hematopoietic support *in vitro*, suggest that they may represent *bona fide*, *in vivo*, hematopoietic niche- (re) generating cells. These cells have previously been defined as skeletal stem cells (SSCs), clonogenic skeletal progenitors capable of establishing the hematopoietic microenvironment (Sacchetti et al., 2007).

To test whether LNGFR+ ECs-derived mesenchymal cells contain SSCs, we exploited a previously established protocol of human MSC culturing as 3D pellets in chondrogenic priming conditions followed by subcutaneous implantation in mice (Farrell et al., 2011).

LNGFR$^+$ ECs-derived mesenchymal cells obtained from fetal bone were subjected to chondrogenic differentiation as 3D pellets for 3 weeks (Figure 4A). This resulted in 3D cartilage pellet formation as shown by glycosaminoglycan production (toluidine blue and thionine staining) (Figure 4B). Chondrogenic differentiation at this point was further confirmed by expression of the chondrogenic markers *COL2A1* and *ACAN* by qRT-PCR analysis

(data not shown). Subsequently, pellets were subcutaneously implanted in recipient mice (6 pellets/pocket). After 10 weeks, µCT scans demonstrated mineralization of the pellets (Figure 4C). Following harvesting of the pellets, histological analyses revealed heterotopic ossicle formation in all harvested pellets with presence of bone, cartilage, adipocytes, blood vessels, and hematopoietic tissue (Figure 4D), establishing the *in vivo* multi-lineage skeletogenic differentiation and hematopoietic niche-forming capacity of LNGFR$^+$ ECs.

Endothelial-derived mesenchymal cells contribute to the hematopoietic niche in mice

The identification of an EC with hematopoietic niche forming capacity raises the question whether such a cell represents a mesodermal precursor for both endothelial and mesenchymal cells (a mesenchymo-angioblast) (Slukvin and Kumar, 2018) or is the result of ECs undergoing EndMT in the human BM. The transcriptional landscape of LNGFR$^+$ ECs, including drivers of EndMT, strongly suggest the latter possibility. To formally demonstrate that endothelial-derived MSCs contribute to the hematopoietic niche in mammalian development, lineage tracing experiments were performed using *VE-Cadherin-Cre*;*LoxP-tdTomato* mice (Chen et al., 2009; Madisen et al., 2010). In these mice, CD144$^+$ ECs and their downstream developmental progeny are permanently marked by tdTomato fluorescence. In line with previous reports establishing the concept of EHT (endothelial to hematopoietic transition) (Boisset et al., 2010; Chen et al., 2009), the majority of CD45$^+$ hematopoietic cells, as well as CD31$^+$CD144$^+$ ECs in 3 week old mice, expressed the tdTomato reporter (data not shown).

Strikingly, a significant proportion (50.2% ± 1.7%) of highly purified BM stromal cells, defined by CD45$^-$lin$^-$CD31$^-$CD144$^-$Sca1$^+$CD51$^+$(Pdgfrα$^+$) marker expression and known to contain SSCs/MSCs (Morikawa et al., 2009b; Pinho et al., 2013; Schepers et al., 2012), was found to be of endothelial origin as indicated by tdTomato expression (Figure 5A and 5C). In addition, a substantial subset (27.0% ± 2.6%) of the downstream osteo/chondrolineage (progenitor) cells (OLCs) (CD45$^-$lin$^-$CD31$^-$CD144$^-$Sca1$^-$CD51$^+$ cells) (Lundberg et al., 2007; Schepers et al., 2012) was also derived from ECs (Figure 5A and 5C). *VE-Cadherin-Cre*-negative;*LoxP-tdTomato* mice were used as a negative control to determine positive tdTomato fluorescence signal (Figure 5B).

Massive parallel RNA sequencing of endothelial-derived (tdTomato positive) vs non-endothelial-derived (tdTomato negative) MSC and OLC subsets confirmed the mesenchymal nature of both subsets (high expression of mesenchymal markers vs absence of endothelial markers) (Figure S5A-B). The endothelial origin of a subset of BM stromal cells was further confirmed by a robust contribution of tdTomato+ cells to non-endothelial stromal cultures, established from whole BM of 3-week old *VE-Cadherin-Cre*;*LoxP-tdTomato* mice (Figure S5C).

Endothelial-derived mesenchymal cells were transcriptionally strikingly distinct, as defined by hierarchical clustering (Figure 5D). Differential gene expression included markedly higher expression of genes encoding key HSC regulatory factors (including *Cxcl12*, *Angpt1*, *Kitl*) (Figure 5E-F), as well as genes encoding markers previously used to define HSC niche cells (*Lepr*, *Nestin*, *Prrx1* and *Mcam*) (Greenbaum et al., 2013; Méndez-Ferrer et al., 2010; Sacchetti et al., 2007; Zhou et al., 2014) (Fig 5G) and gene set enrichment indicative of cytokine regulation (Figure 5H). These endothelial-derived mesenchymal cells also over-expressed genes typically associated with osteogenesis and osteoblast maturation (Figure S5D). Non-endothelial-derived mesenchymal cells, in contrast, displayed a striking differential expression of genes associated with chondrogenesis, including those encoding transcription factors (*Sox5* and *Sox9*) and substituents of the collagenous extracellular matrix, such as *Acan*, *Col9a3*, *Col11a1*, and *Col11a2* (Fig S5E), reflected in enrichment of gene signatures indicative of chondrogenic matrix-formation (Fig S5F-H).

Taken together, the data reveal the existence of a distinct osteogenic subset of mesenchymal cells in the murine BM that is of endothelial origin and differentially expresses key HSC regulatory factors, in line with the notion that these cells may contribute to the hematopoietic niche.

IL-33 is highly expressed in hRECs and drives the endothelial-to-mesenchymal transition of human fetal ECs

The lineage tracing experiments in mice experiments establish that ECs give rise to BM mesenchymal niche cells in development, postulating EndMT as a novel avenue of BM MSC generation. Building on this notion, we sought to demonstrate that human LNGFR$^-$ ECs can give rise to LNGFR$^+$ ECs with mesenchymal characteristics and interrogate the underlying mechanisms that drive EndMT in the human BM. Previously, we identified interleukin (IL)-33 as an anabolic factor in human hematopoiesis, angiogenesis and osteogenesis, driving BM regeneration and development (Kenswil et al., 2018). IL-33 protein was reported to be increased in small subsets of ECs during development and regeneration, in comparison to steady state postnatal ECs (Kenswil et al., 2018), together with factors such as BMP4 and DDP-4, known drivers of EndMT (Medici et al., 2010; Shi et al., 2015). IL-33 was differentially expressed at the transcriptional level in both LNGFR$^+$ hRECs and LNGFR$^-$ hRECs (Figure 6A). As IL-33 is an inflammatory cytokine and inflammation is a known driving force of EndMT, we tested the hypothesis that IL-33 may drive EndMT. To this end, we exposed HUVECs to increasing concentrations of IL-33 and compared its effect to TGF-β1, arguably the best documented and most potent driver of EndMT currently known (Van Meeteren and Ten Dijke, 2012; Zeisberg et al., 2007).

EndMT is associated with a changed transcriptional profile in ECs (Kovacic et al., 2019), which is primarily induced by expression of the transcriptional regulators *SNAI1* (Snail family transcriptional repressor 1), *SNAI2* (Snail family transcriptional repressor 2 or Slug) and *TWIST1* (Souilhol et al., 2018). Exposure of HUVECs to IL-33 (100 ng/ml) led to increased expression of *SNAI2* (*SLUG*) and *TWIST1*, but not of *SNAI1* (Figure 6B-D), strikingly

recapitulating overexpression of these specific transcription factors in primary NGFR⁺ hRECs (Figure 2F).

Concurrent to the increased expression of *SNAI2*, which is a zinc finger transcriptional repressor that can bind to the E-box in the promoters of endothelial lineage genes (Nieto, 2002), the protein expression of the endothelial markers CD31, CD34, and CD144 was decreased in a dose-dependent manner (10ng/ml or 100ng/ml) (Figure 6E-G). Loss of EC identity was corroborated by decreased gene expression of *CDH5*, *PECAM1*, *TEK*, *VEGFR2* and *vWF* by IL-33 (Figure S6A and data not shown).

Concurrent to the increased expression of *TWIST1*, which is a basic helix-loop-helix transcriptional activator of mesenchymal gene expression (Wang et al., 1997), IL-33 induced the protein expression of mesenchymal markers (LNGFR and CD44) in a dose-dependent manner (Figure 6H, I). This was corroborated by demonstrating increased gene expression of other *bona fide* mesenchymal markers such as *FAP*, *TAGLN* (transgelin encoding SM22-α) or and *ACTA2* (actin alpha 2 encoding α-SMA) (Figure S6B).

Remarkably, IL-33 was able to induce EndMT in HUVECS as a single agent to an extent similar to TGF-β1, arguably the most potent inducer of EndMT currently known (Figure S6C-D)

Taken together, the data demonstrate that IL-33 is capable of inducing alterations in HUVECs indicative of cells undergoing EndMT (Dejana et al., 2017), recapitulating characteristics of LNGFR⁺ ECs identified in human BM (Figure 2).

Next, to investigate whether HUVECs not only acquired immunophenotypic changes indicative of EndMT, but also cellular properties congruent with transition towards a mesenchymal cell fate, we interrogated the capacity of IL-33-treated HUVECs to differentiate into the osteogenic and chondrogenic lineage. IL-33-treated cells increased their expression of the extracellular matrix molecules *FN1, COL1A1*, and *COL3A1* (Figure S7A-C). Upon subsequent culture in osteogenic differentiation medium, HUVECs that had undergone EndMT after IL-33 treatment were readily capable of forming calcium deposits in culture as indicated by Alizarin Red binding (Figure 6J) . Similarly, after culture in chondrogenic differentiation medium, HUVECs initially treated with IL-33 exhibited increased glycosaminoglycan (GAG) production compared to vehicle control-treated HUVECs (Figure 6K). This data indicates that IL-33 induced EndMT results in endothelial permissiveness to osteochondrogenic differentiation, congruent with the notion of cellular transition towards mesenchymal cell fates.

IL-33 induces EndMT in adult human ECs through ST2-SNAI2 signaling

While HUVECs are widely used as an *in vitro* model to study EC biology, findings in this venous endothelium of fetal origin may not be applicable to ECs of adult origin, which may have reduced plasticity. To address this, we tested whether IL-33 can also induce EndMT in endothelial colony forming cells (ECFCs) isolated from adult peripheral blood, which have high proliferative potential and are able to contribute to vessel formation in vivo (Critser and Yoder, 2010).

IL-33 (10 ng/ml and 100 ng/ml) induced a dose-dependent decrease of endothelial CD144 expression with a concomitant increase of the mesenchymal markers α-SMA (encoded by *ACTA2*) (Figure S8A), fibronectin (*FN1*) and SM22-α (encoded by *TAGLN*) (Figure S8B), faithfully recapitulating findings in HUVECs (Figure 6E-I).

Similar to findings in HUVECs, exposure to IL-33 induced a permissive state for subsequent osteogenic differentiation of ECs, as indicated by rapid upregulation of early osteogenic differentiation markers (*COL1A1*, *RUNX2*, *OSX*) (Figure S8C-E) and increased formation of calcium deposits (Figure S8F).

Finally, we sought to begin unraveling the underlying molecular mechanisms of IL-33 mediated EndMT in human ECs. IL-33 is thought to function by binding to its cognate receptor ST2 (Kakkar and Lee, 2008). Blocking ST2 signaling in ECFCs by using a neutralizing antibody directed against ST2 (Guo et al., 2014; Suzukawa et al., 2008), resulted in partial rescue of IL-33 mediated EndMT, as shown by attenuated down-regulation of CD144 and up-regulation of fibronectin, in particular at an IL-33 dose of 100 ng/ml (Figure S9A, lower panels). Concomitantly, upregulation of *SNAI2* was impaired by the ST2 neutralizing antibody (Figure S9B).

Taken together, the data demonstrate that LNGFR⁺ 'mesenchyme primed' ECs, as identified in human development and regeneration (Figure 1 and 2), can be derived from fetal and adult human ECs by IL-33, which is highly expressed in hRECs during development and regeneration, and a novel and strong inducer of EndMT at least partially, through ST2-SNAI2 signaling.

DISCUSSION

Stromal cells in the mammalian BM play pivotal roles in tissue maintenance and re-generation. They are likely heterogeneous, with subsets contributing to skeletogenesis, while other sustain hematopoiesis by providing niches to HSPCs. Stromal subsets are thought to originate from tissue resident multipotent mesenchymal stromal cells (MSCs) that are formed during development. However, the developmental origins of such cells remain incompletely understood.

Here, we report the prospective isolation of a human BM EC that has the potential of *de novo* formation of MSCs. LNGFR$^+$ ECs constitute a rare subset of ECs in homeostasis but are more prevalent during fetal development and re-emerge postnatally in the context of regeneration after injury. LNGFR$^+$ ECs can arise from IL-33 driven conversion of LNGFR$^-$ ECs and display transcriptional re-wiring consistent with stemness and EndMT, emanating in their ability to generate *bona fide* MSCs with *in vivo* hematopoietic niche-forming capacity. Formal experimental support for the notion that ECs can transition to distinct stromal cells with HSC supportive characteristics *in vivo* is provided by lineage tracing studies in mice. The data argue for an adapted conceptual view on the origins of the hematopoietic system in mammals, in which ECs not only generate HSCs (through the process of EHT) (Boisset et al., 2010; Chen et al., 2009), but also distinct MSCs that develop into their supportive niches (Figure S10).

The possibility of the *de novo* generation of MSCs through an EC intermediate had previously been suggested by cell culture experiments using embryonic stem cells (ESCs) and induced pluripotent stem cells (iPSCs) demonstrating that MSCs may be generated from (APLNR$^+$) mesenchymo-angioblasts, via an endothelial-stage intermediate (Kumar et al., 2017; Vodyanik et al., 2010). Interestingly, APLNR [as well as its ligand apelin (APLN)], together with IL-33, are highly expressed in the small CD105$^+$ BM EC subset associated with BM development and regeneration in humans (Kenswil et al., 2018) (and data not shown), opening the possibility that LNGFR$^+$CD105$^+$ECs are derived from this small subset of APLN^{high}IL33^{high} CD105$^+$ LNGFR$^-$ ECs.

In vivo precedence for the ability of ECs to transition to mesenchymal cell fates has recently been provided by lineage tracing studies in mice, demonstrating that endocardial ECs are progenitors of pericytes and vascular smooth muscle cells in the murine embryonic heart (Chen et al., 2016a). These EC-derived mesenchymal progenitors lacked the capacity to differentiate into osteogenic or adipogenic cells, suggesting that the multipotent differentiation capacity of mesenchymal progenitors may be tissue-restricted.

Our data furthers the earlier *ex vivo* observation that HUVECs and ECFCs carrying a mutant version of ALK2, can give rise to mesenchymal cells with multilineage differentiation capacity in the context of the human disorder fibrodysplasia ossificans progressiva (FOP) (Medici et al., 2010) (Sánchez-Duffhues et al., 2019). We demonstrate this potential in prospectively isolated cells from the human BM, providing relevance to human physiology.

Whether the pool size of endothelial-derived MSCs is developmentally restricted or can be modulated by *de novo* generation of MSCs through EndMT in times of 'tissue demand' remains unknown at this point. Our finding that ECs that are transitioning towards MSCs with niche forming capacity re-emerge in humans after BM injury clearly suggests the, exciting, latter possibility. Future investigations, including conditional lineage tracing experiments in mice, will likely answer this open question, perhaps opening the way to pharmacologic harnessing of EndMT to foster BM regeneration.

In this context, it is relevant that we identify IL-33 as a novel and potent driver of EndMT with likely relevance to human physiology. Transcriptional profiling of EC subsets emerging during regeneration earlier identified IL-33 as an anabolic factor stimulating hematopoiesis and osteogenesis (Kenswil et al., 2018). Remarkably, IL-33 was able to induce EndMT in HUVECS as a single agent to an extent similar to TGF-β1, arguably the most potent inducer of EndMT currently known. Mechanistically, exposure to IL-33 resulted in synergistic upregulation of *SNAI2* and *TWIST1*, important transcriptional regulators of EndMT through Hedgehog signaling, in line with the molecular profile of LNGFR$^+$ ECs isolated from the human marrow. These observations warrant further research on the effect of this inflammation-associated cytokine in cellular reprogramming including acquisition of stemness features.

Taken together, the data reveal a previously unappreciated potential of specialized BM ECs to convert to niche-generating MSCs. The prospective isolation of this cell type and the elucidation of the associated molecular programs is anticipated to foster investigations into its relevance for development, regeneration and disease.

Figure 1

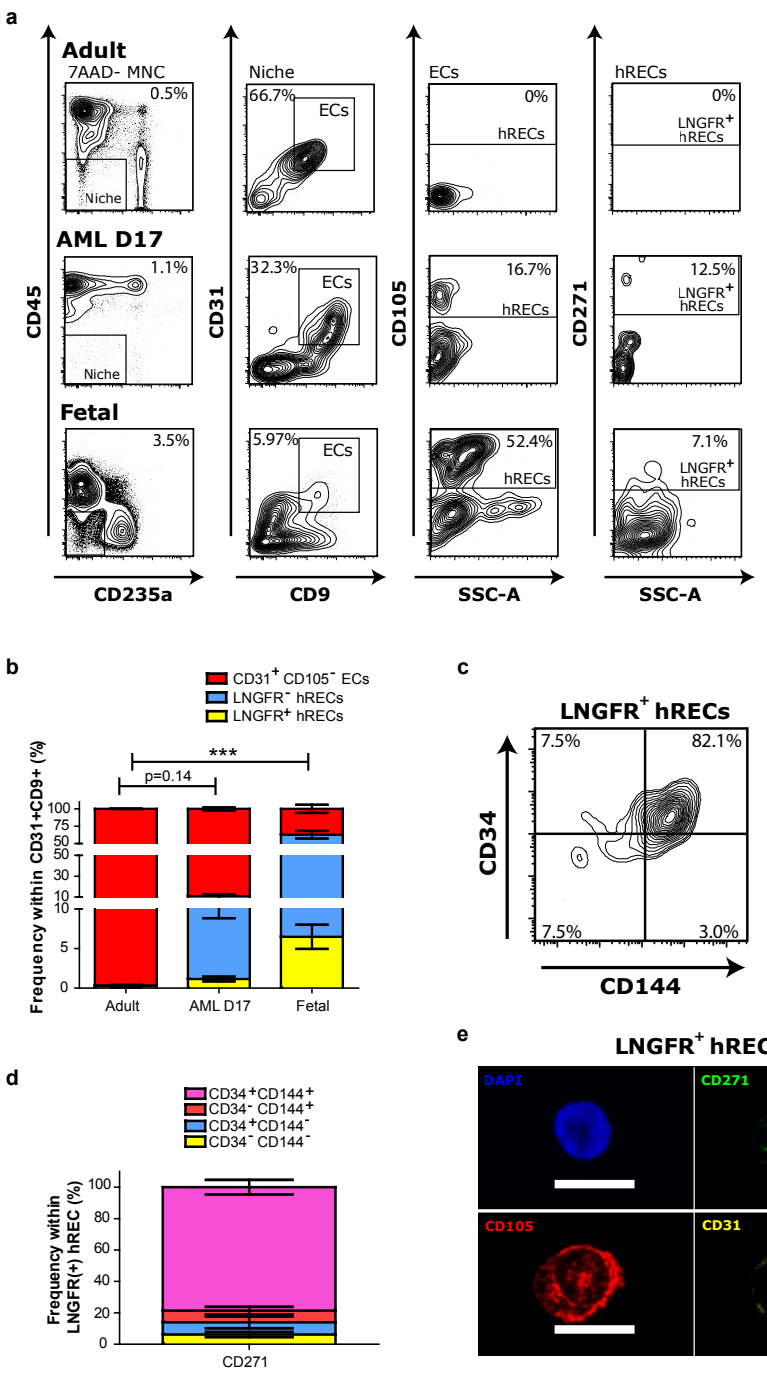

Figure 1. Identification of a rare LNGFR-expressing human EC enriched in regenerative and fetal bone marrow

a. Flow cytometry plots depicting the gating strategy to identify EC subsets. Representative plots of human BM samples demonstrating that a subset of $CD31^{+}CD105^{+}$ ECs (hRECs) express LNGFR (CD271). This subset is enriched in the BM upon regeneration after chemotherapy (middle panel, AML day 17) and fetal development (lower panel, Fetal BM), compared to steady-state adult BM (upper panel, Adult BM).

b. Quantification of EC subset frequencies within the endothelial ($CD31^{+}CD9^{+}$) population of adult steady-state (n=13), regenerative (n=48), and fetal BM (n=15). The one-way analysis of variance (ANOVA) was used to compare the mean frequencies of $LNGFR^{+}$ EC between the three groups. ***p <0.001, one-way ANOVA (p <0.0001) followed by Bonferroni's Multiple Comparison Test. Data represent mean ± S.E.M. S.E.M: Standard error of mean.

c. Representative flow cytometry plots confirming that the majority of the $LNGFR^{+}$ EC in fetal BM express endothelial markers (CD34 and CD144) at protein level.

d. Quantification of CD34 and CD144 expression within the fetal BM $LNGFR^{+}$ EC population, demonstrating that the vast majority of these cells express these endothelial markers (n=13). Data represent mean ± S.E.M.

e. Cropped immunofluorescent image confirming the corresponding cell surface marker expression of CD31, CD105, and CD271 (LNGFR) on FACS-sorted $LNGFR^{+}$ hRECs. White scale bar represents 10 µm. FACS: fluorescence-activated cell sorting.

Figure 2

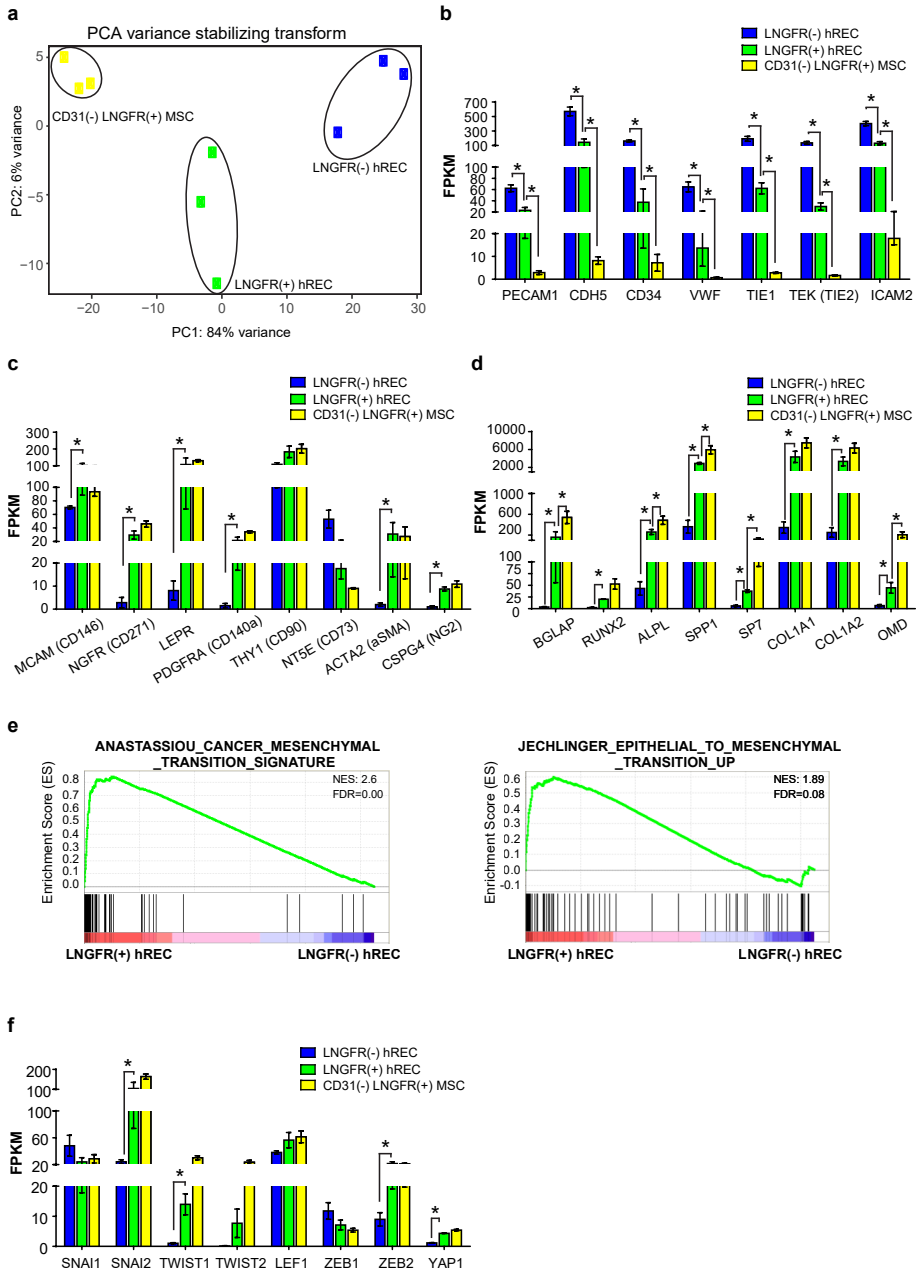

Figure 2. LNGFR-expressing ECs exhibit molecular characteristics of cells undergoing mesenchymal transition
Transcriptomes of CD31⁻LNGFR⁺ MSCs, LNGFR⁺ hRECs, and LNGFR⁻ hRECs were interrogated by massive-parallel RNA-sequencing.

a. Principal component analysis (PCA) on the transcriptomes of CD31⁻LNGFR⁺ MSCs (n=3), LNGFR⁺ hRECs (n=3), and LNGFR⁻ hRECs (n=3) reveal distinct hierarchical clustering of each cell population. LNGFR⁺ hRECs cluster in-between LNGFR⁻ hRECs and CD31⁻LNGFR⁺ MSCs.
b. Expression of genes encoding for known endothelial markers.
c. Expression of genes encoding for known mesenchymal markers.
d. Expression of genes encoding for known osteolineage markers.
e. Activation of transcriptional programs (Also see Figure S2A) associated with mesenchymal transition in LNGFR⁺ hRECs compared to LNGFR⁻ hRECs. NES and FDR value of each gene set is listed. GSEA: gene sets enrichment analysis. NES: normalized enrichment score. FDR: false discovery rate.
f. Expression of genes encoding for known EndMT-drivers.
* FDR<0.05, FDR: false discovery rate. FPKM: fragments per kilobase of exon per million fragments mapped. Data represent mean ± S.E.M. S.E.M: Standard error of mean.

Figure 3

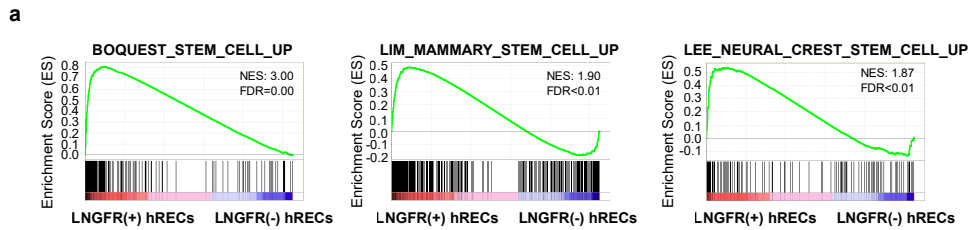

Figure 3. LNGFR-expressing ECs display stemness features and have the capacity to convert to a stem cell like mesenchymal cell

a. Activation of transcriptional programs associated with stemness in LNGFR⁺ hRECs (n=3) compared to LNGFR⁻ hRECs (n=3). NES and FDR value of each gene set is listed. GSEA: gene sets enrichment analysis. NES: normalized enrichment score. FDR: false discovery rate.

b. Bright-field picture of plastic-adherent mesenchymal cells derived from sorted LNGFR⁺ hRECs. 10x magnification. Black scalebar represents 200 µm.

c-d. LNGFR⁺ EC-derived mesenchymal cells fulfill the minimal cell surface marker expression criteria for culture expanded MSCs. Representative flow cytometry plots (of 3 independent experiments with a different fetal bone each experiment) demonstrating that the progeny of LNGFR⁺ hRECs express (c) known MSC makers (CD105, CD73, CD90, CD146, and CD51) and lack expression of (d) endothelial (CD31 and CD34) and hematopoietic markers (CD34 and CD45) at p4.

e. CFU-F frequency of primary sorted single cell CD31⁻LNGFR⁺ MSCs (48 CFU-F out of 254 single cells) and LNGFR⁺ hRECs (26 CFU-F out of 227 single cells). Single cells/well sorted from n=2 independent experiments, 1 fetal bone per experiment. Data represent mean ± S.E.M. CFU-F: Colony-forming unit fibroblast. S.E.M: Standard error of mean.

f. LNGFR⁺ EC-derived mesenchymal cells have tri-lineage differentiation capacity. Culture expanded LNGFR⁺ hREC-derived mesenchymal cells were differentiated towards the osteoblastic (left panel), chondrogenic (middle), and adipogenic (right) lineage. Osteoblasts were stained with Alizarin Red. Cartilage matrix (glycosaminoglycan deposition) is visualized by thionin staining. Adipocytes were stained with Oil Red O. Left and right scalebar represents 100 µm. Middle scalebar represents 200 µm. Representative data from 2 independent experiments with a different fetal bone in each experiment.

Figure 4

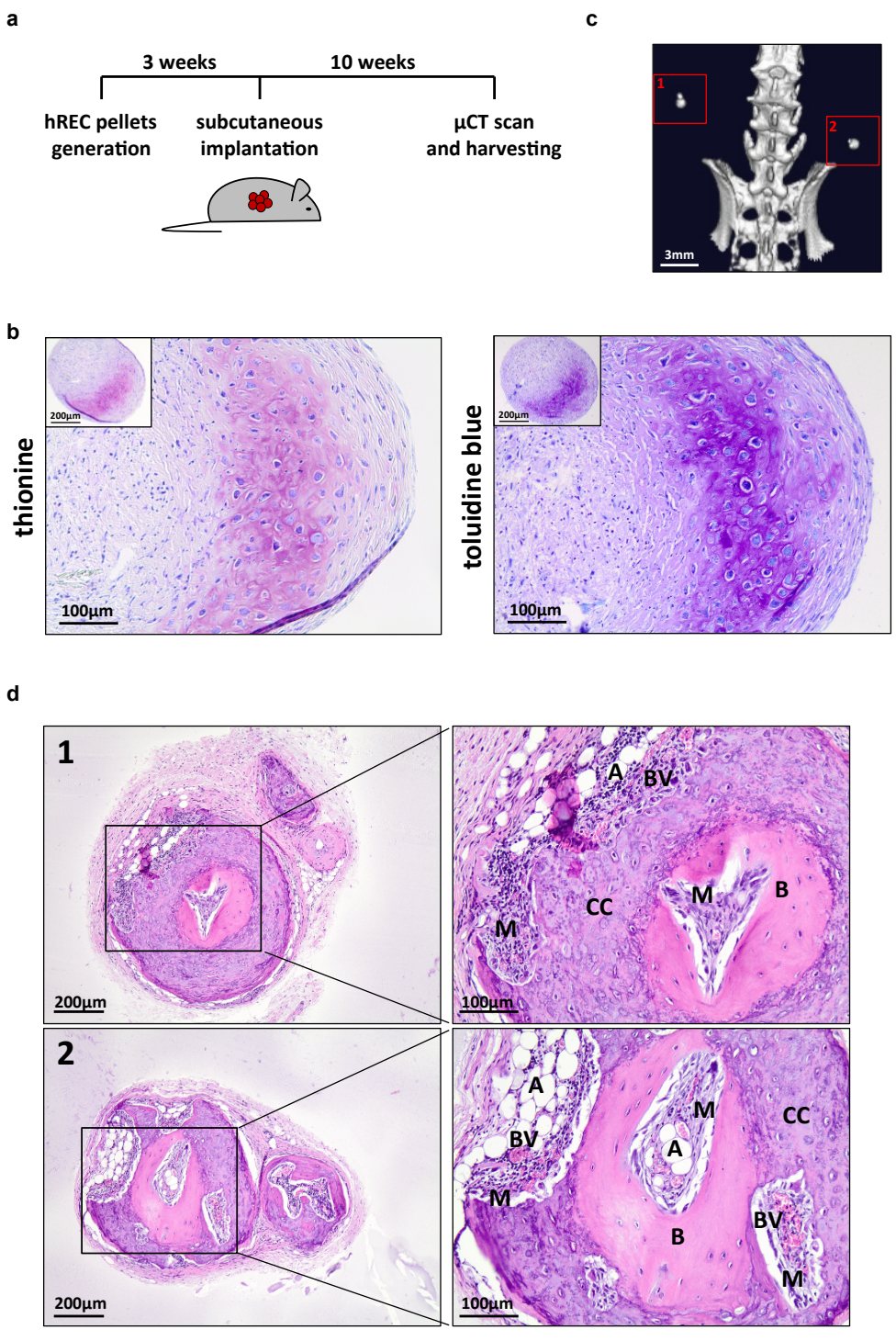

Figure 4. Human LNGFR+ EC-derived mesenchymal cells establish a hematopoietic niche *in vivo*

a. Mesenchymal cells derived from LNGFR-expressing ECs were induced to form 3D pellets and subjected to 3 weeks culture in chondrogenic medium, prior to subcutaneous implantation in athymic nude mice. 10 weeks post-implantation, pellet mineralization was assessed by µCT analysis and the constructs were retrieved for histological processing. Representative data is presented of n=6 transplanted constructs.

b. Glycosaminoglycan production in 3D pellets at the time of implantation was evidenced by thionine (left panel) and toluidine blue (right panel) staining.

c. Representative 3D reconstruction from µCT scans of implanted pellets performed 10 weeks post-implantation.

d. Representative microphotographs of hematoxylin and eosin staining of histological sections of LNGFR^{+} EC-derived bone constructs retrieved 10 weeks post-implantation (B=bone, M=bone marrow, BV=blood vessel, CC=calcified cartilage, A=adipose tissue). Four constructs could be retrieved and sectioned (out of six transplanted). All analyzed constructs (n=4) demonstrated hematopoietic niche formation. Representative images from 2 of the constructs are shown

Figure 5

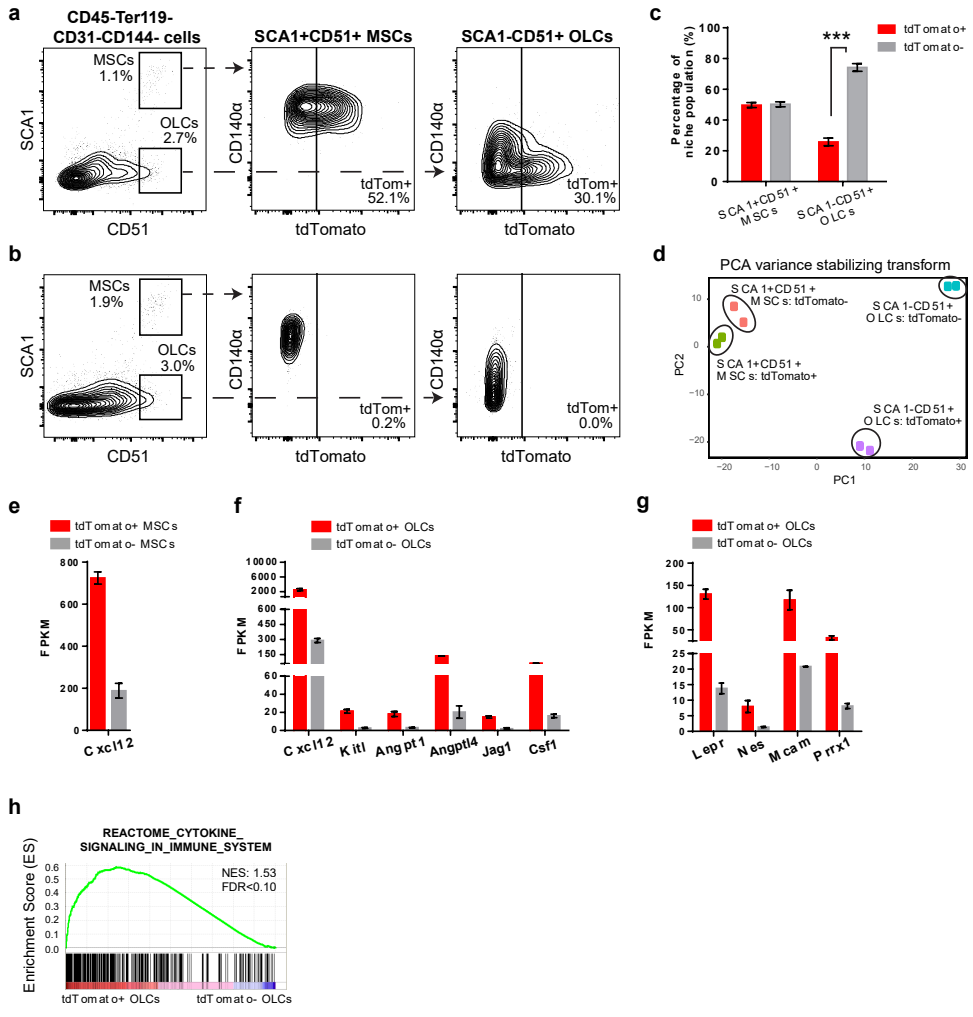

Figure 5. Endothelial-derived mesenchymal cells contribute to hematopoietic niche formation in mice (see also Figure S5)

a-b. Representative flow cytometry plots depicting the gating strategy to identify highly purified mesenchymal populations in the non-endothelial BM niche (defined as CD45$^-$Ter119$^-$CD31$^-$CD144$^-$ cells) of 3-week old *VE-Cadherin-Cre*;*LoxP-tdTomato* mice, containing multipotent stromal cells (MSCs, Sca-1$^+$CD140a$^+$ CD51$^-$ cells) and osteo/chondrolineage progenitor cells (OLCs, Sca-1$^+$CD51$^-$ cells). A substantial subset of these mesenchymal populations are derived from ECs as indicated by tdTomato expression (a). (Also see Figure S5A-C confirming the mesenchymal identity of these tdTomato+ cells). *VE-Cadherin-Cre*-negative;*LoxP-tdTomato* mice (b) were used as a negative control to determine positive tdTomato fluorescence signal.

c. Quantification of the frequency (depicted in %) of tdTomato+ cells within the MSC and OLC population of *VE-Cadherin-Cre*;*LoxP-tdTomato* mice. ***p <0.001, 2-tailed unpaired Student's t test. n=7 mice. Data represent mean ± S.E.M. S.E.M: Standard error of mean.

d. Principal component analysis (PCA) on the transcriptomes of tdTomato$^+$ vs. tdTomato$^-$ MSCs and OLCs showing distinct hierarchical clustering of cell populations. n=2 mice.

e-f. Expression of genes encoding key HSC-regulatory factors in tdTomato+ MSCs compared to tdTomato- MSCs (e), as well as in tdTomato+ OLCs compared to tdTomato- OLCs (f).

g. Expression of genes encoding established HSC niche markers in tdTomato+ OLCs compared to tdTomato- OLCs.

h. Activation of transcriptional programs associated with (hematopoietic) cytokine activity in tdTomato+ OLCs compared to tdTomato- OLCs. NES and FDR value of each gene set is listed. GSEA: gene sets enrichment analysis. NES: normalized enrichment score. FDR: false discovery rate.

FPKM: fragments per kilobase of exon per million fragments mapped. Data represent mean ± S.E.M. S.E.M: Standard error of mean.

Figure 6

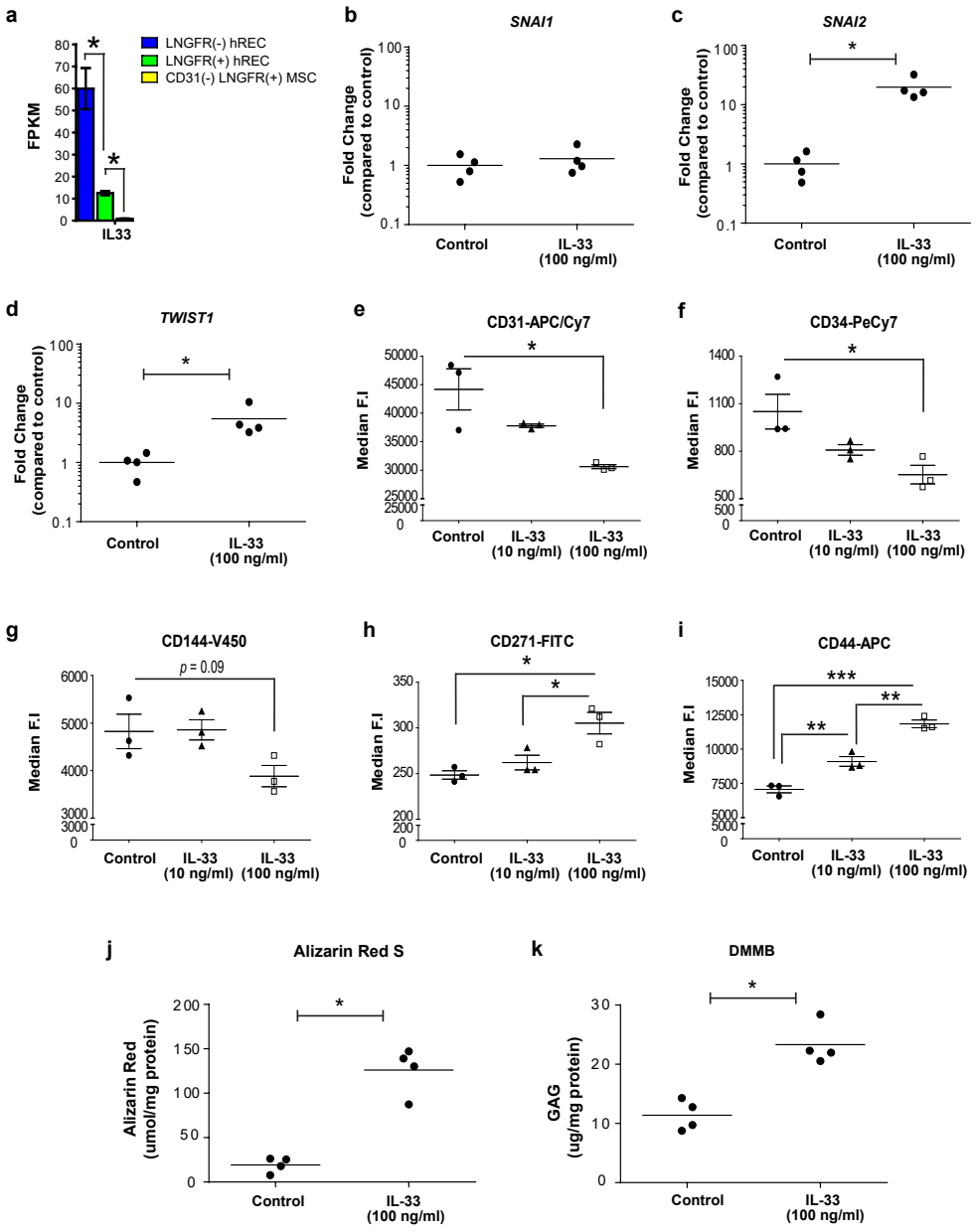

Figure 6. IL-33 drives EndMT and the conversion to mesenchymal cell fates in human fetal ECs (see also Figures S6-9)

a. Expression of IL-33 in different niche subsets in human fetal bone marrow. *FDR<0.05, FDR: false discovery rate. FPKM: fragments per kilobase of exon per million fragments mapped.

b-d. Gene expression levels (by RT-PCR) of transcription factors driving EndMT. HUVECs were treated with IL-33 (100 ng/ml) (n=4) compared with vehicle-control-treated HUVECs (n=4) for four consecutive days. *p<0.05, Mann–Whitney U test.

e-i. Protein expression of endothelial (e-g) and mesenchymal (h-i) markers by HUVEC upon exposure to IL-33 (as assessed by flow cytometry) (vehicle-control vs. IL-33 [n=3 different HUVEC donors]). The one-way analysis of variance (ANOVA) was used to compare the median F.I of each marker, followed by Bonferroni's Multiple Comparison Test. *p< 0.05, **p< 0.01, ***p< 0.001.

j-k. Conversion of HUVECs to mesenchymal (osteochondrogenic) cell fates by IL-33. Calcium deposition (j) after osteogenic stimulation and glycosaminoglycan production (k) after chondrogenic stimulation of HUVECs initially treated IL-33 compared to vehicle-control (n=4). *p<0.05, Mann–Whitney U test. DMMB = Dimethyl methylene blue (DMMB) method. Each "n" represents a different HUVEC donor. F.I: Fluorescence intensity.

Data represent mean ± S.E.M. S.E.M: Standard error of mean.

SUPPLEMENTAL DATA

Figure S1

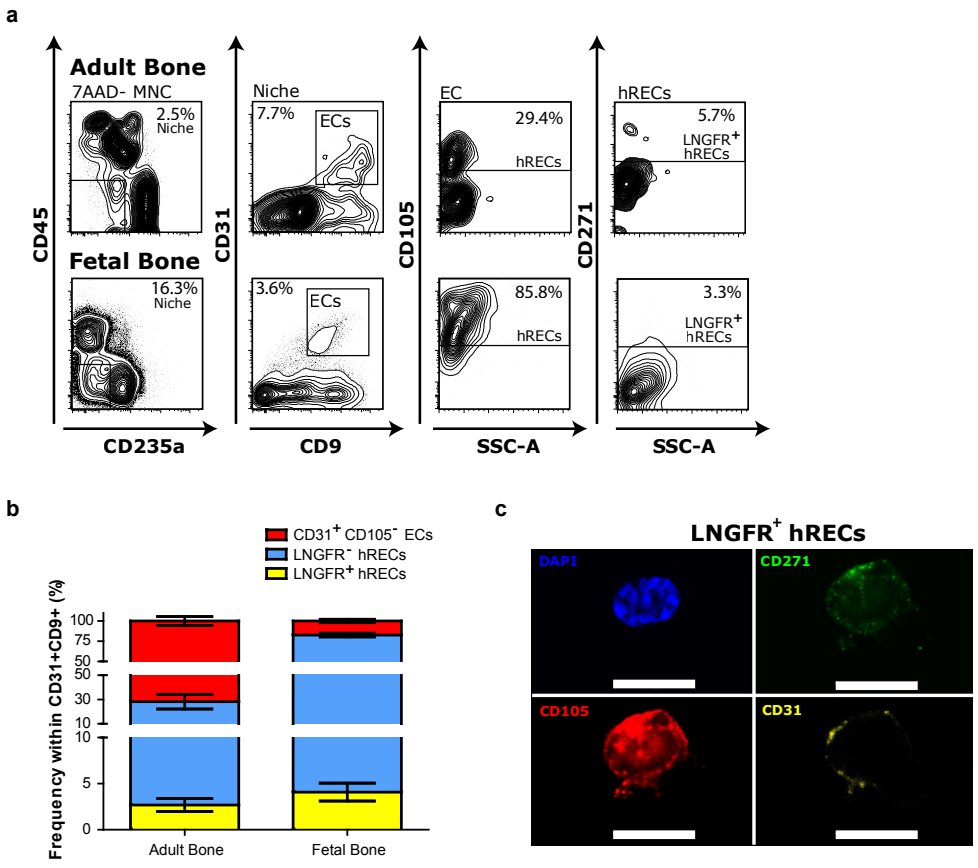

Figure S1. LNGFR-expressing ECs are present in collagenased bone fractions

a. Representative flow cytometry plots of collagenased hip bone from patients undergoing hip replacement surgery, as well as collagenased fetal bone.

b. Quantification of EC subset frequencies within the endothelial population in collagenased bone of patients undergoing hip replacement surgery (n=12), and collagenased fetal bone (n=21). Data represent mean ± S.E.M. S.E.M: Standard error of mean.

c-e. Cropped immunofluorescent images confirming the corresponding cell surface marker expression of CD31, CD105 and LNGFR on FACS-sorted (c) $LNGFR^+$ hRECs, (d) $LNGFR^-$ hRECs and (e) $CD31^-$ $LNGFR^+$ stromal cells. Note high expression of CD31 on $LNGFR^-$ hRECs compared to $LNGFR^+$ hRECs. White scale bar represents 10 µm. FACS: fluorescence-activated cell sorting.

Figure S2

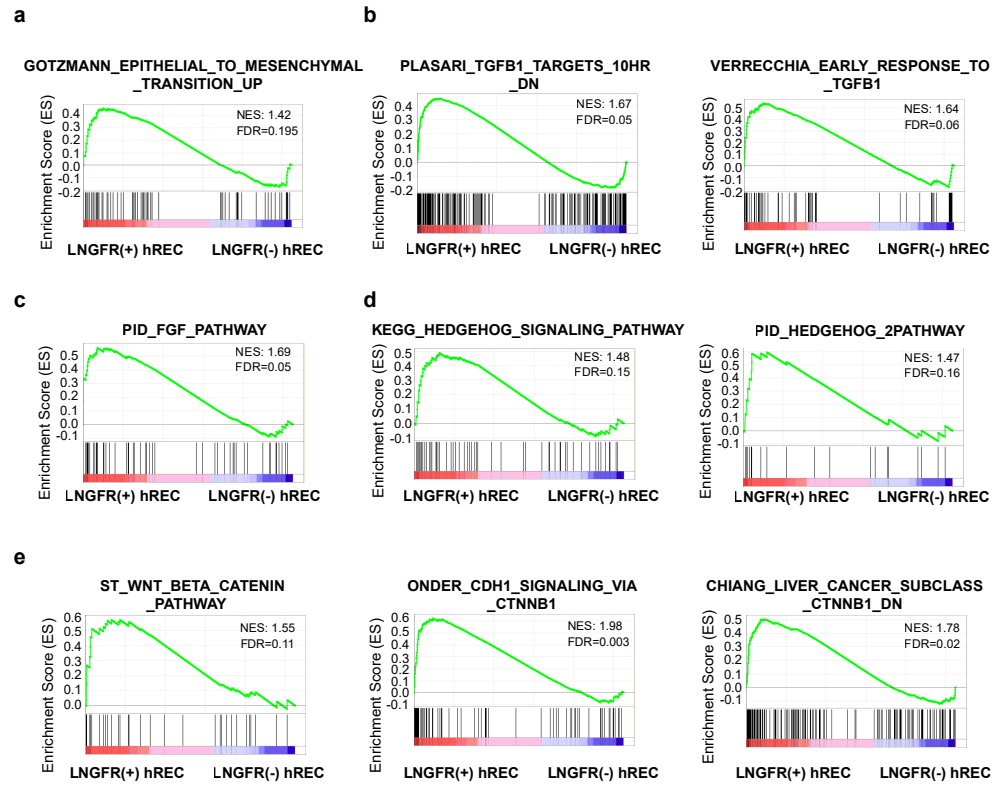

Figure S2. LNGFR-expressing ECs exhibit transcriptional signatures associated with EndMT

a-e. Activation of transcriptional programs associated with (a) mesenchymal transition, (b) TGF-β signaling, (c) FGF signaling, (d) Hedgehog signaling, (e) WNT signaling in LNGFR⁺ hRECs compared to LNGFR⁻ hRECs. NES and FDR value of each gene set is listed. GSEA: gene sets enrichment analysis. NES: normalized enrichment score. FDR: false discovery rate.

Figure S3

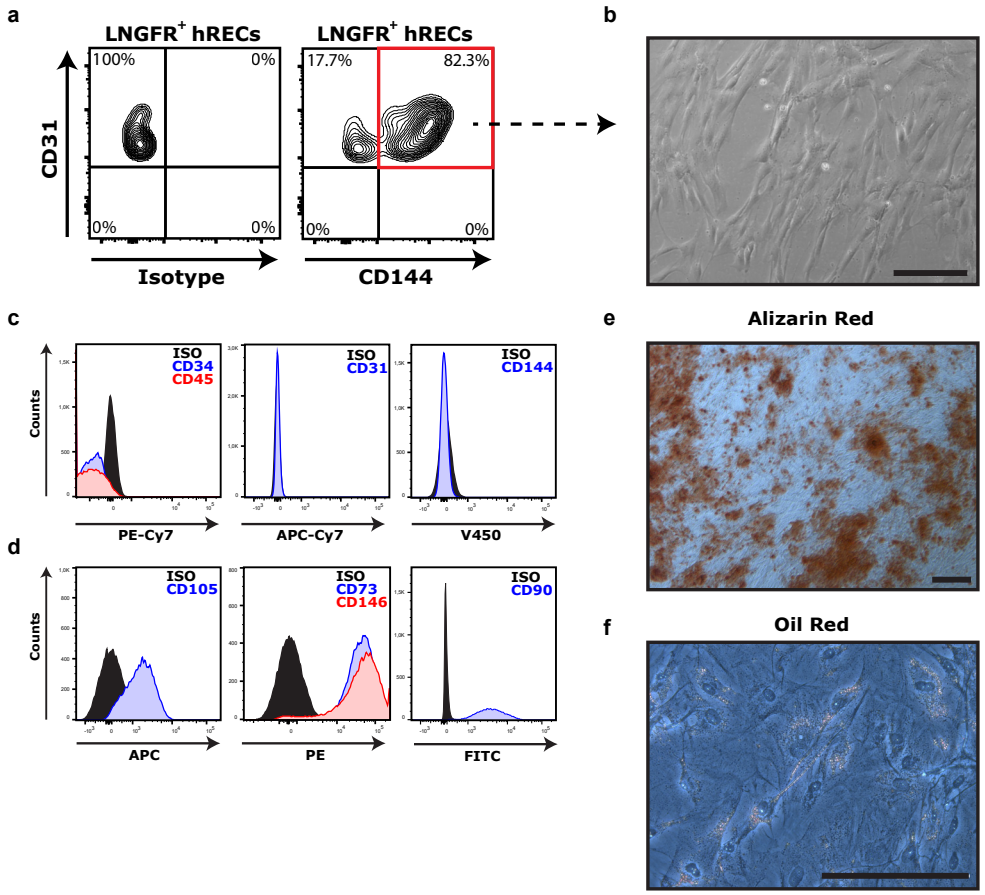

Figure S3. LNGFR⁺CD144⁺ hRECs can form mesenchymal cells with multilineage differentiation capacity

a. Representative flow cytometry plots depicting CD144 (VE-cadherin) expression within the LNGFR⁺ hREC population and gating of LNGFR+CD144+ hRECs.

b. Representative bright-field picture of plastic-adherent mesenchymal cells at p3 derived from sorted primary CD144⁺ LNGFR⁺ hRECs, confirmed in 2 independent experiments (1 fetal bone per experiment). 50 primary cells were initially seeded per well at sorting (n=4 wells from fetal bone 1 and n=6 wells from fetal bone 2). All wells exhibited outgrowth of plastic-adherent mesenchymal cells. 10x magnification. Black scalebar represents 100 µm.

c-d. Representative flow cytometry plots demonstrating that CD144⁺ LNGFR⁺ hREC-derived mesenchymal cells lack expression of endothelial (c) (CD31, CD34 and CD144) and hematopoietic (c) markers (CD34 and CD45) and express known MSC (d) markers (CD105, CD73, CD146, CD90) at p3-4, representative example of n=2 independent experiments.

e-f. Culture expanded CD144⁺ LNGFR⁺ hREC-derived mesenchymal cells (p6) were differentiated towards the osteoblastic (e) and adipogenic (f) lineage. Osteogenic differentiation is assessed by Alizarin Red staining. Adipocytes were stained with Oil Red O. Black scalebar in (e) represents 100 µm. Black scalebar in (f) also represents 100 µm. Representative images of n=2 independent experiments.

Figure S4

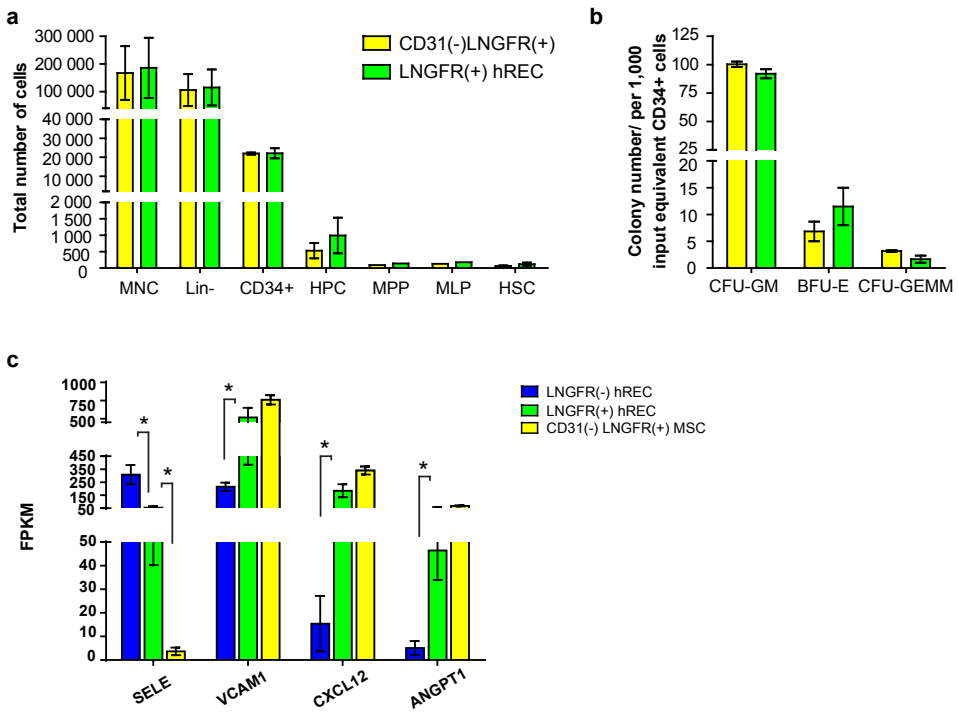

Figure S4. LNGFR⁺ hREC-derived stromal cells display hematopoietic supporting capacity

a-b. Total number of hematopoietic cells (a) and colony forming units (b) formed by 7,500 UCB CD34⁺ cells following one-week of co-culture with the stromal progeny of CD31⁻LNGFR⁺ MSCs or LNGFR⁺ ECs (n=2 independent experiments, each experiment was performed in triplicate). MNC: Mononuclear cells. Lin⁻: Lineage-negative cells. CD34⁺: Lin⁻CD34⁺ cells. HPC: Lin⁻CD34⁺CD38^{lo} cells. MPP: Lin⁻CD34⁺CD38^{lo}CD90⁻CD45RA⁻ cells. MLP: Lin⁻CD34⁺CD38^{lo}CD90⁻CD45RA⁺ cells. HSC: Lin⁻CD34⁺CD38^{lo}CD90⁺CD45RA⁻ cells. Hematopoietic progenitors (HPC), multipotent progenitors (MPP), multilymphoid progenitors (MLP) and hematopoietic stem cells (HSC). CFU-GM: Colony-forming unit–granulocyte-macrophage. BFU-E: Burst forming unit-erythroid. CFU-GEMM: Colony-forming unit –granulocyte-erythrocyte-monocyte-megakaryocyte.

c. Gene expression of known HSC niche-derived factors within CD31⁻LNGFR⁺ MSCs (n=3), LNGFR⁺ hRECs (n=3), and LNGFR⁻ hRECs (n=3) sorted from fetal bone marrow. *FDR<0.05, FDR: false discovery rate. FPKM: fragments per kilobase of exon per million fragments mapped. Data represent mean ± S.E.M. S.E.M: Standard error of mean.

Figure S5. Endothelial-derived mesenchymal cells display distinct transcriptional wiring consistent with bone forming capacity

a-b. MSCs and OLCs (both tdTomato⁺ and tdTomato⁻ subsets) isolated from *VE-Cadherin-Cre*;*LoxP-tdTomato* mice (n=2) express genes encoding mesenchymal transcripts, while lacking expression of genes encoding *bona fide* endothelial genes

c. TdTomato⁺ mesenchymal cells from *VE-Cadherin-Cre*;*LoxP-tdTomato* mice constitute a fraction of cultured bone marrow derived stromal cells. Representative flow cytometry plots depicting mesenchymal marker (CD29 and CD44) expression of plastic-adherent tdTomato⁺ stromal cells after 19 days of culture *ex vivo*. (n=2) (P0). P0 = Passage 0 (before 1st passaging).

d-e. TdTomato⁺ OLCs isolated from *VE-Cadherin-Cre;LoxP-tdTomato* mice display marked overexpression of genes encoding transcripts related to osteogenesis (in comparion to tdTomato⁻ OLCs) (d), while tdTomato⁻ OLCs overexpress transcripts related to chondrogenesis (e).

f-h. Activation of transcriptional programs associated with chondrogenic activity in tdTomato- OLCs compared to tdTomato+ OLCs. NES and FDR value of each gene set is listed. NES: normalized enrichment score. FDR: false discovery rate.

Figure S5

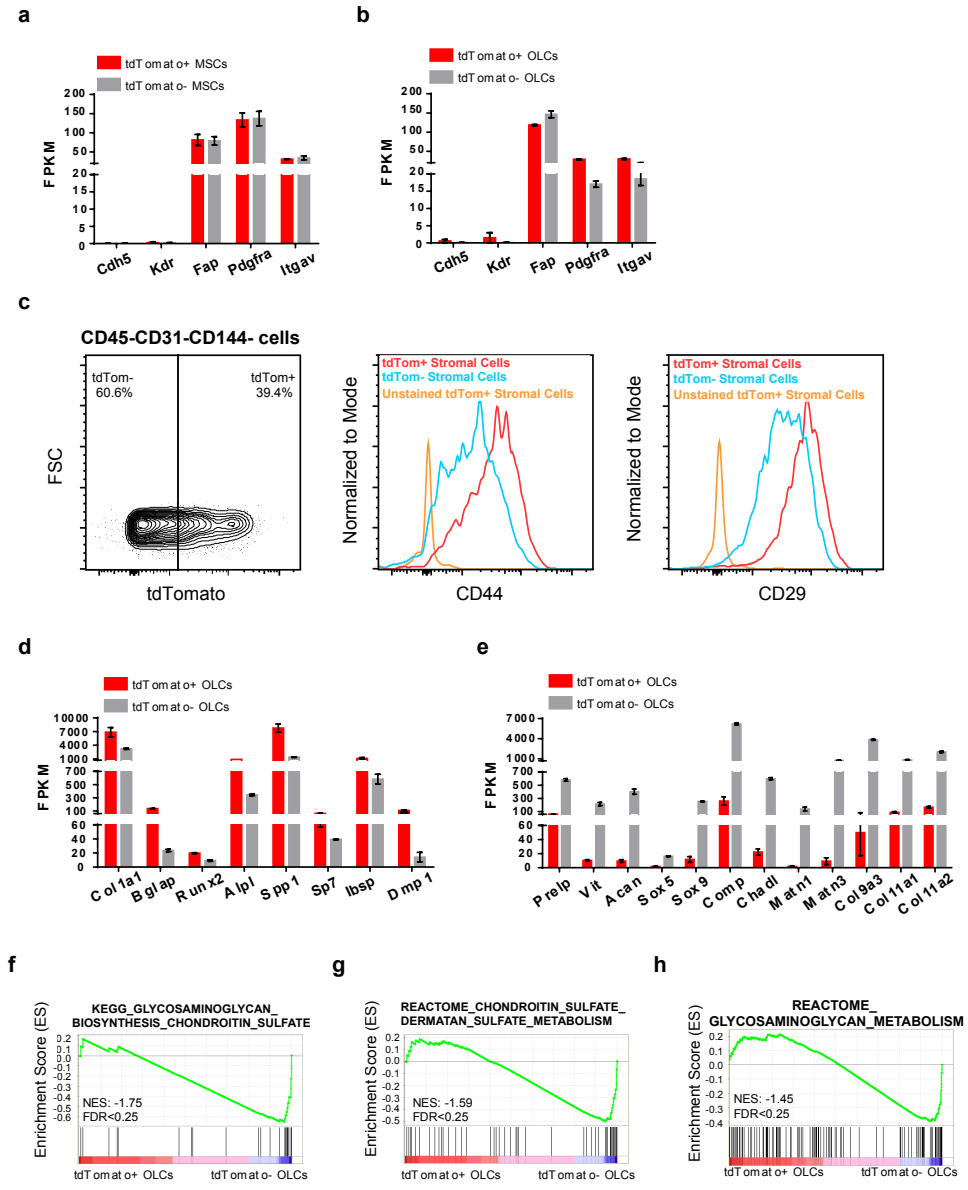

Figure S6

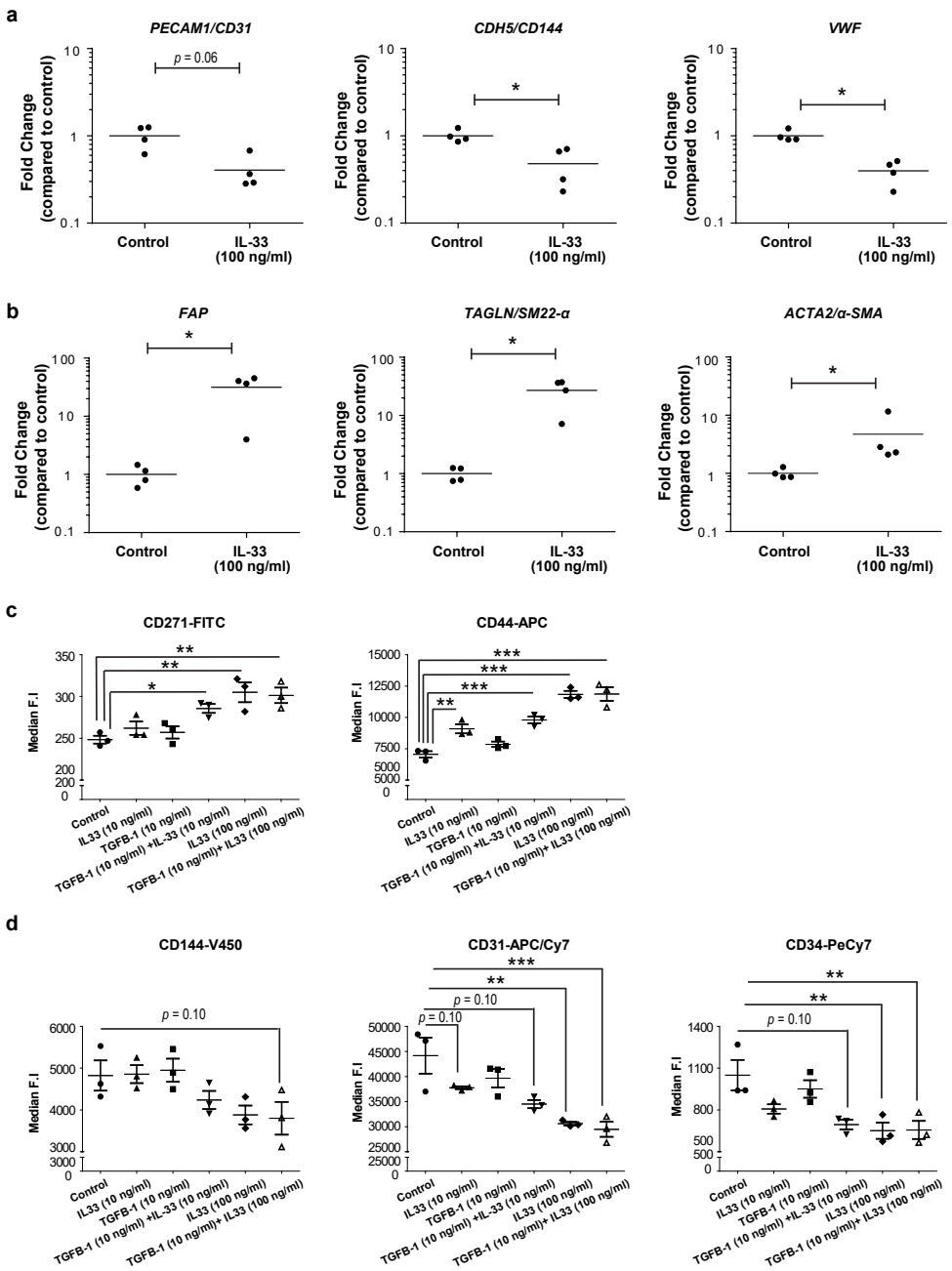

Figure S6. Induction of EndMT in human fetal ECs by IL-33

a-b. Real-time PCR to quantify endothelial (a) and mesenchymal (b) gene expression in HUVECs treated with IL-33 (100 ng/ml) (n=4). Gene expression levels for endothelial lineage genes including, platelet-endothelial cell adhesion molecule (*PECAM*/CD31), VE-Cadherin (*CDH5*), and von Willebrand factor and mesenchymal lineage genes including, Fibronectin (*FN1*), smooth muscle 22-α (*TAGLN*), α-smooth muscle actin (*ACTA2*) were assessed. *p<0.05, Mann–Whitney U test.

c-d. Protein expression of mesenchymal (c) and endothelial markers (d) by HUVECs after treatment with IL-33 (10 ng/ml or 100 ng/ml), or TGF-β1 (10ng/ml), or IL-33 (10 ng/ml or 100 ng/ml) in combination with TGF-β1 (10ng/ml). Combined data of n=3 independent experiments. One-way ANOVA was used to compare the median F.I of each marker, followed by Dunnett's Multiple Comparison Test using untreated HUVECs as the reference group. *p< 0.05, **p< 0.01, ***p< 0.001.

F.I: Fluorescence intensity. Data represent mean ± S.E.M. S.E.M: Standard error mean.

Figure S7

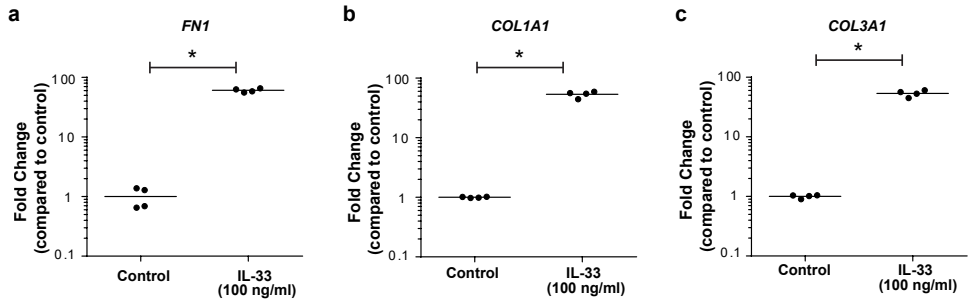

Figure S7. Induction of extracellular matrix genes by IL-33 in human ECs

a-c. Real-time PCR to quantify gene expression of extracellular matrix components in HUVECs treated with IL-33. Gene expression levels for *FN1* (a, encoding for fibronectin), *COL1A1* (b, encoding for Collagen 1α1), and *COL3A1* (c, encoding for Collagen 3α1) were assessed (n=4 independent experiments). *p<0.05, Mann–Whitney U test.

Figure S8. IL-33 induces EndMT and osteogenic differentiation capacity in adult human ECs

a-b. Immunofluorescent pictures depicting reduced endothelial CD144/VE-cadherin (a) and increased mesenchymal markers, including α-SMA (a), fibronectin (b), and transgelin/SM22-α (b) expression by ECFCs following 24 hour exposure to IL-33 (10 and 100 ng/ml). 4',6-diamidino-2-phenylindole (DAPI) staining was used to visualize cell nuclei. Representative data from n=3 independent experiments. White scale bars represents 100 µm.

c-e. Real-time PCR to quantify gene expression of osteogenic differentiation markers in ECFCs treated with IL-33 (10 ng/ml and 100 ng/ml). Gene expression levels for *COL1A1* (encoding for collagen, type I, α1) (c), *RUNX2* (encoding for runt-related transcription factor 2) (d), *FN1* (encoding for fibronectin) (e) were assessed. Data from n=3 independent experiments. ***p <0.001, **p <0.01, one-way ANOVA followed by Bonferroni's Multiple Comparison Test. Data represent mean ± S.E.M. S.E.M: Standard error of mean.

f. Conversion of ECFCs to mesenchymal (osteogenic) cell fate by IL-33. Calcium deposition after culture of ECFCs in osteogenic inductive medium in combination with rhIL-33 at 0 ng/ml (left panel), or 10 ng/ml (middle panel), or 100 ng/ml (right panel). Representative data from n=3 independent experiments.

Figure S8

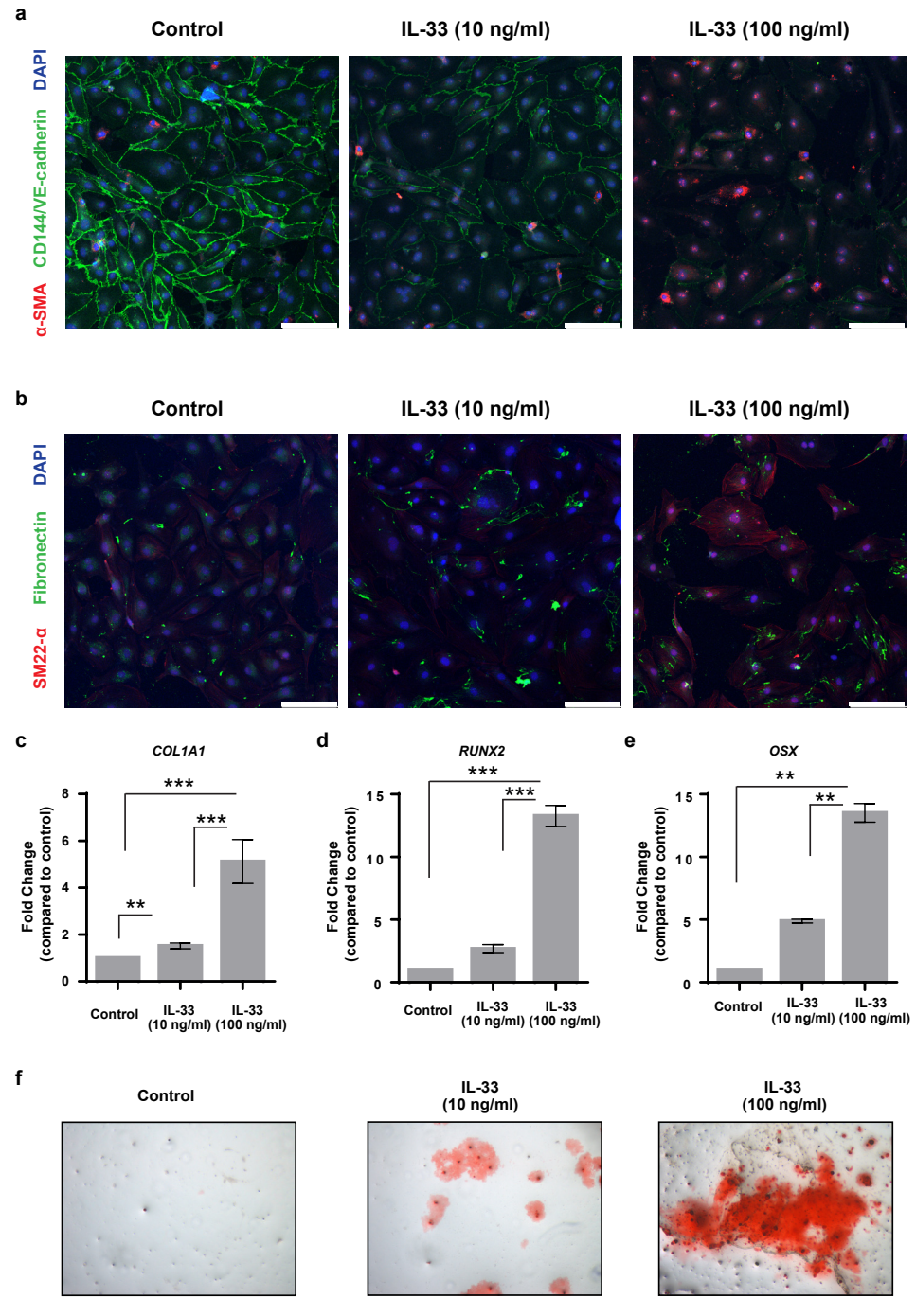

Figure S9

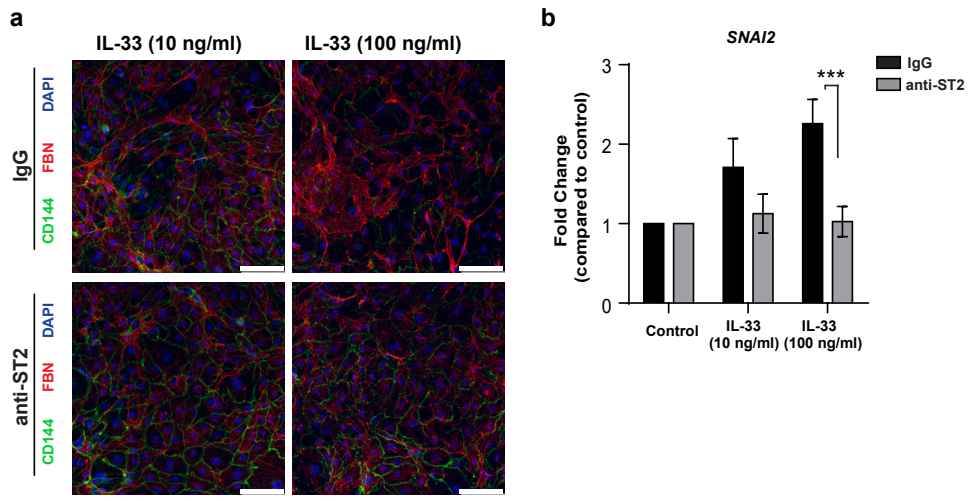

Figure S9. Blockage of ST2 receptor signaling attenuates IL-33 induced EndMT in human ECs

a. Immunofluorescent pictures depicting increased protein expression of CD144/VE-cadherin and reduced fibronectin (FBN) by ECFCs following 24 hour exposure to IL-33 (10 and 100 ng/ml) in combination with an anti-ST2 neutralizing antibody (lower panels) in comparison IgG control antibody (upper panels) (representative data from n=3 independent experiments). DAPI was used to visualize cell nuclei. White scale bars represents 120 µm.

b. *SNAI2* expression by ECFCs exposed to IL-33 (10 and 100 ng/ml) in combination with an IgG control antibody or an anti-ST2 neutralizing antibody after 24 hours. (n=5 independent experiments). ***p <0.001, 2-tailed unpaired Student's t test. Data represent mean ± S.E.M. S.E.M: Standard error of mean.

Figure S10

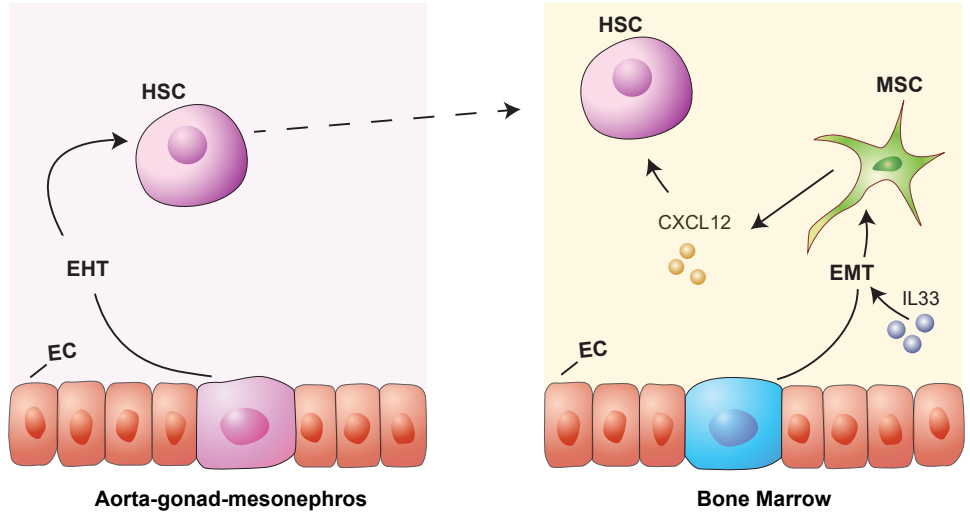

Figure S10. EC contributions to the development of the hematopoietic system in mammals

ECs contribute directly to hematopoiesis by giving rise to hematopoietic stem cells (HSCs) via endothelial-hematopoietic-transition (EHT). In addition, ECs generate mesenchymal multipotent stromal cells (MSCs) that establish the hematopoietic niche via EndMT driven by interleukin (IL)-33.

Table S1

Gene Name	Fetal hRECs FPKM
ENG (CD105)	120.3 ± 47.7
MCAM (CD146)	58.6 ± 31.7
NGFR (CD271)	0.9 ± 0.7
LEPR	5.9 ± 3.4
PDGFRA (CD140a)	1.2 ± 0.7
THY1 (CD90)	26.8 ± 12.5
NT5E (CD73)	5.6 ± 1.8
CSPG4 (NG2)	0.5 ± 0.3

Table S1. Expression of transcripts encoding mesenchymal proteins in fetal ECs
Transcripts encoding mesenchymal markers are expressed in fetal hRECs ($CD45^-CD235^-CD31^+CD9^+CD105^+$) (n=3) (Kenswil et al., 2018). Data represent FPKM values as obtained by massive parallel RNA sequencing. FPKM: fragments per kilobase of exon per million fragments mapped. Data represent mean ± S.E.M. S.E.M: Standard error of mean.

Table S2

GO Term	NES	FDR q-val
ECM remodeling		
GO_PROTEINACEOUS_EXTRACELLULAR_MATRIX	2.36	<0.001
GO_COLLAGEN_FIBRIL_ORGANIZATION	2.32	<0.001
GO_EXTRACELLULAR_MATRIX	2.27	<0.001
GO_COLLAGEN_TRIMER	2.22	<0.001
GO_COLLAGEN_BINDING	2.14	<0.001
Skeletal development		
GO_OSSIFICATION	2.17	<0.001
GO_OSTEOBLAST_DIFFERENTIATION	2.06	<0.01
GO_CHONDROCYTE_DIFFERENTIATION	1.94	<0.05
GO_CARTILAGE_DEVELOPMENT	1.94	<0.05
GO_BONE_MORPHOGENESIS	1.90	<0.05
Neural development		
GO_NEURON_CELL_CELL_ADHESION	1.80	<0.05
GO_NEURON_FATE_SPECIFICATION	1.70	<0.1
GO_POSITIVE_REGULATION_OF_AXONOGENESIS	1.67	<0.1
GO_NEUROBLAST_PROLIFERATION	1.66	<0.1
GO_GLIOGENESIS	1.58	<0.25
(Mesenchymal) Stem cell proliferation		
GO_STEM_CELL_PROLIFERATION	1.82	<0.05
GO_POSITIVE_REGULATION_OF_STEM_CELL_PROLIFERATION	1.79	<0.05
GO_REGULATION_OF_STEM_CELL_PROLIFERATION	1.68	<0.1
GO_POSITIVE_REGULATION_OF_MESENCHYMAL_CELL_PROLIFERATION	1.72	<0.1
GO_REGULATION_OF_MESENCHYMAL_CELL_PROLIFERATION	1.72	<0.1
Wnt pathway		
GO_FRIZZLED_BINDING	1.78	<0.05
GO_REGULATION_OF_CATENIN_IMPORT_INTO_NUCLEUS	1.65	<0.1
GO_REGULATION_OF_CANONICAL_WNT_SIGNALING_PATHWAY	1.56	<0.25
Hedgehog pathway		
GO_REGULATION_OF_SMOOTHENED_SIGNALING_PATHWAY	1.98	<0.01
GO_NEGATIVE_REGULATION_OF_SMOOTHENED_SIGNALING_PATHWAY	1.95	<0.05
GO_POSITIVE_REGULATION_OF_SMOOTHENED_SIGNALING_PATHWAY	1.65	<0.1

Table S2. Gene ontology gene sets enriched in $LNGFR^+$ hRECs in comparison to $LGNFR^-$ hRECs
Gene sets associated with extracellular matrix remodeling, skeletal development, neural development, (mesenchymal) stem cell proliferation, Wnt signaling, and Hedgehog signaling were identified by Gene Ontology (GO) term analysis. NES and FDR value of each gene set is listed. NES: normalized enrichment score. FDR: false discovery rate.

Table S3

Sorted Cells	hREC CD271-	hREC CD271+	CD31-CD105+ CD271-	CD31-CD105+ CD271+
1000	No Stroma	Stroma	No Stroma	Stroma
500	No Stroma	Stroma	No Stroma	Stroma
100	No Stroma	Stroma	No Stroma	Stroma
10	No Stroma	Stroma	No Stroma	Stroma

Table S3. CFU-F capacity of LNGFR$^+$ and LGNFR$^-$ subsets plated at different densities
The capacity to generate mesenchymal stromal cells *in vitro* was confined to LNGFR$^+$ niche populations. Freshly isolated FACS-sorted LNGFR$^+$ hRECs formed stromal layers at comparable cell densities as CD31$^-$LNGFR$^+$ MSCs. Data from 1 fetal bone donor.

EXPERIMENTAL PROCEDURES

Human bone marrow samples

Human bone samples (BM) were collected as previously described (Kenswil et al., 2018). Briefly, BM aspirates of AML patients were collected 17 days after start of chemotherapy (median age: 65 years, range 28-76). All patients were in complete remission after the first cycle of chemotherapy. Control BM was collected by aspiration from healthy individuals that served as donors for allogeneic bone marrow transplantation (median age: 44 years, range 24-58). Bone tissue was obtained from patients undergoing hip replacement surgery (median age: 55 years, range 22-71). Human fetal long bones (median age: 18 gestational weeks, range 15-20) were collected from elective abortions. Gestational age was confirmed by ultrasonic measurement by determining skull diameter and femoral length. The use of human samples was approved by the Institutional Review Board of the Erasmus Medical Center, the Netherlands, in accordance with the declaration of Helsinki with informed consent.

Mice and in vivo procedures

VE-Cadherin-Cre (B6;129-Tg(Cdh5-cre)1Spe/J) mice (Chen et al., 2009), and *Rosa26-tdTomato* (*B6.Cg-Gt(ROSA)26Sortm9(CAG-tdTomato)Hze/J*) mice (Madisen et al., 2010) (Jackson Laboratory), were intercrossed to generate *VE-Cadherin-Cre;LoxP-tdTomato* mice. Animals were maintained in specific pathogen-free conditions in the Experimental Animal Center of Erasmus MC (EDC). All mice were sacrificed by cervical dislocation. Mouse BM and collagenased bone fraction cells were isolated as previously described (Zambetti et al., 2016). Animal studies were approved by the Animal Welfare/Ethics Committee of the EDC in accordance with legislation in the Netherlands.

Cell isolation from human bone (marrow)

Mononuclear cells (MNCs) were isolated from human BM aspirates as previously reported (Kenswil et al., 2018). Briefly, AML Day 17 BM aspirates were mixed 1:25 with red blood cell lysis solution (NH4Cl 0.155 M, KHCO3 0.01 M, EDTA-Na2.2H2O 0.1 M, pH 7.4) to lyse red blood cells. Cryopreserved BM aspirates from healthy individuals were thawed in a waterbath at 37°C. MNCs were collected by centrifugation and washed once with phosphate buffered saline (PBS)+0.5% fetal calf serum (FCS).

Fetal BM MNCs were isolated from fetal long bones, which were first cut into smaller pieces before being gently crushed using a mortar and pestle. BM fraction was filtered through a 40-µm filter and collected in a 50 ml collection tube. Resulting bone fragments were digested with 0.25% collagenase type I (Stem Cell. Cat#07902) for 45 minutes in a waterbath at 37^{o}C to release fetal bone cells. Subsequent BM and bone fragment cell suspensions were washed in PBS+0.5%FCS and cleared from erythrocytes with IOtest3 lysing solution

(Beckman Coulter. Cat#A07799). This was then followed by another washing step with PBS+0.5%FCS. For adult hip bone cells, trabecular bone was also gently crushed using a mortar and pestle and resulting BM and collagenased bone fractions were processed as described for fetal bone cells.

Fluorescence active cells-sorting (FACS) of human niche cells

Cell sorting was performed as previously described (Kenswil et al., 2018). Cells were stained with the following antibodies using optimized dilutions: CD45 (clone HI30, 1:100), CD271 (clone ME20.4, 1:100), CD235a (clone HI264, 1:100), CD31 (clone WM59, 1:100), CD9 (clone HI9a, 1:100) all from Biolegend, and CD105 (clone SN6, 1:50) from eBioscience, and CD144 (clone 55-7H1, 1:50) from BD Biosciences, and subsequently sorted using a FACS ARIAIII Cells Sorter (BD Biosciences). For RNASeq, cells were directly sorted in 800µl Trizol (Ambion) for RNA isolation.

In addition, to determine CD34 and CD144 expression, a number of fetal BM samples were also stained with the following antibodies: CD144 (BD Biosciences, clone 55-7H1, 1:50), and CD34 (Biolegend, clone 581, 1:100).

Flow cytometry on murine bone (marrow) cells

To define and determine the frequencies of murine niche cells, collagenased bone fraction cell suspensions were stained with the following antibodies: anti-CD45.2 (clone 104, 1:100), anti-Ter119 (clone TER-119, 1:25), anti-CD144 (clone BV13, 1:200), anti-CD51 (clone RMV-7, 1:50), anti-Sca1 (clone D7, 1:50) (all from Biolegend), anti-CD140α (clone APA5, 1:100) (eBioscience), and anti-CD31 (clone MEC 13.3, 1:100) (BD Biosciences). Alexa Fluor™ 488-conjugated Streptavidin (S11223, 1:100) (Invitrogen) was used to detect cells marked by biotin anti-CD51 antibody. 7-Amino-Actinomycin D (7-AAD, 1:100) viability dye (A07704, Beckman Coulter) was used to distinguish between living and dead cells.

Immunocytochemistry to detect CD31, CD105, and CD271

To detect CD31, CD105, and CD271 expression on individual niche cells, $CD31^+$ and $CD31^-$ niche cells were sorted in PBS+0.5%FCS and subsequently transferred to poly-l-lysine coated glass slides. To prevent interference from FACS antibodies directed against CD9 and CD105, we excluded these and used the following antibody cocktail for sorting $CD31^+$ and $CD31^-$ niche cells: CD45-BV510 (clone HI30, 1:100), CD235a-PeCy7 (clone HI264, 1:100), CD271-FITC (clone ME20.4, 1:100), and CD31- APC/Cy7 (clone WM59, 1:100), all from Biolegend, and 7AAD (Stem-Kit Reagents) to exclude dead cells.

FACS-sorted niche cells were fixed with 4% paraformaldehyde (PFA)/PBS for 15 minutes on ice, were washed 3 times with PBS, and then incubated in 1%BSA/PBS for 1 hour at room temperature to block aspecific binding sites. Next, cells were stained with rabbit anti-human CD271 (Sigma-Aldrich, HPA004765) and goat anti-human CD105 antibodies (R&D Systems, AF1097-SP). Secondary staining was performed using Alexa Fluor 488-conjugated donkey anti-rabbit (ThermoFisher, A-21206), and Cy3-conjugated donkey anti-goat antibodies (Jackson ImmunoResearch, 705-165-147). After 2 washes in PBS, slides were mounted in VECTASHIELD Mounting Medium with DAPI (Vector Laboratories).

Images were acquired with a Leica TCS SP5 confocal microscope using the LAS software (Leica Microsystems). Alexa Fluor 488 was detected with the 488 laser, Cy3 was detected using the 561 laser, and CD31-APC/Cy7 was detected by using the 633 laser.

RNA Sequencing and geneset enrichment analysis (GSEA)

RNA of sorted cells was extracted according to the manufacturer's instructions for RNA isolation with GenElute LPA (Sigma). cDNA was prepared using the SMARTer procedure with the SMARTer Ultra Low RNA Kit (Clontech) for Illumina Sequencing. The Agilent 2100 Bio-analyzer and the High Sensitivity DNA kit were applied to determine the quantity and quality of the cDNA production. Library preparation and RNA-sequencing was performed as previously described and validated for low cell number-input (Chen et al., 2016b). In brief, prior to sequence alignment, the SMARTer adapters were trimmed using the cutadapt program. The resulting sequences were aligned to the human or murine RefSeq transcriptome using STAR. Sequences that could not be aligned to the RefSeq transcriptome were aligned to the reference genome (build hg19). Normalization and quantification was performed using Cufflinks. The resulting gene expression values are measured as FPKM (Fragments per kilobase of exon per million fragments mapped). Fragment counts were determined per gene with HTSeq-count, utilizing union modes, and subsequently used for differential expression analysis using the DESeq2 package, with standard parameters, in the R environment. Multiple testing correction was performed with the Benjamini-Hochberg procedure to control the False Discovery Rate (FDR). Principle component analysis was performed on the fragment counts using the R environment. Finally, gene set enrichment analysis (GSEA) was performed on the FPKM values using the curated C2 collection of gene sets within MSigDB (Subramanian et al., 2005). Similarly, Gene-ontology (GO) analysis was performed using the curated C5 collection of gene sets.

Fibroblast colony forming efficiency assay

FACS-sorted fetal $LNGFR^+$ hRECs and $CD31^-LNGFR^+$ MSCs were seeded in EGM-2 medium (EBM-2 medium (CC-3156, Lonza) supplemented with EGM-2 SingleQuot growth factors (CC-4176, Lonza), 1 cell per well in a 96-well plate at 37ºC and 5% CO_2. After 2 weeks, cells were fixed with 70% ethanol (vol/vol) and stained with Giemsa. CFU-F colonies were enumerated as previously described (Kenswil et al., 2018).

Human mesenchymal cell culture

Mesenchymal cells derived from FACS-sorted fetal LNGFR$^+$ ECs and CD31$^-$LNGFR$^+$ MSCs were cultured in EGM-2 medium until passage 2 and then transferred to αMEM medium containing 10% FCS and 1% Penicillin-Streptomycin. Cells were subsequently collected at indicated passages for FACS-analyses, differentiation assays and cryopreservation.

Murine mesenchymal cell culture and flow cytometry analyses

5x10^5 whole lysed unfractionated *VE-Cadherin-Cre;LoxP-tdTomato* BM cells/cm^2 were cultured in αMEM medium containing 20% FCS and 1% Penicillin-Streptomycin until reaching confluency. Subsequently, flow cytometric analyses were performed using the following antibodies: anti-CD45.2 (clone 104, 1:100), anti-CD144 (clone BV13, 1:200) (both from Biolegend), anti-CD31 (clone MEC 13.3, 1:100), anti-CD44 (clone IM7, 1:300) (both from BD Biosciences), and anti-CD29 (clone HMb1-1, 1:100) (eBioscience).

Osteogenic, adipogenic, and chondrogenic differentiation assays

For osteogenic differentiation, 3x10^3 mesenchymal cells/cm^2 were cultured in osteogenic induction medium (High glucose DMEM containing glutamax (Invitrogen) supplemented with 10% FCS, 10 mM glycerophosphate (Sigma), 0.1 µM Dexamethasone (Sigma), and 0.1 mM Vitamin-C (Sigma)). Medium was refreshed every 3-4 days at 37°C and 5% CO_2. At end of culture (day 17-21 depending on macroscrope observation of mineralization or cell sheets detaching from outer periphery of well), cells were fixed in 70% ethanol (vol/vol) at 4°C for 1 hour, and after consecutive PBS washes, were stained for 10-20 minutes with an alizarin Red S solution (saturated Alizarin Red S (Sigma) in demineralized water adjusted to pH 4.2 using 0.5% ammonium hydroxide).

For adipogenic differentiation, 2.1X10^4 mesenchymal cells/cm^2 were cultured in adipogenic induction medium (High glucose DMEM containing glutamax supplemented with 10% FCS, 1µm Dexamethasone, 0.2 mM indomethacin (Sigma), 0.01 mg/ml insulin (Sigma), 0.5 mM 3 iso-butyl-l-methyl-xanthine (Sigma). Medium was refreshed every 3-4 days at 37°C and 5% CO_2. At end of culture (day 14), cells were fixed in 4% PFA/PBS for 10 minutes, and stained for 10-15 minutes with an Oil red-O solution (0.5% w/v Oil-red O (in 2-propanol; Sigma)) followed by rinsing in distilled water.

For chondrogenic differentiation, 2x10^5 mesenchymal cells were suspended in complete chondrogenic induction medium (High glucose DMEM containing glutamax supplemented with 1mM Sodium pyruvate (Invitrogen), 40µg/ml Proline (Sigma), 1:100v/v insulin-transferrin-selenium (BD Biosciences), 10 ng/mL TGF-β3 (R&D Systems), 100 nM dexamethasone (Sigma)) in 15mL polypropylene tubes then centrifuged at 200 g for 8 minutes. Medium was refreshed every 3-4 days at 37°C and 5% CO_2. At end of culture (day 21), cell pellets were fixed in 4% PFA/PBS for one hour, embedded in liquid paraffin wax, and cut into 5 µm sections. After deparaffinization, sections were stained for 5 minutes with a Thionine solution (0.04% thionin (Sigma) in 0.01M aqueous sodium acetate pH 4.5).

FACS of mesenchymal cells derived from LNGFR$^+$ ECs and CD31$^-$LNGFR$^+$ MSCs

Mesenchymal cells were collected at P2 and P4, and stained with the following antibodies using optimized dilutions: CD31 (Biolegend, clone WM59, 1:100), CD34 (BD Biosciences, clone 8G12, 1:50), CD45 (Biolegend, clone HI30, 1:50), CD51 (Biolegend, clone NKI-M9, 1:100), CD73 (Biolegend, clone AD2, 1:100), CD90 (eBioscience, clone eBio5E10, 1:100), CD105 (eBioscience, clone SN6, 1:50) and CD146 (BD Biosciences clone P1H12, 1:100) antibodies. Accordingly, cells were also separately incubated with appropriate mouse IgG1, kappa isotype controls: APC/Cy7 (400127), FITC (400107), PE (400111), PE/Cy7 (400125), all from Biolegend, and APC (eBioscience, 17-4714-41). Flow-cytometric analyses was performed using a BD LSRII (BD Biosciences, San Jose, CA, USA) and data was analyzed using FlowJo software (Tree Star Inc, Ashland, OR, USA).

Co-culture of hematopoietic stem progenitor cells with the stromal progeny of LNGFR$^+$ ECs and CD31$^-$LNGFR$^+$ MSCs

Isolation of hematopoietic progenitor/stem cells (HSPCs) from umbilical cord blood (CB) was performed as previously described (Kenswil et al., 2018). Briefly, CD34$^+$ CB cells were isolated using a Ficoll gradient protocol and by magnetic-activated cell sorting (MACS). 24 hours prior to co-culture, to establish a stromal feeder layer, 20.000 stromal cells were seeded per well in a 48-well plate in triplicate. Next, 7.500 HSPCs were seeded on the feeder layers per well and cultured in 350 µl α-MEM containing 10% FCS supplemented with human recombinant stem cell factor (SCF) (25 ng/ml), Thrombopoietin (TPO) (25 ng/ml), FLT3L (25 ng/ml), all from Cellgenix, at 37ºC and 5% CO_2. Medium was refreshed every 3-4 days and cells collected at day 7 for FACs analysis and hematopoietic colony forming-unit (CFU-C) assays, as previously described (Kenswil et al., 2018).

Subsequently, total cell number was quantified by the single-method platform flowcytometric assay (Kenswil et al., 2018). Supernatant containing the non-adherent cultured HSPCs was collected after gentle resuspension and were mixed with adherent cells obtained by trypsinization (TrypLE™ Select (1X), no Phenol Red, #12563011, Gibco). Cells were then incubated with CD34 (348811, BD Biosciences,1:50) and CD45 (304022, Biolegend, 1:50) antibodies to identify HSPCs, and a calibrated number of flow-count fluorosphere beads (7547053, Beckman Coulter). 7AAD (Stem-Kit Reagents) was also included to distinguish between living and non-living cells. The total number of living MNC per µl (n) in a well was calculated using the following formula: n= ((number of MNC events recorded * bead concentration)/ number of recorded single beads)/ (volume cells/ volume beads).

Similarly, the immunophenotype of the cells was determined by staining the cells with hematopoietic lineage-marker cocktail (#22-7778-72, 1:12.5), CD90 (clone eBio5E10, 1:50) antibodies, all from eBiosciences, and CD34 (clone 8G12, 1:50), CD38 (clone HIT2, 1:30), and CD45RA (clone HI100, 1:50) antibodies, all from BD Biosciences. Living cells were identified by excluding 7AAD$^+$ cells. Flowcytometric analysis was performed using a BD LSRII (BD

Biosciences, San Jose, CA, USA) and data was analyzed using FlowJo software (Tree Star Inc, Ashland, OR, USA).

Human hematopoietic colony forming-unit assay

To further assess the hematopoietic potential of cultured HSPCs following co-culture with stromal progeny of LNGFR$^+$ ECs or CD31$^-$LNGFR$^+$ MSCs, we performed a colony-forming unit assay (CFU-C). Input equivalent of 1 x 10^3 cultured CD34$^+$ cells of each condition (LNGFR$^+$ ECs vs CD31$^-$LNGFR$^+$ MSCs) was resuspended in 400 µl Iscove's Modified Dulbecco's Medium (IMDM) and transferred to 3.6 ml of methylcellulose (MethoCult H84434, StemCell Technologies). Cells were then plated in triplicate in 1 cm² petri-dishes (1 ml/dish) and were kept at 37ºC and 5% CO2. Colonies were counted after 12-14 days.

Subcutaneous implantation of chondrogenically primed pellets containing LNGFR$^+$ ECs-derived mesenchymal cells

Mesenchymal cells derived from LNGFR+ ECs were seeded in 15 mL-polypropylene conical tube and centrifuged to form 3D pellets (2 × 10^5 cells/pellet). The pellets were cultured in 500µL DMEM-high-glucose GlutaMAX+ (GIBCO) supplemented with 1.5 µg/mL fungizone, 50 µg/mL gentamicin, 1% ITS+ Premix (Corning), 40 µg/mL L-proline (Sigma-Aldrich), 1 mM sodium pyruvate (GIBCO), 100 nM dexamethasone (Sigma-Aldrich), 25 µg/mL L-ascorbic acid-2-phosphate and 10 ng/mL TGF-β3 (R&D Systems) for 3 weeks. The culture medium was renewed twice a week.

Next, these pellets were implanted subcutaneously on the dorsum of 8 weeks old male athymic nude mice (BALB/cAnNCrl; Charles River). 1h before implantation, animals were given pain medication (buprenorphine, 0.05 mg/kg body weight). Following induction of general anaesthesia (isoflurane), four transverse incisions were created in the skin of the dorsum: two between the shoulder blades and two at the level of the hips. Four subcutaneous pockets were created by blunt dissection and a construct consisting of 6 chondrogenically primed hREC pellets was implanted in each pocket (n=6 constructs). The incisions were closed with staples. 10 weeks post-implantation, pellet mineralization was assessed by Micro-computed tomography (µCT) imaging. µCT scans were performed and reconstructed with the Quantum GX-2 imaging systems (PerkinElmer), using a field of view of 86 mm (90 kV/88 uA, 4 min). Animals were euthanized by cervical dislocation and the constructs were carefully retrieved.

Mice were housed in groups of three under a standard 12 h light/dark cycle, with access to food and water ad libitum. Animal experiments were conducted in the animal facility of the Erasmus MC with approval of the animal ethics committee (project license AVD1010020186166).

Histological analysis of 3D pellets

In vitro chondrogenically primed pellets and *in vivo* bone constructs were fixed for 24h in 4% (w/v) formaldehyde in PBS. *In vivo* samples were further decalcified for 7d in 10% w/v EDTA in PBS, changing the solution twice per week. Next, samples were embedded in paraffin wax. 6 µm-thick sections were cut, deparaffinized, rehydrated and stained with haematoxylin and eosin (H&E) or 0.04% thionine solution (Sigma-Aldrich) to detect glycosaminoglycans (GAGs).

HUVEC culture and stimulation

Human umbilical vein ECs (HUVECs, Lonza, Walkersville, MD) were cultured on 1% gelatin-coated (Sigma, #G9391, St. Louis, MO) flasks or wells. Cells were cultured in endothelial cell medium (ECM) consisting of RPMI 1640 basal medium (Lonza, #BE12-702F, Verviers, Belgium) with heat inactivated Fetal Bovine Serum (Lonza, 20% v/v), Heparin (LEO, #BE013587 5U/ml), EC Growth Factor (ECGF; own preparation 50 µg/ml (Lerner and Harrison, 1990)), penicillin / streptomycin (Gibco, #15140-122, (1%v/v)) and L-Glutamine (Lonza, #BE17-605E 2nM) at 37°C, 5% CO_2. Cells were detached using Trypsin EDTA in PBS (TEP, GIBCO #15400054) solution. Experiments were performed between passages 5 and 6.

HUVECs were either left untreated or stimulated with IL-33 (10 ng/ml or 100 ng/ml, ProSpec), and/ or with TGF-β1 (10 ng/ml, R&D Systems) for 96 hours in ECM without ECGF. Culture medium was refreshed daily during stimulation.

Flow cytometry of HUVECs

HUVECs were stained with the following antibodies using optimized dilutions: CD144 (BD Biosciences, clone 55-7H1, 1:50), CD31 (Biolegend, clone WM59, 1:50), CD34 (BD Biosciences, clone 8G12, 1:50), CD271 (Biolegend, clone ME20.4, 1:100), CD44 (Biolegend, clone IM7, 1:50), CD90 (eBioscience, clone eBio5E10, 1:100), antibodies.

Accordingly, cells were also incubated with appropriate mouse IgG1, kappa isotype controls: APC/Cy7 (400127), FITC (400107), PE (400111), PE/Cy7 (400125), all from Biolegend, V450 (BD Biosciences, 560373) and APC (eBioscience, 17-4714-41). Flow-cytometric analyses was performed using a BD LSRII (BD Biosciences, San Jose, CA, USA) and data was analyzed using FlowJo software (Tree Star Inc, Ashland, OR, USA).

RNA extraction and gene expression analyses of HUVECs

Cells were lysed in TriZOL Reagent (Invitrogen #15596026) and RNA was extracted by Chloroform according to manufacturer's instructions. RNA purity and quantity was assessed using Nanodrop spectrometric analysis. All relative absorbances (A260/280 and A260/230) were >2.0. RNA integrity was assessed on a 1% Agarose gel. 2 µg total RNA was reverse transcribed using the RevertAid First Strand cDNA synthesis kit (Fermentas, #K1622) according to manufacturer's protocol. Quantitative PCR expression analysis was performed

on a reaction mixture containing 10 ng cDNA-equivalent, 0.3 µM sense primers and 0.3 µM antisense primers (Table 1; Sigma) and FastStart SYBR Green (Roche, Almere, The Netherlands). Analyses were run on a Viia7 real-time PCR system (Applied Biosystems).

Table 1. qPCR primers used on RNA isolated from HUVECs

EndMT Transcription factors (sense; antisense)		
SNAI1	GCTGCAGGACTCTAATCCAGA	ATCTCCGGAGGTGGGATG
SNAI2	TGGTTGCTTCAAGGACACAT	GTTGCAGTGAGGGCAAGAA
TWIST1	AAGGCATCACTATGGACTTTCTCT	GCCAGTTTGATCCCAGTATTTT
Endothelial marker genes (sense; antisense)		
CDH5	GTTCACCTTCTGCGAGGATA	GTAGCTGGTGGTGTCCATCT
PECAM1	GCAACACAGTCCAGATAGTCGT	GACCTCAAACTGGGCATCAT
VWF	AGTGAGCCTCTCCGTGTATC	TCACCGGACAGCTTGTAGTA
Mesenchymal marker genes (sense; antisense)		
ACTA2	CTGTTCCAGCCATCCTTCAT	TCATGATGCTGTTGTAGGTGGT
FAP	TGGCGATGAACAATATCCTAGA	ATCCGAACAACGGGATTCTT
TAGLN	CTGAGGACTATGGGGTCATC	TAGTGCCCATCATTCTTGGT

All primers were derived from Sigma.

Glycosaminoglycan production by IL-33-treated HUVECs

The ability of cultured cells to deposit glycosaminoglycans was assessed by the Dimethyl methylene blue (DMMB) method. In short, cells were lysed in 100 µl RIPA buffer (ThermoScientific #89901) and 20 µl of the lysate was mixed with 200 µl DMMB Reagent (Dimethyl methylene blue (100 µM) in 0.6% Acetic acid containing 3 mg.ml-1 Glycine and 1.6mg.ml-1 NaCl, pH 1.5). Samples were incubated at room temperature while shaking for 5 minutes, after which absorbance was measured at A525. Sample glycosaminoglycan content was normalized for protein content as determined by Bradford.

Calcium deposition by IL-33-treated HUVECs

The ability of cultured cells to deposit calcium was assessed by Alizarin Red S (Sigma #A5533). In short, cells were washed in PBS and fixed in 4% formaldehyde at room temperature for 15 mins. The fixative was aspirated and samples washed in diH2O and incubated with Alizarin Red S (40 mM in diH2O). Excess dye was removed by extensive washes with diH2O. Precipitated Alizarin Red was liquified in 10% acetic acid, collected in microcentrifuge tubes and heated to 85°C for 10 minutes. Samples were cooled on ice and pH was adjusted to 4.5 using ammonium hydroxide. The optical density at OD405 was measured and Alizarin Red concentration was calculated against a standard curve of known Alizarin concentrations and normalized for protein content.

ECFC isolation and culture

ECFCs represent an easy source of fully functional highly proliferative ECs from humans. The isolation protocol of humans ECFCs requires withdrawal of 30-60 mL of peripheral blood in citrate-treated collection tubes, after first obtaining written informed consent in accordance with the institutional guidelines. Usually, the first 2 mL of blood were discarded to avoid contamination with skin fibroblasts. The blood was pre-diluted 1:1 with pre-warmed PBS and centrifuged at 740 x g for 30 min in the presence of Ficoll Paque Plus (GE Healthcare Europe GmbH, The Netherlands), in order to separate a fraction containing mononuclear cells (MNCs). These MNCs were subsequently collected and washed three times with M199 (Lonza, Verviers, Belgium) supplemented with 0.1% penicillin/streptomycin (Invitrogen, The Netherlands). Next, these cells were re-suspended in complete EGM-2 (Lonza, Walkerville, MD, USA) supplemented with 10% platelet lysate (PL-EGM) and 0.1% penicillin-streptomycin and seeded at a density of 1.3 x 10^6 cells/cm^2 into 48 well-plates pre-coated with 3 µg/cm^2 human collagen type I prepared according to manufacturer's instructions (#C7624, Sigma Aldrich). After 24 hours, non-adherent cells were carefully removed and fresh medium was added to each well. From this moment, the medium was replaced every day while supernatants were discarded. ECFCs colonies with regular cobblestone morphology appeared within 3-4 weeks.

ECFC quantitative Real Time RT-PCR (qPCR)

Total RNA extraction was performed using NucleoSpin RNA II (Machery Nagel, Düren, Germany). 1 µg of RNA was retro-transcribed using RevertAid First Strand cDNA Synthesis Kits (Fisher Scientific, Landsmeer, The Netherlands), and real-time reverse transcription-PCR experiments were performed using SYBR Green (Bio-Rad, Veenendaal, The Netherlands) and a Bio-Rad CFX Connect device.

Table 2. qPCR primers used on RNA isolated from ECFCs

EndMT Transcription factors (sense; antisense)		
SNAI2	AACAGTATGTGCCTTGGGGG	AAAAGGCACTTGGAAGGGGT
Osteogenic marker genes (sense; antisense)		
Runx2	TGGTTACTGTCATGGCGGGTA	TCTCAGATCGTTGAACCTTGCTA
Osterix	GCCAGAAGCTGTGAAACCTC	GCCAGAAGCTGTGAAACCTC
Col1a1	AAAGGCAATGCTCAAACACC	TCAAAAACGAAGGGGAGATG
Housekeeping gene (sense; antisense)		
GAPDH	TGCACCACCAACTGCTTAGC	GGCATGGACTGTGGTCATGAG

ECFC mineralization assays

For mineralization assays, 5 x 10^4 ECFCs were seeded into 48-well plates and incubated in the presence of IL33 (10, 100 ng/mL) or mQ vehicle-control for 5 days. Subsequently, the medium was replaced by osteogenic medium containing 10^{-8} mol/L dexamethasone, 0.2 mmol/L ascorbic acid and 10 mmol/L β-glycerolphosphate for 21 days. The medium was refreshed every 4 days. Afterwards cells were washed twice with PBS and fixed with 3.7% formaldehyde for 5 minutes. Next, cells were washed twice with distilled water and measurement of calcium deposition was performed by Alizarin Red Staining (ARS), as previously described (Zhang et al., 2012).

ECFC immunofluorescent labelling

For immunofluorescent labeling of ECFCs *in vitro*, cells grown on coverslips were fixed with 4% formaldehyde for 30 minutes at room temperature, washed with glycine for 5 minutes, permeabilized with 0.2% Triton X-100 and blocked in PBS containing 5% bovine serum albumin (BSA) for one hour. Next, the cells were incubated overnight at 4°C in blocking solution containing primary antibody with gentle shaking. Next day, the cells were washed 5 times in washing buffer (PBS containing 0.05% Tween-20 and 1% BSA) and incubated with secondary antibody (Alexa Fluor FITC goat anti-mouse IgG, Alexa-Fluor 555 anti-rabbit IgG (Invitrogen, Breda, the Netherlands), or Cy3 goat anti-mouse IgG (Jackson ImmunoResearch, Suffolk, England; 1:200) in PBS with 0.5% BSA for one hour. Finally, the cells were washed 5 times in washing buffer and mounted in Prolong Gold containing DAPI (Invitrogen). After careful drying, the preparations were imaged in a Leica SP5 confocal scanning laser microscope. A representative picture from each staining is shown (n = 3). The following antibodies were used for immunofluorescent staining: Ve-Cadherin (Cell Signaling, #2158, 1:100), Fibronectin (Sigma-Aldrich, F7387, 1:400), Transgelin (SM22α, abcam, ab14106, 1:400), α-SMA (Sigma-Aldrich,A2547).

Statistics

Statistical analyses were performed using Prism 5 (GraphPad Software) and SPSS 24 (IBM). Unless otherwise specified, unpaired, 2-tailed Student's t test (single test for comparison of 2 means) or 1-way ANOVA followed by Bonferroni correction for multiple comparisons were used to evaluate statistical significance, defined as $p < 0.05$. All results in bar graphs are means ± SEMs. The number of replicates is indicated in the figure legends, including the number of independent experiments.

ACKNOWLEDGEMENTS

We would like to thank Dr. Kirsten van Lom, Dr. Eric Braakman, Lucia Duinhouwer, and Mariëtte ter Borg for providing CD34+ cells and help with human bone marrow sampling; Nathalie Papazian for helping to process fetal tissue; Dr. Elwin Rombouts, Peter van Geel, Paulette van Strien, and Michael Vermeulen for operating the BD FACSARIA III; Onno Roovers, Almira Henić, and Gert-Jan Kremers for providing technical assistance; Esther Siteur-van Rijnstra and Cynthia van der Linden for providing technical assistance and logistic support in handling fetal tissue; Mathias Francois and lab members for help with the lineage tracing experiments; Emma de Pater for advice concerning mouse breeding and members of the ErasmusMC department of Hematology for providing scientific discussion. Egied Simons for assisting with illustrations. This work was supported by an ErasmusMC Fellowship Award to M.H.G.P.R. M-J.G and G.S-D. are supported by the Netherlands CardioVascular Research Initiative grant number 2014-11(awarded to the Reconnect consortium) including collective funding by the Dutch Heart Foundation, Dutch Federation of University Medical Centers, The Netherlands Organization for Health Research and Development, and the Royal Netherlands Academy of Sciences. G.S-D is sponsored by a trampoline grant (#22379) from AFM-Telethon. A.L is supported by the European Union's Horizon 2020 research and innovation programme under grant agreement No 801159.

AUTHOR CONTRIBUTIONS

K.J.G.K designed and performed the experiments, analyzed and visualized the data, and wrote the manuscript. G.S, and A.L designed and performed experiments, analyzed and visualized data. B.V, C.K, A.C.J, C.v.D, and E.M.J.B provided input on and performed experiments, and analyzed data. S.C, and C.v.D performed RNA-seq. R.M.H performed the bioinformatics analyses for the RNA-seq data. M.A.M and M.N.A performed FACS and RNA-seq. B.B provided human fetal samples. P.K.B provided the human hip bone samples and input on the experiments. M.G, and P.t.D provided ECFCs and input on experiments. T.C provided the human fetal samples and input on the experiments. E.F provided BM-derived MSCs and input on the experiments. G.K provided HUVECs, input on the experiments and analyzed data. M.H.G.P.R concepted the program, designed the experiments, analyzed the data, wrote the manuscript, supervised the study, and acquired funding.

DECLARATION OF INTERESTS

The authors declare no competing interests.

REFERENCES

Ansieau, S., Bastid, J., Doreau, A., Morel, A.P., Bouchet, B.P., Thomas, C., Fauvet, F., Puisieux, I., Doglioni, C., Piccinin, S., et al. (2008). Induction of EMT by Twist Proteins as a Collateral Effect of Tumor-Promoting Inactivation of Premature Senescence. Cancer Cell *14*, 79–89.

Azhar, M., Runyan, R.B., Gard, C., Sanford, L.P., Miller, M.L., Andringa, A., Pawlowski, S., Rajan, S., and Doetschman, T. (2009). Ligand-specific function of transforming growth factor beta in epithelial-mesenchymal transition in heart development. Dev. Dyn. *238*, 431–442.

Bianco, P., Robey, P.G., and Simmons, P.J. (2008). Mesenchymal stem cells: revisiting history, concepts, and assays. Cell Stem Cell *2*, 313–319.

Boisset, J., van Cappellen, W., Andrieu-Soler, C., Galjart, N., Dzierzak, E., and Robin, C. (2010). In vivo imaging of haematopoietic cells emerging from the mouse aortic endothelium. Nature *464*, 116–120.

Bracken, C.P., Gregory, P.A., Kolesnikoff, N., Bert, A.G., Wang, J., Shannon, M.F., and Goodall, G.J. (2008). A double-negative feedback loop between ZEB1-SIP1 and the microRNA-200 family regulates epithelial-mesenchymal transition. Cancer Res. *68*, 7846–7854.

Chakraborty, S., Wirrig, E.E., Hinton, R.B., Merrill, W.H., Spicer, D.B., and Yutzey, K.E. (2010). Twist1 promotes heart valve cell proliferation and extracellular matrix gene expression during development in vivo and is expressed in human diseased aortic valves. Dev. Biol. *347*, 167–179.

Chan, C.K.F., Seo, E.Y., Chen, J.Y., Lo, D., McArdle, A., Sinha, R., Tevlin, R., Seita, J., Vincent-Tompkins, J., Wearda, T., et al. (2015). Identification and specification of the mouse skeletal stem cell. Cell *160*, 285–298.

Chen, M.J., Yokomizo, T., Zeigler, B.M., Dzierzak, E., and Speck, N.A. (2009). Runx1 is required for the endothelial to haematopoietic cell transition but not thereafter. Nature *457*, 887–891.

Chen, Q., Zhang, H., Liu, Y., Adams, S., Eilken, H., Stehling, M., Corada, M., Dejana, E., Zhou, B., and Adams, R.H. (2016a). Endothelial cells are progenitors of cardiac pericytes and vascular smooth muscle cells. Nat. Commun. *7*, 12422.

Chen, S., Zambetti, N.A., Bindels, E.M.J., Kenswill, K., Mylona, A.M., Adisty, N.M., Hoogenboezem, R.M., Sanders, M.A., Cremers, E.M.P., Westers, T.M., et al. (2016b). Massive parallel RNA sequencing of highly purified mesenchymal elements in low-risk MDS reveals tissue-context-dependent activation of inflammatory programs. Leukemia *30*, 1938–1942.

Choi, S.H., Hong, Z.Y., Nam, J.K., Lee, H.J., Jang, J., Yoo, R.J., Lee, Y.J., Lee, C.Y., Kim, K.H., Park, S., et al. (2015). A hypoxia-induced vascular endothelial-to-mesenchymal transition in development of radiation-induced pulmonary fibrosis. Clin. Cancer Res. *21*, 3716–3726.

Crisan, M., Yap, S., Casteilla, L., Chen, C.W., Corselli, M., Park, T.S., Andriolo, G., Sun, B., Zheng, B., Zhang, L., et al. (2008). A Perivascular Origin for Mesenchymal Stem Cells in Multiple Human Organs. Cell Stem Cell *3*, 301–313.

Critser, P.J., and Yoder, M.C. (2010). Endothelial colony-forming cell role in neoangiogenesis and tissue repair. Curr. Opin. Organ Transplant. *15*, 68–72.

Dejana, E., Hirschi, K.K., and Simons, M. (2017). The molecular basis of endothelial cell plasticity. Nat. Commun. *8*, 1–11.

Dominici, M., Le Blanc, K., Mueller, I., Slaper-Cortenbach, I., Marini, F.C., Krause, D.S., Deans, R.J., Keating, A., Prockop, D.J., and Horwitz, E.M. (2006). Minimal criteria for defining multipotent mesenchymal stromal cells. The International Society for Cellular Therapy position statement. Cytotherapy *8*, 315–317.

Farrell, E., Both, S.K., Odörfer, K.I., Koevoet, W., Kops, N., O'Brien, F.J., de Jong, R.J.B., Verhaar, J.A., Cuijpers, V., Jansen, J., et al. (2011). In-vivo generation of bone via endochondral ossification by in-vitro chondrogenic priming of adult human and rat mesenchymal stem cells. BMC Musculoskelet. Disord. *12*, 31.

Galipeau, J., and Sensébé, L. (2018). Mesenchymal Stromal Cells: Clinical Challenges and Therapeutic Opportunities. Cell Stem Cell *22*, 824–833.

Greenbaum, A., Hsu, Y.M.S., Day, R.B., Schuettpelz, L.G., Christopher, M.J., Borgerding, J.N., Nagasawa, T., and Link, D.C. (2013). CXCL12 in early mesenchymal progenitors is required for haematopoietic stem-cell maintenance. Nature *495*, 227–230.

Guo, Z., Wu, J., Zhao, J., Liu, F., Chen, Y., Bi, L., Liu, S., and Dong, L. (2014). IL-33 promotes airway remodeling and is a marker of asthma disease severity. J. Asthma *51*, 863–869.

Hurlstone, A.F.L., Haramis, A.P.G., Wienholds, E., Begthel, H., Korving, J., Van Eeden, F., Cuppen, E., Zivkovic, D., Plasterk, R.H.A., and Clevers, H. (2003). The Wnt/β-catenin pathway regulates cardiac valve formation. Nature *425*, 633–637.

Isern, J., García-García, A., Martín, A.M., Arranz, L., Martín-Pérez, D., Torroja, C., Sánchez-Cabo, F., and Méndez-Ferrer, S. (2014). The neural crest is a source of mesenchymal stem cells with specialized hematopoietic stem cell niche function. Elife *3*, 1–28.

Jones, E., English, A., Churchman, S.M., Kouroupis, D., Boxall, S.A., Kinsey, S., Giannoudis, P.G., Emery, P., and McGonagle, D. (2010). Large-scale extraction and characterization of CD271+ multipotential stromal cells from trabecular bone in health and osteoarthritis: Implications for bone regeneration strategies based on uncultured or minimally cultured multipotential stromal cells. Arthritis Rheum. *62*, 1944–1954.

Kakkar, R., and Lee, R.T. (2008). The IL-33/ST2 pathway: Therapeutic target and novel biomarker. Nat. Rev. Drug Discov. *7*, 827–840.

Kenswil, K.J.G., Jaramillo, A.C., Ping, Z., Chen, S., Hoogenboezem, R.M., Mylona, M.A., Adisty, M.N., Bindels, E.M.J., Bos, P.K., Stoop, H., et al. (2018). Characterization of Endothelial Cells Associated with Hematopoietic Niche Formation in Humans Identifies IL-33 As an Anabolic Factor. Cell Rep. *22*, 666–678.

Kfoury, Y., and Scadden, D.T. (2015). Mesenchymal cell contributions to the stem cell niche. Cell Stem Cell *16*, 239–253.

Kokudo, T., Suzuki, Y., Yoshimatsu, Y., Yamazaki, T., Watabe, T., and Miyazono, K. (2008). Snail is required for TGF -induced endothelial-mesenchymal transition of embryonic stem cell-derived endothelial cells. J. Cell Sci. *121*, 3317–3324.

Kovacic, J.C., Dimmeler, S., Harvey, R.P., Finkel, T., Aikawa, E., Krenning, G., and Baker, A.H. (2019). Endothelial to Mesenchymal Transition in Cardiovascular Disease: JACC State-of-the-Art Review. J. Am. Coll. Cardiol. *73*, 190–209.

Kumar, A., D'Souza, S.S., Moskvin, O. V., Toh, H., Wang, B., Zhang, J., Swanson, S., Guo, L.W., Thomson, J.A., and Slukvin, I.I. (2017). Specification and Diversification of Pericytes and Smooth Muscle Cells from Mesenchymoangioblasts. Cell Rep. *19*, 1902–1916.

Kusumbe, A.P., Ramasamy, S.K., and Adams, R.H. (2014). Coupling of angiogenesis and osteogenesis by a specific vessel subtype in bone. Nature *507*, 323–328.

Kusumbe, A.P., Ramasamy, S.K., Itkin, T., Mäe, M.A., Langen, U.H., Betsholtz, C., Lapidot, T., and Adams, R.H. (2016). Age-dependent modulation of vascular niches for haematopoietic stem cells. Nature *532*, 380–384.

Lee, H.T., Lee, J.G., Na, M., and Kay, E.P. (2004). FGF-2 induced by interleukin-1β through the action of phosphatidylinositol 3-kinase mediates endothelial mesenchymal transformation in corneal endothelial cells. J. Biol. Chem. *279*, 32325–32332.

Lerner, C., and Harrison, D.E. (1990). 5-Fluorouracil spares hemopoietic stem cells responsible for long-term repopulation. Exp. Hematol. *18*, 114–118.

Li, H., Ghazanfari, R., Zacharaki, D., Ditzel, N., Isern, J., Ekblom, M., Méndez-Ferrer, S., Kassem, M., and Scheding, S. (2014). Low/negative expression of PDGFR-α identifies the candidate primary mesenchymal stromal cells in adult human bone marrow. Stem Cell Reports *3*, 965–974.

Lundberg, P., Allison, S.J., Lee, N.J., Baldock, P.A., Brouard, N., Rost, S., Enriquez, R.F., Sainsbury, A., Lamghari, M., Simmons, P., et al. (2007). Greater bone formation of Y2 knockout mice is associated with increased osteoprogenitor numbers and altered Y1 receptor expression. J. Biol. Chem. *282*, 19082–19091.

Maddaluno, L., Rudini, N., Cuttano, R., Bravi, L., Giampietro, C., Corada, M., Ferrarini, L., Orsenigo, F., Papa, E., Boulday, G., et al. (2013). EndMT contributes to the onset and progression of cerebral cavernous malformations. Nature *498*, 492–496.

Madisen, L., Zwingman, T.A., Sunkin, S.M., Oh, S.W., Zariwala, H.A., Gu, H., Ng, L.L., Palmiter, R.D., Hawrylycz, M.J., Jones, A.R., et al. (2010). A robust and high-throughput Cre reporting and characterization system for the whole mouse brain. Nat. Neurosci. *13*, 133–140.

Mahmoud, M.M., Serbanovic-Canic, J., Feng, S., Souilhol, C., Xing, R., Hsiao, S., Mammoto, A., Chen, J., Ariaans, M., Francis, S.E., et al. (2017). Shear stress induces endothelial-To-mesenchymal transition via the transcription factor Snail. Sci. Rep. *7*, 1–12.

Medici, D., Shore, E.M., Lounev, V.Y., Kaplan, F.S., Kalluri, R., and Olsen, B.R. (2010). Conversion of vascular endothelial cells into multipotent stem-like cells. Nat. Med. *16*, 1400–1406.

Van Meeteren, L.A., and Ten Dijke, P. (2012). Regulation of endothelial cell plasticity by TGF-β. Cell Tissue Res. *347*, 177–186.

Méndez-Ferrer, S., Michurina, T. V, Ferraro, F., Mazloom, A.R., MacArthur, B.D., Lira, S. a, Scadden, D.T., Ma'ayan, A., Enikolopov, G.N., and Frenette, P.S. (2010). Mesenchymal and haematopoietic stem cells form a unique bone marrow niche. Nature *466*, 829–834.

Morikawa, S., Mabuchi, Y., Niibe, K., Suzuki, S., Nagoshi, N., Sunabori, T., Shimmura, S., Nagai, Y., Nakagawa, T., Okano, H., et al. (2009a). Development of mesenchymal stem cells partially originate from the neural crest. Biochem. Biophys. Res. Commun. *379*, 1114–1119.

Morikawa, S., Mabuchi, Y., Kubota, Y., Nagai, Y., Niibe, K., Hiratsu, E., Suzuki, S., Miyauchi-Hara, C., Nagoshi, N., Sunabori, T., et al. (2009b). Prospective identification, isolation, and systemic transplantation of multipotent mesenchymal stem cells in murine bone marrow. J. Exp. Med. *206*, 2483–2496.

Nieto, M.A. (2002). The snail superfamily of zinc-finger transcription factors. Nat. Rev. Mol. Cell Biol. *3*, 155–166.

Olsen, B.R., Reginato, A.M., and Wang, W. (2000). Bone Development. Annu. Rev. Cell Dev. Biol. *16*, 191–220.

Pardali, E., Sanchez-Duffhues, G., Gomez-Puerto, M.C., and ten Dijke, P. (2017). TGF-β-induced endothelial-mesenchymal transition in fibrotic diseases. Int. J. Mol. Sci. *18*.

Pinho, S., Lacombe, J., Hanoun, M., Mizoguchi, T., Bruns, I., Kunisaki, Y., and Frenette, P.S. (2013). PDGFRα and CD51 mark human Nestin $^{+}$ sphere-forming mesenchymal stem cells capable of hematopoietic progenitor cell expansion. J. Exp. Med. *210*, 1351–1367.

Quirici, N., Soligo, D., Bossolasco, P., Servida, F., Lumini, C., and Deliliers, G.L. (2002). Isolation of bone marrow mesenchymal stem cells by anti-nerve growth factor receptor antibodies. Exp. Hematol. *30*, 783–791.

Rafii, S., Butler, J.M., and Ding, B.-S. (2016). Angiocrine functions of organ-specific endothelial cells. Nature *529*, 316–325.

Ramasamy, S.K., Kusumbe, A.P., and Adams, R.H. (2015). Regulation of tissue morphogenesis by endothelial cell-derived signals. Trends Cell Biol. *25*, 148–157.

Ramasamy, S.K., Kusumbe, A.P., Itkin, T., Gur-Cohen, S., Lapidot, T., and Adams, R.H. (2016). Regulation of Hematopoiesis and Osteogenesis by Blood Vessel–Derived Signals. Annu. Rev. Cell Dev. Biol. *32*, 649–675.

Sacchetti, B., Funari, A., Michienzi, S., Di Cesare, S., Piersanti, S., Saggio, I., Tagliafico, E., Ferrari, S., Robey, P.G., Riminucci, M., et al. (2007). Self-renewing osteoprogenitors in bone marrow sinusoids can organize a hematopoietic microenvironment. Cell *131*, 324–336.

Sanchez-Duffhues, G., Orlova, V., and Ten Dijke, P. (2016). In Brief: Endothelial-to-mesenchymal transition. J. Pathol. *238*, 378–380.

Sánchez-Duffhues, G., Williams, E., Benderitter, P., Orlova, V., van Wijhe, M., Garcia de Vinuesa, A., Kerr, G., Caradec, J., Lodder, K., de Boer, H.C., et al. (2019). Development of Macrocycle Kinase Inhibitors for ALK2 Using Fibrodysplasia Ossificans Progressiva-Derived Endothelial Cells. JBMR Plus *00*, e10230.

Schepers, K., Hsiao, E.C., Garg, T., Scott, M.J., and Passegue, E. (2012). Activated Gs signaling in osteoblastic cells alters the hematopoietic stem cell niche in mice. Blood *120*, 3425–3435.

Shi, S., Srivastava, S.P., Kanasaki, M., He, J., Kitada, M., Nagai, T., Nitta, K., Takagi, S., Kanasaki, K., and Koya, D. (2015). Interactions of DPP-4 and integrin β1 influences endothelial-to-mesenchymal transition. Kidney Int. *88*, 479–489.

Slukvin, I.I., and Kumar, A. (2018). The mesenchymoangioblast, mesodermal precursor for mesenchymal and endothelial cells. Cell. Mol. Life Sci. *75*, 3507–3520.

Souilhol, C., Harmsen, M.C., Evans, P.C., and Krenning, G. (2018). Endothelial-mesenchymal transition in atherosclerosis. Cardiovasc. Res. *114*, 565–577.

Subramanian, A., Tamayo, P., Mootha, V.K., Mukherjee, S., Ebert, B.L., Gillette, M. a, Paulovich, A., Pomeroy, S.L., Golub, T.R., Lander, E.S., et al. (2005). Gene set enrichment analysis: A knowledge-based approach for interpreting genome-wide expression profiles. Proc. Natl. Acad. Sci. *102*, 15545–15550.

Supek, F., Bošnjak, M., Škunca, N., and Šmuc, T. (2011). Revigo summarizes and visualizes long lists of gene ontology terms. PLoS One *6*.

Suzukawa, M., Koketsu, R., Iikura, M., Nakae, S., Matsumoto, K., Nagase, H., Saito, H., Matsushima, K., Ohta, K., Yamamoto, K., et al. (2008). Interleukin-33 enhances adhesion, CD11b expression and survival in human eosinophils. Lab. Investig. *88*, 1245–1253.

Syn, W.K., Jung, Y., Omenetti, A., Abdelmalek, M., Guy, C.D., Yang, L., Wang, J., Witek, R.P., Fearing, C.M., Pereira, T.A., et al. (2009). Hedgehog-Mediated Epithelial-to-Mesenchymal Transition and Fibrogenic Repair in Nonalcoholic Fatty Liver Disease. Gastroenterology *137*, 1478-1488.e8.

Takashima, Y., Era, T., Nakao, K., Kondo, S., Kasuga, M., Smith, A.G., and Nishikawa, S.I. (2007). Neuroepithelial Cells Supply an Initial Transient Wave of MSC Differentiation. Cell *129*, 1377–1388.

Tormin, A., Li, O., Brune, J.C., Walsh, S., Schutz, B., Ehinger, M., Ditzel, N., Kassem, M., and Scheding, S. (2011). CD146 expression on primary nonhematopoietic bone marrow stem cells is correlated with in situ localization. Blood *117*, 5067–5077.

Vodyanik, M.A., Yu, J., Zhang, X., Tian, S., Stewart, R., Thomson, J.A., and Slukvin, I.I. (2010). A Mesoderm-Derived Precursor for Mesenchymal Stem and Endothelial Cells. Cell Stem Cell *7*, 718–729.

Wang, S.M., Coljee, V.W., Pignolo, R.J., Rotenberg, M.O., Cristofalo, V.J., and Sierra, F. (1997). Cloning of the human twist gene: Its expression is retained in adult mesodermally-derived tissues. Gene *187*, 83–92.

Wesseling, M., Sakkers, T.R., de Jager, S.C.A., Pasterkamp, G., and Goumans, M.J. (2018). The morphological and molecular mechanisms of epithelial/endothelial-to-mesenchymal transition and its involvement in atherosclerosis. Vascul. Pharmacol. 0–1.

Worthley, D.L., Churchill, M., Compton, J.T., Tailor, Y., Rao, M., Si, Y., Levin, D., Schwartz, M.G., Uygur, A., Hayakawa, Y., et al. (2015). Gremlin 1 identifies a skeletal stem cell with bone, cartilage, and reticular stromal potential. Cell *160*, 269–284.

Zambetti, N.A., Ping, Z., Chen, S., Kenswil, K.J.G., Mylona, M.A., Sanders, M.A., Hoogenboezem, R.M., Bindels, E.M.J., Adisty, M.N., Van Strien, P.M.H., et al. (2016). Mesenchymal Inflammation Drives Genotoxic Stress in Hematopoietic Stem Cells and Predicts Disease Evolution in Human Pre-leukemia. Cell Stem Cell *19*, 613–627.

Zeisberg, E.M., Tarnavski, O., Zeisberg, M., Dorfman, A.L., McMullen, J.R., Gustafsson, E., Chandraker, A., Yuan, X., Pu, W.T., Roberts, A.B., et al. (2007). Endothelial-to-mesenchymal transition contributes to cardiac fibrosis. Nat. Med. *13*, 952–961.

Zhang, J., Zhang, X., Zhang, L., Zhou, F., Van Dinther, M., and Ten Dijke, P. (2012). LRP8 mediates Wnt/β-catenin signaling and controls osteoblast differentiation. J. Bone Miner. Res. *27*, 2065–2074.

Zhou, B.O., Yue, R., Murphy, M.M., Peyer, J.G., and Morrison, S.J. (2014). Leptin-receptor-expressing mesenchymal stromal cells represent the main source of bone formed by adult bone marrow. Cell Stem Cell *15*, 154–168.

4

IMMUNE CELL COMPOSITION IN REGENERATIVE BONE MARROW AFTER MYELOABLATIVE CHEMOTHERAPY IN ACUTE MYELOID LEUKEMIA PREDICTS HEMATOLOGIC RECOVERY

Keane Jared Guillaume Kenswil[1], Jacqueline Feyen[1], Mariëtte ter Borg[1], Elwin Rombouts[1], Eric Braakman[1], Marc Hermanus Gerardus Petrus Raaijmakers[1,2]

[1]Department of Hematology, Erasmus MC Cancer Institute, Rotterdam 3015CN, The Netherlands
[2]Lead Contact: m.h.g.raaijmakers@erasmusmc.nl

Manuscript in submission

ABSTRACT

Chemotherapy-induced bone marrow (BM) injury is a significant cause of morbidity and mortality in acute myeloid leukemia (AML). Time to hematologic recovery after standard ('3+7') myeloablative chemotherapy can vary considerably between patients, but the factors that drive or predict BM recovery remain incompletely understood.

Here, we assessed the composition of innate and adaptive immune subsets in the regenerating BM (day 17) after induction chemotherapy and related it to hematologic recovery in AML. T cells, and in particular the CD4 central memory (CD4CM) T cell subset, were significantly enriched in the BM after chemotherapy, suggesting relative chemo-resistance of cells providing long-term memory for systemic pathogens. In contrast, B cells and other hematopoietic subsets were depleted. Higher frequencies of the CD4CM T cell subset were associated with delayed hematopoietic recovery, while a high frequency of NK cells related to faster recovery of neutrophil counts. The NK/CD4CM ratio in the BM after chemotherapy was a strong predictor of the time to subsequent neutrophil recovery (Spearman's $\rho = -0.723$, $p < 0.005$; FDR < 0.01). The data provide novel insights into adaptive immune cell recovery after injury and identify the NK/CD4CM index as a putative predictor of hematopoietic recovery in AML.

Keywords

Chemotherapy, bone marrow, regeneration, hematologic recovery, neutropenia, chemo-therapy-induced myelosuppression, immunosuppression, niche

Highlights

1. Standard chemotherapy induces profound B cell depletion with relative resistance of T cell subsets
2. CD4CM T and NK cell frequencies are strongly associated with time to hematopoietic (neutrophil) recovery

INTRODUCTION

Chemotherapy is the main type of treatment for patients with acute myeloid leukemia (AML). The current standard of care for patients, if they are eligible, is conventional "7+3" induction therapy consisting of cytarabine and anthracyclines (Döhner et al., 2017; Tamamyan et al., 2017). This therapeutic modality is typically complicated by a prolonged phase of myelosuppression, resulting in considerable morbidity and mortality, in particular due to opportunistic infections. While the duration of bone marrow (BM) suppression, including neutropenia, may vary substantially between patients, little is known about the factors that support hematopoietic recovery in this setting. Also, we currently lack tools to predict the pace of BM recovery after chemotherapeutic injury.

To achieve hematologic recovery after chemotherapeutic injury, residual normal hematopoietic stem/progenitor cells (HSPCs) in the BM need to replenish mature blood cells. HSPC behavior is tightly regulated by its microenvironment, the so-called HSPC niche (Morrison and Scadden, 2014). Many cell-types contribute to the HSPC niche, including T cells as suggested by some studies (de Bruin et al., 2010; Geerman et al., 2018; Kaplan et al., 2011; Li et al., 2012; Monteiro et al., 2005; Schürch et al., 2014; Tang et al., 2013). The findings in these studies imply that lymphocyte subsets may play a role in hematopoietic recovery following AML chemotherapy, but how lymphocyte subsets are affected by intensive chemotherapy remains largely unknown.

Here, we interrogated the composition of cells comprising the innate and adaptive immunity in the regenerating BM of AML patients after intensive chemotherapy and relate it to hematologic recovery and response to therapy.

RESULTS

Selective depletion of B cells and relative persistence of T cell subsets in AML after intensive chemotherapy

Bone marrow (BM) aspiration during recovery after chemotherapy (e.g. 17-21 days after start of treatment) is standard practice to assess the patient's response status by enumerating the frequency of remaining leukemic blasts. To study the lymphocyte composition in regenerative marrow, BM aspirates of 28 AML patients, 17 days after start of the first cycle of remission induction therapy, were obtained (Supplemental Table 1). All patients displayed an 'empty marrow' with < 5% myeloblasts and a CR/CRi (complete remission with incomplete hematologic recovery) was documented in all patients following subsequent BM examinations following the treatment cycle. These "regenerative" BM samples without morphologic evidence of residual disease were compared to steady-state BM from healthy donors (n=7) using flow cytometry.

First the overall contribution of all lymphocytes to the hematopoietic compartment was determined. Hematopoietic cells (marked by CD45 expression) were identified and subsequently classified into granulocytes (lacking CD14 expression and marked by high side scatter), monocytes (marked by CD14 expression and low side scatter) (Ziegler-Heitbrock, 2015), and lymphocytes (lacking CD14 expression and marked by low side scatter) with flow cytometry (Figure 1A). The frequency of lymphocytes was markedly increased compared to healthy BM (91.5% ± 1.8% versus 22.2% ± 3.8%, FDR < 0.001 by Mann–Whitney U test and adjusted for multiple comparisons using the Benjamini-Hochberg procedure) (Figure 1B), suggesting that lymphoid cells are relatively chemo-resistant. Conversely, the frequency of granulocytes in the regenerative marrow was much lower in comparison to marrow under steady-state conditions (4.2% ± 1.5% versus 72.5% ± 5.3%, FDR < 0.001) (Figure 1C), consistent with the view that chemotherapy depletes neutrophils (Shibayama et al., 2017). Monocyte frequency remained unaltered (4.3% ± 1.0% versus 5.2% ± 1.6%, FDR > 0.05) (Supplemental Figure 1A).

To evaluate the lymphocyte subset composition in regenerative BM, we dissected the lymphoid compartment by analyzing expression of CD16/CD56 (NK and NKT cell marker) (Cooper et al., 2001), CD3 (T cell and NKT cell marker) (Mittag et al., 2005), and CD19 (B cell marker). Flow cytometric assessment revealed that within the lymphoid compartment, T cells were enriched in regenerating marrow compared to healthy marrow (78.2% ± 2.5% versus 62.8% ± 4.3%, FDR < 0.05), seemingly at the cost of B cell frequency (3.4% ± 1.0% versus 20.6% ± 3.6%, FDR < 0.001) (Figure 1D, 1E, 1F). NKT cell frequency within the lymphoid compartment was also increased (6.0% ± 1.0% versus 2.6% ± 0.5%, FDR > 0.05), though this finding was non-significant when corrected for multiple comparisons (Figure 1D, 1H). NK cell frequency varied widely in the regenerative marrow between AML patients, although overall not significantly different from healthy control BM (8.1% ± 1.4% versus 7.9% ± 0.6%, FDR > 0.05) (Figure 1D, 1G). These findings indicate that within the lymphoid fraction specific subsets of lymphocytes may be more susceptible (B cells) or resistant (T cells) to chemotherapy compared to other subsets.

The CD4CM T lymphocyte fraction is increased in regenerative BM

T cells can be further subdivided into CD4- and CD8-expressing T cells which in turn can be grouped into naïve (N), central memory cells (CM), effector memory cells (EM), and CD45RA re-expressing cells (TEMRA) based on CD62L and CD45RA expression (Golubovskaya and Wu, 2016). Dissection of the T cell compartment revealed that the majority of the T cell subset frequencies within the lymphoid compartment were not significantly different between regenerative marrow and healthy BM (Figure 1I, Supplemental Figure 1B-H). Only the frequency of the CD4CM T cell subset was significantly increased in regenerating marrow compared to steady-state BM (25.8% ± 2.7% versus 14.2% ± 1.5%, FDR < 0.05) (Figure 1I, 1J). Taken together these results suggest that T cells (and in particular the CD4CM subset), NK cells and NKT cells are relatively resistant to chemotherapy in comparison to B cells, with the latter being severely reduced within the lymphoid fraction following induction chemotherapy. This is in line with previous reports that found a dramatic depletion of B cells in the peripheral blood of cancer patients following chemotherapy (Mackall et al., 1994; Verma et al., 2016).

The frequency of CD4CM T and NK cells is associated with hematopoietic recovery

Next, we related the frequency of immune subsets to the time needed for hematologic recovery. Hematologic recovery was defined as the time from start of chemotherapy to achieving an absolute neutrophil count (ANC) of ≥ 500/mm^3. 8 patients were excluded from analysis because they were discharged from the hospital before reaching this ANC threshold (Supplemental Table 1), precluding accurate determination of time to recovery. The average time to neutrophil recovery in this subset of patients was 24 days, ranging from 18 to 30 days.

Higher frequencies of T cells within the lymphoid fraction were significantly associated with a delayed neutrophil recovery (Spearman's ρ = 0.633, FDR < 0.05) (Figure 2A). In particular, the frequency of the CD4CM T cell fraction seemed to be relevant, as it was only this T cell subset that was significantly associated with neutrophil recovery (Spearman's ρ = 0.613, FDR < 0.05) (Figure 2B).

Conversely, an inverse relation was found between the frequency of NK cells in the regenerative BM and hematologic recovery. Patients with higher frequencies of NK cells achieved an ANC of 500 cells per mm^3 blood (Figure 2C) faster than patients with lower levels of NK cells (Spearman's ρ = -0.478, p=0.03), although not significant after correcting for multiple comparisons (FDR > 0.05).

Subsequently, we asked if we would find a stronger association between immune subsets and hematologic recovery by creating a NK/CD4CM index, consisting of the two immune subsets' frequencies that showed the strongest association with neutrophil recovery. Indeed, patients with higher NK/CD4CM index scores (proportionally higher NK cell levels relative to lower CD4CM T cell levels) reached an ANC of 500 cells per mm^3 blood (Figure 2D) much faster than patients with a lower NK/CD4CM score (Spearman's $\rho = -0.723$, $p < 0.005$; FDR < 0.01).

Similarly, the association of the NK/CD4CM index to platelet recovery (defined as a count of ≥ 50,000/mm^3) after starting chemotherapy was examined. Of the 28 patients, 6 were excluded from analysis because they were discharged from the hospital before reaching this platelet threshold (Supplemental Table 1), precluding accurate determination of time to recovery. Two other patients were excluded due to the lack of information on their T cell memory subset frequencies. Congruent with the notion that a NK/CD4CM index associates with hematologic recovery, patients with a higher NK/CD4CM index score reached a platelet count of 50,000/mm^3 (Figure 2E) much faster than patients with a lower NK/CD4CM index score (Spearman's $\rho = -0.595$, $p<0.01$; FDR <0.05).

DISCUSSION

Persistent myelosuppression and immunosuppression following chemotherapy predispose cancer patients to opportunistic infections and poses a major cause of morbidity and mortality. The nature of the chemotherapy-induced immunosuppression is incompletely understood and the dynamics of immune subsets in the BM after chemotherapeutic injury has remained largely elusive. Here, we provide data on immune cell composition in the BM following exposure to myeloablative chemotherapy. The data reveal relative preservation of T cell subsets in comparison to other immune cells with a striking association with hematopoietic recovery.

Myeloablative chemotherapy resulted in an increase in the frequency of memory $CD4^+$ T cells, indicative of relative preservation of this subtype of T cells. The BM is an important reservoir for human memory T cells where they are maintained as resting cells in survival niches defined by IL-7-expressing stroma cells (Tokoyoda et al., 2009). They provide long-term polyfunctional memory for systemic pathogens (Di Rosa, 2016; Okhrimenko et al., 2014). Our data indicate that these important immune cells are relatively resistant to chemotherapeutic exposure (perhaps by virtue of their quiescent state in protecting niches), with an increase in their frequency within the lymphocyte compartment upon chemotherapeutic challenge. Although function was not interrogated, data would be in line with the notion that long-term memory against systemic pathogens representing earlier infections may remain relatively intact after myeloablative therapy.

In contrast, B cells were significantly depleted in the marrow after chemotherapy, in line with earlier studies assessing circulating B cell numbers after chemotherapy and relating this finding to impaired humoral immunity in patients (Reilly et al., 2013) (Goswami et al., 2017). Chemotherapy may directly target B cells by inducing apoptosis in these cells (Stahnke et al., 2001) or attenuate their protective vascular niches (Sapoznikov et al., 2008), as chemotherapeutic injury is known to disrupt endothelial niches, at least in murine studies (Hooper et al., 2009; Kopp et al., 2005; Shirota and Tavassoli, 1991).

Interestingly, immune cell composition shortly after chemotherapeutic exposure was strongly correlated with subsequent hematopoietic recovery in AML patients. In particular, the ratio between NK and CD4CM cells was strongly correlated to the duration of neutropenia in this cohort. The association between immune reconstitution and hematopoietic recovery may be a reflection of repopulation kinetics in the marrow in which the most resistant (CD4CM) cells increase after chemotherapeutic challenge with a decline in frequency upon subsequent recovery of other immune subsets. In this context it is noteworthy that indeed NK cells are relatively short-lived cells (exhibiting a half-life of 7-10 days) (Zhang et al., 2007), requiring constant replenishment by active cycling progenitors, likely intrinsically more vulnerable to chemotherapeutic injury. The underlying lineage-specification of the bi-potent NK/T-committed progenitor (Klein Wolterink et al., 2010) implies that a shift in cell

fate decision biased towards NK cell generation may come at the cost of T cell development (Heemskerk et al., 1997; Schotte et al., 2010), potentially further inversely coupling NK and T cell proportions within the lymphoid pool.

Alternatively (albeit not mutually exclusive), certain immune subsets may be active participants in the regeneration of HSPCs and their (myeloid) progeny. T cells have been shown to suppress granulopoiesis directly or indirectly by the release of hematopoietic-inhibitory factors (Broxmeyer et al., 1984; Sallerfors and Olofsson, 1989), while NK cells may produce myelopoiesis-stimulating factors such as IFNγ (Rajagopalan et al., 2001), TNFα (Vitale et al., 2005; Yamashita and Passegué, 2019), and GM-CSF (Levitt et al., 1991).

Of further interest, distinct T cell subsets may have a role in the maintenance of hematopoietic stem cell (HSC) quiescence (Hirata et al., 2018). Our findings prompt future investigations of potential crosstalk between the CD4CM T cell subset and HSPCs.

In addition to providing biologic insights and the instruction of future investigations towards immune cell contributions to hematopoietic recovery, our findings may have clinical relevance. Myelosuppression and persistent neutropenia is an important determinant of treatment related morbidity and mortality in AML. To date, no post-treatment prognostic factors have been identified predicting the duration of neutropenia in AML. Identification of an NK/CD4TM immune-index predicting hematopoietic recovery allows future interrogation of its value to identify patients at increased risk for opportunistic infections. NK cell frequencies varied substantially between patients (Figure 1G) after chemotherapeutic exposure and have been implicated in the direct killing of fungi by recognizing fungal pathogens and eliminating them by releasing lytic granules or by augmenting the antifungal host response (Schmidt et al., 2017). It will be of interest to explore whether the extent of NK cell depletion, in addition to neutropenia, predisposes patients to fungal infections. Insights may facilitate further tailoring of antifungal prophylaxis in AML treatment or the use of hematopoietic growth factors (G-CSF) in selected patients with low NK cell constitution and predicted delayed recovery.

Taken together, the data provide novel insights into immune reconstitution after chemotherapeutic injury and identify the balance between CD4CM and NK cells as a prognostic factor for hematopoietic recovery in AML. Findings are anticipated to prompt future investigations into roles of specific immune subsets in HSPC recovery and instruct potential future tailoring of supportive treatment.

Figure 1

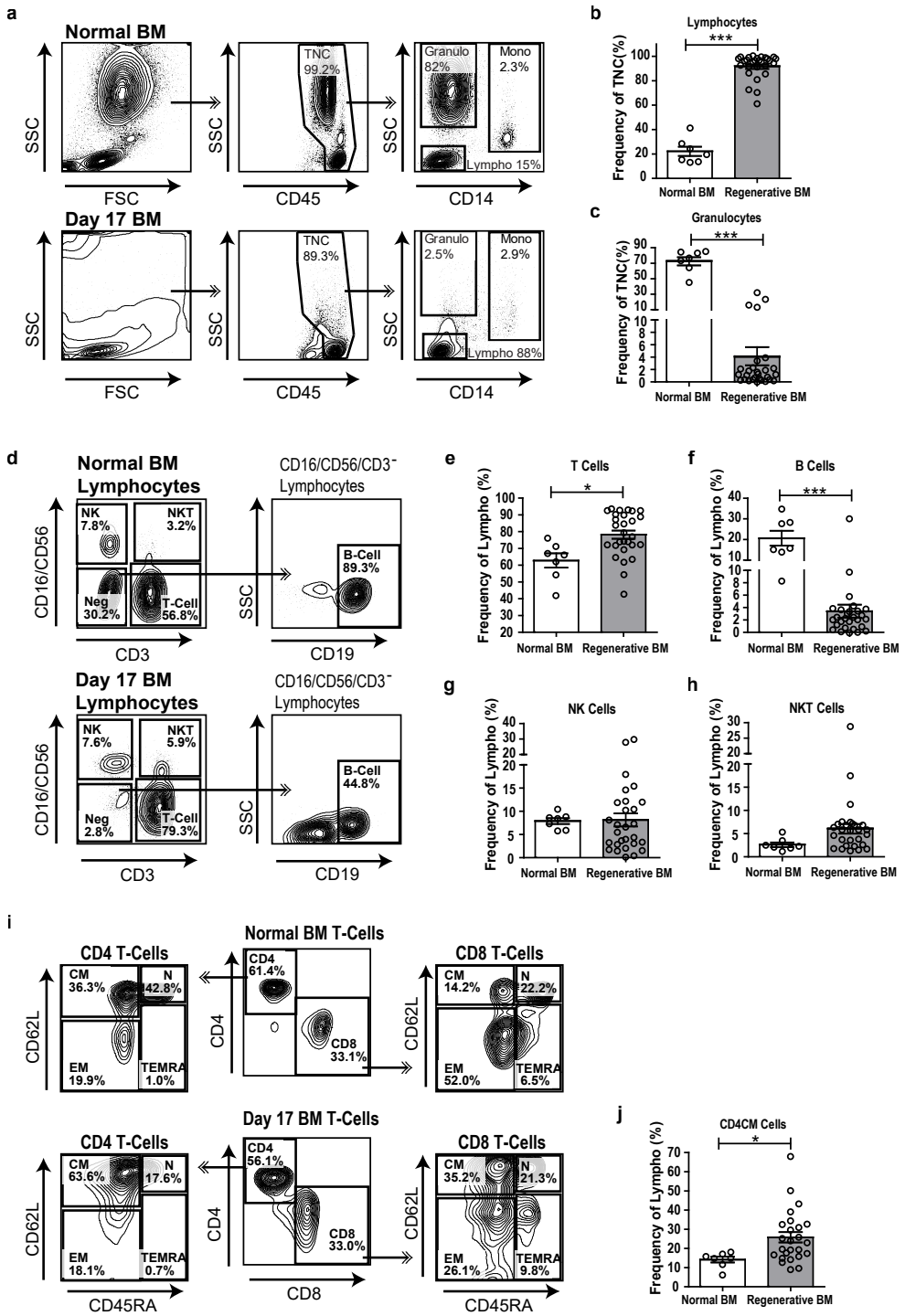

Figure 1. Composition of immune subsets in the BM upon recovery after intensive chemotherapy in AML

a. Representative flow cytometric plots depicting normal steady-state BM (BM) from healthy individuals (upper panels) and BM upon regeneration, 17 days after commencing chemotherapy in AML patients (lower panels). Hematopoietic cells were selected by CD45 expression (middle panels). Granulocytes were identified by high side-scatter characteristics, monocytes by CD14 expression, and lymphocytes by lack of side-scatter properties and CD14 expression (right panels).

b-c. Frequencies of lymphocytes (b) and granulocytes (c) within the total living nucleated cells of normal BM (n=7) and regenerative BM (n=28).

d. Representative flow cytometric plots depicting lymphocyte composition in normal BM (upper panels) and BM upon regeneration (lower panels). Lymphocytes were characterized by CD3 and CD16/CD56 expression, CD16/CD56$^-$CD3$^+$ cells were classified as T cells, whereas CD16/CD56$^+$CD3$^-$, and CD16/CD56$^+$CD3$^+$ cells were identified as NK and NKT cells respectively. B cells were classified as CD16/CD56$^-$CD3$^-$ cells that expressed CD19.

e-h. Frequencies of T cells (e), B cells (f), NK cells (g), and NKT cells (h) within the lymphocyte compartment of normal BM (n=7) and regenerative BM (n=28).

i. Representative flow cytometric plots depicting T cell composition in normal BM (upper panels) and BM upon regeneration (lower panels). T cells were subdivided in CD4 and CD8 T cells (middle panels). Both CD4 and CD8 T cells were further classified as central memory (CM), effector memory (EM), CD45RA re-expressing cells (TEMRA), and naïve (N) subsets based on CD62L and CD45RA expression.

j. Frequency of CD4CM Cells within the lymphocyte compartment of normal BM (n=7) and regenerative BM (n=28).

*FDR<0.05, ***FDR< 0.001, by Mann–Whitney U test and adjusted for multiple comparisons using the Benjamini-Hochberg Procedure. False Discovery Rates (FDR).

Figure 2

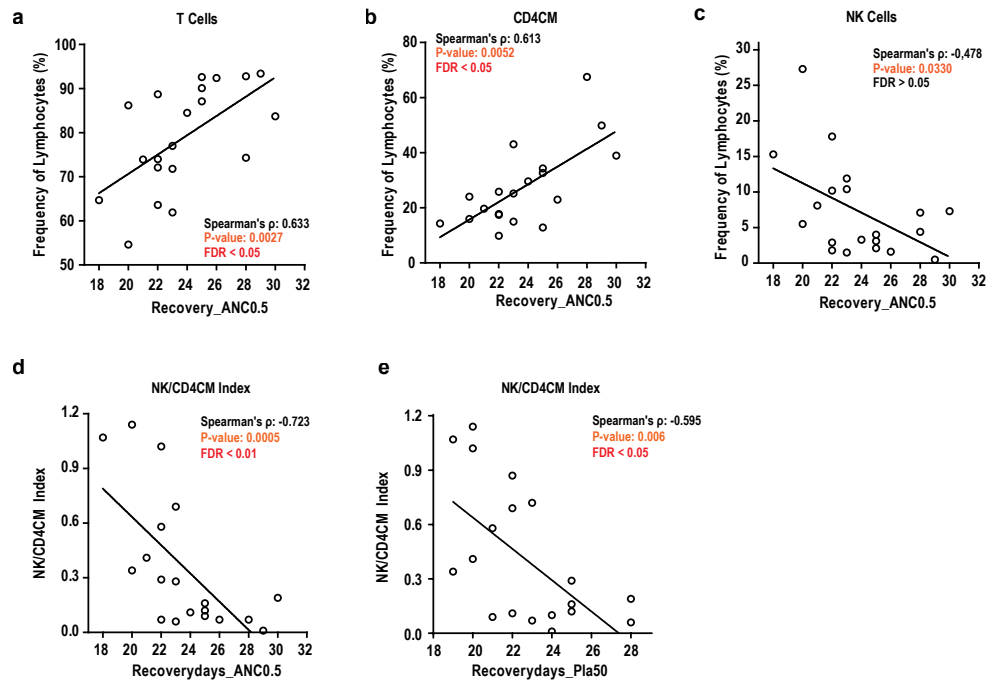

Figure 2. Frequency of CD4CM T and NK cells is associated with neutrophil recovery after chemotherapy in AML

a-c. Correlation plots describing the relationship between the frequencies of specific BM lymphocyte subsets and hematologic recovery (ANC ≥ 500/mm^3 blood), depicted as days after start of chemotherapy:

a. The association between the frequency of T cells and ANC ≥ 500/mm^3 (n=20).

b. The association between the frequency of CD4CM T cells and ANC ≥ 500/mm^3. Data on the memory T cell subsets were missing for one patient, hence (n=19).

c. The association between the frequency of NK cells and ANC ≥ 500/mm^3 (n=20).

d. The association between the NK/CD4CM index, calculated by dividing the "frequency of NK cells" by "the frequency of CD4CM T cells" and ANC ≥ 500/mm^3 (n =19).

e. The association between the NK/CD4CM index and an absolute platelet count of ≥ 50,000/mm^3 (n =20).

Spearman's rank correlation coefficient (to calculate the non-parametric correlation estimate) and corresponding p-values are depicted. P-values were also adjusted for multiple comparisons using the Benjamini-Hochberg procedure and are depicted as False Discovery Rates (FDR).

Table S1

Sample ID	WHO Diagnosis	Response	Age	Gender	ANC0.5 (days)	Pla50 (days)
1	AML with mutated NPM1	CR	65	Male	20	20
2	AML with myelodysplasia-related changes	CR	73	Male	30	**NA**
3	AML with mutated NPM1	CR	57	Male	**NA**	22
4	AML NOS	CR	53	Female	22	20
5	AML NOS	CR	70	Male	23	28
6	AML with mutated NPM1	CR	71	Male	**NA**	24
7	AML with mutated NPM1	CR	69	Male	24	22
8	AML NOS	CR	58	Female	25	21
9	MDS RAEB-2	CRi	72	Female	28	**NA**
10	Therapy related AML	CR	68	Male	20	19
11	AML with myelodysplasia-related changes	CR	68	Male	25	25
12	AML with mutated CEBPA	CR	33	Female	**NA**	24
13	AML with myelodysplasia-related changes	CR	70	Male	**NA**	23
14	Relapse AML	CR	59	Male	29	**NA**
15	AML with t(8;21)	CR	67	Male	**NA**	23
16	AML with t(8;21)	CR	37	Female	25	25
17	AML with mutated CEBPA	CR	27	Male	23	22
18	AML with mutated NPM1	CR	58	Female	26	23
19	AML NOS	CR	28	Female	22	23
20	AML with mutated NPM1	CR	35	Male	**NA**	28
21	AML with mutated NPM1	CR	67	Female	21	20
22	Relapse AML	CRi	67	Female	28	**NA**
23	AML with myelodysplasia-related changes	CR	69	Male	23	**NA**
24	AML with myelodysplasia-related changes	CR	69	Female	18	19
25	AML NOS	CRi	26	Female	**NA**	32
26	Therapy related AML	CR	65	Female	**NA**	**NA**
27	Therapy related AML	CR	65	Male	22	25
28	AML with mutated NPM1	CR	58	Female	22	21

Table S1. Related to Figure 1 and 2. AML patient characteristics
BM was obtained from the HOVON103 and HOVON132 clinical trials. Patient ID, WHO classification based on the 2017 ELN recommendations, therapy response, age, and gender are listed. The time needed to achieve a neutrophil count of ≥ 500/mm^3 blood, and a platelet count of ≥ 50,000/mm^3 blood after start of chemotherapy are also depicted.

Figure S1

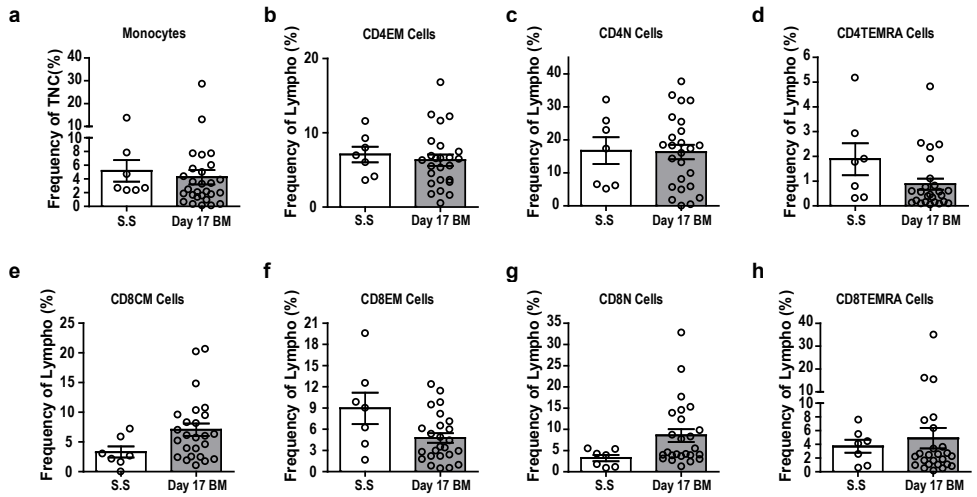

Supplemental Figure 1. Related to Figure 1. Frequencies of immune subsets in normal vs AML regenerative BM
a. The frequency of monocytes within the total living nucleated cells in normal BM (n=7) and regenerative BM (n=28).
b-h. Frequencies of CD4EM T cells (b), CD4N T cells (c), CD4TEMRA T cells (d), CD8CM T cells (e), CD8EM T cells (f), CD8N T cells (g), and CD8TEMRA T cells (h) within the lymphocyte compartment in normal BM (n=7) and regenerative BM (n=28).

EXPERIMENTAL PROCEDURES

BM Aspirates

BM aspirates from AML patients (average: 58 years, range: 20–75 years) were collected at 17 days (range 16-19) after start of remission induction chemotherapy (3+7 schedule of chemotherapy with anthracycline and cytarabine). Control marrow was obtained by aspiration from donors for allogeneic transplantation (average: 64.8 years, range: 47–78 years) after obtaining written informed consent. The use of human samples with informed consent was approved by the Institutional Review Board of the Erasmus Medical Center (the Netherlands) in accordance with the Declaration of Helsinki.

Cell isolation and Flow Cytometry

Mononuclear cells (MNCs) were isolated from BM aspirates as previously reported (Kenswil et al., 2018). Briefly, cryopreserved BM aspirates from healthy individuals were thawed in a waterbath at 37°C. Subsequently, BM aspirates underwent centrifugation and were washed once with PBS+0.5% FCS.

Next, BM aspirates were divided in two and were either stained with one of the following two antibody cocktails: one cocktail (1) to determine the frequencies of monocytes, B cells, T cells, NK cells, B cells and the other cocktail (2) to determine the frequencies of naïve and memory T cell subsets. For (1) we used CD14 (Cat. No: 560180, BD Pharmingen) and a multitest mix (Cat. No: 342417, Becton Dickson) containing CD45, CD3, CD16/CD56, and CD19, while for (2) we used CD45 (Cat. No: 11-9459-42, eBioscience), CD45RA (Cat. No: 46-0468-42, eBioscience), CD3 (Cat. No: 12-0039-42, eBioscience), CD4 (Cat. No: 317443, Biolegend), CD8 (Cat. No: 561423, BD Pharmingen), and CD62L (Cat. No: 17-0629-42, eBioscience).

The BM aspirates were then mixed 1:10 with 1x IOTest3 Lysing solution (Cat. No: A07799, Beckman Coulter) to lyse red blood cells.

Flow-cytometric analyses were performed using a BD FACSCanto™ II (BD Biosciences, San Jose, CA, USA) and data were analyzed using FlowJo software (Tree Star Inc, Ashland, OR, USA).

Statistics

To compare the mean differences between different (patient) groups the Mann–Whitney U test was applied. To measure the degree of correlation between immune subsets and hematologic recovery, the Spearman's rank correlation coefficient was. Concomitantly, corresponding p-values were also calculated. In addition, P-values were adjusted for multiple comparisons when needed using the Benjamini-Hochberg procedure and are depicted as False Discovery Rates (FDR).

Software

Statistical analyses were performed using IBM SPSS 25. Graphs were generated by using Prism 5 (GraphPad Software). Final figures were completed in Adobe Illustrator CC.

ACKNOWLEDGEMENTS

We would like to thank the following people for their contributions to this paper: Larissa de Graaf for providing access to BM samples obtained from healthy donors and flow cytometry measurements of these samples, and Ayşegül Öcal Sahin for flow cytometry measurements of a number of AML patient samples.

COMPETING INTERESTS

The authors have declared that no competing interests exist.

REFERENCES

Broxmeyer, H.E., Juliano, L., Lu, L., Platzer, E., Dupont, B., 1984. HLA-DR human histocompatibility leukocyte antigens-restricted lymphocyte-monocyte interactions in the release from monocytes of acidic isoferritins that suppress hematopoietic progenitor cells. J. Clin. Invest. 73, 939–953. https://doi.org/10.1172/JCI111318

Cooper, M.A., Fehniger, T.A., Caligiuri, M.A., 2001. The biology of human natural killer-cell subsets. Trends Immunol. 22, 633–640. https://doi.org/10.1016/S1471-4906(01)02060-9

de Bruin, A.M., Buitenhuis, M., van der Sluijs, K.F., van Gisbergen, K.P.J.M., Boon, L., Nolte, M. a, 2010. Eosinophil differentiation in the bone marrow is inhibited by T cell-derived IFN-gamma. Blood 116, 2559–69. https://doi.org/10.1182/blood-2009-12-261339

Di Rosa, F., 2016. Two Niches in the Bone Marrow: A Hypothesis on Life-long T Cell Memory. Trends Immunol. 37, 503–512. https://doi.org/10.1016/j.it.2016.05.004

Döhner, H., Estey, E., Grimwade, D., Amadori, S., Appelbaum, F.R., Büchner, T., Dombret, H., Ebert, B.L., Fenaux, P., Larson, R.A., Levine, R.L., Lo-Coco, F., Naoe, T., Niederwieser, D., Ossenkoppele, G.J., Sanz, M., Sierra, J., Tallman, M.S., Tien, H., Wei, A.H., Löwenberg, B., Bloomfield, C.D., 2017. Diagnosis and management of AML in adults: 2017 ELN recommendations from an international expert panel. Blood 129, 424–447. https://doi.org/10.1182/blood-2016-08-733196

Geerman, S., Brasser, G., Bhushal, S., Salerno, F., Kragten, N.A., Hoogenboezem, M., de Haan, G., Wolkers, M.C., Pascutti, M.F., Nolte, M.A., 2018. Memory CD8+ T cells support the maintenance of hematopoietic stem cells in the bone marrow. Haematologica 103, e230–e233. https://doi.org/10.3324/haematol.2017.169516

Golubovskaya, V., Wu, L., 2016. Different subsets of T cells, memory, effector functions, and CAR-T immunotherapy. Cancers (Basel). 8. https://doi.org/10.3390/cancers8030036

Goswami, M., Prince, G., Biancotto, A., Moir, S., Kardava, L., Santich, B.H., Cheung, F., Kotliarov, Y., Chen, J., Shi, R., Zhou, H., Golding, H., Manischewitz, J., King, L., Kunz, L.M., Noonan, K., Borrello, I.M., Smith, B.D., Hourigan, C.S., 2017. Impaired B cell immunity in acute myeloid leukemia patients after chemotherapy. J. Transl. Med. 15, 1–16. https://doi.org/10.1186/s12967-017-1252-2

Heemskerk, M.H.M., Blom, B., Nolan, G., Stegmann, A.P.A., Bakker, A.Q., Weijer, K., Res, P.C.M., Spits, H., 1997. Inhibition of T Cell and Promotion of Natural Killer Cell Development by the Dominant Negative Helix Loop Helix Factor Id3. J. Exp. Med. 186, 1597–1602. https://doi.org/10.1084/jem.186.9.1597

Hirata, Y., Furuhashi, K., Ishii, H., Li, H.W., Pinho, S., Ding, L., Robson, S.C., Frenette, P.S., Fujisaki, J., 2018. CD150highBone Marrow Tregs Maintain Hematopoietic Stem Cell Quiescence and Immune Privilege via Adenosine. Cell Stem Cell 22, 445-453.e5. https://doi.org/10.1016/j.stem.2018.01.017

Hooper, A.T., Butler, J.M., Nolan, D.J., Kranz, A., Iida, K., Kobayashi, M., Kopp, H.-G., Shido, K., Petit, I., Yanger, K., James, D., Witte, L., Zhu, Z., Wu, Y., Pytowski, B., Rosenwaks, Z., Mittal, V., Sato, T.N., Rafii, S., 2009. Engraftment and Reconstitution of Hematopoiesis Is Dependent on VEGFR2-Mediated Regeneration of Sinusoidal Endothelial Cells. Cell Stem Cell 4, 263–274. https://doi.org/10.1016/j.stem.2009.01.006

Kaplan, M.H., Glosson, N.L., Stritesky, G.L., Yeh, N., Kinzfogl, J., Rohrabaugh, S.L., Goswami, R., Pham, D., Levy, D.E., Brutkiewicz, R.R., Blum, J.S., Cooper, S., Hangoc, G., Broxmeyer, H.E., 2011. STAT3-dependent IL-21 production from T helper cells regulates hematopoietic progenitor cell homeostasis. Blood 117, 6198–6201. https://doi.org/10.1182/blood-2011-02-334367

Klein Wolterink, R.G.J., García-Ojeda, M.E., Vosshenrich, C.A.J., Hendriks, R.W., Di Santo, J.P., 2010. The intrathymic crossroads of T and NK cell differentiation. Immunol. Rev. 238, 126–37. https://doi.org/10.1111/j.1600-065X.2010.00960.x

Kopp, H.G., Avecilla, S.T., Hooper, A.T., Shmelkov, S. V., Ramos, C.A., Zhang, F., Rafii, S., 2005. Tie2 activation contributes to hemangiogenic regeneration after myelosuppression. Blood 106, 505–513. https://doi.org/10.1182/blood-2004-11-4269

Levitt, L.J., Nagler, A., Lee, F., Abrams, J., Shatsky, M., Thompson, D., 1991. Production of granulocyte/macrophage-colony-stimulating factor by human natural killer cells: Modulation by the p75 subunit of the interleukin 2 receptor and by the CD2 receptor. J. Clin. Invest. 88, 67–75. https://doi.org/10.1172/JCI115306

Li, J.-Y., Adams, J., Calvi, L.M., Lane, T.F., DiPaolo, R., Weitzmann, M.N., Pacifici, R., 2012. PTH expands short-term murine hemopoietic stem cells through T cells. Blood 120, 4352–4362. https://doi.org/10.1182/blood-2012-06-438531

Mackall, C.L., Fleisher, T.A., Brown, M.R., Magrath, I.T., Shad, A.T., Horowitz, M.E., Wexler, L.H., Adde, M.A., McClure, L.L., Gress, R.E., 1994. Lymphocyte depletion during treatment with intensive chemotherapy for cancer. Blood 84, 2221–8.

Mittag, A., Lenz, D., Gerstner, A.O.H., Sack, U., Steinbrecher, M., Koksch, M., Raffael, A., Bocsi, J., Tárnok, A., 2005. Polychromatic (eight-color) slide-based cytometry for the phenotyping of leukocyte, NK, and NKT subsets. Cytom. Part A 65A, 103–115. https://doi.org/10.1002/cyto.a.20140

Monteiro, J.P., Benjamin, A., Costa, E.S., Barcinski, M.A., Bonomo, A., 2005. Normal hematopoiesis is maintained by activated bone marrow CD4+ T cells. Blood 105, 1484–1491. https://doi.org/10.1182/blood-2004-07-2856

Morrison, S.J., Scadden, D.T., 2014. The bone marrow niche for haematopoietic stem cells. Nature 505, 327–34. https://doi.org/10.1038/nature12984

Okhrimenko, A., Grun, J.R., Westendorf, K., Fang, Z., Reinke, S., von Roth, P., Wassilew, G., Kuhl, A.A., Kudernatsch, R., Demski, S., Scheibenbogen, C., Tokoyoda, K., McGrath, M.A., Raftery, M.J., Schonrich, G., Serra, A., Chang, H.-D., Radbruch, A., Dong, J., 2014. Human memory T cells from the bone marrow are resting and maintain long-lasting systemic memory. Proc. Natl. Acad. Sci. 111, 9229–9234. https://doi.org/10.1073/pnas.1318731111

Rajagopalan, S., Fu, J., Long, E.O., 2001. Cutting Edge: Induction of IFN- Production but Not Cytotoxicity by the Killer Cell Ig-Like Receptor KIR2DL4 (CD158d) in Resting NK Cells. J. Immunol. 167, 1877–1881. https://doi.org/10.4049/jimmunol.167.4.1877

Reilly, A., Kersun, L.S., Luning Prak, E., Boyer, J., McDonald, K., Jawad, A.F., Sullivan, K.E., 2013. Immunologic consequences of chemotherapy for acute myeloid leukemia. J. Pediatr. Hematol. Oncol. 35, 46–53. https://doi.org/10.1097/MPH.0b013e318266c0c8

Sallerfors, B., Olofsson, T., 1989. Cell-mediated inhibition of granulopoiesis in vitro in patients with acute myeloid leukemia in remission. Eur. J. Haematol. 42, 164–172. https://doi.org/10.1111/j.1600-0609.1989.tb01206.x

Sapoznikov, A., Pewzner-Jung, Y., Kalchenko, V., Krauthgamer, R., Shachar, I., Jung, S., 2008. Perivascular clusters of dendritic cells provide critical survival signals to B cells in bone marrow niches. Nat. Immunol. 9, 388–395. https://doi.org/10.1038/ni1571

Schmidt, S., Tramsen, L., Lehrnbecher, T., 2017. Natural killer cells in antifungal immunity. Front. Immunol. 8, 1–10. https://doi.org/10.3389/fimmu.2017.01623

Schotte, R., Dontje, W., Nagasawa, M., Yasuda, Y., Bakker, A.Q., Spits, H., Blom, B., 2010. Synergy between IL-15 and Id2 Promotes the Expansion of Human NK Progenitor Cells, Which Can Be Counteracted by the E Protein HEB Required To Drive T Cell Development. J. Immunol. 184, 6670–6679. https://doi.org/10.4049/jimmunol.0901508

Schürch, C.M., Riether, C., Ochsenbein, A.F., 2014. Cytotoxic CD8+ T cells stimulate hematopoietic progenitors by promoting cytokine release from bone marrow mesenchymal stromal cells. Cell Stem Cell 14, 460–472. https://doi.org/10.1016/j.stem.2014.01.002

Shibayama, Y., Tsukahara, T., Emori, M., Murata, K., Mizushima, E., Hirohashi, Y., Kanaseki, T., Nakatsugawa, M., Kubo, T., Yamashita, T., Sato, N., Torigoe, T., 2017. Implication of chemo-resistant memory T cells for immune surveillance in patients with sarcoma receiving chemotherapy. Cancer Sci. 108, 1739–1745. https://doi.org/10.1111/cas.13319

Shirota, T., Tavassoli, M., 1991. Cyclophosphamide-induced alterations of bone marrow endothelium: implications in homing of marrow cells after transplantation. Exp. Hematol. 19, 369–73.

Stahnke, K., Fulda, S., Friesen, C., Strauss, G., Debatin, K.M., 2001. Activation of apoptosis pathways in peripheral blood lymphocytes by in vivo chemotherapy. Blood 98, 3066–73. https://doi.org/10.1182/blood.v98.10.3066

Tamamyan, G., Kadia, T., Ravandi, F., Borthakur, G., Cortes, J., Jabbour, E., Daver, N., Ohanian, M., Kantarjian, H., Konopleva, M., 2017. Frontline treatment of acute myeloid leukemia in adults. Crit. Rev. Oncol. Hematol. 110, 20–34. https://doi.org/10.1016/j.critrevonc.2016.12.004

Tang, Q., Jiang, D., Alonso, S., Pant, A., Martínez Gómez, J.M., Kemeny, D.M., Chen, L., Schwarz, H., 2013. CD137 ligand signaling enhances myelopoiesis during infections. Eur. J. Immunol. 43, 1555–1567. https://doi.org/10.1002/eji.201243071

Tokoyoda, K., Zehentmeier, S., Hegazy, A.N., Albrecht, I., Grün, J.R., Löhning, M., Radbruch, A., 2009. Professional Memory CD4+ T Lymphocytes Preferentially Reside and Rest in the Bone Marrow. Immunity 30, 721–730. https://doi.org/10.1016/j.immuni.2009.03.015

Verma, R., Foster, R.E., Horgan, K., Mounsey, K., Nixon, H., Smalle, N., Hughes, T.A., Carter, C.R.D., 2016. Lymphocyte depletion and repopulation after chemotherapy for primary breast cancer. Breast Cancer Res. 18, 1–12. https://doi.org/10.1186/s13058-015-0669-x

Vitale, M., Della Chiesa, M., Carlomagno, S., Pende, D., Aricò, M., Moretta, L., Moretta, A., 2005. NK-dependent DC maturation is mediated by TNFα and IFNγ released upon engagement of the NKp30 triggering receptor. Blood 106, 566–571. https://doi.org/10.1182/blood-2004-10-4035

Yamashita, M., Passegué, E., 2019. TNF-α Coordinates Hematopoietic Stem Cell Survival and Myeloid Regeneration. Cell Stem Cell 25, 357-372.e7. https://doi.org/10.1016/j.stem.2019.05.019

Zhang, Y., Wallace, D.L., De Lara, C.M., Ghattas, H., Asquith, B., Worth, A., Griffin, G.E., Taylor, G.P., Tough, D.F., Beverley, P.C.L., Macallan, D.C., 2007. In vivo kinetics of human natural killer cells: The effects of ageing and acute and chronic viral infection. Immunology 121, 258–265. https://doi.org/10.1111/j.1365-2567.2007.02573.x

Ziegler-Heitbrock, L., 2015. Blood monocytes and their subsets: Established features and open questions. Front. Immunol. 6, 1–5. https://doi.org/10.3389/fimmu.2015.00423

5

GENERAL DISCUSSION AND CONCLUSION

5.1 Summary

The work presented in this thesis focuses on how the bone marrow (BM) microenvironment, in particular BM endothelial cells (ECs), can contribute to BM regeneration following chemotherapy-induced injury in humans.

Recent work using experimental mouse models to investigate the cellular and molecular pathways underlying hematologic recovery after injury revealed that BM ECS can mediate BM regeneration in a perfusion-independent manner (Poulos et al., 2013; Winkler et al., 2012), for example by the release of paracrine growth factors (Doan et al., 2013; Himburg et al., 2018; Xu et al., 2018). While multiple studies before have demonstrated the importance of BM ECs for hematopoiesis (Ding and Morrison, 2013; Ding et al., 2012; Hooper et al., 2009), newer studies have identified and characterized a subset of these ECs (type H endothelium) that also couple angiogenesis (blood vessel development) to osteogenesis (bone formation) (Kusumbe et al., 2014; Ramasamy et al., 2014). However, the relevance of these findings for human biology is not well established due to the lack of studies in humans that have attempted to unravel the specific contributions of BM ECs to BM regeneration.

To address this issue, in **Chapter 2,** we characterized BM ECs ($CD31^+CD9^+$ cells) enriched in the human BM in conditions of generation (development) and regeneration (after injury). The frequency of human BM ECs, marked by endoglin (CD105) expression, was increased in the niche of acute myeloid leukemia (AML) patients recovering from myeloablative chemotherapy compared to healthy controls. Similarly, we also observed an increased proportion of CD105-expressing ECs in mice treated with chemotherapy. The enrichment of CD105-expressing ECs during recovery after chemotherapeutic injury suggested that this cell type could be implicated in mammalian regeneration and hematopoietic niche formation. This notion was further supported by the predominance of $CD105^+$ cells within the endothelial compartment of fetal BM at gestational week 15–20, when hematopoiesis is migrating from the fetal liver to the bone marrow in humans. Like BM regeneration after injury, BM formation during fetal development involves orchestrated interplay between many heterotypic cells that coordinate timely activation of angiogenesis, osteogenesis, and hematopoiesis (Chan et al., 2009; Maes et al., 2010). $CD105^+$ ECs were enriched in collagenased bones in ontogeny (fetal stage) and in adults, and the trabecular localization of ECs expressing CD105 was confirmed with *in situ* immunofluorescence. Collectively, these findings and in particular the enrichment of this cell type during regenerative states after injury, prompted us to name this EC type “human regeneration-associated EC” (hREC).

The phenotypic characteristics of hRECs were reminiscent of the type H endothelium previously characterized in mice, and raised the possibility that hRECs may be the human equivalent of mouse type H endothelium. Comprehensive transcriptional characterization of fetal hRECs revealed a striking molecular similarity to murine type H endothelium, including overexpression of transcripts encoding canonical HSPC regulatory factors, as well as anabolic regulators of angiogenesis and osteogenesis. Gene set enrichment analysis (GSEA) of fetal hRECs further demonstrated activation of the NOTCH signaling pathway, which was previously shown to mediate the coupling of angiogenesis and osteogenesis by type H endothelium (Ramasamy et al., 2014).

These data indicate that hRECs have a transcriptional wiring consistent with the coupling of angiogenesis, osteogenesis, and hematopoiesis. This made us hypothesize that further interrogation of the transcriptome of hRECs might allow for the identification of (novel) angiocrine factors that can facilitate these processes in development and regeneration. Focusing on genes encoding secreted factors, overexpressed in both fetal hRECs and ECs from regenerative marrow, led to the identification of interleukin-33 (IL-33). Subsequent *in vitro* and *in vivo* experiments revealed that IL-33 was able to promote the expansion of distinct subsets of hematopoietic precursor cells, ECs, as well as osteogenic differentiation of mesenchymal precursor cells. Treatment of mice with recombinant mouse IL-33 (rmIL-33) resulted in an increased number of myeloid and lymphoid progenitors, which was accompanied by a relative increase of various cells within the niche, including $CD31^+CD105^+$ (ECs) and $CD31^-Sca^-CD51^+$ niche cells (mesenchymal precursor and osteolineage cells). Collectively, the data demonstrate the existence of a human EC subtype associated with regeneration and human niche formation, similar to the type H endothelium described in mice. In addition, the identification of IL-33 provides proof of principle for the notion that transcriptome analyses of these hRECs allows for the discovery of novel candidate angiocrine and anabolic niche factors.

Among the enriched transcripts in fetal hRECs were transcripts normally associated with non-endothelial stromal (mesenchymal) cells, which led us to hypothesize in **Chapter 3** that hRECs harbored a subset of cells undergoing the process of endothelial-to-mesenchymal transition (EndMT) during BM (re)generation. First we confirmed that a subset of hRECs expresses the protein CD271 (LNGFR), encoded by one of the up-regulated mesenchymal transcripts and a well-known marker of primary human BM mesenchymal cells. These $CD271^+$ hRECs exhibited a transcriptome consistent with cells undergoing EndMT and acquiring stem cell-like properties. Functionally, $(CD144^+)CD271^+$ hRECs were able to generate colony-forming unit fibroblasts (CFU-Fs) with multilineage skeletogenic differentiation capacity *ex vivo*. The skeletogenic differentiation capacity and ‘niche-forming capacity’ of these mesenchymal cells was also confirmed using *in vivo* transplantation assays demonstrating that $CD271^+$hREC-derived mesenchymal cells had the capacity to reconstitute the entire hematopoietic niche in immunodeficient recipient mice. These findings strongly suggested that a small subset of primary (fetal) ECs is capable of converting to skeletal stem/progenitor cells that contribute to hematopoietic niche formation during mammalian ontogeny.

To confirm this notion and assess the alleged contribution of EndMT to the formation of the BM niche during fetal ontogeny, we performed genetic endothelial-lineage tracing studies using *VEcad-cre;LoxP-tdTomato* mice. In these mice tdTomato expression, labeling ECs and their descendants and driven by the promotor of *VEcad* (which encodes for VE-cadherin/

CD144), at 3 weeks after birth revealed that ±50% of the CD144$^-$CD31$^-$Sca1$^+$CD51$^+$(Pdgfrα+) mesenchymal niche cells (previously shown to be a highly purified fraction of BM stromal cells containing skeletal stem cells) were derived from ECs. In addition, ±27% of the CD144$^-$CD31$^-$SCA1$^-$CD51$^+$ niche cells (osteoblastic cells) were also of endothelial origin. These results indicate that ECs provide a significant contribution to the mesenchymal compartment of the hematopoietic niche. Interestingly, endothelial-derived mesenchymal cells had a distinct transcriptional wiring, characterized by expression of genes previously associated with the subset of mesenchymal cells forming the HSC niche (*Lepr, Nestin*), as well as key HSC regulatory genes (such as *Cxcl12, Kitl, Angpt1* and others). Together, these experiments provide experimental support for the novel conceptual view that endothelial cells generate mesenchymal multipotent cells with hematopoietic-niche forming capacity through a process of EndMT.

Next, we sought to identify the underlying signaling pathways mediating EndMT of hRECs in humans. Notably, multiple known regulators of EndMT, such as BMP4 and DPP-4, had been shown in **Chapter 2** to be overexpressed in hRECs. Building on these observations, we focused our attention on IL-33, the inflammatory cytokine with anabolic effects in the hematopoietic system, as identified in chapter 2. *In vitro* experiments utilizing two independent models of endothelium revealed that rhIL-33 treatment induced transcriptional alterations consistent with EndMT (down-regulation of endothelial marker expression accompanied by up-regulation of mesenchymal marker expression) in a dose-dependent manner, which was confirmed at the protein level. Induction of EndMT programs by IL-33 resulted in functional transition of ECs to a cellular state permissive of differentiation towards skeletal fates (cartilage and bone), as demonstrated by the production of calcific (osteogenic) matrix and glycosaminoglycan (GAG) (chondrogenic differentiation). Mechanistically, signaling through the ST2 receptor and upregulation of *SNAI2* was identified as a pathway of IL33-induced EndMT in experiments exploiting neutralizing antibody directed against ST2.

Collectively, the data reveal that endothelium-derived mesenchymal (stem) cells contribute to hematopoietic niche formation in mammals during ontogeny through the process of EndMT. IL-33 is identified as a novel and strong mediator of this process in this context. The observation that ECs undergoing EndMT occur upon recovery after chemotherapeutic injury, raises the exciting prospect that this process may be reinforced during regeneration after injury.

In **Chapter 4** we switched gears and sought to better characterize the *hematopoietic* cells potentially involved in BM regeneration by interrogating the hematopoietic composition of the BM upon early regeneration after chemotherapeutic injury (day 17 after starting induction chemotherapy). Hematopoietic cells at this point consisted predominantly of lymphoid cells (low side scatter, CD45$^+$CD14$^-$ cells) in regenerative marrow from AML patients.

Notably, T cells (in particular the CD4CM T cell subset) were enriched in the regenerative BM. On the other hand, B cells were relatively depleted as these exhibited a more than 5 fold-decrease compared to their counterparts in normal BM. Subsequently, we related the frequencies of the various lymphoid subsets to the time needed to achieve an absolute neutrophil count of ≥ 500/mm^3 blood (a parameter of hematologic recovery). We observed that higher frequencies of T cells were associated with slower hematologic recovery. Specifically, the CD4CM T cell subset seemed to be driving this association, as it was the only T cell subset significantly associated with the duration of neutrophil recovery. Conversely, we found that higher frequencies of NK cells were associated with faster hematologic recovery. Combining the frequencies of both CD4CM T cells and NK cells into a NK/CD4CM index further strengthened the association of immune composition with the time to recovery. Together these findings provide insights on the recovery of immune subsets following chemotherapeutic injury. These findings may be of clinical use in predicting the time to hematopoietic recovery and pave the way to further studies addressing the biological contribution of immune subsets to BM regeneration.

5.2 Organ-specific endothelial cells in (re)generation

ECs provide instructive signals that support the formation, maintenance, and regeneration of multiple organs in mammals. For instance, it has been reported that during embryonic development ECs direct liver morphogenesis by suppressing WNT and NOTCH signaling in hepatic endoderm (Han et al., 2011). Subsequent work has shown that homeostasis of the adult liver is governed by WNT ligands (WNT2 and WNT9B) derived from central vein ECs of the liver (Wang et al., 2015), whereas in response to injury, liver sinusoidal ECs (LSECs) direct reconstitution of liver mass and function by releasing WNT2 (Ding et al., 2010), hepatocyte growth factor (HGF) (Ding et al., 2010) and angiopoietin 2 (ANG2) (Hu et al., 2014). Likewise, the vasculature of the lungs is regarded to guide tissue development and regeneration in a perfusion-independent manner. While the exact molecular cues are unknown, it is thought that angiocrine factors released from primitive pulmonary capillaries contribute to early lung patterning (Lazarus et al., 2011). Others have shown that endothelial-derived matrix metalloproteinase-14 (MMP14)(Ding et al., 2011) and thrombospondin-1 (Lee et al., 2014) (TSP1) mediate repair of pulmonary epithelium by regulating proliferation and differentiation of bronchoalveolar stem cells.

ECs can also directly contribute to organogenesis by transdifferentiation, for example by endothelial-to-mesenchymal transition (EndMT). It has been reported that embryonic pulmonary ECs contribute to neointimal formation of the pulmonary artery wall by giving rise to mesenchymal cells (Arciniegas et al., 2005) and that endocardial ECs generate pericytes and vascular smooth muscle cells of the murine embryonic heart by first converting into mesenchymal progenitors (Chen et al., 2016b).

Endothelial cells in the hematopoietic system

Intriguingly, most hematopoietic cells can be considered of endothelium origin, since the definitive hematopoietic stem cells (HSCs) emerge from hemogenic endothelium of the embryonic dorsal aorta, in a process termed endothelial-to-hematopoietic transition (EHT). It is important to note that non-hemogenic ECs surrounding the hemogenic endothelium reportedly function as niche cells by providing angiocrine signals, such as endothelial-derived Jagged1 (Gama-Norton et al., 2015) and SCF (Azzoni et al., 2018), which are required for HSC specification or maturation.

ECs continue to fulfill their role as niche cells for HSPCs in adulthood. Seminal work demonstrated that ECs are needed for HSC maintenance (Ding and Morrison, 2013; Ding et al., 2012), as well as hematopoietic regeneration after injury (Hooper et al., 2009). Subsequent studies revealed that ECs can mediate hematopoietic regeneration by expressing various signaling molecules, including membrane-bound factors such as Jagged-1 (Poulos et al., 2013), and E-selectin (Winkler et al., 2012), or paracrine factors like pleiotrophin (Himburg et al., 2018), and epidermal growth factor (EGF) (Doan et al., 2013). Furthermore, a subset of BM ECs coupling angiogenesis and osteogenesis in mice has recently been identified and extensively characterized (Kusumbe et al., 2014; Ramasamy et al., 2014). These studies indicate that ECs play an important role in mammalian BM regeneration after injury.

Insights into endothelial contributions to bone marrow (re)generation: relevance for human biology*?*

Although these studies (discussed in depth in the introduction of this thesis) have greatly increased our understanding of the instructive-role of ECs in guiding tissue homeostasis and (re)generation, the relevance for human biology has remained largely speculative. Specifically, there are a number of unresolved questions concerning the (angiocrine) contributions of ECs to bone BM (re)generation in humans. These include: (1) Do specialized subsets of BM ECs, like those in described mice, exist in humans? (2) Are the molecular pathways driving endothelial-mediated BM (re)generation in mice also activated in humans? (3) Do human BM ECs possess the capacity to convert to other cell-types during BM formation or regeneration after injury?

The work described in this dissertation attempted to address these questions and consequently provides novel insights on the molecular and cellular components underlying endothelial-mediated BM (re)generation in humans. Our findings underscore the versatile (direct and indirect) contributions of the endothelial niche to BM development during fetal development and recovery after injury.

Chapter 2 identifies and characterizes a previously unrecognized human EC population (hRECs), including its potential angiocrine profile, associated with BM formation and hematopoietic recovery after chemotherapy. The chapter further identifies interleukin (IL)-33, highly expressed in hRECs as a novel driver of human BM regeneration through anabolic effects on both hematopoietic and mesenchymal/endothelial niche cells.

Chapter 3 revealed that a subset of hRECs converts to non-endothelial hematopoiesis-supportive stromal cells with the capacity to form cells with the ability to reconstitute the hematopoietic niche after *in vivo* transplantation. The concept of endothelial-derived mesenchymal cells as constituents of the HSPC niche is confirmed in genetic lineage-tracing experiments in mice. IL-33 is identified as a molecular driver of this conversion.

5.3 Characterization of human bone marrow endothelium during ontogeny and regeneration

The findings in **Chapter 2** revealed that some human BM ECs share many immunophenotypic and molecular similarities with BM ECs of mice, such as with the recently characterized type H endothelium, marked by high expression of CD31 and endomucin (Kusumbe et al., 2014, 2016; Ramasamy et al., 2014).

The specific human BM ECs described in **Chapter 2** were enriched during fetal development and during recovery after chemotherapeutic insult, and hence termed human regeneration-associated ECs (hRECs). *Phenotypically*, hRECs resembled type H endothelium by being enriched at endosteal regions, being prevalent during fetal development (Langen et al., 2017), being reduced in frequency upon aging, being resistant to genotoxic stress, and expressing markers typical for both arteriolar and sinusoidal blood vessels, including (high expression of) CD31 and endomucin. These hRECs, distinguished from steady-state ECs ($CD31^+CD9^+$ cells) by up-regulated expression of the TGF-b1 receptor endoglin (CD105), were distinct from human sinusoidal vessels, as the latter lacked/exhibited low expression of CD31. This is line with the high expression of CD31 found in type H endothelium of mice, which was also reportedly distinct from sinusoidal blood vessels and characterized as endosteal capillaries. Importantly, these endosteal capillaries, also referred to as transition zone vessels since they connect arterioles to downstream sinusoidal vessels, are functionally distinct from other BM ECs because they couple bone formation and blood vessel growth. This coupling of osteogenesis and angiogenesis, as well as the survival of type H ECs was demonstrated to be dependent on endothelial NOTCH and HIF1 signaling. Interestingly, Nombela-Arrieta, et al. showed that CD105-expessing ECs, closely associated with elevated HIF-1a expression, were found throughout the BM cavity of mice upon regeneration after 5-flourouracil (5-FU), a chemotherapeutic agent, treatment (Nombela-Arrieta et al., 2013). Follow-up work revealed that type H transitional vessels in fact also express CD105 (Gomariz et al., 2018). Similar to humans, we found that mice also exhibited enrichment of $CD105^+$ BM ECs after myeloablative chemotherapy (**Chapter 2**, Figure 2A-C), thereby establishing broader relevance for mammalian biology.

Transcriptional profiling of hRECs revealed many **molecular** commonalities between hRECs and murine BM ECs, especially with the type H ECs. These commonalities included transcriptional activation of the *NOTCH* and *HIF1* signaling pathways, which was further supported by the up-regulated expression of multiple NOTCH components by hRECs, such as

JAG1, *DLL4*, *NOTCH1*, and *NOTCH4*. These molecular commonalities indicate that hRECs, like type H ECs in mice, have a similar transcriptional wiring that facilitates both osteogenesis and angiogenesis. This notion is reinforced by the finding that hRECs displayed increased expression of genes encoding for anabolic regulators of both of these biological processes, such as *SEMA3A* (Serini et al., 2003; Tamagnone and Giordano, 2006), *EDN1* (Clines et al., 2007; Salani et al., 2000), *IGF2* (Chen et al., 2010; Ritter et al., 2002), *POSTN* (Oshima et al., 2002; Shao et al., 2004) and *EFNA1* (Edwards and Mundy, 2008; Kuijper et al., 2007). These molecular commonalities between hRECs and type H ECs, suggest that hRECs are the human counterpart of type H endothelium.

Additional molecular similarities of hRECs with other murine BM ECs include expression of genes encoding for previously discovered angiocrine factors known to regulate HSC function (like proliferation and differentiation), such as *JAG1* (Poulos et al., 2013), *ESELE* (Winkler et al., 2012), *TMBD* (Gur-Cohen et al., 2015), *TFPI* (Khurana et al., 2013), *PLAT* (Ibrahim et al., 2014), and *TNC* (Nakamura-Ishizu et al., 2012). Another molecular commonality of hRECs with regeneration-associated BM ECs in mice was elevated expression of *TNFRSF1A*, the gene encoding for one of the canonical receptors for tumor necrosis factor-α (TNFα). A recent report revealed that TNFα-mediated regeneration of murine BM ECs (which in turn promoted hematopoietic recovery) was dependent on binding of TNFα to this specific receptor (Bowers et al., 2018). These commonalties between human and mouse BM ECs indicate that there is a considerable degree of evolutionary conservation across these species.

These findings also indicate that the molecular makeup of BM ECs is quite distinct from other organotypic ECs. One of the distinctive features of BM ECs (compared to other tissue-specific ECs) is the ability to regulate the function of heterotypic stem cells, such as HSCs and skeletal stem cells (SCCs). This executive function of BM ECs is especially important during endochondral ossification which requires extensive crosstalk between many different types of cells, such as, chondrocytes, osteolineage-cells (Ben Shoham et al., 2016), osteoclasts (Romeo et al., 2019), and hematopoietic progenitors, which is thought to greatly dependent on angiocrine signals derived from blood vessels invading the mesenchymal condensation (primordium of a long bone) (Sivaraj and Adams, 2016). BM ECs seem to deploy a different set of angiocrine factors for the fine-tuned regulation of tissue-specific stem cells (in this case HSCs and SSCs) than other ECs. For example, while LSEC-derived WNT2 (Ding et al., 2010; Wang et al., 2015) and WNT9B (Wang et al., 2015) may play a prominent role in mediating liver function, these angiocrine factors were not expressed by hRECs. Also, the regenerative function of some angiocrine factors may be restricted to their organ, such as HGF (Ding et al., 2010) and ANG2 (Hu et al., 2014) (both were expressed in hRECs, but not elevated), the latter reportedly inhibiting the HSC-supportive function of angiopoietin 1 (ANG1) (Gomei et al., 2010).

Another prime example of how BM ECs seem distinct from other organotypic ECs is the tissue-dependent response induced by endothelial-Notch activation. While the endothelial-Notch pathway has convincingly been shown to play a beneficial role in mediating BM regeneration (Butler et al., 2010; Chen et al., 2016a; Guo et al., 2017; Kusumbe et al., 2016; Poulos et al., 2013; Ramasamy et al., 2014; Shao et al., 2019), activation of endothelial-Notch signaling in other organs, such as the liver (Duan et al., 2018), lung (Cao et al., 2016) and kidney (Kida et al., 2016), reportedly promotes fibrosis in these organs and is thereby detrimental to tissue regeneration after injury.

Differences between hRECs and type H ECs

While hRECs and type H ECs exhibit a number of similarities in their angiocrine profile, including expression of angiocrine factors that regulate angiogenesis (EFNB2, DLL4, Jagged1) (Ramasamy et al., 2014) and hematopoiesis (SCF and CXCL12) (Kusumbe et al., 2016), there are some differences with regard to the expression of osteogenic growth factors. For instance, it was reported that type H endothelium overexpressed *Pdgfa*, *Pdgfb*, *Tgb1*, *Tgb3* and *Fgf1* compared to type L endothelium (sinusoidal BM ECs). Of these only *PDGFB* was found to be significantly up-regulated in hRECs. Most notably expression of transcripts encoding for Noggin, a secreted antagonist of bone morphogenetic protein (BMP) signaling and strongly indicated to be an angiocrine regulator of osteogenesis (Ramasamy et al., 2014), was very low/absent in hREC.

Of note, it was demonstrated that EC-specific overexpression of *Pdgfb* led to HSC expansion in the BM, presumably in an indirect manner, since this expansion of HSCs was accompanied by increased number of PDGFRβ/NG2-expressing mesenchymal stromal cells and cellular levels of SCF (Kusumbe et al., 2016). This demonstrates that BM ECs can directly regulate the behaviour of HSPCs, for example by the release of hematopoietic-supporting angiocrine factors, or indirectly by releasing angiocrine factors that support the maintenance or HSPC-regulatory function of other niche cells.

These findings suggests that despite BM ECs of mice and humans exhibiting many molecular similarities, including activation of the same molecular programs, i.e Notch and HIF1 signaling, the downstream angiocrine factors underlying BM formation or hematopoietic regeneration after injury are not necessarily always the same in these ECs from different mammalian species. This further argues that while the knowledge acquired from studies using transgenic mice is valuable, work in humans will be needed to validate these findings in order to provide relevance to human regenerative medicine.

5.4 Regenerative factors expressed by human hRECs: Identification of IL-33 as a driver of hematopoietic recovery and niche formation

The identification of an endothelial subset associated with BM (re)generation in **Chapter 2** provided the opportunity to interrogate its transcriptional programs for putatively novel BM regenerating factors. HRECs expressed a number of genes encoding for soluble or

membrane-bound proteins with a mostly unknown role, at the time of writing **Chapter 2**, in (mediating) hematopoietic recovery after injury. This provided us with a list of candidate angiocrine factors that were perhaps capable of regulating hematopoiesis, osteogenesis, and/or angiogenesis, including laminin α4 (LAMA4), and interleukin-33 (IL-33) (**Chapter 2**, Figure 5). Strikingly, subsequent experiments to unravel the angiocrine potential of IL-33 revealed that IL-33 was capable of facilitating hematopoiesis, angiogenesis, **and** osteogenesis *in vitro*. This provided proof of concept that elucidation of the transcriptome of human BM ECs associated with BM formation or regeneration can support the identification of novel angiocrine factors. Of note, **Chapter 2** also now complements a follow-up study revealing that niche-derived LAMA4 controls the cycling and homing of hematopoietic stem and progenitor cells (HSPCs) (Susek et al., 2018) by indicating BM endothelium as a possible source of LAMA4.

Importantly, IL-33 expression was also detected in $CD105^+$ BM ECs of mice and was up-regulated following chemotherapy-induced injury (**Chapter 2,** Figure 2D-E). This is congruent with the notion that BM ECs of mice and humans express the same angiocrine factors. Though the number of studies is limited to date, endothelial IL-33 expression in the BM of mice has been confirmed by other groups (Mager et al., 2015; Nolan et al., 2013), specifically one group indicated that IL-33 was mainly restricted to a subset of sinusoidal blood vessels (Mager et al., 2015). The other group attempting to characterize endothelium from different organs during homeostasis and regeneration revealed modest *Il33* expression in BM endothelium during steady-state conditions (Nolan et al., 2013). However, both of these studies did not report whether IL-33 was differentially expressed after injury, such as myelosupression. Whether the proposed counterpart of hRECs in mice, the type H capillaries, express IL-33 as well, has not been reported.

IL-33 induces expansion of multipotent hematopoietic progenitors

Chapter 2 also provides insights on how angiocrine factors expressed by human BM ECs might support BM formation and regeneration after injury. Due to the limitations inherent to the study of human cells, as well as the inability to propagate hRECs ex vivo without loss of their endothelial phenotype (**Chapter 3**), providing direct experimental support for the notion that hRECs support BM formation and regeneration after injury was hampered. Therefore, strategic focus was placed on dissecting the hREC transcriptome to establish the potential angiocrine profile of these cells and identify angiocrine factors possibly involved in endothelial-driven reconstitution of HSPCs or formation of the hematopoietic niche. This strategy led to the discovery that IL-33, one of the candidate angiocrine factors overexpressed in hRECs, was able to support hematopoiesis, osteogenesis, and angiogenesis.

Originally described to be an inducer of T helper 2 (T_H2) cytokines upon its discovery (Schmitz et al., 2005), IL-33 is now regarded to be a pleiotropic cytokine and is best known for its role in immunity and inflammation (Cayrol and Girard, 2014). The hematopoiesis-

supportive effect of IL-33 was initially suggested in **Chapter 2** by the *ex vivo* capacity of human recombinant IL-33 (rhIL-33) to expand $CD34^+$ myeloid and lymphoid hematopoietic progenitor cells (HPCs) isolated from umbilical cord blood (UCB), without exhausting immunophenotypic HSCs. These observations build upon previous findings revealing that in response to rhIL-33 treatment, $CD34^+$ HPCs release hematopoietic-stimulatory cytokines (Allakhverdi et al., 2009), such as granulocyte-macrophage colony-stimulating factor (GM-CSF) and interleukin-6 (IL-6). The *in vivo* effects of IL-33 on hematopoiesis were demonstrated in mice treated with recombinant murine IL-33 (rmIL-33) (**Chapter 2**, Figure 7 and S6), which revealed enhanced myelopoiesis characterized by splenomegaly (data not shown) and increased number of mature myeloid cells in the peripheral blood and BM in rmIL-33-treated mice. Similar to the effects of rhIL-33, rmIL-33 treatment increased the number of hematopoietic precursor cells in the BM of mice, including multipotent progenitors with both myeloid and lymphoid potential (Oguro et al., 2013), and in particular more committed cells, such as granulocyte-macrophage progenitors (GMPs), lymphoid-committed precursors with T cell, B cell, and natural killer (NK) cell potential (Kumar et al., 2008), and innate lymphoid cells (Brickshawana et al., 2011), without compromising immunophenotypic HSC number.

Importantly, recent follow-up work in mice demonstrated that recombinant IL-33 is a potent inducer of HSPC, as well as, common lymphoid progenitor cell (CLP) mobilization into peripheral blood, indicating that recombinant IL-33 is capable of targeting these cells (Alt et al., 2019). This notion is supported by a prior study revealing that the canonical receptor of IL-33, ST2, is expressed by various subsets of hematopoietic progenitor cells, including Lin^-, $cKit^+$, $Sca\text{-}1^+$ (LKS) cells and CLPs (Le et al., 2013). Subsequent work uncovered similar effects of recombinant IL-33 on hematopoiesis, congruent with those described in **Chapter 2**, demonstrating that administration of rmIL-33 not only promoted myelopoiesis, but also splenic lymphopoiesis, and enhanced host defense against opportunistic infections (Kim et al., 2014). In particular, recombinant IL-33 was found to be capable of inducing expansion and activation of a subset of B cells (Komai-Koma et al., 2011), which further supports the notion that IL-33 can also enhance lymphopoiesis.

These studies complement the findings in **Chapter 2**, and indicate that IL-33 is capable of supporting myelopoiesis, as well, as lymphopoiesis, which may have considerable clinical relevance, specifically for patients with delayed immune reconstitution after receiving chemotherapy and consequently at risk for opportunistic infections. For example, we observed that patients with decreased levels of NK cells after chemotherapy tended to have delayed hematopoietic recovery (**Chapter 4**). Interestingly, it has been demonstrated that NK cells express ST2 and that IL-33 can amplify expansion of these cells (Bourgeois et al., 2009; Nabekura et al., 2015), making it tempting to speculate whether delayed hematopoietic recovery seen in patients may in fact also coincide with lower levels of IL-33. Formal demonstration of endothelial-derived IL-33 supporting hematopoietic regeneration after injury will have to await *in vivo* endothelial-targeted deletion experiments in mice.

Nevertheless, a very recent study has indicated that at the least recombinant IL-33 is able to enhance HSC regeneration and overall survival after myelosuppressive irradiation (Kim et al., 2014).

IL-33-mediated BM regeneration by supporting BM niche cells

The findings in **Chapter 2** also indicate that IL-33 may support hematopoiesis by (re) building the BM microenvironment for HSPCs. The BM microenvironment, also known as the hematopoietic niche, consists of BM stromal subsets, including ECs and osteolineage/ skeletal cells.

Previous studies have shown that regeneration of BM endothelium (angiogenesis) precedes, and is required for, proper HSPC reconstitution (Bowers et al., 2018; Hooper et al., 2009; Zhou et al., 2015). Abrogating *IL33* expression in HUVECs disrupted expansion of these ECs (**Chapter 2**, Figure 6C), indicating that IL-33 is a positive regulator of EC proliferation (an important feature of angiogenesis). This is in line with earlier work suggesting IL-33 is capable of stimulating vessel sprouting of ECs *in vitro* (Choi et al., 2009; Shan et al., 2016; Stojkovic et al., 2014) and promoting angiogenesis *in vivo* (Choi et al., 2009; Shan et al., 2016). Other work has indicated that the angiogenic effects of IL-33 may be tissue-specific, suggested by the observation that recombinant IL-33 inhibited neovascularization in the eye (Theodoropoulou et al., 2017). Likewise, Notch signaling has been demonstrated to have similar tissue-specific effects on angiogenesis, with activated Notch signaling inhibiting retinal angiogenesis (Hellström et al., 2007), while promoting angiogenesis in the BM(Ramasamy et al., 2014). Provocatively, Notch signaling has been reported to drive expression of IL-33 (Sundlisæter et al., 2012), which may further support the notion that the angiogenic effect of IL-33 is tissue-specific.

It is also interesting to speculate how IL-33 could mediate BM angiogenesis during regeneration after injury. While *in vitro* studies suggest a direct effect of IL-33 on EC proliferation, it is possible that IL-33 may affect other cells mediating BM angiogenesis. In light of the recent observation that granulocytes accelerate blood vessel regeneration following irradiation (Bowers et al., 2018), and considering that IL-33 reportedly facilitates neutrophil recruitment (Alves-Filho et al., 2010; Verri et al., 2010) and increases neutrophil number (**Chapter 2**, Figure S6D-E), these findings raise the possibility that IL-33 might contribute to hematopoietic recovery by acting on neutrophils mediating vascular regeneration. Furthermore, it has been shown that neutrophil-derived proteases are able to cleave full-length IL-33, resulting in bio-active IL-33 with ~10-fold higher activity (Lefrançais et al., 2012), which makes it tempting to speculate that IL-33 derived from injured/activated endothelium may create an inflammatory feed-forward loop to jumpstart BM regeneration. Of note, another indirect effect of angiocrine-derived IL-33 facilitating endothelial-mediated hematopoietic regeneration could be by inducing expression of HSPC-stimulatory cytokines in (other) ECs. This possibility was raised by a previous study demonstrating that exogenous

IL-33 is capable of stimulating GM-CSF and macrophage colony-stimulating factor (M-CSF) production in ECs (Montanari et al., 2016). Interestingly, we also observed that *CSF1*, encoding for M-CSF, was overexpressed in hRECs (data not shown).

Chapter 2 (Figure 6A-B) also revealed that BM-derived stromal cells (BMDSCs) cultured in osteogenic medium supplemented with rhIL-33 exhibited enhanced mineralization capacity, suggesting that IL-33 may help establish the BM microenvironment by supporting matrix deposition by osteogenic cells. The enhanced mineralization capacity of rhIL-33-treated BMDSCs was in line with a previous report demonstrating that IL-33 can cause a two-fold increase in mineral deposition by mouse osteoblasts *ex vivo* (Saleh et al., 2011). It is tempting to speculate that the stimulatory effect of IL-33 on osteogenesis might come into play during BM formation in fetal development, since mineralization is a hallmark feature of endochondral ossification. While previous work has shown that bone formation in mice deficient for the IL-33 receptor, ST2, was normal (Schulze et al., 2011), indicating that the IL-33/ST2 signaling axis is not essential for skeletogenesis, it does not exclude the possibility that IL-33 plays a role in the emergence of BM.

What drives endothelial IL-33 expression and release?

The induction of IL-33 expression following chemotherapy-induced tissue damage is congruent with a previous study showing that gene expression of IL-33 and secretion by HUVECs are increased after irradiation, which, like chemotherapy, can cause extensive tissue damage (Lee et al., 2015). The notion that endothelial IL-33 expression is induced by tissue damage raises a number of questions. These include the nature of the cues that induce endothelial *IL33* expression and the mechanism/trigger for IL-33 release. While the findings in this dissertation cannot comprehensively answer these questions, they might be able to provide some clues on how these specific processes could unfold.

For one, IL-33 expression in ECs *in vitro* has been associated with cellular quiescence (Küchler et al., 2008) and was suggested to be driven by Notch signaling (Sundlisæter et al., 2012). While we did not interrogate the cell cycle status of hRECs, these findings might partly explain why $CD105^{+}$ BM ECs are relatively chemo-resistant (**Chapter 2**, Figure 1C-D and Figure 2A-B) and are also in line with the transcriptional activation of Notch signaling observed in hRECs (**Chapter 2**, Figure 4E-F). Secondly, subsequent work revealed that IL-33 expression was up-regulated in ECs with an activated DNA damage response (Stav-Noraas et al., 2017), indicating that DNA damage might be involved in regulating IL-33 expression, which is interesting considering that chemotherapy is a potent inducer of DNA damage. In addition, chemotherapy can also cause tissue damage by the generation of reactive oxygen species (ROS) (Angsutararux et al., 2015; Wojcik et al., 2015) and subsequent inflammation (Mittal et al., 2014). The latter has been linked with up-regulated endothelial IL-33 expression in mice, indicated by the observation of elevated protein expression of IL-33 in and around the blood vessels of inflamed organs (colon and liver) (Pichery et al.,

2012). Another possible mediator of endothelial IL-33 expression is Oncostatin M (OSM). OSM has recently been reported to induce murine IL-33 expression by vascular ECs of the liver and LSECs (Arshad et al., 2015). Provocatively, transcript expression of genes encoding for components of the receptor complex capable of binding OSM (*IL6ST*, *OSMR*, and *LIFR*) were highly overexpressed in hRECs compared to steady-state BM ECs, which is compatible with the view that OSM might be able to regulate IL-33 expression by hRECs.

The cellular release of IL-33 by ECs is a somewhat contentious subject. IL-33 is mainly known to act as an "alarmin" released by cells undergoing necrosis after tissue damage (Cayrol and Girard, 2018), however, there have been some studies suggesting that IL-33 can be released by active secretion from bio-mechanically stressed fibroblasts (Kakkar et al., 2012) or ECs (Chen et al., 2015) (without undergoing necrosis). Furthermore, another recent report proposed that the release of IL-33 in the absence of cell death was possible through extracellular secretion of adenosine triphosphate (ATP) mediated by the generation of ROS (Uchida et al., 2017), which is appealing to link with hRECs in the context of chemotherapy-associated ROS. IL-33 preferentially localizes to the nucleus of cells due to an evolutionarily conserved homeodomain-like helix–turn–helix motif within its N-terminal domain (Bertheloot and Latz, 2017). This nuclear location of IL-33 was recently demonstrated to be a strong regulator of extracellular IL-33 by acting as a "sink", as expression of a N-terminally truncated IL-33 in mice resulted in excessive IL-33 release and subsequent lethal inflammation (Bessa et al., 2014). In the case of hRECs, IL-33 expression was detected in both the nucleus and cytoplasm (**Chapter 2**, Figure 5B), with the cytoplasmic localization suggesting that IL-33 is being released based on the reports described above. The notion of active IL-33 secretion by hRECs, instead of release induced by necrosis, is further supported by the flow cytometric observation that hRECs are 7AAD negative, indicating that hRECs are viable cells (**Chapter 2**, Figure 1A). Considering these findings, we speculate that chemotherapy-induced ROS caused tissue/cellular damage without inducing necrosis of ECs, but enough to trigger endothelial IL-33 release.

The findings in **Chapter 2** suggest that IL-33 is up-regulated and released by living cells upon chemotherapeutic challenge, which might be mediated by endothelial-Notch activation. Further research will be needed to uncover the exact molecular mechanisms underlying IL-33 up-regulation and secretion by ECs upon BM regeneration and development.

5.5 Endothelium-derived mesenchymal cells contribute to the hematopoietic niche in development

Chapter 3 reveals that a subset of hRECs, characterized by co-expression of low-affinity nerve growth factor receptor (LNGFR)/CD271, undergoes EndMT *ex vivo*, giving rise to non-endothelial stromal (also known as mesenchymal) cells capable of supporting hematopoiesis and differentiating into various BM microenvironmental/skeletal cells, including chondrocytes, osteoblasts, adipocytes. These LNGFR$^+$ hRECs exhibited a transcriptional wiring consistent with EndMT, including overexpression of mesenchymal markers concomitant with down-regulated expression of endothelial markers in comparison with LNGFR$^-$ hRECs.

These findings are somewhat reminiscent of earlier *ex vivo* observations that HUVECs, harboring a mutated form of ALK2 that causes fibrodysplasia ossificans progressiva (FOP), were able to generate multipotent mesenchymal cells (Medici et al., 2010). The process of EndMT is thought to normally occur during times of organ morphogenesis (Kovacic et al., 2019), such as cardiac and pulmonary development, and seems to re-emerge postnatally in pathological conditions involving organ-specific fibrosis (Pardali et al., 2017). Now for the first time, evidence is presented that prospectively isolated ECs of the primitive human BM can generate non-endothelial stromal cells **with** skeletogenic differentiation capacity, providing relevance to developmental physiology of human BM.

The stromal progeny of LNGFR$^+$ hRECs contains bona fide human skeletal progenitors

While formal proof for the conversion of *human* LNGFR$^+$ ECs into mesenchymal cells under physiological conditions is lacking (due to limitations inherent to the study of human cells), **Chapter 3** does provide conclusive evidence that LNGFR$^+$hREC-derived mesenchymal cells harbor *in vivo* skeletogenic differentiation capacity. The LNGFR$^+$hREC-derived mesenchymal cells were capable of establishing an ectopic hematopoietic microenvironment (comprising bone, cartilage, endothelium and hematopoietic tissue) upon xenogeneic transplantation in mice. Given this evidence and the finding that hRECs reside in skeletal tissue *in situ* (enriched in fetal and regenerative BM), the stromal progeny of LNGFR$^+$ hRECs can at the least be considered (novel) skeletal progenitor cells for now. Additional clonal and serial transplantation *in vivo* assays are planned to assess their self-renewal ability and test whether they constitute bona fide multipotent SSCs, i.e. stem cells residing in skeletal tissue capable of generating cartilage-forming, bone-forming, and/or fat-forming cells, as well as hematopoiesis-supportive stroma *and* possessing the capacity for self-renewal.

The identification of human endothelial-derived skeletal progenitor cells in **Chapter 3** adds to a larger body of work that has greatly improved our understanding of the BM stromal cells (BMSCs) associated with the human skeletal system (Chan et al., 2018; Pinho et al., 2013; Sacchetti et al., 2007; Tormin et al., 2011). These previous studies described various, and often partially overlapping, SSCs within the BMSC pool.

Seminal work from the late Paulo Bianco's group was the first to prospectively isolate human SSCs, demonstrating that these SSCs, marked by CD146 protein expression, displayed a perivascular localization in the BM and possessed osteochondroadipogenic potential (Sacchetti et al., 2007). A subsequent study revealed that the CD146$^+$ cells (containing SSCs) constitute a subset of CD271$^+$ BMSCs and that the CD146$^-$CD271$^+$ subset also contained SSCs with tri-lineage potential similar to their CD146$^+$CD271$^+$ counterparts, but unlike their counterparts, localized preferentially at endosteal sites (Tormin et al., 2011). It is tempting

to speculate that LNGFR+ hRECs might give rise to both CD271+ BMSC subsets *in vivo*, due to their shared expression of CD271 and their similar skeletogenic differentiation capacity.

It is important to scrutinize that the SSCs in the aforementioned studies were obtained from adult BM. The specific cell-surface markers used to prospectively isolate these cells may not carry over to skeletal tissue at different developmental stages. In fact, while follow-up work showed that PDGFR-α^{low}CD271$^+$ BMSCs are highly enriched for SSCs in adult BM (Ghazanfari et al., 2016; Li et al., 2014b), another paper proposed that combinatory expression of PDGFR-α and CD51 marks Nestin$^+$ SSC-like cells, which were especially enriched for HSC-supportive factors, in fetal bone (Pinho et al., 2013). Expression of LNGFR by fetal PDGFR-α$^+$CD51$^+$ SSC-like cells was not reported, and it remains to be seen to if the LNGFR$^+$hREC-derived stromal cells would overlap with these cells.

In an systematic attempt to define the hierarchical organization of BMSCs, a recent study identified a PDPN$^+$CD146$^-$CD73$^+$CD164$^+$ SSC enriched in the growth plate of fetal and adult skeletal tissue that was capable of giving rise to osteo- and chondrogenic progenitor cells, but not adipogenic cells (Chan et al., 2018). This latter work further stresses that humans BMSCs are very heterogeneous, with some subsets differentiating into specific skeletal subsets with restricted differentiation capacity, while other stromal subsets sustain hematopoiesis by providing niches to HSPCs (Chan et al., 2018). Our data indicate that LNGFR$^+$ EC-derived stromal cells may exert both functions, emanating in their ability to create ectopic BM niches containing cells from diverse skeletal lineages (fat, bone, cartilage), and support nascent hematopoiesis. These data also indicate that the LNGFR$^+$hREC-derived stromal cells are distinct from the PDPN$^+$CD146$^-$CD73$^+$CD164$^+$ SSC and its downstream progeny considering that the latter exhibited a more restricted skeletogenic (osteochondrogenic) differentiation capacity.

Untangling the origins of the hematopoietic niche/skeletal stem cells in mice

The observation of ECs undergoing mesenchymal transition in the context of human BM (re)generation prompted the question whether this process occurs *in vivo* in mammals and what the contribution of endothelial-derived mesenchymal cells would be to the stromal/skeletal BM microenvironment. To this end, we performed genetic fate mapping in transgenic mice labeling ECs and their descendants. This revealed that in 3-week old mice a significant proportion of mesenchymal/skeletal progenitors (±50%), and osteo-lineage cells (±27%) were derived from ECs (**Chapter 3**, Figure 5), indicating that ECs contribute to the skeletal compartment of the hematopoietic niche of young mice. These findings support the notion that mammalian ECs can convert into mesenchymal cells under physiological conditions/in mammalian ontogeny.

Notably, endothelial contribution to the hematopoietic niche of mice was unanticipated based on previous work attempting to define the origins of SSCs. So far, multiple studies using transgenic mice have indicated that murine skeletal stem/progenitor cells can be

derived from multiple developmental sources, with some first appearing during early skeletal development (endochondral ossification) (Isern et al., 2014; Ono et al., 2014b, 2014a; Worthley et al., 2015) or postnatally(Zhou et al., 2014), either at the perichondrium (Isern et al., 2014; Ono et al., 2014a) or in the growth plate (Mizuhashi et al., 2018), and existing transiently (Takashima et al., 2007) or persisting well into adulthood (Zhou et al., 2014). Specifically, different groups have shown that SSCs are either derived from the neural crest or from the lateral plate mesoderm (LPM) (Robey, 2018). This has been suggested by fate-mapping studies performed with specific reporter mice labeling either neural crest-derived cells (P0-Cre, Sox1-Cre, Wnt1-Cre, Nes-CreERT, SOX10-CreERT) (Isern et al., 2014; Morikawa et al., 2009; Takashima et al., 2007) and (lateral plate) mesodermal-derived cells (Prx1-Cre, Mesp1-Cre and Hoxb6-CreER) (Greenbaum et al., 2013; Isern et al., 2014; Komada et al., 2012). Basically, despite the great heterogeneity of SSCs in time and space, the prevailing dogma asserts that SSCs are of non-hematopoietic and non-endothelial origin (Ambrosi et al., 2019).

Although the studies above have not demonstrated that SSCs can be derived via an endothelial-intermediate stage, these studies have not explicitly ruled out that all the SSCs in the BM lack an endothelial-origin, especially in situations after myeloablative insult for example (Figure 1). Considering the mesodermal origin of endothelium (Dyer and Patterson, 2010), it is not likely that endothelial-derived SSCs would overlap with neural-crest derived SSCs, since the neural crest and mesoderm are two distinct embryonic tissues. However, this does raise the possibility that at a certain point during mammalian ontogeny some mesodermal-derived SSCs, or perhaps precursor SSCs, arise from "skeletogenic endothelium" via EndMT, a developmental event/process perhaps not too dissimilar from HSC generation from hemogenic endothelium via EHT (Figure 1).

It has been proposed that endothelium itself can be derived from two types of mesoderm: the paraxial mesoderm and the splanchnopleuric layer of the LPM (Dyer and Patterson, 2010). The former predominately generates the blood vessels of the kidney and body wall, whereas the latter form endothelial precursors that vascularize visceral organs and contribute to aortic floor and intra-aortic hematopoietic cell clusters (Dyer and Patterson, 2010). In this context, it is noteworthy that a very recent report indicated that the entire avian BM vasculature is derived from the paraxial mesoderm (Yvernogeau et al., 2019). Although we cannot currently deduce which type of ECs generated the immunophenotypic SSCs we observed in our mouse model (**Chapter 3**), the human data suggest that fetal BM ECs give rise to skeletal progenitor cells. Creating a novel reporter line specifically marking ECs (CDH5) and the paraxial mesoderm (Mesp-1?) could help shed light on the question whether BM ECs contribute to (paraxial) mesodermal-derived SSCs.

Mesenchymal-like BM ECs and LNGFR-expressing BMSCs in mice: parallels with LNGFR$^+$ hRECs?

Considering the potential of LNGFR$^+$ hRECs to give rise to skeletogenic progenitor cells, it is noteworthy that in a recent study, characterizing multipotent BMSCs marked by CD73-EGFP, a subset of ECs with mesenchymal properties was identified in the BM of adult mice (Breitbach et al., 2018). This endothelial subset shared remarkable resemblance with the LNGFR$^+$ hREC identified in **Chapter 3**. Commonalities include the overexpression of *CD73* (in association with the expression of *bona fide* endothelial markers), the transcriptional upregulation of a stromal stem cell signature (Boquest_Stem_Cell_up signature), including overexpression of *COL1A1*, *COL1A2*, and the overexpression of 'hematopoietic niche' genes (*ESELE*, *VCAM1*, *CXCL12*). The skeletogenic differentiation capacity of this subset of ECs was not interrogated in mice (hampered due to the limited population doublings of these cells in culture), but our findings in humans (**Chapter 3**) revealed the potential of similar cells to convert into skeletal progenitor cells.

LNGFR is also expressed by a distinct BMSC in mice. Using mass cytometry (to measure protein expression of several BM stromal markers at single-cell level) the Scadden group demonstrated that BMSCs in adult mice can be divided into different clusters based on their cell-surface protein expression (Severe et al., 2019). Interestingly, one family of stromal clusters defined by their CD73 expression, was enriched for CFU-Fs, was the least sensitive to radiotherapy, and displayed the highest expression of HSPC-regulatory factors during homeostatic and stress conditions. In particular, within this family, one cluster distinguished by LNGFR expression, expressed the highest level of cytokines and was highly enriched following irradiation. These findings, together with the observation that these LNGFR$^+$CD73$^+$ stromal cells were also enriched during fetal development, further reinforce the notion that LNGFR is a marker of hematopoiesis-supportive BMSCs enriched during BM (re)generation in both humans and mice.

IL-33 mediates the conversion of human BM ECs into mesenchymal cells with skeletogenic potential

The findings in **Chapter 3** also uncover a role for IL-33 as an inducer of EndMT in two different types of ECs (fetal vs adult) *in vitro*. Strikingly, the resulting "mesenchymal" progeny possessed skeletogenic differentiation capacity: The stromal progeny of HUVECs were capable of producing calcific deposits (osteogenic) and cartilaginous extracellular matrix after treatment with rhIL-33. In parallel, the stromal cells derived from rhIL33-treated ECFCs, isolated from adult peripheral blood, obtained the capacity to undergo osteogenic differentiation. Additional experiments to test the adipogenic capacity, as well as the chondrogenic capacity for ECFC-derived stromal cells, are planned and will be necessary to test if IL-33 endowed the stromal progeny of these culture expanded ECs with multipotent skeletogenic differentiation capacity. In addition, xenogeneic transplantation

of these endothelial-derived stromal cells in mice will elucidate if these cells acquired bona fide in vivo skeletogenic differentiation capacity.

A number of clues pointed to the potential of IL-33 as an EndMT factor. First, the angiocrine profile of hRECs (Chapter 2) already contained other well-established EndMT factors, such as DPP-4 (Kanasaki et al., 2014; Shi et al., 2015), BMP4 (Medici et al., 2010), and EDN1 (Widyantoro et al., 2010), suggesting that there might be other factors inducing EndMT within the angiocrine profile of hRECs. Furthermore, as IL-33 is widely recognized to be an inflammatory cytokine, and vascular inflammation is associated with EndMT (Kovacic et al., 2019), we hypothesized that IL-33 could convert ECs into non-endothelial stromal cells. This hypothesis was further supported by a previous study demonstrating that IL-1β, an inflammatory cytokine which strongly resembles IL-33 at a structural level, enhances EndMT (Maleszewska et al., 2013). The ability of IL-33 to endow endothelial-derived stromal cells with skeletogenic differentiation capacity, on top of inducing EndMT, is remarkable considering that only BMP4 (Medici et al., 2010) and TGF-β (Medici et al., 2010) have been shown to have similar effects, and further highlights the pleiotropic nature of IL-33.

The *de novo* generation of non-endothelial stromal cells – with skeletogenic differentiation capacity – through an EC intermediate stage had previously been suggested in cell culture experiments using embryonic stem cells (ESCs) and induced pluripotent stem cells (iPSCs) demonstrating that mesenchymal cells with multilineage differentiation capacity can be generated from apelin receptor (APLNR)-expressing mesenchymoangioblasts, via an endothelial-intermediate (Kumar et al., 2017; Vodyanik et al., 2010). Interestingly while, *APLNR*, as well as transcripts encoding for the corresponding ligand Apelin, are highly expressed in hRECs lacking LNGFR expression, expression of *APLNR* and *APLN* is more subdued in the LNGFR$^+$ hREC subset, opening the possibility that IL-33^{high}APLNR^{high}LNGFR$^-$ hRECs gave rise to the smaller LNGFR$^+$ hRECs subset (via autocrine signaling).

Our *in vitro* findings on the role of IL-33 in EndMT likely have relevance to human BM physiology. HUVECs treated with rhIL-33 exhibited increased expression of LNGFR (**Chapter 3**, Figure 6H), as well as, (up-regulated expression of) other mesenchymal markers concomitant with decreased expression of endothelial markers, indicating that IL-33 can initiate by extension EndMT in LNGFR$^-$ hRECs by inducing expression of LNGFR (and other mesenchymal markers) *in vivo*. This notion is corroborated by the finding that LNGFR$^+$ hRECs and IL-33-treated HUVECs exhibited similar expression of transcriptional drivers of EndMT, in particular *SNAI2* and *TWIST1* (**Chapter 3**, Figure 2F and Figure 6B-D).

Our observations warrant further research on the effect of IL-33 in cellular reprogramming including acquisition of skeletal progenitor features. Specifically, relevance of IL-33 to mammalian BM physiology will require abrogation of *IL33* expression in vertebrate model systems during BM development (niche formation) and upon regeneration after injury.

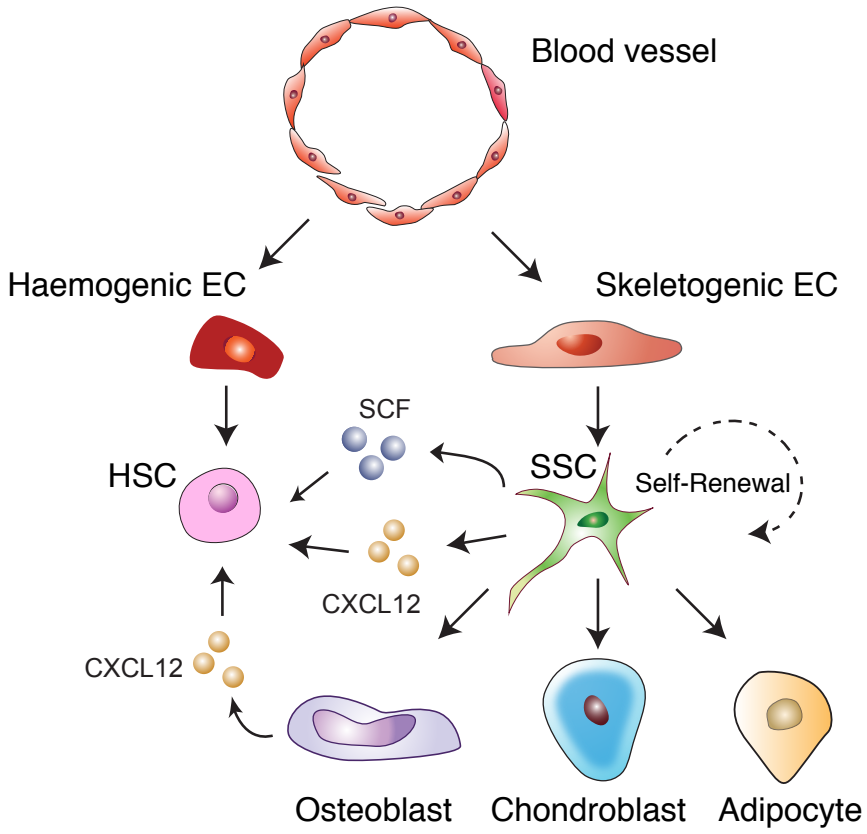

Figure 1. An adapted view on the ontogeny of the hematopoietic system: Concerted generation of stem cells and their niches by endothelial cells? We propose that endothelial cells can generate skeletal progenitor/stem cells that form the BM microenvironment that nourish hematopoietic stem/progenitor cells. In this new model the endothelium lies at the apex of all the BM cells.

5.6 Immune cells associate with hematopoietic recovery

ECs are not the only established niche cells in the BM regulating HSPC function. The progeny of HSCs can relay signals back to HSCs and establish regulatory feedback loop (Hirata et al., 2018b, 2018a; Schürch et al., 2014). Therefore, we also explored if mature hematopoietic cells are involved in mediating BM regeneration after injury, exploiting our resource of bone marrow after chemotherapeutic injury.

Chapter 4 set out to determine the hematopoietic composition of the HSPC niche, with a special focus on lymphoid cells of the innate and adaptive immune system, and identify immune cells associated with hematopoietic regeneration. The subsequent findings in

Chapter 4 indicate that specific immune subsets, such as T cells, are preserved in comparison to other immune cells after myeloablative chemotherapy and are associated with the time needed for hematopoietic recovery (duration of neutropenia), and also provide insights on chemotherapy-induced immunosuppression.

In particular, memory $CD4^+$ T Cells were enriched after myeloablative chemotherapy (**Chapter 4**, Figure 1), indicating that these memory cells are relatively resistant to myeloablative therapy. This resistance could be due to relative quiescence of memory $CD4^+$ T cells conferred by survival niches, which is supported by earlier work demonstrating that memory T cells, associated with IL-7-expressing stromal cells, are kept in a non-cycling state (i.e. resting) (Tokoyoda et al., 2009). On the other hand, B cells were dramatically depleted in the BM following chemotherapy (**Chapter 4**, Figure 1), congruent with previous studies revealing a disproportional reduction in circulating B cell numbers and an impaired humoral immunity in patients (Goswami et al., 2017; Reilly et al., 2013). While it is possible that chemotherapy directly targeted these cells by inducing apoptosis (Stahnke et al., 2001), indirect effects on B cells via their niches is also a possibility. For instance, multiple studies have shown that the BM vasculature is disrupted following myeloablative chemotherapy (Hooper et al., 2009; Kopp et al., 2005; Shirota and Tavassoli, 1991), which may have detrimental consequences for the perivascular niches of B cells (Sapoznikov et al., 2008). Low levels of B cells may have clinical implications for chemotherapy-induced immunosuppression, considering that humoral immune deficiency may leave patients at risk for recurrent infections from polysaccharide-capsulated bacteria (Papanicolaou and Mehta, 2011). In this context it might be worthwhile to reiterate that recombinant IL-33 was found to be capable of inducing expansion and activation of a subset of B cells (Komai-Koma et al., 2011), which suggests that IL-33 might play a role in the reconstitution of B cells after chemotherapy.

The observation that immune composition after chemotherapeutic exposure was strongly associated with subsequent hematopoietic recovery in acute myeloid leukemia (AML) patients (**Chapter 4**, Figure 2) provides biological insights on repopulation dynamics and/or the potential role of immune cells in hematopoietic recovery. The strong correlation between the NK/CD4CM index and the duration of neutropenia might be a matter of specific repopulation kinetics in the BM with the more chemo-resistant (CD4CM T) cells being enriched after myeloablative chemotherapy followed by a progressive decline in frequency upon subsequent recovery of other immune subsets. This notion is congruent with the limited lifespan of NK cells, which are relatively short-lived cells (exhibiting a half-life of 7-10 days) (Zhang et al., 2007) and requiring constant replenishment by active cycling progenitors, indicating that NK cell levels are likely more sensitive to chemotherapy. In addition, the underlying lineage-specification of the bi-potent NK/T-committed progenitor (Klein Wolterink et al., 2010) implies that a shift in cell fate decision biased towards NK cell generation may come at the cost of T cell development (Heemskerk et al., 1997; Schotte et al., 2010), potentially further coupling NK and T cell proportions within the lymphoid

pool. In this scenario, lymphoid subsets would be merely "passive bystanders" in regards to mediating hematopoietic recovery after myeloablative chemotherapy. Alternatively (albeit not entirely mutually exclusive), T and NK cells may be active participants in the reconstitution of HSPCs and their (myeloid) progeny. T cells have been suggested to suppress granulopoiesis directly or indirectly by the release of hematopoietic-inhibitory factors (Broxmeyer et al., 1984; Sallerfors and Olofsson, 1989)(Sallerfors and Olofsson, 1989). Both NK and T cells can secrete various HSPC-regulatory cytokines and growth factors, such as IFNγ (Rajagopalan et al., 2001; Villegas-Mendez et al., 2012), TNFα (von Fliedner et al., 1992; Vitale et al., 2005), and GM-CSF (Levitt et al., 1991; Shi et al., 2006), which may provide a possible means for these immune cells to mediate granulopoiesis. In addition, distinct T cell subsets have been suggested to maintain hematopoietic stem cell (HSC) quiescence (Hirata et al., 2018a). The findings in **Chapter 4** warrant future investigations into the potential contributions of NK and T cells to HSPC reconstitution.

In addition to providing biologic insights on chemotherapy-induced immunosuppression and instructing future investigations towards immune cell contributions to hematopoietic recovery, our findings may also have additional clinical relevance. Persistent neutropenia following chemotherapy is an important determinant of treatment related morbidity and mortality in AML. To date, no post-treatment prognostic factor has been identified predicting the duration of neutropenia in AML. Identification of an NK/CD4TM immune-index predicting hematopoietic recovery enables future interrogation of its value to identify patients vulnerable to opportunistic infections. The substantial variance in NK cell frequencies between patients (**Chapter 4**, Figure 1G) may also have some clinical implications for patient recovery after chemotherapy, since NK cells have been implicated in the direct killing of fungi by recognizing fungal pathogens and eliminating them by releasing lytic granules or by augmenting the antifungal host response (Schmidt et al., 2017). It will be of interest to explore whether the extent of NK cell depletion, in addition to neutropenia, predisposes patients to fungal infections. Additional insights may facilitate further tailoring of antifungal prophylaxis in AML treatment or the use of hematopoietic growth factors (G-CSF) in selected patients with low NK cell constitution and predicted delayed recovery.

Taken together, the data provide novel insights into immune reconstitution after chemotherapeutic injury and identify the balance between CD4CM and NK cells as a prognostic factor for hematopoietic recovery in AML. Findings are anticipated to prompt future investigations into roles of specific immune subsets in HSPC recovery and instruct potential future tailoring of supportive treatment.

5.7 Perspectives and future directions

Overall, the findings in this dissertation support the notion that humans BM ECs, like those found in mice, play an important role in regulating organ morphogenesis and tissue regeneration after injury. Our work has a number of implications for the field of endothelial

biology and (BM) tissue regeneration. The findings indicate that (1) there is considerable evolutionary conversation of BM endothelial cell subsets between mammalian species (human and mice), (2) characterization of endothelial subsets isolated from humans may instruct the identification of specialized ECs and proteins involved in BM niche formation and hematopoietic recovery after injury. This could be used as a platform for the development of novel therapeutic strategies, such as endothelial cell-based transplantations for tissue regeneration or the delivery of angiocrine factors to support the reconstitution of stem and progenitor cells.

Future research

This dissertation addressed the role of the HSPC niche in BM regeneration and development, in particular focusing on ECs and (endothelial-derived) IL-33. The data show that mammalian BM contains specialized BM EC subsets and express angiocrine factors (in particular IL-33) capable of mediating the niche function of ECs. We demonstrated that a distinct subset of skeletal progenitor cells is derived from ECs, providing for the first time *in vivo* evidence that BM endothelium can directly contribute to BM formation (and regeneration) by EndMT. These findings raise a number of questions and hypotheses worth tackling.

For one, we were not able to maintain, let alone expand, LNGFR$^-$ hRECs in culture, which precluded co-culture experiments to directly address (the question) whether these cells are capable of supporting hematopoiesis. Interestingly, transcriptional profiling of hRECs revealed overexpression of genes encoding for secreted factors as well as their receptors (**Chapter 2**, Figure S2D), suggesting the potential relevance of autocrine signaling in the biology of hRECs and perhaps providing clues on how to optimize culture conditions for hREC maintenance. Alternatively, introducing the advenoviral E4ORF1 gene product into hRECs may provide another method to maintain hREC survival *ex vivo*, as it has been previously been demonstrated that lentiviral introduction of E4ORF1 in human primary ECs increased the long-term survival of these cells in serum/cytokine-free conditions while preserving their *in vivo* angiogenic potential (Seandel et al., 2008), and enabled the identification of distinct HSPC-regulatory angiocrine factors (Kobayashi et al., 2010).

Furthermore, in addition to IL-33, we identified a number of other candidate angiocrine factors possibly expressed by hRECs (**Chapter 2**, Figure 5A). It could be worthwhile to test the capacity of these factors to support hematopoiesis, angiogenesis, osteogenesis or EndMT *ex vivo*. For instance, by overexpressing or knocking-down these factors in HUVECs, and then using these modified HUVECs in a co-culture system with HSPCs or mesenchymal elements to test the effect on HSPC expansion or skeletogenic differentiation, respectively. In addition modified HUVECs can be tested for their capacity for endothelial tube formation or proliferation, or if they are coerced to undergo EndMT. It would also be of particular (clinical) interest to assess the effects of candidate angiocrine factors, especially recombinant IL-33, on the reconstitution of HSPCs and their progeny following myeloablative conditioning, for

instance in mice challenged with 5-FU or undergoing BM transplantation after irradiation.
While the findings in **Chapter 3** revealed that LNGFR$^+$ hRECs can generate skeletal progenitor cells, the question remains whether these skeletal progenitors arose from a single LNGFR$^+$ hREC, or if different LNGFR$^+$ hRECs gave rise to committed skeletal progenitors, for example stromal cells specifically differentiating into osteogenic, chondrogenic, or adipogenic cells. Clonal assays in which single cells of LNGFR$^+$ hRECs are sorted and subsequently expanded and transplanted in mice to test their skeletogenic differentiation capacity can potentially resolve this issue. Similarly, single cell RNA sequencing could provide additional insights on the distinct molecular profile of LNGFR$^+$ hRECs and their non-endothelial stromal progeny in relation to "conventional" SSCs (Chan et al., 2018). Furthermore, it would be of interest to test if the heterotopic ossicles generated by the progeny of LNGFR$^+$ hRECs contain phenotypically identical serially transplantable niche-generating non-endothelial stromal cells, or even LNGFR$^+$ hRECs themselves.
The findings in **Chapter 2** and especially **Chapter 3** may also have relevance for the pathophysiology of myeloproliferative neoplasms (MPNs), in particular for primary myelofibrosis (PMF), a disease characterized by expansion of stromal elements in the marrow, including myelofibrosis, extensive ossification, and increased angiogenesis (Arora et al., 2004; Panteli et al., 2004; Ponce et al., 2014). This increased angiogenesis, accompanied by elevated levels of angiogenic growth factors (Ponce et al., 2014; Di Raimondo et al., 2001b, 2001a), raises the possibility that BM ECs might be involved in the pathology of PMF. In fact, a recent reported suggested the occurrence of EndMT in the BM and spleen of PMF patients, including excessive extracellular matrix production (fibronectin) (Erba et al., 2017). Notably, LNGFR$^+$ hRECs exhibited activation of transcriptional programs of fiber organization and ossification (**Chapter 3**, Figure S2F and Table S2), hallmarks of PMF, and were capable of generating non-endothelial stromal cells capable of skeletogenic differentiation (**Chapter 3**, Figure 4), making it tempting to speculate that LNGFR$^+$ hRECs may contribute to PMF by generating myofibroblasts. Interestingly, CD105$^+$ BM ECs were shown to be associated with the degree of fibrosis in PMF (Medinger and Passweg, 2014; Ponzoni et al., 2004), congruent with the notion that hRECs (CD31$^+$CD9$^+$CD105$^+$ BM ECs) might be involved in the development of PMF.
The increased angiogenesis observed in PMF may partially be explained by IL-33, considering its angiogenic effects, demonstrated in **Chapter 2** (Figure 6C and Figure S7B) and also by other studies. In fact, IL-33 was recently shown to be involved in the pathogenesis of MPNs, and amongst the other MPN sub-types, IL-33 expression was the most pronounced in PMF (Mager et al., 2015). Intriguingly, downstream signaling induced by IL-33 has been shown to be mediated by activating Jak2 (Funakoshi-Tago et al., 2011), and considering that constitutive JAK2 signaling (JAK2V617F) drives MPN development, this further reinforces the notion that IL-33 is involved in the pathogenesis of PMF. These implications, in conjunction with the findings in this dissertation, warrant further examinations to test whether IL-33 contributes to accelerated collagen production and ossification in the pathogenesis of PMF, perhaps by driving the conversion of LNGFR$^-$ ECs to LNGFR$^+$ ECs. Of note IL-33 has also been suggested to be involved in the fibrotic diseases of other organs, including the lung (Fanny et al., 2018; Li et al., 2014a) and liver (Marvie et al., 2010; Mchedlidze et al., 2013) (though the fibrosis did not seem to involve EndMT).

Therapeutic avenues
The findings in this dissertation may help instruct the development of novel targeted therapies. For instance, multiple studies in mice have shown that direct injection of ECs can support hematopoiesis following myelosuppression, in particular, recent work revealed that co-transplantation of BM ECs with HSPCs in mice enhanced hematopoietic recovery after myleoablation (Rabbany et al., 2017). Future studies building upon these findings using BM ECs, specifically hRECs, might lead to the development of novel cell-based therapies to augment BM regeneration in patients following myelosuppression. In addition, with IL-33 providing proof of principle, further elucidation of the hREC transcriptome might instruct the discovery of additional angiocrine factors facilitating angiogenesis, osteogenesis, and/or hematopoiesis (**Chapter 2**, Figure 5A). This could lead to the development of therapeutic agents based on novel angiocrine factors. In fact, a long-acting IL-33 has recently been engineered for its potential use as a HSPC mobilizing agent (Alt et al., 2019).
Administration of this long-acting IL-33 for example could be used to accelerate BM regeneration after injury. This engineered IL-33 could support BM regeneration by directly acting on hematopoietic precursor cells or more indirectly by actively supporting the regeneration of the BM microenvironment by inducing conversion of BM ECs into skeletal progenitor cells. Another therapeutic approach could be targeted modulation of endothelial-signaling pathways, for example by targeting endothelial-Notch activity. The group of Ralf Adams provided proof of principle of this concept by activating endothelial-HIF1α signaling using deferoxamine mesylate (DFM) to enhance bone formation in mice (Kusumbe et al., 2014). Conversely, inhibitors directed against specific signaling pathways, for example IL-33, may attenuate development of fibrotic diseases.
In closing, this dissertation validates many findings obtained in mice studies and provides relevance for these studies to human BM physiology. Our findings reveal novel (direct and indirect) contributions of human BM ECs to BM regeneration and development and also warrant future investigations interrogating the precise role of the BM microenvironments in regulating hematopoiesis, angiogenesis, and osteogenesis. Transcriptional profiling human BM ECs may serve as an important resource instructing discovery of novel angiocrine factors.

REFERENCES

Allakhverdi, Z., Comeau, M.R., Smith, D.E., Toy, D., Endam, L.M., Desrosiers, M., Liu, Y.J., Howie, K.J., Denburg, J.A., Gauvreau, G.M., et al. (2009). CD34+ hemopoietic progenitor cells are potent effectors of allergic inflammation. J. Allergy Clin. Immunol. *123*, 472–479.

Alt, C., Yuan, S., Wu, F., Stankovich, B., Calaoagan, J., Schopies, S., Wu, J.Y., Shen, J., Schneider, D., Zhu, Y., et al. (2019). Long-Acting IL-33 Mobilizes High-Quality Hematopoietic Stem and Progenitor Cells More Efficiently Than Granulocyte Colony-Stimulating Factor or AMD3100. Biol. Blood Marrow Transplant. *000*, 1–11.

Alves-Filho, J.C., Snego, F., Souto, F.O., Freitas, A., Verri, W.A., Auxiliadora-Martins, M., Basile-Filho, A., McKenzie, A.N., Xu, D., Cunha, F.Q., et al. (2010). Interleukin-33 attenuates sepsis by enhancing neutrophil influx to the site of infection. Nat. Med. *16*, 708–712.

Ambrosi, T.H., Longaker, M.T., and Chan, C.K.F. (2019). A Revised Perspective of Skeletal Stem Cell Biology. Front. Cell Dev. Biol. *7*.

Angsutararux, P., Luanpitpong, S., and Issaragrisil, S. (2015). Chemotherapy-Induced Cardiotoxicity: Overview of the Roles of Oxidative Stress. Oxid. Med. Cell. Longev. *2015*.

Arciniegas, E., Neves, C.Y., Carrillo, L.M., Zambrano, E.A., and Ramírez, R. (2005). Endothelial-Mesenchymal Transition Occurs during Embryonic Pulmonary Artery Development. Endothelium *12*, 193–200.

Arora, B., Ho, C.-L., Hoyer, J.D., Mesa, R.A., and Tefferi, A. (2004). Bone marrow angiogenesis and its clinical correlates in myelofibrosis with myeloid metaplasia. Haematologica *89*, 1454–1458.

Arshad, M.I., Guihard, P., Danger, Y., Noel, G., Le Seyec, J., Boutet, M.A., Richards, C.D., L'Helgoualc'h, A., Genet, V., Lucas-Clerc, C., et al. (2015). Oncostatin M induces IL-33 expression in liver endothelial cells in mice and expands ST2+CD4+ lymphocytes. Am. J. Physiol. - Gastrointest. Liver Physiol. *309*, G542–G553.

Azzoni, E., Frontera, V., McGrath, K.E., Harman, J., Carrelha, J., Nerlov, C., Palis, J., Jacobsen, S.E.W., and Bruijn, M.F. (2018). Kit ligand has a critical role in mouse yolk sac and aorta–gonad–mesonephros hematopoiesis. EMBO Rep. *19*, 1–17.

Bertheloot, D., and Latz, E. (2017). HMGB1, IL-1α, IL-33 and S100 proteins: dual-function alarmins. Cell. Mol. Immunol. *14*, 43–64.

Bessa, J., Meyer, C.A., de Vera Mudry, M.C., Schlicht, S., Smith, S.H., Iglesias, A., and Cote-Sierra, J. (2014). Altered subcellular localization of IL-33 leads to non-resolving lethal inflammation. J. Autoimmun. *55*, 33–41.

Bourgeois, E., van, L.P., Samson, M., Diem, S., Barra, A., Roga, S., Gombert, J.M., Schneider, E., Dy, M., Gourdy, P., et al. (2009). The pro-Th2 cytokine IL-33 directly interacts with invariant NKT and NK cells to induce IFN-γ production. Eur. J. Immunol. *39*, 1046–1055.

Bowers, E., Slaughter, A., Frenette, P.S., Kuick, R., Pello, O.M., and Lucas, D. (2018). Granulocyte-derived TNFα promotes vascular and hematopoietic regeneration in the bone marrow. Nat. Med. *24*, 95–102.

Breitbach, M., Kimura, K., Luis, T.C., Fuegemann, C.J., Woll, P.S., Hesse, M., Facchini, R., Rieck, S., Jobin, K., Reinhardt, J., et al. (2018). In Vivo Labeling by CD73 Marks Multipotent Stromal Cells and Highlights Endothelial Heterogeneity in the Bone Marrow Niche. Cell Stem Cell *22*, 262-276.e7.

Brickshawana, A., Shapiro, V.S., Kita, H., and Pease, L.R. (2011). Lineage(-)Sca1+c-Kit(-)CD25+ cells are IL-33-responsive type 2 innate cells in the mouse bone marrow. J. Immunol. *187*, 5795–5804.

Broxmeyer, H.E., Juliano, L., Lu, L., Platzer, E., and Dupont, B. (1984). HLA-DR human histocompatibility leukocyte antigens-restricted lymphocyte-monocyte interactions in the release from monocytes of acidic isoferritins that suppress hematopoietic progenitor cells. J. Clin. Invest. *73*, 939–953.

Butler, J.M., Nolan, D.J., Vertes, E.L., Varnum-Finney, B., Kobayashi, H., Hooper, A.T., Seandel, M., Shido, K., White, I.A., Kobayashi, M., et al. (2010). Endothelial Cells Are Essential for the Self-Renewal and Repopulation of Notch-Dependent Hematopoietic Stem Cells. Cell Stem Cell *6*, 251–264.

Cao, Z., Lis, R., Ginsberg, M., Chavez, D., Shido, K., Rabbany, S.Y., Fong, G.H., Sakmar, T.P., Rafii, S., and Ding, B. Sen (2016). Targeting of the pulmonary capillary vascular niche promotes lung alveolar repair and ameliorates fibrosis. Nat. Med. *22*, 154–162.

Cayrol, C., and Girard, J.P. (2014). IL-33: An alarmin cytokine with crucial roles in innate immunity, inflammation and allergy. Curr. Opin. Immunol. *31*, 31–37.

Cayrol, C., and Girard, J.P. (2018). Interleukin-33 (IL-33): A nuclear cytokine from the IL-1 family. Immunol. Rev. *281*, 154–168.

Chan, C.K.F., Chen, C.-C., Luppen, C.A., Kim, J.-B., DeBoer, A.T., Wei, K., Helms, J.A., Kuo, C.J., Kraft, D.L., and Weissman, I.L. (2009). Endochondral ossification is required for haematopoietic stem-cell niche formation. Nature *457*, 490–494.

Chan, C.K.F., Gulati, G.S., Sinha, R., Tompkins, J.V., Lopez, M., Carter, A.C., Ransom, R.C., Reinisch, A., Wearda, T., Murphy, M., et al. (2018). Identification of the Human Skeletal Stem Cell. Cell *175*, 43-56.e21.

Chen, J.J., Gao, X.T., Yang, L., Fu, W., Liang, L., Li, J.C., Hu, B., Sun, Z.J., Huang, S.Y., Zhang, Y.Z., et al. (2016a). Disruption of Notch signaling aggravates irradiation-induced bone marrow injury, which is ameliorated by a soluble Dll1 ligand through Csf2rb2 upregulation. Sci. Rep. *6*, 1–11.

Chen, L., Jiang, W., Huang, J., He, B.C., Zuo, G.W., Zhang, W., Luo, Q., Shi, Q., Zhang, B.Q., Wagner, E.R., et al. (2010). Insulin-like growth factor 2 (IGF-2) potentiates BMP-9-induced osteogenic differentiation and bone formation. J. Bone Miner. Res. *25*, 2447–2459.

Chen, Q., Zhang, H., Liu, Y., Adams, S., Eilken, H., Stehling, M., Corada, M., Dejana, E., Zhou, B., and Adams, R.H. (2016b). Endothelial cells are progenitors of cardiac pericytes and vascular smooth muscle cells. Nat. Commun. *7*, 12422.

Chen, W.Y., Hong, J., Gannon, J., Kakkar, R., and Lee, R.T. (2015). Myocardial pressure overload induces systemic inflammation through endothelial cell IL-33. Proc. Natl. Acad. Sci. U. S. A. *112*, 7249–7254.

Choi, Y., Choi, H., Min, J., Pyun, B., Maeng, Y., Park, H., Kim, J., Kim, Y., and Kwon, Y. (2009). ST2 / TRAF6-mediated endothelial nitric oxide production Interleukin-33 induces angiogenesis and vascular permeability through ST2 / TRAF6-mediated endothelial nitric oxide production. Blood *114*, 3117–3126.

Clines, G. a, Mohammad, K.S., Bao, Y., Stephens, O.W., Suva, L.J., Shaughnessy, J.D., Fox, J.W., Chirgwin, J.M., and Guise, T. a (2007). Dickkopf Homolog 1 Mediates Endothelin-1-Stimulated New Bone Formation. Mol. Endocrinol. *21*, 486–498.

Ding, L., and Morrison, S.J. (2013). Haematopoietic stem cells and early lymphoid progenitors occupy distinct bone marrow niches. Nature *495*, 231–235.

Ding, B. Sen, Nolan, D.J., Butler, J.M., James, D., Babazadeh, A.O., Rosenwaks, Z., Mittal, V., Kobayashi, H., Shido, K., Lyden, D., et al. (2010). Inductive angiocrine signals from sinusoidal endothelium are required for liver regeneration. Nature *468*, 310–315.

Ding, B. Sen, Nolan, D.J., Guo, P., Babazadeh, A.O., Cao, Z., Rosenwaks, Z., Crystal, R.G., Simons, M., Sato, T.N., Worgall, S., et al. (2011). Endothelial-derived angiocrine signals induce and sustain regenerative lung alveolarization. Cell *147*, 539–553.

Ding, L., Saunders, T.L., Enikolopov, G., and Morrison, S.J. (2012). Endothelial and perivascular cells maintain haematopoietic stem cells. Nature *481*, 457–462.

Doan, P.L., Himburg, H.A., Helms, K., Russell, J.L., Fixsen, E., Quarmyne, M., Harris, J.R., Deoliviera, D., Sullivan, J.M., Chao, N.J., et al. (2013). Epidermal growth factor regulates hematopoietic regeneration after radiation injury. Nat. Med. *19*, 295–304.

Duan, J.L., Ruan, B., Yan, X.C., Liang, L., Song, P., Yang, Z.Y., Liu, Y., Dou, K.F., Han, H., and Wang, L. (2018). Endothelial Notch activation reshapes the angiocrine of sinusoidal endothelia to aggravate liver fibrosis and blunt regeneration in mice. Hepatology *68*, 677–690.

Dyer, L., and Patterson, C. (2010). Development of the Endothelium: An Emphasis on Heterogeneity. Semin. Thromb. Hemost. *36*, 227–235.

Edwards, C.M., and Mundy, G.R. (2008). Eph receptors and ephrin signaling pathways: A role in bone homeostasis. Int. J. Med. Sci. *5*, 263–272.

Erba, B.G., Gruppi, C., Corada, M., Pisati, F., Rosti, V., Bartalucci, N., Villeval, J.L., Vannucchi, A.M., Barosi, G., Balduini, A., et al. (2017). Endothelial-to-Mesenchymal Transition in Bone Marrow and Spleen of Primary Myelofibrosis. Am. J. Pathol. *187*, 1879–1892.

Fanny, M., Nascimento, M., Baron, L., Schricke, C., Maillet, I., Akbal, M., Riteau, N., Bert, M. Le, Quesniaux, V., Ryffel, B., et al. (2018). The IL-33 receptor ST2 regulates pulmonary inflammation and fibrosis to bleomycin. Front. Immunol. *9*, 1–12.

von Fliedner, V., Miescher, S., Gérain, J., Gallati, H., Barras, C., Heumann, D., and Cerottini, J.C. (1992). Production of tumor necrosis factor-α by naive or memory T lymphocytes activated via CD28. Cell. Immunol. *139*, 198–207.

Funakoshi-Tago, M., Tago, K., Sato, Y., Tominaga, S.I., and Kasahara, T. (2011). JAK2 is an important signal transducer in IL-33-induced NF-κB activation. Cell. Signal. *23*, 363–370.

Gama-Norton, L., Ferrando, E., Ruiz-Herguido, C., Liu, Z., Guiu, J., Islam, A.B.M.M.K., Lee, S.U., Yan, M., Guidos, C.J., López-Bigas, N., et al. (2015). Notch signal strength controls cell fate in the haemogenic endothelium. Nat. Commun. *6*.

Ghazanfari, R., Li, H., Zacharaki, D., Lim, H.C., and Scheding, S. (2016). Human Non-Hematopoietic CD271pos/CD140alow/neg Bone Marrow Stroma Cells Fulfill Stringent Stem Cell Criteria in Serial Transplantations. Stem Cells Dev. *25*, 1652–1658.

Gomariz, A., Helbling, P.M., Isringhausen, S., Suessbier, U., Becker, A., Boss, A., Nagasawa, T., Paul, G., Goksel, O., Székely, G., et al. (2018). Quantitative spatial analysis of haematopoiesis-regulating stromal cells in the bone marrow microenvironment by 3D microscopy. Nat. Commun. *9*.

Gomei, Y., Nakamura, Y., Yoshihara, H., Hosokawa, K., Iwasaki, H., Suda, T., and Arai, F. (2010). Functional differences between two Tie2 ligands, angiopoietin-1 and -2, in regulation of adult bone marrow hematopoietic stem cells. Exp. Hematol. *38*, 82-89.e1.

Goswami, M., Prince, G., Biancotto, A., Moir, S., Kardava, L., Santich, B.H., Cheung, F., Kotliarov, Y., Chen, J., Shi, R., et al. (2017). Impaired B cell immunity in acute myeloid leukemia patients after chemotherapy. J. Transl. Med. *15*, 1–16.

Greenbaum, A., Hsu, Y.M.S., Day, R.B., Schuettpelz, L.G., Christopher, M.J., Borgerding, J.N., Nagasawa, T., and Link, D.C. (2013). CXCL12 in early mesenchymal progenitors is required for haematopoietic stem-cell maintenance. Nature *495*, 227–230.

Guo, P., Poulos, M.G., Palikuqi, B., Badwe, C.R., Lis, R., Kunar, B., Ding, B.-S., Rabbany, S.Y., Shido, K., Butler, J.M., et al. (2017). Endothelial jagged-2 sustains hematopoietic stem and progenitor reconstitution after myelosuppression. J. Clin. Invest. *127*, 4242–4256.

Gur-Cohen, S., Itkin, T., Chakrabarty, S., Graf, C., Kollet, O., Ludin, A., Golan, K., Kalinkovich, A., Ledergor, G., Wong, E., et al. (2015). PAR1 signaling regulates the retention and recruitment of EPCR-expressing bone marrow hematopoietic stem cells. Nat. Med. *21*, 1307–1317.

Han, S., Dziedzic, N., Gadue, P., Keller, G.M., and Gouon-Evans, V. (2011). An endothelial cell niche induces hepatic specification through dual repression of Wnt and notch signaling. Stem Cells *29*, 217–228.

Heemskerk, M.H.M., Blom, B., Nolan, G., Stegmann, A.P.A., Bakker, A.Q., Weijer, K., Res, P.C.M., and Spits, H. (1997). Inhibition of T Cell and Promotion of Natural Killer Cell Development by the Dominant Negative Helix Loop Helix Factor Id3. J. Exp. Med. *186*, 1597–1602.

Hellström, M., Phng, L.K., Hofmann, J.J., Wallgard, E., Coultas, L., Lindblom, P., Alva, J., Nilsson, A.K., Karlsson, L., Gaiano, N., et al. (2007). Dll4 signalling through Notch1 regulates formation of tip cells during angiogenesis. Nature *445*, 776–780.

Himburg, H.A., Termini, C.M., Schlussel, L., Kan, J., Li, M., Zhao, L., Fang, T., Sasine, J.P., Chang, V.Y., and Chute, J.P. (2018). Distinct Bone Marrow Sources of Pleiotrophin Control Hematopoietic Stem Cell Maintenance and Regeneration. Cell Stem Cell *23*, 370-381.e5.

Hirata, Y., Furuhashi, K., Ishii, H., Li, H.W., Pinho, S., Ding, L., Robson, S.C., Frenette, P.S., and Fujisaki, J. (2018a). CD150highBone Marrow Tregs Maintain Hematopoietic Stem Cell Quiescence and Immune Privilege via Adenosine. Cell Stem Cell *22*, 445-453.e5.

Hirata, Y., Kakiuchi, M., Robson, S.C., and Fujisaki, J. (2018b). CD150high CD4 T cells and CD150high Tregs regulate hematopoietic stem cell quiescence via CD73. Haematologica haematol.2018.198283.

Hooper, A.T., Butler, J.M., Nolan, D.J., Kranz, A., Iida, K., Kobayashi, M., Kopp, H.-G., Shido, K., Petit, I., Yanger, K., et al. (2009). Engraftment and Reconstitution of Hematopoiesis Is Dependent on VEGFR2-Mediated Regeneration of Sinusoidal Endothelial Cells. Cell Stem Cell *4*, 263–274.

Hu, J., Srivastava, K., Wieland, M., Runge, A., Mogler, C., Besemfelder, E., Terhardt, D., Vogel, M.J., Cao, L., Korn, C., et al. (2014). Endothelial Cell-Derived Angiopoietin-2 Controls Liver Regeneration as a Spatiotemporal Rheostat. Science. *343*, 416–419.

Ibrahim, A.A., Yahata, T., Onizuka, M., Dan, T., Van Ypersele De Strihou, C., Miyata, T., and Ando, K. (2014). Inhibition of plasminogen activator inhibitor type-1 activity enhances rapid and sustainable hematopoietic regeneration. Stem Cells *32*, 946–958.

Isern, J., García-García, A., Martín, A.M., Arranz, L., Martín-Pérez, D., Torroja, C., Sánchez-Cabo, F., and Méndez-Ferrer, S. (2014). The neural crest is a source of mesenchymal stem cells with specialized hematopoietic stem cell niche function. Elife *3*, 1–28.

Kakkar, R., Hei, H., Dobner, S., and Lee, R.T. (2012). Interleukin 33 as a mechanically responsive cytokine secreted by living cells. J. Biol. Chem. *287*, 6941–6948.

Kanasaki, K., Shi, S., Kanasaki, M., He, J., Nagai, T., Nakamura, Y., Ishigaki, Y., Kitada, M., Srivastava, S.P., and Koya, D. (2014). Linagliptin-mediated DPP-4 inhibition ameliorates kidney fibrosis in streptozotocin-induced diabetic mice by inhibiting endothelial-to-mesenchymal transition in a therapeutic regimen. Diabetes *63*, 2120–2131.

Khurana, S., Margamuljana, L., Joseph, C., Schouteden, S., Buckley, S.M., and Verfaillie, C.M. (2013). Glypican-3-mediated inhibition of CD26 by TFPI: a novel mechanism in hematopoietic stem cell homing and maintenance. Blood *121*, 2587–2595.

Kida, Y., Zullo, J.A., and Goligorsky, M.S. (2016). Endothelial sirtuin 1 inactivation enhances capillary rarefaction and fibrosis following kidney injury through Notch activation. Biochem. Biophys. Res. Commun. *478*, 1074–1079.

Kim, J., Kim, W., Le, H.T., Moon, U.J., Tran, V.G., Kim, H.J., Jung, S., Nguyen, Q.-T., Kim, B.-S., Jun, J.-B., et al. (2014). IL-33–Induced Hematopoietic Stem and Progenitor Cell Mobilization Depends upon CCR2. J. Immunol. *193*, 3792–3802.

Klein Wolterink, R.G.J., García-Ojeda, M.E., Vosshenrich, C.A.J., Hendriks, R.W., and Di Santo, J.P. (2010). The intrathymic crossroads of T and NK cell differentiation. Immunol. Rev. *238*, 126–137.

Kobayashi, H., Butler, J.M., O'Donnell, R., Kobayashi, M., Ding, B.-S., Bonner, B., Chiu, V.K., Nolan, D.J., Shido, K., Benjamin, L., et al. (2010). Angiocrine factors from Akt-activated endothelial cells balance self-renewal and differentiation of haematopoietic stem cells. Nat. Cell Biol. *12*, 1046–1056.

Komada, Y., Yamane, T., Kadota, D., Isono, K., Takakura, N., Hayashi, S.-I., and Yamazaki, H. (2012). Origins and Properties of Dental, Thymic, and Bone Marrow Mesenchymal Cells and Their Stem Cells. PLoS One *7*, e46436.

Komai-Koma, M., Gilchrist, D.S., McKenzie, A.N.J., Goodyear, C.S., Xu, D., and Liew, F.Y. (2011). IL-33 Activates B1 Cells and Exacerbates Contact Sensitivity. J. Immunol. *186*, 2584–2591.

Kopp, H.G., Avecilla, S.T., Hooper, A.T., Shmelkov, S. V., Ramos, C.A., Zhang, F., and Rafii, S. (2005). Tie2 activation contributes to hemangiogenic regeneration after myelosuppression. Blood *106*, 505–513.

Kovacic, J.C., Dimmeler, S., Harvey, R.P., Finkel, T., Aikawa, E., Krenning, G., and Baker, A.H. (2019). Endothelial to Mesenchymal Transition in Cardiovascular Disease: JACC State-of-the-Art Review. J. Am. Coll. Cardiol. *73*, 190–209.

Küchler, A.M., Pollheimer, J., Balogh, J., Sponheim, J., Manley, L., Sorensen, D.R., De Angelis, P.M., Scott, H., and Haraldsen, G. (2008). Nuclear Interleukin-33 Is Generally Expressed in Resting Endothelium but Rapidly Lost upon Angiogenic or Proinflammatory Activation. Am. J. Pathol. *173*, 1229–1242.

Kuijper, S., Turner, C.J., and Adams, R.H. (2007). Regulation of Angiogenesis by Eph–Ephrin Interactions. Trends Cardiovasc. Med. *17*, 145–151.

Kumar, A., D'Souza, S.S., Moskvin, O. V., Toh, H., Wang, B., Zhang, J., Swanson, S., Guo, L.W., Thomson, J.A., and Slukvin, I.I. (2017). Specification and Diversification of Pericytes and Smooth Muscle Cells from Mesenchymoangioblasts. Cell Rep. *19*, 1902–1916.

Kumar, R., Fossati, V., Israel, M., and Snoeck, H.-W. (2008). Lin-Sca1+Kit- Bone Marrow Cells Contain Early Lymphoid-Committed Precursors That Are Distinct from Common Lymphoid Progenitors. J. Immunol. *181*, 7507–7513.

Kusumbe, A.P., Ramasamy, S.K., and Adams, R.H. (2014). Coupling of angiogenesis and osteogenesis by a specific vessel subtype in bone. Nature *507*, 323–328.

Kusumbe, A.P., Ramasamy, S.K., Itkin, T., Mäe, M.A., Langen, U.H., Betsholtz, C., Lapidot, T., and Adams, R.H. (2016). Age-dependent modulation of vascular niches for haematopoietic stem cells. Nature *532*, 380–384.

Langen, U.H., Pitulescu, M.E., Kim, J.M., Enriquez-Gasca, R., Sivaraj, K.K., Kusumbe, A.P., Singh, A., Di Russo, J., Bixel, M.G., Zhou, B., et al. (2017). Cell-matrix signals specify bone endothelial cells during developmental osteogenesis. Nat. Cell Biol. *19*, 189–201.

Lazarus, A., Del-Moral, P.M., Ilovich, O., Mishani, E., Warburton, D., and Keshet, E. (2011). A perfusion-independent role of blood vessels in determining branching stereotypy of lung airways. Development *138*, 2359–2368.

Le, H., Kim, W., Kim, J., Cho, H.R., and Kwon, B. (2013). Interleukin-33: A Mediator of Inflammation Targeting Hematopoietic Stem and Progenitor Cells and Their Progenies. Front. Immunol. *4*, 1–9.

Lee, E.-J., Kim, J.W., Yoo, H., Kwak, W., Choi, W.H., Cho, S., Choi, Y.J., Lee, Y.-J., and Cho, J. (2015). Single high-dose irradiation aggravates eosinophil-mediated fibrosis through IL-33 secreted from impaired vessels in the skin compared to fractionated irradiation. Biochem. Biophys. Res. Commun. *464*, 20–26.

Lee, J.H., Bhang, D.H., Beede, A., Huang, T.L., Stripp, B.R., Bloch, K.D., Wagers, A.J., Tseng, Y.H., Ryeom, S., and Kim, C.F. (2014). Lung stem cell differentiation in mice directed by endothelial cells via a BMP4-NFATc1-thrombospondin-1 axis. Cell *156*, 440–455.

Lefrançais, E., Roga, S., Gautier, V., Gonzalez-de-Peredo, A., Monsarrat, B., Girard, J.P., and Cayrol, C. (2012). IL-33 is processed into mature bioactive forms by neutrophil elastase and cathepsin G. Proc. Natl. Acad. Sci. U. S. A. *109*, 1673–1678.

Levitt, L.J., Nagler, A., Lee, F., Abrams, J., Shatsky, M., and Thompson, D. (1991). Production of granulocyte/macrophage-colony-stimulating factor by human natural killer cells: Modulation by the p75 subunit of the interleukin 2 receptor and by the CD2 receptor. J. Clin. Invest. *88*, 67–75.

Li, D., Guabiraba, R., Besnard, A.G., Komai-Koma, M., Jabir, M.S., Zhang, L., Graham, G.J., Kurowska-Stolarska, M., Liew, F.Y., McSharry, C., et al. (2014a). IL-33 promotes ST2-dependent lung fibrosis by the induction of alternatively activated macrophages and innate lymphoid cells in mice. J. Allergy Clin. Immunol. *134*, 1422-1432.e11.

Li, H., Ghazanfari, R., Zacharaki, D., Ditzel, N., Isern, J., Ekblom, M., Méndez-Ferrer, S., Kassem, M., and Scheding, S. (2014b). Low/negative expression of PDGFR-α identifies the candidate primary mesenchymal stromal cells in adult human bone marrow. Stem Cell Reports *3*, 965–974.

Maes, C., Kobayashi, T., Selig, M.K., Torrekens, S., Roth, S.I., Mackem, S., Carmeliet, G., and Kronenberg, H.M. (2010). Osteoblast precursors, but not mature osteoblasts, move into developing and fractured bones along with invading blood vessels. Dev. Cell *19*, 329–344.

Mager, L.F., Riether, C., Schürch, C.M., Banz, Y., Wasmer, M.H., Stuber, R., Theocharides, A.P., Li, X., Xia, Y., Saito, H., et al. (2015). IL-33 signaling contributes to the pathogenesis of myeloproliferative neoplasms. J. Clin. Invest. *125*, 2579–2591.

Maleszewska, M., Moonen, J.R.A.J., Huijkman, N., van de Sluis, B., Krenning, G., and Harmsen, M.C. (2013). IL-1β and TGFβ2 synergistically induce endothelial to mesenchymal transition in an NFκB-dependent manner. Immunobiology *218*, 443–454.

Marvie, P., Lisbonne, M., L'Helgoualc'h, A., Rauch, M., Turlin, B., Preisser, L., Bourd-Boittin, K., Théret, N., Gascan, H., Piquet-Pellorce, C., et al. (2010). Interleukin-33 overexpression is associated with liver fibrosis in mice and humans. J. Cell. Mol. Med. *14*, 1726–1739.

Mchedlidze, T., Waldner, M., Zopf, S., Walker, J., Rankin, A.L., Schuchmann, M., Voehringer, D., McKenzie, A.N.J., Neurath, M.F., Pflanz, S., et al. (2013). Interleukin-33-dependent innate lymphoid cells mediate hepatic fibrosis. Immunity *39*, 357–371.

Medici, D., Shore, E.M., Lounev, V.Y., Kaplan, F.S., Kalluri, R., and Olsen, B.R. (2010). Conversion of vascular endothelial cells into multipotent stem-like cells. Nat. Med. *16*, 1400–1406.

Medinger, M., and Passweg, J. (2014). Angiogenesis in myeloproliferative neoplasms, new markers and future directions. Memo - Mag. Eur. Med. Oncol. *7*, 206–210.

Mittal, M., Siddiqui, M.R., Tran, K., Reddy, S.P., and Malik, A.B. (2014). Reactive oxygen species in inflammation and tissue injury. Antioxidants Redox Signal. *20*, 1126–1167.

Mizuhashi, K., Ono, W., Matsushita, Y., Sakagami, N., Takahashi, A., Saunders, T.L., Nagasawa, T., Kronenberg, H.M., and Ono, N. (2018). Resting zone of the growth plate houses a unique class of skeletal stem cells. Nature *563*, 254–258.

Montanari, E., Stojkovic, S., Kaun, C., Lemberger, C.E., de Martin, R., Rauscher, S., Gröger, M., Maurer, G., Neumayer, C., Huk, I., et al. (2016). Interleukin-33 stimulates GM-CSF and M-CSF production by human endothelial cells. Thromb. Haemost. *116*, 317–327.

Morikawa, S., Mabuchi, Y., Niibe, K., Suzuki, S., Nagoshi, N., Sunabori, T., Shimmura, S., Nagai, Y., Nakagawa, T., Okano, H., et al. (2009). Development of mesenchymal stem cells partially originate from the neural crest. Biochem. Biophys. Res. Commun. *379*, 1114–1119.

Nabekura, T., Girard, J.-P., and Lanier, L.L. (2015). IL-33 Receptor ST2 Amplifies the Expansion of NK Cells and Enhances Host Defense during Mouse Cytomegalovirus Infection. J. Immunol. *194*, 5948–5952.

Nakamura-Ishizu, A., Okuno, Y., Omatsu, Y., Okabe, K., Morimoto, J., Uede, T., Nagasawa, T., Suda, T., and Kubota, Y. (2012). Extracellular matrix protein tenascin-C is required in the bone marrow microenvironment primed for hematopoietic regeneration. Blood *119*, 5429–5437.

Nolan, D.J., Ginsberg, M., Israely, E., Palikuqi, B., Poulos, M.G., James, D., Ding, B. Sen, Schachterle, W., Liu, Y., Rosenwaks, Z., et al. (2013). Molecular Signatures of Tissue-Specific Microvascular Endothelial Cell Heterogeneity in Organ Maintenance and Regeneration. Dev. Cell *26*, 204–219.

Nombela-Arrieta, C., Pivarnik, G., Winkel, B., Canty, K.J., Harley, B., Mahoney, J.E., Park, S.-Y., Lu, J., Protopopov, A., and Silberstein, L.E. (2013). Quantitative imaging of haematopoietic stem and progenitor cell localization and hypoxic status in the bone marrow microenvironment. Nat. Cell Biol. *15*, 533–543.

Oguro, H., Ding, L., and Morrison, S.J. (2013). SLAM family markers resolve functionally distinct subpopulations of hematopoietic stem cells and multipotent progenitors. Cell Stem Cell *13*, 102–116.

Ono, N., Ono, W., Mizoguchi, T., Nagasawa, T., Frenette, P.S., and Kronenberg, H.M. (2014a). Vasculature-associated cells expressing nestin in developing bones encompass early cells in the osteoblast and endothelial lineage. Dev. Cell *29*, 330–339.

Ono, N., Ono, W., Nagasawa, T., and Kronenberg, H.M. (2014b). A subset of chondrogenic cells provides early mesenchymal progenitors in growing bones. Nat. Cell Biol. *16*, 1157–1167.

Oshima, A., Tanabe, H., Yan, T., Lowe, G.N., Glackin, C.A., and Kudo, A. (2002). A novel mechanism for the regulation of osteoblast differentiation: Transcription of periostin, a member of the fasciclin I family, is regulated by the bHLH transcription factor, Twist. J. Cell. Biochem. *86*, 792–804.

Panteli, K., Zagorianakou, N., Bai, M., Katsaraki, A., Agnantis, N.J., and Bourantas, K. (2004). Angiogenesis in chronic myeloproliferative diseases detected by CD34 expression. Eur. J. Haematol. *72*, 410–415.

Papanicolaou, G., and Mehta, J. (2011). Infections in Patients with Hematologic Malignancies. In Principles and Practice of Cancer Infectious Diseases, (Totowa, NJ: Humana Press), pp. 27–38.

Pardali, E., Sanchez-Duffhues, G., Gomez-Puerto, M.C., and ten Dijke, P. (2017). TGF-β-induced endothelial-mesenchymal transition in fibrotic diseases. Int. J. Mol. Sci. *18*.

Pichery, M., Mirey, E., Mercier, P., Lefrancais, E., Dujardin, A., Ortega, N., and Girard, J.-P. (2012). Endogenous IL-33 Is Highly Expressed in Mouse Epithelial Barrier Tissues, Lymphoid Organs, Brain, Embryos, and Inflamed Tissues: In Situ Analysis Using a Novel Il-33–LacZ Gene Trap Reporter Strain. J. Immunol. *188*, 3488–3495.

Pinho, S., Lacombe, J., Hanoun, M., Mizoguchi, T., Bruns, I., Kunisaki, Y., and Frenette, P.S. (2013). PDGFRα and CD51 mark human Nestin $^{+}$ sphere-forming mesenchymal stem cells capable of hematopoietic progenitor cell expansion. J. Exp. Med. *210*, 1351–1367.

Ponce, C.C., Chauffaille, M. de L.L.F., Ihara, S.S.M., and Silva, M.R.R. (2014). Increased angiogenesis in primary myelofibrosis: Latent transforming growth factor-β as a possible angiogenic factor. Rev. Bras. Hematol. Hemoter. *36*, 322–328.

Ponzoni, M., Savage, D.G., Ferreri, A.J.M., Pruneri, G., Viale, G., Servida, P., Bertolini, F., and Orazi, A. (2004). Chronic idiopathic myelofibrosis: Independent prognostic importance of bone marrow microvascular density evaluated by CD105 (endoglin) immunostaining. Mod. Pathol. *17*, 1513–1520.

Poulos, M.G., Guo, P., Kofler, N.M., Pinho, S., Gutkin, M.C., Tikhonova, A., Aifantis, I., Frenette, P.S., Kitajewski, J., Rafii, S., et al. (2013). Endothelial Jagged-1 Is Necessary for Homeostatic and Regenerative Hematopoiesis. Cell Rep. *4*, 1022–1034.

Rabbany, S.Y., Ramalingam, P., Llanos, P., Poulos, M.G., Butler, J.M., Gutkin, M.C., and Gilleran, K. (2017). Endothelial transplantation rejuvenates aged hematopoietic stem cell function. J. Clin. Invest. *127*, 4163–4178.

Di Raimondo, F., Azzaro, M.P., Palumbo, G.A., Bagnato, S., Stagno, F., Giustolisi, G.M., Cacciola, E., Sortino, G., Guglielmo, P., and Giustolisi, R. (2001a). Elevated vascular endothelial growth factor (VEGF) serum levels in idiopathic myelofibrosis. Leukemia *15*, 976–980.

Di Raimondo, F., Palumbo, G.A., Molica, S., and Giustolisi, R. (2001b). Angiogenesis in chronic myeloproliferative diseases. Acta Haematol. *106*, 177–183.

Rajagopalan, S., Fu, J., and Long, E.O. (2001). Cutting Edge: Induction of IFN- Production but Not Cytotoxicity by the Killer Cell Ig-Like Receptor KIR2DL4 (CD158d) in Resting NK Cells. J. Immunol. *167*, 1877–1881.

Ramasamy, S.K., Kusumbe, A.P., Wang, L., and Adams, R.H. (2014). Endothelial Notch activity promotes angiogenesis and osteogenesis in bone. Nature *507*, 376–380.

Reilly, A., Kersun, L.S., Luning Prak, E., Boyer, J., McDonald, K., Jawad, A.F., and Sullivan, K.E. (2013). Immunologic consequences of chemotherapy for acute myeloid leukemia. J. Pediatr. Hematol. Oncol. *35*, 46–53.

Ritter, M.R., Dorrell, M.I., Edmonds, J., Friedlander, S.F., and Friedlander, M. (2002). Insulin-like growth factor 2 and potential regulators of hemangioma growth and involution identified by large-scale expression analysis. Proc. Natl. Acad. Sci. U. S. A. *99*, 7455–7460.

Robey, P.G. (2018). Skeletal Stem Cells/Bone Marrow Stromal Cells. In Genetics of Bone Biology and Skeletal Disease, (Elsevier), pp. 241–260.

Romeo, S.G., Alawi, K.M., Rodrigues, J., Singh, A., Kusumbe, A.P., and Ramasamy, S.K. (2019). Endothelial proteolytic activity and interaction with non-resorbing osteoclasts mediate bone elongation. Nat. Cell Biol. *21*, 430–441.

Sacchetti, B., Funari, A., Michienzi, S., Di Cesare, S., Piersanti, S., Saggio, I., Tagliafico, E., Ferrari, S., Robey, P.G., Riminucci, M., et al. (2007). Self-renewing osteoprogenitors in bone marrow sinusoids can organize a hematopoietic microenvironment. Cell *131*, 324–336.

Salani, D., Taraboletti, G., Rosanò, L., Di Castro, V., Borsotti, P., Giavazzi, R., and Bagnato, A. (2000). Endothelin-1 Induces an Angiogenic Phenotype in Cultured Endothelial Cells and Stimulates Neovascularization In Vivo. Am. J. Pathol. *157*, 1703–1711.

Saleh, H., Eeles, D., Hodge, J.M., Nicholson, G.C., Gu, R., Pompolo, S., Gillespie, M.T., and Quinn, J.M.W. (2011). Interleukin-33, a target of parathyroid hormone and oncostatin m, increases osteoblastic matrix mineral deposition and inhibits osteoclast formation in vitro. Endocrinology *152*, 1911–1922.

Sallerfors, B., and Olofsson, T. (1989). Cell-mediated inhibition of granulopoiesis in vitro in patients with acute myeloid leukemia in remission. Eur. J. Haematol. *42*, 164–172.

Sapoznikov, A., Pewzner-Jung, Y., Kalchenko, V., Krauthgamer, R., Shachar, I., and Jung, S. (2008). Perivascular clusters of dendritic cells provide critical survival signals to B cells in bone marrow niches. Nat. Immunol. *9*, 388–395.

Schmidt, S., Tramsen, L., and Lehrnbecher, T. (2017). Natural killer cells in antifungal immunity. Front. Immunol. *8*, 1–10.

Schmitz, J., Owyang, A., Oldham, E., Song, Y., Murphy, E., McClanahan, T.K., Zurawski, G., Moshrefi, M., Qin, J., Li, X., et al. (2005). IL-33, an interleukin-1-like cytokine that signals via the IL-1 receptor-related protein ST2 and induces T helper type 2-associated cytokines. Immunity *23*, 479–490.

Schotte, R., Dontje, W., Nagasawa, M., Yasuda, Y., Bakker, A.Q., Spits, H., and Blom, B. (2010). Synergy between IL-15 and Id2 Promotes the Expansion of Human NK Progenitor Cells, Which Can Be Counteracted by the E Protein HEB Required To Drive T Cell Development. J. Immunol. *184*, 6670–6679.

Schulze, J., Bickert, T., Beil, F.T., Zaiss, M.M., Albers, J., Wintges, K., Streichert, T., Klaetschke, K., Keller, J., Hissnauer, T.N., et al. (2011). Interleukin-33 is expressed in differentiated osteoblasts and blocks osteoclast formation from bone marrow precursor cells. J. Bone Miner. Res. *26*, 704–717.

Schürch, C.M., Riether, C., and Ochsenbein, A.F. (2014). Cytotoxic CD8+ T cells stimulate hematopoietic progenitors by promoting cytokine release from bone marrow mesenchymal stromal cells. Cell Stem Cell *14*, 460–472.

Seandel, M., Butler, J.M., Kobayashi, H., Hooper, A.T., White, I.A., Zhang, F., Vertes, E.L., Kobayashi, M., Zhang, Y., Shmelkov, S. V., et al. (2008). Generation of a functional and durable vascular niche by the adenoviral E4ORF1 gene. Proc. Natl. Acad. Sci. U. S. A. *105*, 19288–19293.

Serini, G., Valdembri, D., Zanivan, S., Morterra, G., Burkhardt, C., Caccavari, F., Zammataro, L., Primo, L., Tamagnone, L., Logan, M., et al. (2003). Class 3 semaphorins control vascular morphogenesis by inhibiting integrin function. Nature *424*, 391–397.

Severe, N., Karabacak, N.M., Gustafsson, K., Baryawno, N., Courties, G., Kfoury, Y., Kokkaliaris, K.D., Rhee, C., Lee, D., Scadden, E.W., et al. (2019). Stress-Induced Changes in Bone Marrow Stromal Cell Populations Revealed through Single-Cell Protein Expression Mapping. Cell Stem Cell 1–14.

Shan, S., Li, Y., Wang, J., Lv, Z., Yi, D., Huang, Q., Corrigan, C.J., Wang, W., Quangeng, Z., and Ying, S. (2016). Nasal administration of interleukin-33 induces airways angiogenesis and expression of multiple angiogenic factors in a murine asthma surrogate. Immunology *148*, 83–91.

Shao, L., Sottoriva, K., Palasiewicz, K., Zhang, J., Hyun, J., Soni, S.S., Paik, N.Y., Gao, X., Cuervo, H., Malik, A.B., et al. (2019). A Tie2-Notch1 signaling axis regulates regeneration of the endothelial bone marrow niche. Haematologica haematol.2018.208660.

Shao, R., Bao, S., Bai, X., Blanchette, C., Anderson, R.M., Dang, T., Gishizky, M.L., Marks, J.R., and Wang, X. (2004). Acquired expression of periostin by human breast cancers promotes tumor angiogenesis through up-regulation of vascular endothelial growth factor receptor 2 expression. Mol. Cell. Biol. *24*, 3992–4003.

Shi, S., Srivastava, S.P., Kanasaki, M., He, J., Kitada, M., Nagai, T., Nitta, K., Takagi, S., Kanasaki, K., and Koya, D. (2015). Interactions of DPP-4 and integrin β1 influences endothelial-to-mesenchymal transition. Kidney Int. *88*, 479–489.

Shi, Y., Liu, C.H., Roberts, A.I., Das, J., Xu, G., Ren, G., Zhang, Y., Zhang, L., Zeng, R.Y., Tan, H.S.W., et al. (2006). Granulocyte-macrophage colony-stimulating factor (GM-CSF) and T-cell responses: What we do and don't know. Cell Res. *16*, 126–133.

Shirota, T., and Tavassoli, M. (1991). Cyclophosphamide-induced alterations of bone marrow endothelium: implications in homing of marrow cells after transplantation. Exp. Hematol. *19*, 369–373.

Ben Shoham, A., Rot, C., Stern, T., Krief, S., Akiva, A., Dadosh, T., Sabany, H., Lu, Y., Kadler, K.E., and Zelzer, E. (2016). Deposition of collagen type I onto skeletal endothelium reveals a new role for blood vessels in regulating bone morphology. Development *143*, 3933–3943.

Sivaraj, K.K., and Adams, R.H. (2016). Blood vessel formation and function in bone. Development *143*, 2706–2715.

Stahnke, K., Fulda, S., Friesen, C., Strauss, G., and Debatin, K.M. (2001). Activation of apoptosis pathways in peripheral blood lymphocytes by in vivo chemotherapy. Blood *98*, 3066–3073.

Stav-Noraas, T.E., Edelmann, R.J., Poulsen, L.L.C., Sundnes, O., Phung, D., Küchler, A.M., Müller, F., Kamen, A.A., Haraldsen, G., Kaarbø, M., et al. (2017). Endothelial IL-33 Expression Is Augmented by Adenoviral Activation of the DNA Damage Machinery. J. Immunol. *198*, 3318–3325.

Stojkovic, S., Kaun, C., Heinz, M., Krychtiuk, K.A., Rauscher, S., Lemberger, C.E., de Martin, R., Gröger, M., Petzelbauer, P., Huk, I., et al. (2014). Interleukin-33 induces urokinase in human endothelial cells-possible impact on angiogenesis. J. Thromb. Haemost. *12*, 948–957.

Sundlisæter, E., Edelmann, R.J., Hol, J., Sponheim, J., Kchler, A.M., Weiss, M., Udalova, I.A., Midwood, K.S., Kasprzycka, M., and Haraldsen, G. (2012). The alarmin IL-33 is a notch target in quiescent endothelial cells. Am. J. Pathol. *181*, 1099–1111.

Susek, K.H., Korpos, E., Huppert, J., Wu, C., Savelyeva, I., Rosenbauer, F., Müller-Tidow, C., Koschmieder, S., and Sorokin, L. (2018). Bone marrow laminins influence hematopoietic stem and progenitor cell cycling and homing to the bone marrow. Matrix Biol. *67*, 47–62.

Takashima, Y., Era, T., Nakao, K., Kondo, S., Kasuga, M., Smith, A.G., and Nishikawa, S.I. (2007). Neuroepithelial Cells Supply an Initial Transient Wave of MSC Differentiation. Cell *129*, 1377–1388.

Tamagnone, L., and Giordano, S. (2006). Semaphorin pathways orchestrate osteogenesis. Nat. Cell Biol. *8*, 545–547.

Theodoropoulou, S., Copland, D.A., Liu, J., Wu, J., Gardner, P.J., Ozaki, E., Doyle, S.L., Campbell, M., and Dick, A.D. (2017). Interleukin-33 regulates tissue remodelling and inhibits angiogenesis in the eye. J. Pathol. *241*, 45–56.

Tokoyoda, K., Zehentmeier, S., Hegazy, A.N., Albrecht, I., Grün, J.R., Löhning, M., and Radbruch, A. (2009). Professional Memory CD4+ T Lymphocytes Preferentially Reside and Rest in the Bone Marrow. Immunity *30*, 721–730.

Tormin, A., Li, O., Brune, J.C., Walsh, S., Schutz, B., Ehinger, M., Ditzel, N., Kassem, M., and Scheding, S. (2011). CD146 expression on primary nonhematopoietic bone marrow stem cells is correlated with in situ localization. Blood *117*, 5067–5077.

Uchida, M., Anderson, E.L., Squillace, D.L., Patil, N., Maniak, P.J., Iijima, K., Kita, H., and O'Grady, S.M. (2017). Oxidative stress serves as a key checkpoint for IL-33 release by airway epithelium. Allergy *72*, 1521–1531.

Verri, W.A., Souto, F.O., Vieira, S.M., Almeida, S.C.L., Fukada, S.Y., Xu, D., Alves-Filho, J.C., Cunha, T.M., Guerrero, A.T.G., Mattos-Guimaraes, R.B., et al. (2010). IL-33 induces neutrophil migration in rheumatoid arthritis and is a target of anti-TNF therapy. Ann. Rheum. Dis. *69*, 1697–1703.

Villegas-Mendez, A., Greig, R., Shaw, T.N., de Souza, J.B., Gwyer Findlay, E., Stumhofer, J.S., Hafalla, J.C.R., Blount, D.G., Hunter, C.A., Riley, E.M., et al. (2012). IFN-γ–Producing CD4 + T Cells Promote Experimental Cerebral Malaria by Modulating CD8 + T Cell Accumulation within the Brain. J. Immunol. *189*, 968–979.

Vitale, M., Della Chiesa, M., Carlomagno, S., Pende, D., Aricò, M., Moretta, L., and Moretta, A. (2005). NK-dependent DC maturation is mediated by TNFα and IFNγ released upon engagement of the NKp30 triggering receptor. Blood *106*, 566–571.

Vodyanik, M.A., Yu, J., Zhang, X., Tian, S., Stewart, R., Thomson, J.A., and Slukvin, I.I. (2010). A Mesoderm-Derived Precursor for Mesenchymal Stem and Endothelial Cells. Cell Stem Cell *7*, 718–729.

Wang, B., Zhao, L., Fish, M., Logan, C.Y., and Nusse, R. (2015). Self-renewing diploid Axin2 + cells fuel homeostatic renewal of the liver. Nature *524*, 180–185.

Widyantoro, B., Emoto, N., Nakayama, K., Anggrahini, D.W., Adiarto, S., Iwasa, N., Yagi, K., Miyagawa, K., Rikitake, Y., Suzuki, T., et al. (2010). Endothelial cell-derived endothelin-1 promotes cardiac fibrosis in diabetic hearts through stimulation of endothelial-to-mesenchymal transition. Circulation *121*, 2407–2418.

Winkler, I.G., Barbier, V., Nowlan, B., Jacobsen, R.N., Forristal, C.E., Patton, J.T., Magnani, J.L., and Lévesque, J.-P. (2012). Vascular niche E-selectin regulates hematopoietic stem cell dormancy, self renewal and chemoresistance. Nat. Med. *18*, 1651–1657.

Wojcik, T., Buczek, E., Majzner, K., Kolodziejczyk, A., Miszczyk, J., Kaczara, P., Kwiatek, W., Baranska, M., Szymonski, M., and Chlopicki, S. (2015). Comparative endothelial profiling of doxorubicin and daunorubicin in cultured endothelial cells. Toxicol. Vitr. *29*, 512–521.

Worthley, D.L., Churchill, M., Compton, J.T., Tailor, Y., Rao, M., Si, Y., Levin, D., Schwartz, M.G., Uygur, A., Hayakawa, Y., et al. (2015). Gremlin 1 identifies a skeletal stem cell with bone, cartilage, and reticular stromal potential. Cell *160*, 269–284.

Xu, C., Gao, X., Wei, Q., Nakahara, F., Zimmerman, S.E., Mar, J., and Frenette, P.S. (2018). Stem cell factor is selectively secreted by arterial endothelial cells in bone marrow. Nat. Commun. *9*, 1–13.

Yvernogeau, L., Gautier, R., Petit, L., Khoury, H., Relaix, F., Ribes, V., Sang, H., Charbord, P., Souyri, M., Robin, C., et al. (2019). In vivo generation of haematopoietic stem/progenitor cells from bone marrow-derived haemogenic endothelium. Nat. Cell Biol. *21*, 1334–1345.

Zhang, Y., Wallace, D.L., De Lara, C.M., Ghattas, H., Asquith, B., Worth, A., Griffin, G.E., Taylor, G.P., Tough, D.F., Beverley, P.C.L., et al. (2007). In vivo kinetics of human natural killer cells: The effects of ageing and acute and chronic viral infection. Immunology *121*, 258–265.

Zhou, B.O., Yue, R., Murphy, M.M., Peyer, J.G., and Morrison, S.J. (2014). Leptin-receptor-expressing mesenchymal stromal cells represent the main source of bone formed by adult bone marrow. Cell Stem Cell *15*, 154–168.

Zhou, B.O., Ding, L., and Morrison, S.J. (2015). Hematopoietic stem and progenitor cells regulate the regeneration of their niche by secreting Angiopoietin-1. Elife *2015*, 1–25.

A

ADDENDUM

LIST OF ABBREVIATIONS

5FU	5-fluorouracil
α-SMA	Alpha smooth muscle actin
ADM	Adrenomedullin
AGM	Aorta-gonad-mesonephros
AML	Acute myeloid leukemia
ANC	Absolute neutrophil count
ANOVA	One-way analysis of variance
APLN	Apelin
BF	Bone fraction
BM	Bone marrow
BMP4	Bone morphogenetic protein 4
BMDSC	BM-derived stromal cells
BMSC	Bone marrow stromal cell
BrdU	5-bromodeoxyuridine
CAR	CXCL12-abundant reticular
CD	Cluster of differentiation
CFU-C	Colony-forming unit cell
CFU-F	Colony-forming unit fibroblast
CFU-GM	Colony-forming unit granulocyte-monocyte
CLP	Common lymphoid progenitor
CM	Central memory
CMP	Common myeloid progenitor
CXCL4	C-X-C motif ligand 4
CXCL12	C-X-C motif chemokine ligand 12
D17	Day 17
DKK1	Dickkopf-1
E	Embryonic day
EC	Endothelial cell
ECFC	Endothelial colony forming cell
EDN1	Endothelin 1
EFNA1	Ephrin A1
EGF	Epidermal growth factor
EHT	Endothelial-to-hematopoietic transition
EM	Effector memory
EMT	Epithelial-to-mesenchymal transition
EndMT	Endothelial-to-mesenchymal transition
ES	Enrichment score

ESELE	Selectin E
FACS	Fluorescence activated cell sorting
FC	Fold change
FDR	False discovery rate
FGF1	Fibroblast growth factor 1
FOP	Fibrodysplasia ossificans progressiva
FPKM	Fragments per kilobase of exon per million fragments mapped
G-CSF	Granulocyte colony-stimulating factor
GAG	Glycosaminoglycan
GM-CSF	Granulocyte-macrophage colony-stimulating factor
GMP	Granulocytic/macrophage progenitor
GO	Gene ontology
GSEA	Gene set enrichment analysis
HPC	Hematopoietic progenitor cell
hREC	Human regeneration-associated EC
HUVEC	Human umbilical vein endothelial cell
HSC	Hematopoietic stem cell
HSPC	Hematopoietic stem and progenitor cell
IL-1β	Interleukin 1 β
IL-33	Interleukin 33
IR	Ionizing radiation
Jag1	Jagged-1
Jag2	Jagged-2
LEPR	Leptin receptor
LNGFR	Low-affinity nerve growth factor receptor
LT-HSC	Long-term HSC
MACS	Magnetic-activated cell sorting
MEP	Megakaryocytic/erythroid progenitor
MFI	Mean fluorescence intensity
MLP	Multilymphoid progenitor
MMRN2	Multimerin 2
MNC	Mononuclear cell
MPP	Multipotent progenitor
MSC	Mesenchymal stromal cell
NES	Normalized enrichment score
NK	Natural killer cell
N	Naive
OBC	Osteoblastic cell
OLC	Osteo/chondrolineage (progenitor) cell
Ocn	Osteocalcin
PCA	Principal component analysis
PLAT	Tissue-type plasminogen activator
PTN	Pleiotrophin
RBC	Red blood cell
rmIL-33	Recombinant murine IL-33
rhIL-33	Recombinant human IL-33
ROS	Reactive oxygen species
Sca-1	Stem cell antigen 1
SCF	Stem cell factor
S.E.M	Standard error of the mean
SEMA3A	Semaphorin-3A
SLAM	Signaling lymphocyte activation molecule
SNAI1	Snail family transcriptional repressor 1
SNAI2	Snail family transcriptional repressor 2
SNS	Sympathetic nervous system
ST-HSC	Short-term HSC
TEMRA	CD45RA re-expressing cells
TNC	Tenascin C
TFPI	Tissue Factor Pathway Inhibitor
TGF-β	Transforming Growth Factor Beta
TMBD	Thrombomodulin
TNFα	Tumor necrosis factor-alpha
TPO	Thrombopoietin
TWIST1	Twist Family BHLH Transcription Factor 1
UCB	Umbilical cord blood
WBC	White blood cell
VC	Vehicle Control
VEGFR2	Vascular endothelial growth factor receptor 2

ENGLISH SUMMARY

Red blood cells, white blood cells, and platelets are important for our (human) survival. Red blood cells take care of the transport of oxygen and waste products, while white blood cells make up our immune system. Platelets are needed for proper blood clotting. The continuous production of new blood cells (hematopoiesis) in adults occurs in the bone marrow (BM). Hematopoiesis is maintained by a relatively rare population of blood (hematopoietic) stem cells (HSCs) that have the potential to develop into every type of blood cell. Hematopoiesis is strongly influenced by the microenvironment for HSCs in the BM. The BM microenvironment, also knowns as the HSC niche, can be considered a supportive network of heterogeneous cells that facilitate the proliferation and differentiation of HSCs and their progeny, for example by producing signaling molecules that affect neighbouring cells (paracrine growth factors).
Chemotherapy is one of the most common types of treatments for cancer patients. However, a possible adverse effect of chemotherapy is BM damage, including the disruption of hematopoiesis. The focus of the work presented in this thesis is how the BM microenvironment, in particular endothelial cells (ECs), contributes to BM recovery (and in extension also hematopoiesis) after chemotherapy-induced injury in humans.

Recent work in mice attempting to identify the cellular and molecular factors pathways underlying hematologic recovery after injury revealed that BM ECs can facilitate BM regeneration in a perfusion-independent manner (not simply dependent on blood flow) by expressing distinct growth factors. While multiple studies have previously shown the importance of BM ECs for hematopoiesis, newer studies have now identified and characterized a specialized subset of these ECs in mice (type H endothelium) that actively link blood vessel development (angiogenesis) to bone formation (osteogenesis).
These latest studies, and other studies (discussed in more detail in the introduction of this thesis), have greatly increased our understanding of the instructive role of BM ECs in guiding tissue maintenance and regeneration. However, the relevance of the findings from these studies for humans remains largely unknown due to lack of studies focusing on the role of BM ECs in BM regeneration in humans (for example by identifying the relevant paracrine growth factors derived from ECs, which are also known as “angiocrine” factors). The goal of this thesis is to shed more light on this important issue, and answer the following outstanding questions:

(1) Do specialized subtypes of BM ECs, similar to those found in mice, also exist in humans?
(2) Are the molecular pathways driving endothelial-mediated BM (re)generation in mice, also activated in humans?
(3) Do human BM ECs have the capacity to convert to other cell-types during BM formation or upon regeneration after injury?

To answer the first two questions, in **Chapter 2**, we characterized ECs (defined as $CD31^+CD9^+$ cells) that were enriched in the BM of humans in conditions of generation (fetal development) and upon regeneration (after injury). We found that these BM ECs, marked by protein expression of endoglin (CD105), were increased in patients with acute myeloid leukemia (AML; a type of blood cancer) fully recovering from myeloablative chemotherapy in comparison with healthy controls. Similarly, we also observed an increased proportion of CD105-expressing BM ECs in mice treated with chemotherapy.

Similar to BM regeneration after injury, BM formation during fetal development involves orchestrated interplay between different types of (heterotypic) cells that coordinate timely activation of angiogenesis, osteogenesis, and hematopoiesis. The enrichment of $CD105^+$ BM ECs during recovery after chemotherapy-induced damage in both humans and mice suggested that this EC subtype could be involved in mammalian regeneration and hematopoietic niche formation. This notion was further supported by the predominance of $CD105^+$ cells within the endothelial-compartment of human fetal BM at gestational week 15-20, the phase in which hematopoiesis shifts from the fetal liver to the BM. These findings and in particular the enrichment of this cell type during regenerative states after injury, prompted us to name this EC type "human regeneration-associated EC" (hREC).

The phenotypic characteristics of hRECs reminded us of the type H endothelium previously characterized in mice, and suggested that hRECs might be the human equivalent of mouse type H endothelium. By characterizing the gene expression of fetal hRECs in depth, we further observed a remarkable molecular similarity between hRECs and type H endothelium, such as over-expression of genes encoding for HSPC-regulatory factors, as well as genes encoding for regulators of angiogenesis and osteogenesis. Gene set enrichment analysis (GSEA) of fetal hRECs revealed activation of the NOTCH signaling pathway, which was previously shown to drive the coupling of angiogenesis and osteogenesis by type H endothelium. These data indicate that hRECs exhibit a gene expression profile consistent with the coupling of angiogenesis, osteogenesis, and hematopoiesis.

This led us to hypothesize that we could identify (novel) angiocrine factors, capable of facilitating the abovementioned processes in development and regeneration, by further analyses of the gene expression profile of hRECs. By specifically focusing on genes encoding for secreted factors, over-expressed in both fetal hRECs and ECs of regenerative BM, we identified interleukin-33 (IL-33) as a candidate angiocrine factor. Subsequent *in vitro* and *in vivo* experiments demonstrated that IL-33 was capable of promoting expansion of distinct subsets of hematopoietic progenitor cells, human umbilical vein ECs, as well as enhancing osteogenic differentiation of mesenchymal precursor cells. Mice treated with recombinant murine IL-33 (rmIL-33) exhibited an increased levels of myeloid and lymphoid progenitor cells along with a relative increase of various stromal cells, including $CD31^+CD105^+$ (ECs) and $CD31^-Sca^-CD51^+$ niche cells (mesenchymal precursor and osteolineage cells). Collectively, the data revealed the existence of a human EC subtype associated with regeneration and niche formation, reminiscent of the type H endothelium of mice. In addition, the identification of IL-33 provides proof of principle for the notion that interrogation of the gene expression profile of hRECs enables the discovery of novel angiocrine and anabolic niche factors.

Among the over-expressed genes in fetal hRECs were genes typically expressed in non-endothelial stromal (mesenchymal) cells. This observation made us hypothesize in **Chapter 3** that hRECs contain a subset of cells that is undergoing the process of endothelial-to-mesenchymal transition (EndMT) during BM (re)generation.

First we confirmed that a subset of the hRECs expressed the protein LNGFR (CD271), encoded by one of the over-expressed mesenchymal genes and a well-known marker of human BM mesenchymal cells. These $CD271^+$ hRECs exhibited a gene expression profile consistent with cells undergoing EndMT and acquiring stem cell-like properties. Functionally, these $(CD144^+)CD271^+$ hRECs were able to generate mesenchymal cells, specifically colony-forming-unit fibroblasts (CFU-Fs), with the capacity to differentiate to cells of different skeletal lineages *ex vivo*. The skeletal differentiation capacity and "niche-forming capacity" of these mesenchymal cells were confirmed using *in vivo* transplantation-assays. These revealed that $CD271^+$hREC-derived mesenchymal cells harbored the capacity to generate the entire hematopoietic niche in immunodeficient recipient mice. These findings strongly suggested that a small subset of primary (fetal) ECs is capable of converting to skeletal stem/progenitor-like cells that contribute to hematopoietic niche formation during the ontogeny of mammals.

To confirm this notion and to evaluate the alleged contribution of EndMT to BM niche formation during fetal ontogeny, we tracked the cells derived from endothelium in genetic endothelial-lineage tracing studies using *VEcad-cre;LoxP-tdTomato* mice. In these mice expression of tdTomato (a fluorescent reporter) is driven by gene regulatory elements of *VEcad* (a gene which encodes for VE-cadherin/CD144 and is only expressed in ECs), and thereby labels ECs and their descendants. In these mice, at 3 weeks after birth, ±50% of the $CD144^-CD31^-Sca1^+CD51^+$(Pdgfrα+) mesenchymal niche cells were derived from ECs (as indicated by tdTomato expression). These mesenchymal cells were previously shown to be a highly purified fraction of BM stromal cells containing skeletal stem cells. In addition, ±25% of the $CD144^-CD31^-SCA1^-CD51^+$ niche cells (osteolineage cells) were also of endothelial origin. These results indicate that ECs are a significant source of mesenchymal cells in the hematopoietic nice. Interestingly, the endothelial-derived mesenchymal cells exhibited a distinct gene expression profile, characterized by expression of genes previously associated with specific mesenchymal cells that generate the HSC niche (*Lepr* and *Nestin*), as well as important HSC-regulatory genes (like *Cxcl12*, *Kitl*, *Angpt1* and others). Collectively, these findings provide experimental support for the novel concept that ECs give rise to multipotent mesenchymal cells with hematopoietic niche-forming capacity via the process of EndMT.

Next we sought to identify the signaling pathways driving EndMT in hRECs. Notably, multiple

known regulators of EndMT, like BMP4 and DPP-4, were also shown in **Chapter 2** to be over-expressed in hRECs. Building on these observations and since inflammation is also a known driver of EndMT, we again turned our focus to IL-33, the pro-inflammatory cytokine with anabolic effects on the hematopoietic system. *In vitro* experiments with two independent models of endothelium demonstrated that recombinant human IL-33 (rhIL-33) induced gene expression alterations consistent with EndMT-like characteristics, including down-regulation of endothelial marker expression concomitant with up-regulation of expression of mesenchymal markers. This effect was dose-dependent and was also confirmed on the protein level. Induction of EndMT programs by IL-33 led to a functional transition of ECs to a cellular state permissive of differentiation into skeletal cells (cartilage and bone). This was shown by the production of calcific matrix (osteogenic differentiation) and glycosaminoglycan (CAG) (chondrogenic differentiation). Mechanistically, signaling through the ST2-receptor (the known receptor for IL-33) and downstream up-regulation of *SNAI2* was identified as the signaling pathway mediating IL-33-induced EndMT in experiments utilizing neutralizing antibody directed against ST2.

Taken together, these findings revealed that endothelial-derived mesenchymal (stem-like) cells can contribute to hematopoietic niche formation in mammals during fetal development through the process of EndMT. In this context IL-33 is identified as a novel and strong mediator of EndMT. The observation that ECs undergoing EndMT exist upon recovery after chemotherapy-induced injury, raises the exciting prospect that this process could be (clincally) enhanced during regeneration after injury.

In Chapter 4 we switched gears and sought to better characterize the *hematopoietic* cells possibly involved in BM regeneration by determining the hematopoietic composition of the BM in an early phase of regeneration after chemotherapeutic injury (day 17 after start of induction chemotherapy). At this time-point hematopoietic cells predominately consisted of lymphoid cells (low side scatter, $CD45^{+}CD14^{-}$ cells), in particular T-cells (specifically the CD4CM T-cell subset) were enriched in the regenerative BM of AML-patients. On the other hand, B-cells were relatively decreased, and exhibited a more than 5-fold decrease in comparison with their normal counterparts in healthy BM.

Subsequently, we related the frequencies of the different lymphoid subsets to the time needed to achieve an absolute neutrophil (a type of white blood cell) count of ≥500/mm^3 blood (a parameter commonly used to assess hematologic recovery). Interestingly, we observed that higher frequencies of T-cells were associated with slower hematologic recovery. In particular, the CD4CM T-cell subset seemed to drive this association, since this was the only T-cell subset that was significantly associated with the duration of neutrophil recovery. Conversely, we found that a higher frequencies of NK-cells were associated with faster hematologic recovery. Combining the frequencies of both CD4CM T-cells and NK-cells into a NK/CD4CM-index (the frequency of NK-cells divided by the frequency of CD4CM T-cells) provided an even stronger association of immune composition with the time to recovery.

Taken together, these results provide insights on the recovery (kinetics) of immune cells following chemotherapy-induced injury. These findings may be of clinical use in predicting the time to hematopoietic recovery and pave the way to further studies addressing the biological contribution of immune cells to BM regeneration.

DUTCH SUMMARY (NEDERLANDSE SAMENVATTING)

Rode bloedcellen, witte bloedcellen en bloedplaatjes zijn essentieel om te overleven. Rijpe bloedcellen zorgen onder andere voor het transport van zuurstof en afvalstoffen, en spelen een belangrijke rol in het immuunsysteem. De continue aanmaak van nieuwe bloedcellen (hematopoëse) in volwassen mensen vindt plaats in het beenmerg (BM). Hematopoëse wordt gehandhaafd door een zeer kleine populatie van hematopoëtische stamcellen (HSCs) die zich tot elk type bloedcel kunnen ontwikkelen. Hematopoëse wordt sterk beïnvloed door de micro-omgeving van HSCs in het BM. De BM micro-omgeving, ook wel bekend als de HSC niche, kan men beschouwen als een ondersteunend netwerk van uiteenlopende celsoorten die de differentiatie en proliferatie van HSCs en hun nageslacht (HSPCs) kunnen aansturen, bijvoorbeeld door het afscheiden van paracriene groeifactoren (signaalstoffen die inwerken op naburige cellen).

Chemotherapie is een van de meest gebruikte behandelingen voor patiënten met kanker. Een mogelijke bijwerking van chemotherapie is schade aan het BM, waardoor hematopoëse verstoord kan raken. Het in dit proefschrift gepresenteerde werk richt zich erop hoe de BM micro-omgeving, in het bijzonder BM-endotheelcellen (ECs), kan bijdragen aan het herstel van BM (en in het verlengde daarvan hematopoëse) na door chemotherapie-geïnduceerde schade bij mensen.

Recent werk in muizen, met als doel de cellulaire en moleculaire factoren te identificeren die ten grondslag liggen aan herstel van hematopoëse na schade, heeft aangetoond dat BM-ECs hematologisch herstel op een perfusie-onafhankelijke manier kunnen mediëren door bepaalde groeifactoren tot expressie te brengen. Hoewel meerdere studies eerder het belang van BM-ECs voor hematopoëse hebben laten zien, hebben nieuwere studies ondertussen een gespecialiseerde subgroep van BM-ECs in muizen (type H-endotheel) geïdentificeerd en gekarakteriseerd. Kenmerkend aan deze type ECs was het vermogen om angiogenese (ontwikkeling van bloedvaten) aan osteogenese (botvorming) te koppelen.

Deze en andere studies (in meer detail besproken in de introductie van dit proefschrift) hebben ons begrip van de rol van ECs in weefsel-homeostase en (re)generatie enorm vergroot. Echter, de relevantie van deze bevindingen voor de mens is onduidelijk vanwege het gebrek aan studies over de specifieke bijdragen van gespecialiseerde BM-ECs aan BM (re)generatie in mensen (zoals de betrokken paracriene groeifactoren afkomstig van ECs, ook bekend als “angiocriene” factoren). Het doel van dit proefschrift is om meer licht te werpen op deze belangrijke kwestie, op zoek naar antwoorden op de volgende openstaande vragen:

(1) Bestaan gespecialiseerde subtypes van BM-ECs, zoals die beschreven in muizen, ook in mensen?
(2) Zijn de moleculaire paden, die endotheel-gemedieerde BM (re)generatie bij muizen aansturen, ook bij mensen geactiveerd?
(3) Hebben menselijke BM-ECs het vermogen om tijdens BM-vorming of herstel na schade zichzelf om te zetten in andere celtypen?

Om de eerste twee vragen te beantwoorden, hebben we in **hoofdstuk 2** BM-ECs (gedefinieerd als $CD31^+CD9^+$ cellen), die verrijkt waren in BM van mensen tijdens generatie (ontwikkeling) en regeneratie (na schade), gekarakteriseerd. De frequentie van deze humane BM-ECs, die gekenmerkt waren door expressie van endoglin (CD105), was verhoogd bij acute myeloïde leukemie (AML; een type bloedkanker) patiënten die herstelden van myeloablatieve chemotherapie, in vergelijking met gezonde controles. Evenzo zagen we in muizen die chemotherapie kregen, een toegenomen frequentie van BM-ECs die CD105 tot expressie brachten.
Net als BM-regeneratie na schade, omvat de vorming van BM ook tijdens de foetale ontwikkeling een georkestreerd samenspel tussen verschillende soorten (heterotypische) cellen die tijdige activering van angiogenese, osteogenese en hematopoëse coördineren. De verrijking van $CD105^+$ BM-ECs tijdens herstel na schade door chemotherapie suggereerde dat dit celtype betrokken zou kunnen zijn bij zowel regeneratie als hematopoëtische nichevorming van zoogdieren. Deze gedachte werd verder ondersteund door de overheersing van $CD105^+$ ECs binnen het endotheel-compartiment van foetaal BM van 15-20 zwangerschapsweken oud, de fase waarin de hematopoëse bij mensen zich verschuift van de foetale lever naar het BM. $CD105^+$ ECs waren ook verrijkt in botfracties, zowel gedurende de foetale ontwikkeling) als in volwassenen. De trabeculaire lokalisatie van $CD105^+$ ECs werd met *in situ* immunofluorescentie bevestigd. Gezamenlijk hebben deze bevindingen, en in het bijzonder de verrijking van dit celtype tijdens regeneratieve condities na chemotherapie, ons ertoe aangezet dit type BM-EC “humane regeneratie-geassocieerde EC” (hREC) te benoemen.
De fenotypische kenmerken van hRECs deden ons denken aan het type H-endotheel dat eerder in muizen werd gekarakteriseerd, en suggereerde dat hRECs mogelijk het menselijke equivalent van type H-endotheel waren. Uitgebreide transcriptionele karakterisering van foetale hRECs onthulde een opvallende moleculaire gelijkenis met het type H-endotheel, inclusief over-expressie van transcripten die coderen voor typische HSPC-regulerende factoren, evenals anabole regulatoren van angiogenese en osteogenese. Gene set enrichment analyse (GSEA) van foetale hRECs toonde onder andere activering van de NOTCH-signalering, waarvan eerder werd aangetoond dat deze de koppeling van angiogenese en osteogenese door type H-endotheel medieert. Deze data geven aan dat hRECs een transcriptioneel profiel bezitten die overeen komt met een rol in de koppeling van angiogenese, osteogenese en hematopoëse.

Dit leidde naar onze hypothese dat we door verdere analyse van het transcriptoom van hRECs (nieuwe) angiocriene factoren, die misschien bovengenoemde processen in ontwikkeling en regeneratie faciliteren, zouden kunnen ontdekken. De strategie om ons te concentreren op genen die coderen voor factoren die uit een cel gesecerneerd kunnen worden, tot over-expressie gebracht in zowel foetale hRECs als ECs uit regeneratief BM, bracht ons naar de identificatie van interleukine-33 (IL-33). Daaropvolgende *in vitro* en *in vivo* experimenten leerden ons dat IL-33 in staat was de expansie van specifieke subgroepen van hematopoëtische voorlopercellen, ECs, evenals osteogene differentiatie van mesenchymale voorlopercellen te stimuleren. Behandeling van muizen met recombinant muizen IL-33 (rmIL-33) resulteerde in een verhoogd aantal myeloïde en lymfoïde voorlopercellen, wat gepaard ging met een relatieve toename van verschillende cellen in de niche, inclusief $CD31^+CD105^+$ (ECs) en $CD31^-Sca^-CD51^+$ niche-cellen (mesenchymale voorloper- en botcellen). Gezamenlijk tonen de data het bestaan aan van een menselijk EC-subtype, geassocieerd met regeneratie en menselijke nichevorming, vergelijkbaar met het type H-endotheel beschreven in muizen. Bovendien levert de identificatie van IL-33 bewijs voor het idee dat transcriptoom-analyse van hRECs het mogelijk maakt om nieuwe angiocriene en anabole niche-factoren te ontdekken.

Onder de verrijkte transcripten in foetale hRECs waren transcripten die normaal met niet-endotheliale stromale (mesenchymale) cellen worden geassocieerd. Deze bevinding leidde ons naar de hypothese in **hoofdstuk 3** dat hRECs een groep cellen bevatten die het proces van endotheel-naar-mesenchymale transitie (EndMT) ondergaan tijdens BM (re)generatie.
Eerst bevestigden we dat een subgroep binnen de hRECs het eiwit CD271 (LNGFR) tot expressie brengt, dat wordt gecodeerd door één van de verrijkte mesenchymale transcripten en een bekende marker van primaire menselijke BM-mesenchymale cellen. Deze $CD271^+$ hRECs vertoonden een transcriptioneel profiel consistent met cellen die EndMT ondergaan en stamcel-achtige eigenschappen verwerven. Functioneel konden deze ($CD144^+$) $CD271^+$ hRECs kolonie-vormende eenheid fibroblasten (CFU-Fs) genereren met de *ex vivo* capaciteit om te differentiëren naar cellen van verschillende soorten skeletale weefsels. De skeletogene differentiatiecapaciteit en ‘niche-vormende capaciteit’ van deze mesenchymale cellen werd ook bevestigd met behulp van *in vivo* transplantatie-assays. Deze toonden aan dat van $CD271^+$ hREC-afgeleide mesenchymale cellen het vermogen hadden om de gehele hematopoëtische niche in immunodeficiënte ontvangende muizen te reconstrueren. Deze bevindingen suggereerden sterk dat een klein subtype van primaire (foetale) ECs in staat is om te converteren naar skeletstam/voorlopercellen die bijdragen aan hematopoëtische nichevorming tijdens de ontogenese van zoogdieren.
Om dit idee te bevestigen en de vermeende bijdrage van EndMT aan de vorming van de BM-niche tijdens de foetale ontogenese te evalueren, hebben wij genetische endotheel-lijn natrekstudies met behulp van *VEcad-cre;LoxP-tdTomato* muizen uitgevoerd. TdTomato-expressie in deze muizen, aangedreven door de promotor van *VEcad* (dat codeert voor

VE-cadherin/CD144) en dus ECs en hun nakomelingen permanent bestempelen, onthulde dat ±50% van de $CD144^{-}CD31^{-}Sca1^{+}CD51^{+}(Pdgfr\alpha^{+})$ mesenchymale niche-cellen afkomstig was van ECs in 3-weken oude muizen. Deze $CD144^{-}CD31^{-}Sca1^{+}CD51^{+}(Pdgfr\alpha^{+})$ mesenchymale niche-cellen werden eerder aangetoond een zeer zuivere fractie van BM-stromacellen te zijn die skeletstamcellen bevatten. Bovendien bleek ±25% van de $CD144^{-}CD31^{-}SCA1^{-}CD51^{+}$ niche-cellen (bot-voorlopercellen) ook van endotheliale origine. Deze resultaten geven aan dat ECs een significante bijdrage leveren aan het mesenchymale compartiment van de hematopoëtische niche. Interessant is dat de van endotheel-afgeleide mesenchymale cellen een bijzonder transcriptioneel profiel hadden, gekenmerkt door expressie van genen die eerder waren geassocieerd met specifieke mesenchymale cellen die de HSC-niche vormen (*Lepr* en *Nes*), evenals genen die coderen voor belangrijke HSC-regulerende eiwitten (zoals *Cxcl12*, *Kitl*, *Angpt1* en anderen). Gezamenlijk zijn deze bevindingen een experimentele ondersteuning van het nieuwe concept dat ECs multipotente mesenchymale cellen met hematopoëtische niche-vormingscapaciteit genereren via een proces van EndMT.

Vervolgens probeerden we de onderliggende signaleringroutes te identificeren die EndMT in hRECs mediëren. Opvallend was dat van meerdere bekende regulatoren van EndMT, zoals BMP4 en DPP-4, ook in **hoofdstuk 2** werd aangetoond dat die tot over-expressie in hRECs kwamen. Gebaseerd op onder andere deze observaties, richtten we onze aandacht op IL-33, de pro-inflammatoire cytokine met anabole effecten in het hematopoëtische systeem. *In vitro* experimenten met twee onafhankelijke endotheel-cellijnen onthulden dat behandeling met recombinant humaan IL-33 (rhIL-33) transcriptionele veranderingen teweegbracht met EndMT-achtige kenmerken, namelijk down-regulatie van endotheliale marker expressie gelijktijdig met up-regulatie van mesenchymale marker expressie. Dit gebeurde op een dosis-afhankelijke manier, wat op eiwitniveau werd bevestigd. Inductie van EndMT-programma's door IL-33 resulteerde in functionele overgang van ECs naar een cellulaire staat, die differentiatie toeliet naar skeletachtige cellen (kraakbeen- en botvormende cellen). Dit werd aangetoond door de productie van kalkhoudende (osteogene differentiatie) matrix en glycosaminoglycaan (GAG) (chondrogene differentiatie). Signalering via de ST2-receptor met up-regulatie van *SNAI2* als gevolg werd geïdentificeerd als de signaleringroute die IL33-geïnduceerd EndMT aandreef, door experimenten met een neutraliserend antilichaam gericht tegen ST2.

Gezamenlijk onthullen deze bevindingen dat endotheel-afgeleide mesenchymale (stam) cellen aan de hematopoëtische nichevorming bij zoogdieren bijdragen tijdens de ontogenese van zoogdieren via EndMT. IL-33 blijkt in dit verband een nieuwe en sterke bemiddelaar van dit proces. De observatie dat ECs die EndMT ondergaan geïdentificeerd werden bij herstel na chemotherapie-geïnduceerde schade, opent de belangrijke mogelijkheid dat dit proces gestuurd kan worden om regeneratie te bevorderen.

In hoofdstuk 4 probeerden we juist de *hematopoëtische* cellen (en niet de niche cellen) die mogelijk betrokken zijn bij BM-herstel beter te karakteriseren door de hematopoëtische samenstelling van het BM in kaart te brengen in een vroeg stadium van herstel (dag 17 na het starten van inductiechemotherapie). Op dit moment (dag 17) bestonden hematopoëtische cellen voornamelijk uit lymfoïde cellen (low side scatter, CD45+ CD14-cellen). Vooral T-cellen (in het bijzonder de CD4CM T-celsubset) waren verrijkt in het regeneratief beenmerg van AML-patiënten. Aan de andere kant waren de B-cellen relatief laag, zij vertoonden een meer dan 5-voudige afname in vergelijking met hun tegenhangers in normaal BM. Deze bevindingen laten zien dat de 'geheugen' cellen van onze cellulaire afweer blijkbaar goed bestand zijn tegen chemotherapie-geïnduceerde celdood (in tegenstelling tot andere 'uitvoerende' componenten van de afweer zoals neutrofielen en B-cellen).

Vervolgens hebben we de frequenties van de verschillende lymfoïde subsets gerelateerd aan de tijd die nodig is om een absoluut aantal neutrofielen (een type witte bloedcel) van ≥500/mm^3 bloed te bereiken (een parameter voor hematologisch herstel). We zagen dat hogere frequenties van T-cellen geassocieerd waren met langzamer hematologisch herstel. Vooral de CD4CM T-cel subset leek deze associatie te bewerkstelligen, omdat het de enige T-cel subset was die significant geassocieerd was met de duur van neutrofiel herstel. Omgekeerd vonden we dat hogere frequenties van NK-cellen geassocieerd waren met sneller hematologisch herstel. Het combineren van de frequenties van zowel CD4CM T-cellen als NK-cellen in een NK/CD4CM-index versterkte verder de associatie van immuun-samenstelling met de tijd tot herstel. Gezamenlijk bieden deze bevindingen niet alleen inzichten in het herstel van immuun-subsets na chemotherapie-geïnduceerde schade, maar kunnen ze ook bijdragen aan het voorspellen van de tijd tot hematopoëtisch herstel. Ze maken verder de weg vrij voor verder onderzoek naar de biologische bijdrage van specifieke immuun-subsets (zoals CD4CM T-cellen) aan BM-herstel.

CURRICULUM VITAE

Keane Kenswil was born on the 9th of May 1989 in Paramaribo, Suriname. In 2001 he moved to the Netherlands after living in St. Maarten for 6 years. He attended Het Citycollege St. Franciscus high school in Rotterdam (The Netherlands) from 2001 until 2007 where he obtained his VWO diploma. In 2007 he started his study Biomedical Sciences at the LUMC in Leiden, where he did his bachelor and master with a focus on biomedical research. He did his first master internship in 2011 at the department of Surgery at LUMC in the group of Prof. dr. Paul Quax, where he tried to unravel the signaling pathways mediating arteriogenesis in a murine model of hind limb ischemia. His second master internship was performed at the Erasmus MC in Rotterdam in the group of Prof.dr. Raaijmakers at the deparment of Hematology in 2013. During this internship he focused on setting up an *ex vivo* culture system to study the potential effects of candidate (niche-derived) ligands on hematopoietic stem/progenitor cell proliferation and differentiation. At the end of this internship, in 2014, he decided to continue this project as a PhD-candidate, and also expanded the scope of his work. This included characterizing the human niche cells involved in bone marrow formation during fetal development, as well as bone marrow regeneration after chemotherapy-induced injury. Here he found that endothelial cells have an important role and express regulatory factors that can facilitate angiogenesis, osteogenesis, and hematopoiesis. Detailed results are presented in this thesis.

LIST OF PUBLICATIONS

Keane J.G. Kenswil, Adrian C. Jaramillo, Zhen Ping, Si Chen, Remco M. Hoogenboezem, Maria A. Mylona, Maria N. Adisty, Eric M. J. Bindels, Pieter K. Bos, Hans Stoop, King Hong Lam, Bram van der Eerden, Tom Cupedo, Marc H.G.P. Raaijmakers. Characterization of Endothelial Cells Associated with Hematopoietic Niche Formation in Humans Identifies IL-33 As an Anabolic Factor. *Cell Rep*. 2018 Jan 16;22(3):666-678

Keane J.G. Kenswil, Gonzalo Sánchez-Duffhues, Andrea Lolli, Claire van Dijk, Callie Knuth, Byambasuren Vanchin, Adrian Christopher Jaramillo, Remco Michiel Hoogenboezem, Tom Cupedo, Eric Moniqué Johannes Bindels, Bianca Blom, Pieter Koen Bos, Marie-Jose Goumans, Peter ten Dijke, Eric Farrell, Guido Krenning, Marc Hermanus Gerardus Petrus Raaijmakers. Endothelial-derived Mesenchymal Cells Contribute to Hematopoietic Niche Formation in Humans. *Manuscript Submitted*

Jasper J. Koning, Tanja Konijn, Kim A. Lakeman, Tom O'Toole, **Keane J. G. Kenswil**, Marc H. G. P. Raaijmakers, Tatyana V. Michurina, Grigori Enikolopov and Reina E. Mebius. Nestin-Expressing Precursors Give Rise to Both Endothelial as well as Nonendothelial Lymph Node Stromal Cells. *The Journal of Immunology*. 2016 Oct 1;197(7):2686-94

Noemi A. Zambetti, Zhen Ping, Si Chen, **Keane J.G. Kenswil**, Maria A. Mylona, Mathijs A. Sanders, Remco M. Hoogenboezem, Eric M.J. Bindels, Maria N. Adisty, Paulina M.H. van Strien, Cindy S. van der Leije, Theresia M. Westers, Eline M.P. Cremers, Chiara Milanese, Pier G. Mastroberardino, Johannes P.T.M. van Leeuwen, Bram C.J. van der Eerden, Ivo P. Touw, Taco W. Kuijpers, Roland Kanaar, Arjan A. van de Loosdrecht, Thomas Vogl, Marc H.G.P. Raaijmakers. Mesenchymal Inflammation Drives Genotoxic Stress in Hematopoietic Stem Cells and Predicts Disease Evolution in Human Pre-leukemia. *Cell Stem Cell*. 2016 Nov 3;19(5):613-627

Zhen Ping, Si Chen, Sjoerd J. F. Hermans, **Keane J. G. Kenswil**, Jacqueline Feyen, Claire van Dijk, Eric M. J. Bindels, Athina M. Mylona, Niken M. Adisty, Remco M. Hoogenboezem, Mathijs A. Sanders, Eline M. P. Cremers, Dicky J. Lindenbergh-Kortleve, Janneke N. Samsom, Arjan A. van de Loosdrecht, Marc H. G. P. Raaijmakers. Activation of NF-κB driven inflammatory programs in mesenchymal elements attenuates hematopoiesis in low-risk myelodysplastic syndromes. *Leukemia*. 2019 Feb;33(2):536-541

Hongzhe Li, Hooi Ching Lim, Dimitra Zacharaki, Xiaojie Xian, **Keane J.G. Kenswil**, Sandro Bräunig, Marc HGP Raaijmakers, Niels-Bjarne Woods, Jenny Hansson, Stefan Scheding. Early Growth Response 1 Regulates Hematopoietic Support And Proliferation In Human Primary Bone Marrow Stromal Cells. *Haematologica*. 2019 Aug 1. pii: haematol.2019.216648

PHD PORTFOLIO

Name PhD Student: Keane Kenswil
Erasmus MC Department: Hematology
Research School: Molecular Medicine (MolMed)

PhD Period: January 2014 – January 2020
Promoters: Prof.dr. H.G.P. Raaijmakers
Prof.dr. I.P. Touw

1. PhD Training Year

	Year	ECTS
General Courses		
Photoshop and Illustrator workshop	2014	0.3
Research management for PhD-students	2014	1.0
Research integrity course	2016	0.3
Biomedical English writing course	2017	2.0
Annual Course on Molecular Medicine	2018	0.6
In-depth Courses and Workshops		
Molecular aspects of hematological disorders (4x)	2014-2017	2.8
The course on R	2016	1.8
Basic course on SPSS	2018	1.0
Basic course on Python	2019	1.7
Basic course on Microsoft Access	2019	0.3
Two-days Course Bayesians statistics and JASP: Basic & Advanced	2019	0.6
Advanced course on Excel	2019	0.4
Scientific Meetings Department of Hematology		
Work discussions (Weekly)	2013-2018	8
Journal club / literature discussions (bi-montly)	2013-2018	7
PhD lunch with invited speaker (Monthly)	2014-2018	2.5
Erasmus Hematology Lectures (Monthly)	2014-2018	2
National/International conferences		
Molecular Medicine Day (4x) (Rotterdam)	2014-2017	1.5
European School of Haematology International Conference (Lisbon, Portugal)	2015	0.3
Dutch Hematology Congress (2x) (Arnhem)	2016-2017	0.6
Annual Conference of American Society of Hematology (Atlanta, USA)	2018	0.3
Presentations		
Departmental work discussions (Oral, 6x) (Rotterdam)	2014-2017	3.0
Journal clubs (Oral, 3x) (Rotterdam)	2014-2017	1.5
Dutch Hematology Congress (Oral, 1x)	2017	1.0
Academic Center for Stem Cells and Organoids in REgenerative medicine (ACE-SCORE) Day (Oral, 1x)	2017	1.0
Annual Conference of American Society of Hematology (Atlanta, US (Poster, 1x)	2018	1.0
2. Teaching, Supervision & Organization Activities		
Organization and supervision PhD lunch with invited speakers	2015-2016	0.2
Total		**41.7**

WORD OF THANKS

Perhaps I'm exaggerating by stating that I never expected to be writing my acknowledgments (at least any time soon), but there were times I genuinely thought I'd never reach this point in my PhD programme. Achieving this milestone would not have been possible without my own niche; in particular the people – to whom I will forever be indebted to for their continuous support over the past years – who I would like to thank in the following paragraphs.

Allereerst wil ik mijn promotor **Prof.dr. Raaijmakers**, **Marc**, bedanken: U nam mij niet alleen aan als een masterstudent, heel lang geleden al, maar u zag (gelukkig voor mij) genoeg potentie in mij om mijn onderzoek als volwaardige promovendus voort te zetten. De afgelopen jaren heeft u duidelijk aan mij gemaakt wat nodig is om succesvol te zijn in wetenschappelijk onderzoek. Naast imponeren met uw gladde praatjes, bent u ook gewoon het schoolvoorbeeld geweest van hard werken, hoe vaak ben ik u wel niet tegengekomen nog laat in de avond, of in het weekend, op werk. En misschien was de allerbelangrijkste les: gericht werken en bewust zijn van wat "the bigger picture" is. Dit heeft mij uiteindelijk ook immens geholpen met het (leren) schrijven. Verder heeft u mij ook geleerd om door te zetten als het tegenzit en dat tegenslagen in de wetenschap de normaalste zaak van de wereld is; uw enthousiasme en gedrevenheid voor onderzoek wist me vaak ook gewoon weer te motiveren wanner het nodig was. We waren misschien regelmatig niet met elkaar over eens over hoe bepaalde vraagstukken (realistisch) aangepakt moesten worden, maar dat was waarschijnlijk ook beter zo, anders had ik niet veel geleerd tijdens mijn periode in de Raaijmakers' groep. Ik ben heel dankbaar hiervoor en wens u en uw groep veel succes toe in het maken van nieuwe wetenschappelijke ontdekkingen.

Prof.dr. Touw, **Ivo**, mijn tweede promotor, ik heb veel geleerd, en me ook goed vermaakt, van uw moeilijke (en ook gewoon legitieme) vragen die vaak levendige discussies deed oplaaien tijdens de werkbesprekingen. U stelde ook vaak relevante vragen over mijn experimenten, deze hielpen ons het onderzoek naar een hoger niveau te brengen, maar voorkwam ook dat we voorbarige conclusies trokken. Verder kon u ook tegengewicht bieden aan Marc en kon ik gelukkig naar jou toe gaan voor duidelijk advies wanneer ik er soms niet uitkwam met hem. Misschien op de eerste oogopslag niet heel erg wetenschappelijk, maar ik stelde ook altijd op prijs hoe je altijd verschillende gerechten wist klaar te maken voor de eet-evenementen van onze afdeling. Oh en natuurlijk ook bedankt voor het grondig nakijken van mijn proefschrift!

I would also like to thank my assessment committee for critically evaluating and approving my manuscript. **Prof.dr. P. ten Dijke**, ik heb u persoonlijk (nog) niet ontmoet, maar u bent wel nauw betrokken geweest bij mijn onderzoek, vooral met de meest recente studie over EndMT, waar u (en uw groep) ook kritisch aan heeft bijgedragen. Nog bedankt hiervoor. **Prof.dr. W. E. Fibbe**, ook u heb ik (nog) niet ontmoet, maar u heeft ook een belangrijke bijdrage geleverd door mijn proefschrift snel op tijd grondig door te nemen, zelfs na wat

kleine mankementen met het *Hora Finita* systeem. Dank hiervoor. **Dr. E. Farrell**, I'm very grateful for our long-time ongoing collaboration that has turned out to be very fruitful, and which will hopefully lead to a very nice publication! Your willingness to extend a helping hand to our group helped us answer some very important questions brought up by the peer reviewers. I would also like to thank you for being the secretary of the committee, and keeping Marc updated through the whole process, who in turn could keep me informed on the latest developments.

I would also like to extend my gratitude to the other members of my doctoral committee for willing to participate in my defence ceremony. **Prof.dr. J.P.T.M van Leeuwen**, ik voel me vereerd dat u als decaan deel kan nemen in mijn promotieplechtigheid. Ik herinner me dat één van mijn eerste collaboratieve bijeenkomsten met jouw onderzoeksgroep was, namelijk de "Bone-HSC" meetings op de vijfde verdieping. Dit leidde gelijk naar één van de eerste samenwerkingen in mijn onderzoek, wat heel goed verliep, bedankt hiervoor. **Dr. T. Cupedo**, **Tom**, ik ben u ook heel erg dankbaar voor de verschillende manieren hoe jij mij hebt geholpen. Jij hebt je niet alleen (letterlijk) ingespannen om foetaal materiaal voor mijn onderzoek te regelen, maar jij heb ook veel constructieve feedback geleverd in twee van mijn belangrijkste studies. Ik vond de collaboratieve bijeenkomsten met jouw onderzoeksgroep ook altijd heel erg leerzaam. Jouw onderzoeksgroep was ook altijd bereid om mij te helpen, en is in zekere mate een weerspiegeling van jou. **Dr. G. Krenning**, **Guido**, jouw groep heeft ook belangrijke bijdragen geleverd aan mijn werk naar EndMT. Jij hebt ook zelf ervoor gezorgd dat nadat jouw PhD-student, Byamba, terug naar Mongolië was vertrokken dat onze samenwerking nog vlekkeloos verliep. Bedankt hiervoor. **Dr. R. Schneider**, **Rebekka**, while I maybe have not worked as closely as my other (former) colleagues with your group, I really still appreciate your input and the help you and your group have provided me along the way. I hope the common themes shared between our groups will continue to foster close (future) collaborations, in particular when it comes to resolving the potential role of IL-33 in myelofibrosis.

Verder wil ik ook de andere groepsleiders van de afdeling Hematologie bedanken die ik heb meegemaakt. Speciale dank aan **Bob** die ik nog regelmatig tegenkwam en mij altijd heel erg vrolijk groette, ook al kende u mij eigenlijk niet, en die ook nog vaak de Friday floor meetings bijwoonde en daar ook interessante vragen stelde. Dit geldt ook voor **Pieter**, **Frank**, **Jan**, **Ruud**, **Moniek**, **Peter**, **Eric**, **Mojca**, **Stefan** en **Emma**, jullie hebben allemaal op één of andere manier mij geholpen, bijvoorbeeld door het doneren van bepaalde protocollen, reagenten, cellen, weefsel, of zelfs met het opzetten van nieuwe muizen-breedings. Ook was het gezellig om met jullie te babbelen of grappen te maken over jullie eigen PhD-studenten tijdens de borrels.

Of course I would also like to thank my fellow group members, be it former, contemporary, as well as recently arrived colleagues, you all had your part in helping me to complete my PhD studies.

First of all I would like to thank **Noemi**, you were my daily supervisor during my master internship despite you not really benefiting from this task due to our projects not being directly related. Nonetheless you still took your time to teach me basic stuff, such as cell culture and genotyping, and helped me to get on my way to conduct my own research independently. I appreciated your more hands-off (progressively over time) approach in supervising me and liked that you didn't mind me slacking off from time to time to socialize with other fellow (master)students. I think you also set a great example for the rest of the students in the lab, and I think this is partly why Marc has such high standards for his PhD students, so thanks for that ☺.

Athina, while I did not end up being your student, you still helped me out with any questions I had for you, even though you already had left the group by then. Also thank you for helping to set up the group before I arrived!

Niken, apppaaa, how I miss our KFC feasts we shared with our fellow (Asian) group members. Thank you so much for helping with out with genotyping, FACS and RNA-Sequencing, without you the group barely managed to scrape by.

Si, another of the original KFC-crew members! I'm impressed by how you always managed to stick to your goals and never got too distracted, despite whatever stressful situations were occurring in the lab. It's particularly impressive that you managed to graduate with minimal delays, which is not an easy task in this group. You also have a real knack for presenting, and I hope you keep putting it to good use in Singapore! I would like to thank you for giving me a lot of constructive feedback during our group-meetings, at least when you were not falling asleep haha, and also for organizing a lot of fun social (read: eating a lot of food) events with our other lab-mates.

Ping, the honour and privilege is mine. We have been through so much, and even lived together for a while, though I actually did not see you much socially back then since you were usually slaving away in the lab until the early morning hours. This was often, if you were not procrastinating in the lab or getting distracted by me, due to your dedication to getting stuff done perfectly. Because, indeed, what's the point of doing something if it's not done properly? This is a sentiment I agree strongly with you, and I think this is also why I get a long with you not only at professional level, but also a personal level. In fact, we see eye to eye on a lot on a lot stuff, in particular what it means to have honor. That said we also had some disagreements, and inevitable tensions in the lab, like about Tibet/Taiwen, but we always managed to keep it respectful. I have to keep it brief, but I'm sincerely grateful that I shared an office, our own private fridge, many dinners, karaoke-borrels, fun festivals, and many crazy parties over the years. Also special thanks for helping me out with my mice experiments whenever my hands were too shaky!

Adrian, you bloody Mexican! We both know I would never have gotten to this point without you laying the groundwork for me when it comes to the Day 17 and fetal samples. For this I will always be grateful to you. Besides these critical scientific contributions, you

were also one hell of a roommate to have! The many nights out, but also the nights at our place hosting costume parties, including the toga, yoga, Halloween, murder-mystery, and Christmas sweater themed events; the utter debauchery would have made Caligula blushed. And then not to speak of the countless concerts we attended, such as Nils Vroom, The Beach Pixies, Blossoms, Corvalis, Small Blacks, Yucks, Dinosaur Sr., Sonic Seniors, The Serial Killer from No Country for Old Men, and The Robert Smiths, what a time to be alive indeed. I really hope we manage to attend another festival with the gang~~bang~~ before all it is said and done. There are many more stuff I'm grateful for, but I have to keep it brief. I will spare you the platitudes, and simply wish you good luck in whatever you still need to do to finish your PhD. Trust the dice.

Claire, ik wilde net schrijven dat alles gelukkig eindelijk achter de rug is, maar we hebben misschien binnenkort nog revisies voor de EndMT paper :')! Maar nu even serieus, ik ben je zeer dankbaar dat jij mijn projecten voorlopig (en niet eventjes) wist over te nemen. Zonder jou zouden de foetale monsters in Amsterdam niet verwerkt zijn geweest, en dat was ook allemaal net op tijd gebeurd. Jij hebt niet alleen praktisch werk gedaan, zoals FACs en RNASeq, maar jij hebt ook gewoon in zijn geheel kunnen bijdragen door jouw eigen wetenschappelijke inzichten te verschaffen, zoals bijvoorbeeld bij het analyseren van de scRNASeq data, en andere momenten die ik me nu natuurlijk niet meer kan herinneren :p. Ik geloof oprecht dat je geschikt zou zijn om zelf een PhD-traject te voltooien! Jij hebt in ieder geval het IQ en passie ervoor. Verder was het ook heel gezellig met jou; en hoop ik binnenkort met jou en PaOla te kunnen sushi'n.

Jacqueline, you are the bridge from the former generation to the current one. I'm really impressed to see how you've developed over time as researcher, like me also starting off as a master student, and becoming more confident and taking charge of your own experiments. Not only that, but you have also kind of taken up a senior-ish role in the group, making sure everyone is doing well or doing stuff properly in the group. I'm really grateful for the several times you helped me out with my projects, be it with HiX to help me out with the AML day 17 samples, or preparing antibody orders, or even performing flow cytometry experiments for the EndMT project. I'm sure you will continue to do well in your PhD, and wish you good luck in carrying the torch for the newer generation!

To the other former Post-Docs in our group: **Yongyi** and **Tamar**, it's too bad our periods didn't overlap much in the lab, I would have really liked to soak up more of your knowledge. I wish you well in your future scientific pursuits! All active PhD-candidates or Post-Docs in our group, **Eline**, **Isabel**, **LanPeng**, and **Martijn**, I haven't worked or interacted much with you at all, but I still want to thank you for the times I chatted or distracted you in the office or hallways and wish you well with your studies! Also a special mention to all former students in our group, like **Sjoerd**, I enjoyed nerding out about stuff like Twitch, I felt like I was teenager again.

Last but not least of the Raaijmakers' group, I want to thank **PaOla**, I often say time is a flat circle, and working closely with you these past weeks on the submission for the EndMT paper, made me believe this all the more: I started my studies on the niche with a feisty, short, intelligent Italian brunette, only for it to finish with another fire-y, small, smart, Italian brunette. Though my thesis was technically already approved, you still helped me elevate the EndMT paper to another level, not only stylistically with your choice of colours, but also literally at a single cell level. For this I really want to say thank you. I'm happy "my project" is in your hands now, and I'm sure you will do well. Also like I told Claire, I look forward to our sushi dinner to discuss not only how the project is progressing, but also to figure out which political system, instead of democracy, would be the best to meet the needs of society.

I would also like to name a lot of other people from the lab that have helped me out. Special thanks to **Eric-Sensei**, I don't think I'm exaggerating when I call you the Godfather, or maybe even the babysitter of our group, without your guidance we would not gotten much done (efficiently or properly) over the past years. I'm especially grateful for the many times you helped me out with those pesky western blots and with the shRNA knockdowns. In addition, I also appreciated your fine taste in music (most of the times), in particular when it comes to our shared love for (post)punk music or The National. We even attended a Sigur Rós concert together once with Mr.O! **Mr.O**, what up my ginger! It's time to plan Iceland part II, it has to happen! Thanks for organizing the many epic (ambrosia) nights, and being part of all the crazy adventures we've experienced over the years. We also worked a bit in this period, and I also want to thank you for helping me out in the lab, be it with confocal, getting me extra screen for the PC, or providing me shiny antibodies for immunofluorescence. Thanks man! **Paulette!** Hoe vaak moest jij wel niet lang op het lab blijven, omdat jij mij aan het helpen was met FACS-sorteren. Verder hielp jij mij ook zo vaak met het preppen van mijn samples voor RNASeq, en was jij ook altijd oprecht geïnteresseerd in hoe het met mij ging, en ook met de anderen in de groep, door een luisterend oor aan te bieden. Je was soms eigenlijk gewoon een technician binnen onze groep (en ik zou het helemaal niet erg gevonden hebben als jij naar de Raaijmakers' groep was overgelopen), en wil je hiervoor hartelijk bedanken! Ik wil ook **Nathalie** bedanken, jij hebt me ook zo vaak geholpen met het sorteren en het verwerken van de foetale botten. Ook vond jij het nooit een probleem als ik regelmatig antilichamen kwam gebruiken van jouw groep. Verder kon ik wel lachen om je grappen, zoals over "The Great Wall of China".

Remco, ik vond het heel gezellig met jou op de 19de verdieping toen ik aanvankelijk begon als een masterstudent, en dat bleef ook zo nadat we zelf een eigen plek op de 13de hadden gevonden. Ik wil jou ook hartelijk bedanken voor jouw inzet om gedegen RNASeq/GSEA analyses uit te voeren. Dit geldt ook voor **Mathijs**, en ik wil jullie allebei bedanken voor jullie geduld met onze vragen over statistiek, bijvoorbeeld wanneer iets nou echt als significant beschouwd kan worden. Ik wil ook **Elodie** bedanken voor het bouwen van de RNASeq-database website.

Verder wil ik nog meer mensen bedanken, waaronder de flow-cytometrie operators: **Elwin**, **Peter** en **Michael**. Jullie werkten altijd nauwkering en bleven geduldig en flexibel wanneer ik samples (nog laat) moest sorteren. Ik wil in het bijzonder Elwin verder bedanken, want jij hebt mij ook ontzettend veel geholpen met het vierde hoofdstuk van mijn proefschrift. Samen met **Lucia** hebben jullie mij ook geholpen met opzetten van mijn masterstage. Ik wil ook **Mariëtte** bedanken, jij hebt mij veel geholpen met het isoleren van $CD34^+$ cellen uit navelstrengbloed, en je hebt mij vaak cellen gedoneerd. **Jasper** en **Joyce**, ik heb misschien niet veel direct met jullie gewerkt, maar ik kon altijd leuke grappen met jullie maken. To err is human to arr is pirate.

I would also like to give special thanks to my collaborators, who helped me finish my studies. **Bram** en **Marijke**, dank jullie wel voor de MSCs en ook voor het duidelijk maken aan mij hoe ik ALP-assays moest uitvoeren. **Byamba** and **Callie**, thank you for all the cell culture and (differentiation assays) you guys performed for the EndMT paper. Callie, it's about time we find another festival or event to celebrate that we can put our PhD-adventure behind us! **Gonzalo** and **Andrea Lolli**, I also want to thank you for your critical contributions to the EndMT paper, I hope you guys don't mind if I keep pestering you about experimental details if any questions pop-up, especially if we end up doing revisions! **Dr. Pieter Koen Bos** en **Dr. King Lam** bedankt voor de humane (bot) monsters die ik heb kunnen gebruiken in mijn studies. **Dr. Hans Stoop**, jou wil ik ook bedanken voor al de immunohistochemie die jij voor mij hebt gedaan, en ik wens je nog succes toe met je jazz-optredens! Ik wil ook het **BMT** lab bedanken voor al de BM samples die jullie aan mij hebben gegeven. Speciale dank aan **Hennie** die mij heeft geleerd hoe ik kolonies moet tellen.

I'm also much obliged to the colleagues who I shared my office with over the years. **Emanuele**, my paranymph and dear friend, hopefully you have survived the corona-scare with Matteo, and will manage to make my ceremony. If not, you will be very difficult to replace, as I don't see anyone easily replicating your rather care-free, bordering on the lackadaisical, attitude that is very much appreciated by me. In fact, I'm rather fond of this approach to life as it led to many eggtastic eggperiences. At the same time your attitude keeps my rather neurotic and impulsive behaviour in check, and whenever we almost came to blows you always knew when to walk away (cause you'd get your ass kicked). Kidding aside, as Ping would put it, it's been an honour to have gotten to know you. I look forward to visiting your hometown one day so we can play some basketball and eat arrosticini with the locals. Having said that I hope I already partially repaid my debt to you by finding you your first Dutch GF. P.S. Sorry for dragging you to Welcome to the Future, but it's your own fault you got sick from eating bad fish. Anywho, good luck with your own writing. **Cansuuu**, thank you for bestowing upon me my cute "Keannuu" nickname, I think it actually suits me quite well. You and your daddy have made my final years of my PhD so much fun, I'm happy that we not only saw each other so often in the lab, but also outside of it! I'm in particularly impressed by how you can keep up with me, Ping and your daddy when it comes to eating yummy food. With Ping, me, and also your daddy leaving soon, I hope you won't get too lonely, but I'm sure you'll manage, since you probably will just keep laughing like a maniac, as you always do. Good luck with finishing your projects, you can do it!! **Mira**, you were never officially my officemate, but you practically were with how often you came to visit us. Luckily, you never did become part of our office, otherwise I would have gone crazy with the nonstop chit-chat between you and Cansu. That said I did appreciate your presence most of the times, even though I admittedly was a bit too mean sometimes (sorry, not sorry, for that). I am grateful for the times you helped me out with my experiments. While things didn't work out at the EMC, I'm pretty sure you'll do fine in the LUMC, and I hope I'm also invited for your PhD ceremony when that time arrives!! **Michiyo**, you were one of the most polite officemates I had, and it was so much fun talking to you about Japan, and even going out and eating Ramen with you and the rest of the gang. **Farshid**, thank you for providing me a lot of career advice, and welcoming me into your office that you were already sharing with **Lucilla**, who always had a story or two to tell.

I still have many people to thank, and I'd like to continue with the technicians in the Delwel Group. **Claudia** and **Andrea**, thank you for the pleasant and very considerate conversations, you guys were always nice to me. Andrea one day we will definitely attend a salsa party or bachata event with one of my good friends, ahah. **Marijke**, bedankt voor jouw hulp in het ML-II lab. Ook wil ik de andere technici van onze afdeling bedanken, in het bijzonder **Hans** en **Dennis**; ik vond de bierproeverij en andere sociale evenementen altijd goed geslaagd, alleen was het jammer dat ik geen pittige ketchup meer van jullie kon krijgen. **Inge**, ik ben je ook dank verschuldigd, jij had me geholpen met het verwerken van muizen-botten voor immuno-kleuringen, nog bedankt hiervoor!

I also want to thank former and current Post-Docs in the lab, **Julien** (also magic cola lol), **Ferry**, **Leonie**, **Jess, and Nils**. Thank you for all the times you helped me out with FACS-sorting, providing general career advice, engaging scientific discussions, or just exchanging simple pleasantries.

I also owe a lot to the (PhD-)students that have come before me. Very special thanks to **Kasia** and **Jana**, original founders of the EMC-techno club, it was such a blast to get to know the playful side of my fellow colleagues of the lab, and much respect to you OGs for setting the tone for the younger generation. I'd like to give even more props to Jana for introducing me to her fellow MolMed students. And thank you Kasia for giving me not only career advice, but also advice about life in general. **Monica** you deserve a special mention as well, you also helped me out a couple of times with FACS-sorting, and you were also very fun to party with, especially with Julien, I hope you are doing well in Vancouver! Shout-out to **Patricia D** (you also had a very fine musical taste), and **Marshall**, hope you are doing well in MAGA-land! As for you, **Roberto**, I hope our lengthy conversations, which still have continued and hopefully will keep on going for a long time, made it clear how much I appreciate having you around. You have also been very considerate of others, in addition to being a deep-thinker

without ever being pretentious or arrogant. Having you and Adrian as roommates was so much fun, and I'm happy we managed to arrange this and experience so many, as you put it, "moments" together. Cause in the end, that's all what matters no? I wish you all the best, and hopefully I will see you again soon. Perhaps one day we can all see Solar Fields together? Ostia.

I also want to thank the other PhD students that are close to graduating or are getting there: **Davine**, **Tim**, **Patricia O**, **Adil**, **Sophie**, and **Roger**, zet hem op! I wish you the best with finishing your studies. To the newer PhD students that I have gotten to know a bit: **Bella** totally awesome that you returned to Hematology, hope you keep listening to good indie music, and perhaps I'll bump into you in one of those random ADE parties. **Madelon**, het was leuk om je te leren kennen tijdens de Python cursus, houd me op de hoogte als je ooit een documentaire heb geregisseerd! Verder wens ik je nog succes met Paola in je kantoor, ik ben er heel bewust van dat ze best veel kan praten ☺.

Ik wil ook nog andere collega's van de afdeling Hematologie bedanken: **Ans**, **Annelies**, **Eaudia**, **Tessa**, en **Leenke**, ik wil jullie bedanken voor het regelen van al mijn afspraken met Marc en Ivo, verder waren jullie altijd behulpzaam als ik vragen had, bijvoorbeeld over hoe ik bepaalde reagenten het beste kon verzenden. **Egied**, ik wil jou ook hartelijk bedanken voor al jouw hulp met mijn proefschrift, zonder jou zou ik de tijd niet hebben gehad om mij goed te concentreren op mijn schrijfwerk. Verder ben ik heel tevreden over hoe mijn proefschrift eruit gaat zien.

Over the years I also met a lot of fellow students outside of Hematology that made my EMC-experience all the more fun! Special thanks to **Lena**, I enjoyed our talks about free will/ determinism, you playing my musical requests during your DJ-set at BAR, and not to forget the many karaoke events! You also helped me realize that for some reason most of the cool people from Greece are from Thessaloniki, case in point **Irene** and **Isabella**! I had a great time with you girls at BKS, and many other events, perhaps we can find another festival soon. Maybe the one Ping will be attending this August, the music won't be Radiohead or The Cure, but it I'm pretty sure it will be awesome! I also want to wish you both good luck with your PhDs. Also a special thank you to Irene for introducing me to the girl who took over your old room, haha. Also please give some hugs and kisses to Nefeli and Len for me! I also want to thank another expat from Thessaloniki, **Simy**, especially for giving me plenty of extra discounts at the EMC-cafeteria, good look with your egg studies! I also want to mention **Anika** and **Liz**, you guys were one of the first master students I started to hang out with when I first started out at the EMC. Thanks for having me over in Atlanta Liz, and I wish you good luck at the CDC! Anika good luck finishing up your PhD in Switzerland, and get that €€€. Also shout-out to the people I met from Infection & Immunology, **Jurre, Anusha**, and **Simone** who were always up for parties! I'd also like to give special thanks to the people form MolMed-school, **Rodrigo** and **Pablo** it was fun playing basketball with you guys from time to time, and having many BBQ sessions (in the park)! **Diana** and **Adna**, you guys also joined for basketball a couple of times and even more special, I really had great time visiting you guys in your home countries and showing me around. I think it made me understand you guys better knowing where you came from, I guess haha. Diana, I wish you good luck in Memphis, just don't get shot by those crazy Americans okay? Adna, hopefully you can manage finding a position in the EU and maybe see you at **Tania**'s and **Alex**' wedding?! Very special thanks to these lovebirds for letting me stay at your place, so many times. It really felt like my third home. And besides that it has been so much fun going to (karaoke-)parties and festivals, such as Expedition and Bangface, with you guys. Take care of each other, and also good luck with writing your thesis Tania!

The fun was not limited to the EMC, and I also have to mention some other awesome people, in particular the my fellow Bisons. Special thanks to **Raz** who has been the driving force behind all the awesome Bisons events. Shout-out to **Ian**, maybe the craziest Bison of them all, and that says a lot considering I know Adrian. I also want to thank **Lorenzo**, **Thomas**, **Livia**, **Matteo**, the Italian (Schopare?) branch of the Bison group, thanks for all the memorable parties and BBQs in the park.

Ik heb gelukkig nog meer vrienden, denk ik, onder andere **Esther** en **Sanders**, die ik ook wil bedanken voor het bijwonen van allerlei concerten, en hopelijk blijft dit ook de komende jaren zo doorgaan. Alleen moet DIIV wel weer goede muziek maken. Ik moet natuurlijk de Lamers-squad ook opnoemen, zonder jullie zou ik mij veel minder hebben vermaakt de afgelopen jaren, vooral bedankt voor jullie geduld met mijn trollings, in het bijzonder **Nilton** en **Kachon** (die het ook vaak verdienen). Jullie hebben mij regelmatig geholpen met verhuizen, en ik ben eigenlijk de tel kwijt, thanks boys. **Nahuel** en **Ali**, cool dat jullie naar IJsland mee waren gekomen, kom maar nog een keer, alleen wel met extra verzekering voor de huurauto. Ik ben nu wel betere driver, of niet Nahuek? Verder GG met alle gaming sessies, en kom snel weer een paar potjes PES doen. Shout-out to fellow OG SXM'r strongman **Rugene**, I appreciated your heavy-lifting, not only during my moving, but also during my mom's. It was also cool playing Pokemon Go with you for a bit, and I wish you the best in becoming a Pokemon master, if not yu-gi-oh/salsa/bachata master. Oh ja, ik wil ook nog succes aan **Shiraaz** toewensen met het afronden van jouw PhD. Ik wil nog één speciaal iemand van het EMC bedanken, en dat is **Frank van Vliet**, dank je voor al die keren dat je naar me luisterde over mijn problemen, advies hebt gegeven, fondsen voor mij hebt geregeld, en ook gewoon de gezelligheid die jij altijd aanbood met ons etentjes en drankjes. Hopelijk doe jij zelf de komende tijd ook rustig aan en hoef jij het niet zo druk te hebben met werk.

Ik wil ook even mijn familie bedanken, waaronder mijn neven en nichten, **Bryan**, **Edsard**, en **Amy**, wat leuk dat **oma** ons allemaal heeft weten samen te brengen, door haar hebben we allerlei familie-uitjes kunnen maken afgelopen tijd. Wel jammer dat we voorlopig niet veel kunnen tot 1 juni, maar ik weet zeker dat we daarna snel iets vinden om mijn promotie goed te vieren. Verder echt tof dat je nog mee was gekomen naar Malta Bryan toen we

Roberto opzochten, alleen volgende keer niet zo goedkoop parkeren in Eindhoven! Sowieso nog bedankt dat je me paranimf wil zijn! Verder wil ik ook mijn zusje **Abygail** bedanken, jij hebt me zo vaak moeten ophalen bij het vliegveld als er weer eens problemen waren, zelfs ook helemaal uit Brussel. Ook heb je vaak andere dingen voor mij gedaan en vervoerd, bijvoorbeeld wanneer **mama** eten wilde langsbrengen. Ik zal mijn best doen om aardiger tegen jou te zijn, en ook vaker bubbeltea meennemen naar huis voor jou. Ik wens je nog succes met het afronden van je studie. **Ma**, bedankt voor al het eten, en alle ontelbare dingen die jij voor mij hebt geregeld. Jij hebt misschien gelijk dat ik vaker naar je moet luisteren, maar ik zal altijd koppig blijven. Ik ben wel dankbaar naar **jou** en **papa**, dat jullie Abygail en mij naar Nederland hebben gebracht, want uiteindelijk hebben we hier een heel goed leven weten op te bouwen. **Pa**, ook bedankt voor al je aanmoedigingen en steun, onder andere door telkens te vragen wanneer mijn proefschrift af zal zijn. Het is eindelijk gelukt.

And to cap it all off, I want to also to give special thanks **Nina**, my cutiepie. I have put you through a lot all these years of me trying to obtain my PhD title. Still the longer you waited the more I felt I had to finish; otherwise that waiting would have been for nothing. Luckily you are very patient (haha) and the time has finally arrived that we can take the next step, not only in our career, but life in general. I want to thank you for hanging in there, and also for the pretty cover you and your friend **Lydia**, made for me. Where-ever our adventures may lead us, I hope I'll be good enough to stand by your side.

Well that's it, I probably forgot to mention a couple of people, and for that I have to apologize, but I need to print this dissertation in time, kthxbye.